Characterisation of the Interaction between FAT10 and its Substrate Protein p62

Dissertation

zur Erlangung des akademischen Grades
eines Doktors der Naturwissenschaften (Dr. rer. nat.)
an der Universität Konstanz (Fachbereich Biologie)

Vorgelegt von

Kathrin Christiane Kluge

Tag der mündlichen Prüfung: 10.04.14
1. Referent: Prof. Dr. Marcus Groettrup, Universität Konstanz
2. Referent: Prof. Dr. Elisa May, Universität Konstanz

Danksagung

An erster Stelle möchte ich mich ganz besonders herzlich bei Herrn Prof. Dr. Marcus Groettrup für die Bereitstellung des Themas und des Arbeitsplatzes sowie für die sehr gute wissenschaftliche und menschliche Betreuung dieser Arbeit bedanken. Vielen Dank auch für das stets offene Ohr in allen fachlichen und persönlichen Belangen.

Mein Dank gilt auch meinen Gutachtern und Prüfern, für ihre freundliche Bereitschaft diese Aufgaben zu übernehmen.

Des Weiteren möchte ich mich beim Graduiertenkolleg RTG1331 für die finanzielle Unterstützung und bei seinen Mitgliedern für die vielen anregenden wissenschaftlichen Diskussionen bedanken.

Mein ganz besonderer Dank gilt Frau Dr. Annette Aichem, die mir als FAT10-Expertin während der gesamten Promotion mit sehr wertvollem Rat und sehr hilfreicher Tat zur Seite stand und von deren überaus großer Erfahrung ich sehr viel lernen konnte.

Vielen Dank auch an die anderen Mitarbeiter des BIT*g*'s für den sehr regen wissenschaftlichen und materiellen Austausch, die herzliche Aufnahme als „Tagesgast" inkl. der exzellenten Verköstigung und an Nicola Catone, für seine großartige Hilfe bei der Herstellung des rekombinanten GST-FAT10-Proteins.

Bei all meinen Kollegen auf P11 möchte ich mich für die tolle Atmosphäre und die sehr schöne Zeit bedanken! Durch eure ausnahmslose Freundlichkeit und Hilfsbereitschaft habe ich mich hier im Süden sehr schnell eingelebt und bin immer gern zur Arbeit gegangen.

Ich möchte mich insbesondere bei Andrea, Annette S., Valentina, Sonja E., Rich, Gretl, Valerie und Stella für die vielen unglaublich lustigen Momente, die schönen gemeinsamen Erlebnisse und vor allem für eure bedingungslose Unterstützung in allen Lebenslagen bedanken. Ihr seid mir während der Promotionszeit sehr gute Freunde geworden.

Tina danke ich dafür, dass sie durch ihre Hundegeschichten und ihren unvergleichlichen Humor den Laboralltag sehr aufgelockert hat. Für die wöchentlichen Spieltaganalysen und die vielen heiteren Gespräche danke ich Marc, Michi und Gerado. Für ihre Hilfsbereitschaft, sei es bei Problemen mit dem technischen Equipment, Blumen-Sitting oder verschenkten Schneeketten, danke ich Ulli. Unserer guten Seele Brigitte danke ich für ihre Unterstützung bei allen computertechnischen und formellen Angelegenheiten. Vielen Dank auch an Gunter Schmidtke (*f.k.a* Maniatis?!), dessen Wissen und Erfahrung in der Biochemie und Molekularbiologie mindestens genauso riesig sind wie seine Sprüche- und Anekdotensammlung. Auch allen anderen ehemaligen und gegenwärtigen Kollegen, die ich hier aus Platzgründen nicht alle aufzählen kann, gilt mein Dank für die angenehme Zusammenarbeit.

Ebenfalls bedanken möchte ich mich bei meinen Konstanzer Freunden Sonja G., Kathi & Andi, Finn, Sophie, Becci & Philipp M., für die vielen gemütlichen Kaffeerunden, gemeinsamen sportlichen Aktivitäten, Ausflüge, Spieleabende und Gespräche. Für unsere lange Freundschaft danke ich meinen „alten" Freunden Alex, Steffi, Siggi, Anna, Philipp P., Vroni, Bea, Claudia, Michi P., Kathi S., Anne, Mirka, Karina, Diana und Mirko, die mir den Rücken stärken und die ich nicht mehr missen möchte.

Meiner Familie danke ich für den tollen Zusammenhalt, obwohl die Entfernung leider nicht immer so viele Besuche ermöglicht.

Schlussendlich gilt mein Dank vor allem meinen Eltern, für all ihre bedingungslose Liebe und Unterstützung aus der ich immer Mut, Kraft und Zuversicht schöpfen kann!

Table of content

1 Zusammenfassung/Summary

1.1 Deutsch

Das Ubiquitin verwandte Protein FAT10 bildet über ein C-terminales Glycin-Glycin Motiv Isopeptide Brücken mit den Lysinen in seinen Substratproteinen. Die biologische Funktion von FAT10, neben dem proteasomalen Abbau der modifizierten Proteine, ist noch weitestgehend ungeklärt. Das Protein Sequestosome 1 (SQSTM1/p62) wird an verschiedenen Lysinen mono-FAT10yliert und interagiert auch nicht-kovalent mit FAT10. Die FAT10ylierung von p62 führt zu dessen proteasomalen Abbau. Durch die Interaktion mit einer großen Anzahl von Proteinen, übt p62 viele verschiedene Funktionen aus. Es ist zum Beispiel an der Bildung von Ubiquitin positiven Protein Aggregaten beteiligt und führt diese zum autophagosomalen Abbau.

Das Ziel dieser Studie war es, die Interaktionen zwischen FAT10 und p62 zu charakterisieren. Hierzu wurden *in vitro* Interaktionsstudien mit rekombinanten Proteinen und mit in HEK293T Zellen exprimierten Proteinen durchgeführt. Bei einer Lysin-freien p62 Mutante war die FAT10ylierung nicht immer vollständig verhindert. p62 Mutanten mit fehlenden Domänen wurden für die Identifizierung der kovalenten und nicht-kovalenten Interaktionsdomänen verwendet. Bei den p62 Mutanten ohne PB1, NPI, TRAF oder N-terminalen PEST Domäne waren keine FAT10-p62 Konjugate detektierbar. Die Analyse einzelner p62 Lysin Mutanten ergab, dass die für die FAT10ylierung verwendeten Lysine vermutlich redundant sind. Die ZZ, die LIR, die CPI Domäne und der C-Terminus der C-terminalen PEST Domäne von p62 sind scheinbar für die nicht-kovalente Interaktion mit FAT10 verzichtbar. Anhand von nicht phosphorylierbaren, „phospho-mimicking“ und nicht oligomerisierenden p62 Mutanten wurde gezeigt, dass weder der Phosphorylierungsstatus an Serin 403 noch die Fähigkeit von p62 Oligomere zu bilden Voraussetzungen für die Interaktion mit FAT10 sind. Mit einer isolierten p62 PB1 Domäne wurde gezeigt, dass diese weder kovalent noch nicht-kovalent mit p62 interagiert. Ein Cycloheximide „Chase“ ergab, dass das Proteasom der bevorzugte Abbauweg für das FAT10-p62 Konjugat ist. Die Untersuchung der autophagosomalen Adapterproteinen NBR1, NDP52 und OPTN auf ihre Interaktionsfähigkeit mit FAT10 blieb ohne weitere Treffer.

1.2 English

The ubiquitin-like modifier FAT10 has a C-terminal diglycine motif which is required for the conjugation to lysines (K) in its substrate proteins via isopeptide bonds. The biological function of FAT10, besides the proteasomal degradation of substrate proteins remains obscure. Sequestosome 1 (SQSTM1/p62) was found to be mono-FAT10ylated at several lysines and a non-covalent interaction between FAT10 and p62 was detectable too. The FAT10ylation of p62 leads to its proteasomal degradation. p62 can interact with a large number of proteins and changes its face by altering the binding partner(s). It is required for the formation of ubiquitylated protein aggregates and was found to act as a shuttling factor which links those aggregates to the autophagy machinery.

The aim of this study was to further characterise the covalent and non-covalent interaction between FAT10 and p62. Therefore, *in vitro* interaction studies with either recombinant proteins or proteins which were expressed in HEK293T cells were performed. By using a lysineless p62 mutant, the FAT10ylation was not always completely abolished. p62 deletion proteins were used in order to identify the covalent and non-covalent interaction domains. The deletion of the PB1, the NPI, the TRAF or the N-terminal PEST domain of p62 were found to impede the FAT10ylation. By the mutation of single lysines, it was shown that the lysines of p62 which become FAT10ylated seem to be redundant. For the non-covalent interaction with FAT10, the ZZ, the LIR, the CPI and the C-terminus of the C-terminal PEST domain of HA-p62 seem to be dispensable. By using non-phosphorylation, phospho-mimicking and non-oligomerisation p62 mutants it was shown that neither the phosphorylation status at seine 403, nor the oligomerisation capability of p62 seem to be prerequisites for the interaction with FAT10. An isolated PB1 domain of p62 did not interact with Flag-FAT10, neither covalently or non-covalently. According to the cycloheximide chase, proteasomal degradation rather than autophagosomal degradation is involved in the degradation of the FAT10-p62 conjugate. There was no interaction detectable between FAT10 and other autophagic adaptor proteins such as NBR1, NDP52 and OPTN.

2 Introduction

2.1 Protein homeostasis

Due to the permanently changing quantitative and qualitative protein demand of cells, their proteomes are highly dynamic. Proteins are constantly synthesised; they traffic intracellularly, adopt their functional conformation and are ultimately degraded (Kettern, Dreiseidler et al. 2010).

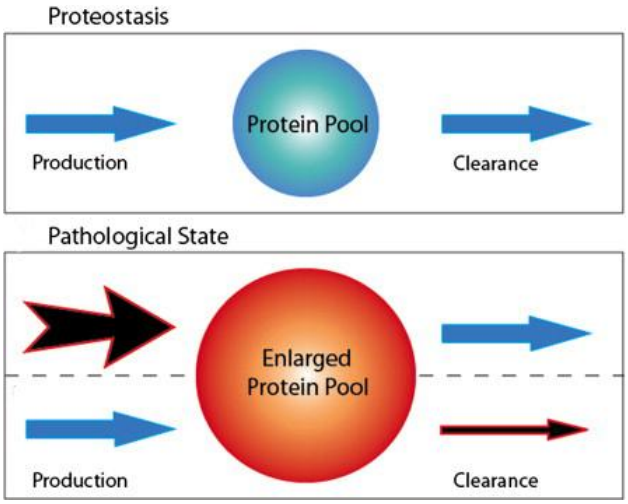

Figure 1: Defects in extracellular protein homeostasis result in protein accumulation. Under normal conditions, proteins are maintained at a concentration appropriate for their function. The mechanisms of production and degradation are the main events of proteostasis. The proteostasis machinery is adjustable in order to maintain the protein concentration during fluctuations in production or clearance. An increased protein production (large black arrow) without an increase in clearance as well as defects in the protein clearance (thin black arrow), may cause an increase in protein concentration (Wyatt, Yerbury et al. 2012).

To maintain the proteome is a major challenge, considering that proteins must fold and function in the crowded environment of a cell that is exposed to physical, metabolic and environmental stresses (Kettern, Dreiseidler et al. 2010). The indelible accumulation of disused and defective proteins would be cytotoxic and could also lead, in the long term, to a lack of amino acids for the synthesis of new proteins. Therefore, cells have evolved a complex network of components that ensure protein homeostasis (proteostasis) (Kettern, Dreiseidler et al. 2010). The main events of the proteostasis are the mechanisms of production and degradation. The synthesis of proteins is precisely regulated either epigenetically (methylation of the DNA, histone

modification) or at the transcriptional level (via enhancer/promoter properties and transcription factors) or at the translational level (modification of translation initiation factors and regulatory protein complexes) (Gebauer and Hentze 2004). For the degradation of proteins mainly two systems are responsible: the ubiquitin-proteasome system (UPS) and the autophagosomal degradation system.

This proteostasis network balances the folding, misfolding, aggregation and degradation of proteins in an adjustable manner. It adapts to physiological stimuli (such as growth factor, cytokines and hormone signalling), and to environmental insults (such as heat or oxidative stress) (Kettern, Dreiseidler et al. 2010).

2.2 The ubiquitin-proteasome system (UPS)

The proteasome is a protein complex which contains several proteases. It selectively degrades proteins that are marked by a small protein called ubiquitin. Proteasomal degradation is required for the rapid removal of proteins and mainly degrades proteins with short half-lives (Lecker, Goldberg et al. 2006). The specific destruction of proteins results in the termination of the processes involving these proteins and to changes in the cell composition. Thus it permits the adaptation to new physiological conditions. The UPS is involved in the regulation of gene transcription, cell signalling pathways, the protein quality control and in the “major histocompatibility complex” (MHC) class I antigen presentation (Lecker, Goldberg et al. 2006).

2.3 The proteasome

The 26S proteasome is composed of more than thirty distinct subunits (Matyskiela and Martin 2013) which are arranged in subcomplexes: the catalytic 20S core particle and one or two regulatory 19S particles (Besche, Peth et al. 2009, Xie 2010). These subunits perform different functions including the recognition, unfolding, translocation and cleavage of protein substrates (Gallastegui and Groll 2010). The proteasome cleaves the substrate proteins into short oligopeptides with an average length distribution of 7–8 amino acids (Groll, Bochtler et al. 2005).

Upon stress, in mammalian, the proteasome genes are inducible by the transcription factor “nuclear factor erythroid-derived 2-related factor 2” (NRF2) (Xie 2010). NRF2 is a very short-lived protein which itself becomes degraded by the proteasome (Xie

2010). Since NRF2 doesn't play a major role in basal expression of proteasome genes, there may be two distinct systems to regulate the expression of the proteasome genes: one for the basal level and one for the feedback up-regulation (Xie 2010).

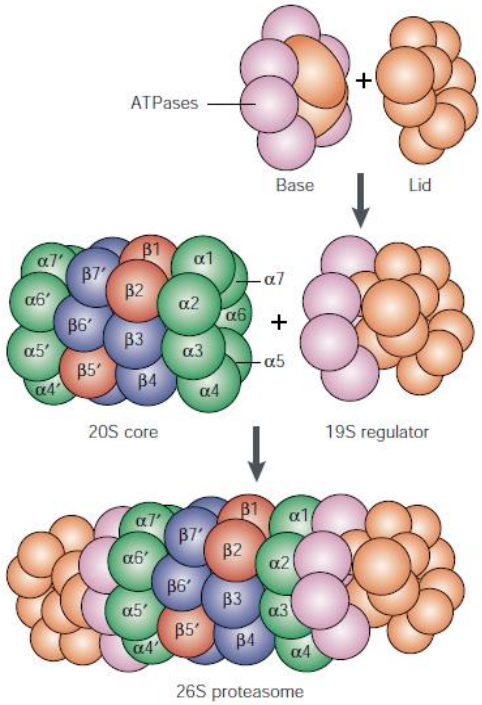

Figure 2: The proteasome composition. The barrel shaped 20S core particle consists of the seven different α- and β-subunits [α1–α7 (green), β1–β7 (blue and red)]. The β1, β2 and β5 subunits (red) harbour the catalytic active sites. The 19S subunit comprises two substructures, the base and the lid. The base is composed of ATPase (purple) and non-ATPase subunits (orange) whereas the lid contains non-ATPase subunits (orange) only (Kloetzel 2004).

2.3.1 The core particle

The proteolytic 20S core particle (20S proteasome) is a barrel shaped structure, composed of twenty-eight subunits (14 α and 14 β subunits) arranged in four stacked heptameric rings (fig.2) which create a sequestered internal chamber (Voges, Zwickl et al. 1999, Matyskiela and Martin 2013). In eukaryotes, there are seven different α- and β-subunits (α1–7 and β1-7) (Voges, Zwickl et al. 1999, Gallastegui and Groll 2010).The rings consist of either all-α1-7 or of all-β1-7-type subunits, stacked in an α1-7–β1-7–β1-7–α1-7 pattern (fig.2) (Voges, Zwickl et al. 1999, Matyskiela and Martin 2013).

The α-type subunits N-terminally project into the centre of the proteolytic chamber and form a gate which restricts the access to the internal cavity and thus protects the cell from unregulated protein degradation. This gate can only be opened in a strictly regulated manner through the binding of regulatory particles (Groll, Bajorek et al. 2000, Gallastegui and Groll 2010, Jung and Grune 2012). The N-termini of three β-type subunits (β1, β2, β5) (fig.2) contain the proteolytic residues (Gallastegui and Groll 2010). Each endopeptidase has a different specificity: the β1, β2, and β5 subunits generate caspase-like, trypsin-like, and chymotrypsin-like activities, respectively (Kisselev, Garcia-Calvo et al. 2003, Murata, Yashiroda et al. 2009). β1 selectively cleaves after acidic residues, β2 after basic residues, and β5 after hydrophobic residues (Gallastegui and Groll 2010, Jung and Grune 2012). This enables the core particle to cleave most, if not all, peptide bonds (Smalle and Vierstra 2004). These differentiated active sites likely facilitate the complete destruction of diverse protein substrates into short peptides. (Gallastegui and Groll 2010)

2.3.2 The regulatory particle

To form the 26S proteasome holoenzyme, the 20S core particle in eukaryotes is capped at one or both sites by a multi-subunit regulatory complex, called the 19S proteasome, regulatory particle, PA700 or proteasome activator (Glickman and Ciechanover 2002, Murata, Yashiroda et al. 2009). Regulatory particles are attached to the outer α-rings of the 20S core particle (fig.2) (Glickman and Ciechanover 2002). They are involved in the recognition, unfolding and translocation of ubiquitylated substrates and also regulate the entry of selected substrates into the core particle (Gallastegui and Groll 2010, Matyskiela and Martin 2013). Each regulatory particle itself can be further dissected into two multi subunit substructures, a ring shaped base and a lid (fig.2) (Glickman and Ciechanover 2002).

The base

The base binds to the 20S proteasome (fig.2) and consists out of the six homologue AAA+ ATPase subunits, “regulatory particle triple-A protein” (RPT) RPT1–RPT6, and four non-ATPase subunits, “regulatory particle non-ATPase” (RPN) RPN1, RPN2, RPN10 and RPN13 (Jung and Grune 2012, Lander, Estrin et al. 2012). The ATPases form hetero-hexameric rings (RPT1, 2, 6, 3, 4 and 5) and the energy of the ATP

hydrolysis is used to unfold substrate proteins and to translocate the polypeptides into the proteolytic chamber of the core particle (Lander, Estrin et al. 2012). The RPT2, RPT3 and RPT5 subunits play a role in the gate opening of the α-subunits of the 20S proteasome (Jung and Grune 2012). The integral ubiquitin receptors RPN10 and RPN13 recognize polyubiquitylated substrates directly (Finley 2009).

The lid

The lid (fig.2) is composed of nine non-ATPase subunits: RPN3, RPN5–RPN9, RPN11, RPN12 and RPN15 (Kaneko, Hamazaki et al. 2009, Jung and Grune 2012, Tanaka 2013). So far, the only known biochemical function of the lid is to capture and deubiquitylate substrate proteins in order to facilitate their degradation (Tanaka 2013). RPN11 deubiquitylates the substrate proteins prior to their degradation (Kaneko, Hamazaki et al. 2009, Jung and Grune 2012, Lasker, Forster et al. 2012, Tanaka 2013).

2.4 Proteasome subtypes

Despite constitutive proteasomes, there are also tissue- and developmental specific, as well as cytokine inducible proteasome subtypes that vary with regard to their subunit composition, activity and cellular distribution. These subtypes exhibit different enzymatic characteristics (Dahlmann, Ruppert et al. 2000). This heterogeneity in proteasome subtypes does not only exist between different tissues, but also within a single cell. Subpopulations of proteasomes can also be located within different cellular compartments (Dahlmann, Ruppert et al. 2000).

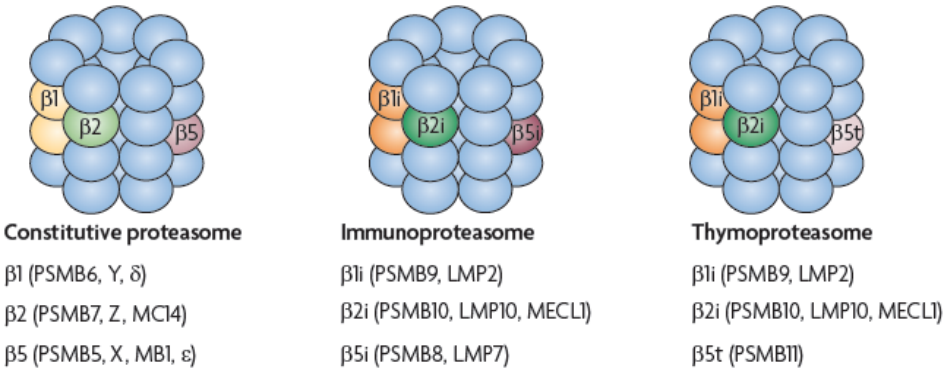

Figure.3: The subunit composition of the active sites of the constitutive proteasome, immunoproteasome and thymoproteasome. The alternative nomenclatures of the proteolytic subunits are mentioned in the brackets. Compared with the constitutive proteasome, the immunoproteasome has a strongly decreased caspase-like activity and an increased chymotrypsin-like activity, whereas the thymoproteasome has a decreased chymotrypsin-like activity (Groettrup, Kirk et al. 2010). The catalytic β5t subunit was found to be expressed exclusively in "cortical thymic epithelial cells" (cTECs) (Murata, Sasaki et al. 2007, Tomaru, Ishizu et al. 2009, Tanaka 2013). It was suggest that β5t plays a key role in generating the MHC class I–restricted $CD8^+$ T cell repertoire during thymic positive selection (Murata, Sasaki et al. 2007).

2.4.1 The immunoproteasome

The UPS represents a major pathway for supplying peptides for MHC class I mediated antigen presentation. This immune function of the UPS can be improved by an "Interferon-γ" (IFNγ), "Tumor necrosis factor-α" (TNFα) or lipopolysaccharide (LPS) inducible isoenzyme of the 26S proteasome, the so called immunoproteasome (Groettrup, Kirk et al. 2010, Jung and Grune 2012). In the immunoproteasome, the proteolytic subunits of the constitutive proteasome β1, β2 and β5 are replaced by their inducible equivalents β1i, β2i and β5i, also called "low-molecular-weight protein 2" (LMP2), "multicatalytic endopeptidase-like-complex-1" (MECL1), and LMP7, respectively (fig.3). Therefore the whole proteasome has to be assembled *de novo* (Basler, Kirk et al. 2013, Ebstein, Voigt et al. 2013). The immunoproteasome has an increased chymotrypsin-like activity compared to the standard proteasome. This chymotrypsin-like activity is thought to be important for the production of antigenic peptides with high affinities for MHC class I clefts, which serve as peptide-binding pockets (Groettrup, Kirk et al. 2010, Tanaka 2013). In fact, the immunoproteasome knockout mice display defects in the antigen processing and consequently have compromised immune responses (Sijts and Kloetzel 2011, Kincaid, Che et al. 2012, Tanaka 2013).

In the lymphoid tissues such as thymus, spleen and lymph nodes, immunoproteasome subunits are constitutively expressed (Sijts and Kloetzel 2011). Whereas in “dendritic cells” (DCs) the immunoproteasome is express at high levels constitutively (Macagno, Gilliet et al. 1999, Morel, Levy et al. 2000), the immunoproteasome levels in macrophages, T cells and B cells depend on their differentiation states. In unstimmulated non-lymphoid peripheral tissues however, the immunoproteasome expression is rather low (Sijts and Kloetzel 2011). Immunoproteasomes have a much shorter half-life (about 27 hours) compared to the constitutive 20S proteasome (about 8–12 days). Thus the immunoproteasomes can be expressed very quickly and removed very fast (Jung and Grune 2012). Immunoproteasomes do not always contain the inducible catalytic subunits exclusively. Also mixed forms are found which contain both, the inducible βi-subunits and the constitutive ones (Jung and Grune 2012, Basler, Kirk et al. 2013).

The role of the immunoproteasome in antigen presentation is neither exclusive nor indisputable. LMP2 for example, has been shown by the group of Michael J. Ross, to play a key role in the degradation of phosphorylated IκBα and the subsequent NF-κB activation (Gong, Canaan et al. 2010). In 2010, Seifert et al. published that immunoproteasomes substantially contribute to preserve the protein homeostasis upon interferon induced oxidative stress rather than having a specific role in the production of class I antigens (Seifert, Bialy et al. 2010). They argue that the immunoproteasome, has an increased clearance efficiency of damaged protein aggregates, compared to the constitutive proteasome and therefore helps to maintain cell viability under IFN-induced oxidative stress conditions (Seifert, Bialy et al. 2010). In contrast, Nathan et al. reported in 2013 that 26S immunoproteasomes do have similar binding and degradation capacities for polyubiquitylated proteins, as constitutive proteasomes (Nathan, Spinnenhirn et al. 2013).

2.5 Ubiquitin and ubiquitin-like proteins

The structure and thus the function of proteins are regulated via posttranslational modifications. After being synthesised by ribosome’s, the polypeptide chains undergo various posttranslational modifications such as folding or cutting to become the mature protein product. Also the posttranslational attachment of inorganic groups

(such as phosphorylation, hydroxylation nitrosylation or sulfation) or organic groups (such as glycosylation, formylation, acetylation or methylation) to the residues of certain amino acids within the polypeptide chain alter the properties of the proteins. Even whole proteins such as ubiquitin are covalently attached to the polypeptide chains posttranslational.

2.6 Ubiquitin

Ubiquitin is a posttranslational modifier which contains 76 amino acids and is highly conserved in eukaryotes. Its characteristic three-dimensional structure is formed by a β-grasp fold, called the ubiquitin fold (Grabbe and Dikic 2009, Hochstrasser 2009). Via its C-terminal diglycine motif ubiquitin reversibly binds to substrate proteins. The covalent attachment of an ubiquitin monomer or a polyubiquitin chain to a substrate protein is called ubiquitylation (Kravtsova-Ivantsiv and Ciechanover 2012). Ubiquitin is one of the most frequent and prominent examples for a posttranslational modification by a protein. In 2004, Aaron Ciechanover, Avram Hershko, and Irwine Rose received the Noble Prize in chemistry for the discovery of the most prominent function of ubiquitylation: the degradation of the substrate proteins by the 26S proteasome (Ciechanover, Elias et al. 1980, Hershko, Ciechanover et al. 1980, Spasser and Brik 2012). Via the ubiquitylation of certain substrate proteins, ubiquitin controls a large number of cellular processes, including protein degradation, DNA repair, chromatin remodelling, cell cycle regulation, endocytosis, and kinase signalling pathways (Komander, Clague et al. 2009).

Intracellularly, ubiquitin exists either as a free or a substrate bound form (Kimura and Tanaka 2010). The balance between these two pools is generally maintained by the opposing activities of ubiquitin ligating factors that catalyse the synthesis of chains and deubiquitylating enzymes (DUBs) which disassemble them again (Shabek and Ciechanover 2010). When cells are exposed to different insults, more aberrant proteins are produced. Thus more ubiquitin conjugates are formed and the ratio between the conjugated and free pool increases transiently (Shabek and Ciechanover 2010). To provide the cell with sufficient ubiquitin amounts and to cover the greater consumption during stress, also the expression of ubiquitin is increased (Shabek and Ciechanover 2010). Besides the transcriptional activation, the levels of

free ubiquitin can also be increased by accelerating the disassembly of ubiquitin chains (Dantuma and Lindsten 2010). Upon removal of the insulting agent or adaptation to the stress, the transcription of ubiquitin returns to basal level and the conjugated ubiquitin is degraded along with the substrate(s) (Shabek and Ciechanover 2010).

2.6.1 Ubiquitylation

Ubiquitin is synthesised as an inactive precursor protein. In order to make the C-terminal diglycine motif available for conjugation, it has to be processed by a specific protease (called ubiquitin carboxy-terminal hydrolase) (Muller, Hoege et al. 2001). Ubiquitylation requires the coordinated action of three types of enzymes known as ubiquitin activating enzymes (E1), ubiquitin conjugating enzymes (E2), and ubiquitin ligases (E3). These enzymes link the C-terminal α-carboxyl group of the ubiquitin backbone to the ε-amino group of a lysine (K) in the substrate protein through an isopeptide bond (Spasser and Brik 2012). In a few rare cases however, ubiquitin has been found to be conjugated to the α-amino groups of the N-terminal residues or to residues other than lysines [cysteines (C), serines (S) and threonines (T)] of its substrate proteins (Kravtsova-Ivantsiv and Ciechanover 2012).

The E1 enzymes efficiently select the correct UBLs for their respective downstream pathways (Schulman 2011). While the E3 enzymes are the main determinants of the substrate specificity, the E2 enzymes have a major role in determining the linkage type (Ye and Rape 2009).

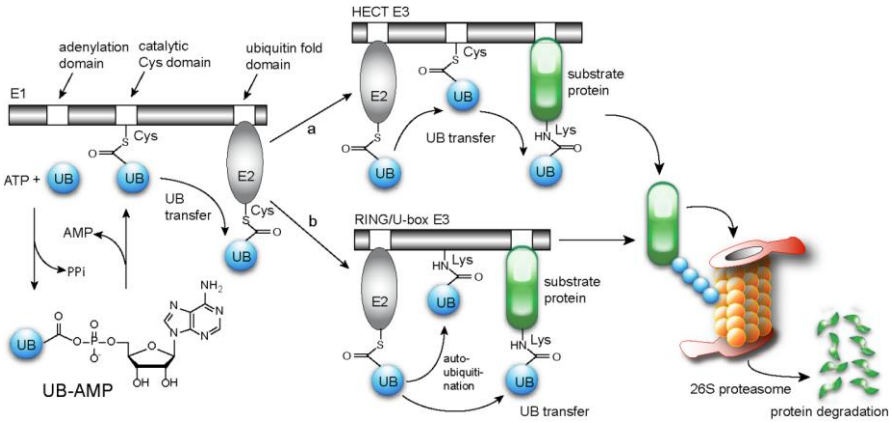

Figure 4: The ubiquitin conjugation machinery. Ubiquitin is transferred through an E1-E2-E3 enzymatic cascade to cellular proteins to regulate their degradation and biological functions in the cell. The figure was taken from the homepage of Dr. Jun Yin from the Department of Chemistry at the Georgia State University. URL: http://chemistry.gsu.edu/Yin.php (04.02.2014).

As depicted in figure 4, the E1 enzyme first binds ATP and subsequently ubiquitin and then it catalyses the ubiquitin adenylate formation with release of pyrophosphate. The adenylated ubiquitin is transferred onto the active site cysteine residue of the E1 enzyme to form an E1-ubiquitin thioester with AMP as by-product (Kerscher, Felberbaum et al. 2006, Herrmann, Lerman et al. 2007). The E1 then binds a second ATP and ubiquitin to again form an ubiquitin adenylate. The resulting fully loaded E1-ubiquitin complex contains two ubiquitin molecules, one as a thioester at the catalytic cysteine and one as adenylate and is competent for transferring ubiquitin to the active site cysteine residue of its cognate E2 enzyme (Kerscher, Felberbaum et al. 2006, Herrmann, Lerman et al. 2007). The ubiquitin-charged E2 enzyme and the specific substrate protein are then both bound by an E3 enzyme which catalyses the transfer of the activated ubiquitin onto the substrate protein (Kerscher, Felberbaum et al. 2006, Herrmann, Lerman et al. 2007).

After releasing ubiquitin, the discharged E2 dissociates from the E3, allowing a second charged E2 to interact with the E3, facilitating a second round of ubiquitin transfer, either by attacking a lysine residue in ubiquitin itself or of a different lysine in the substrate. Multiple E2 cycles of E1-mediated ubiquitin loading and subsequent unloading – through a variety of mechanisms lead to polyubiquitylation of the substrate (Deshaies and Joazeiro 2009, Schulman and Harper 2009). However there is also evidence for ubiquitin chains being built on E2 or E3 enzymes and transferred to their substrates “en bloc” (Metzger, Hristova et al. 2012). In some cases,

multiubiquitylation requires the additional activity of ubiquitin-chain elongation factors (E4 enzymes) (Hoppe 2005).

The enzymatic conjugation machinery for ubiquitin is composed of two E1 enzymes UBE1 (UBA1) and UBA6 (UBE1L2/ E1-L2/MOP4) (Chiu, Sun et al. 2007, Pelzer, Kassner et al. 2007), 30–40 E2 enzymes, and several hundred E3 ligases (Schulman 2011, Kulathu and Komander 2012).

Concerning UBE1 and UBA6 it was the first time that two different E1 enzymes were shown to be able to activate the same member of the ubiquitin family and the two enzymes were shown not to be redundant (Chiu, Sun et al. 2007, Pelzer, Kassner et al. 2007, Groettrup, Pelzer et al. 2008).

The known E2 enzymes for ubiquitin are grouped into four classes: E2s which are charged by UBA1 only, E2s which are charged equally by UBA1 and UBA6 as well as E2 enzymes which can be charged by neither UBA1, nor by UBA6. The E2 enzyme “UBA6-specific E2” (USE1) is loaded by UBA6 only (Jin, Li et al. 2007). Some E2s possess a core ubiquitin-conjugating (UBC) domain, which contains the catalytic cysteine residue which accepts ubiquitin from the E1. Others also have a UBC domain but lack an active-site cysteine residue (Ye and Rape 2009).

The E3 enzymes range from single polypeptide chains to large multi subunit complexes in which substrate recognition and ubiquitin conjugation are relegated to distinct subunits (Pickart 2001). There is increasing evidence for autoubiquitylation as part of the normal physiological function of some E3s, which results in their rapid degradation (Fang and Weissman 2004). There are two major superfamilies of E3s: the “Really Interesting New Gene” (RING)-domain E3s and the “homologous to the E6-AP C terminus” (HECT)-domain E3s. The HECT E3s catalyse the formation of the isopeptide bonds by utilising a catalytic cysteine residue, which forms a transient thioester intermediate between ubiquitin and the E3 (Spasser and Brik 2012). The RING-finger, and the RING-related U-box family lack a classical catalytic active site (Spasser and Brik 2012). They appear to function as adaptors which position the substrates in close proximity to the reactive E2-ubiquitin thioester bonds (Hochstrasser 2006). By forming complexes with many alternative substrate-recognition subunits, certain RING domain proteins add great diversity to the E3 family. The cullin family proteins scaffold the assembly of multi-subunit “cullin-RING

E3 ubiquitin ligase" (CRL) complexes, the largest family of E3 ligases. Cullin proteins tether substrate-recognition subunits and the RING finger components. Thus, the cullin-organized CRL positions a substrate in close proximity to the RING-bound E2 enzyme which catalyses the transfer of ubiquitin to the substrate (Deshaies and Joazeiro 2009, Sarikas, Hartmann et al. 2011).

2.6.2 The ubiquitin chains

Usually, the ubiquitylation reaction does not stop after the first ubiquitin moiety is attached to the substrate protein but continues so that additional ubiquitin moieties are attached to a lysine of the preceding ubiquitin moiety. Consequently, long ubiquitin chains are formed on the substrates (Schrader, Harstad et al. 2009). Ubiquitin contains seven lysines, namely K6, K11, K27, K29, K33, K48 and K63, all of which have been shown to form polyubiquitin chains on substrate proteins *in vivo* (fig.5) (Trempe 2011, Kulathu and Komander 2012).

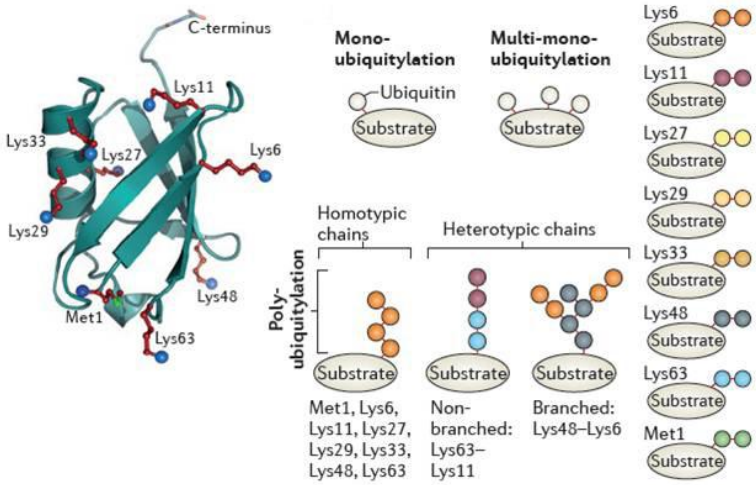

Figure 5: The different forms of ubiquitylation. In the 3D structure of ubiquitin on the left panel, the seven lysine residues and the N terminal methionine of ubiquitin are shown as red sticks and the amino groups that are modified with ubiquitin during the chain formation are shown as blue spheres. On the right panel, there is an overview of the various forms of ubiquitylation. Substrates can be modified by mono-, multi-mono- or polyubiquitin. Ubiquitin chains are coloured according to linkage-type. Polyubiquitin can consist of a single type of linkage (homotypic chains) or more than one linkage type (heterotypic chains). Heterotypic chains are either branched (also termed 'forked') or non-branched (Kulathu and Komander 2012).

Protein substrates tagged by polyubiquitin chains of different linkages undergo different fates (Trempe 2011). While monoubiquitylation is typically associated with

cellular trafficking and the regulation of gene expression, the functionality of polyubiquitylation is depending on the respective ubiquitin lysine residue or N-terminus which serves as the linkage site of polymerisation (Nakayasu, Ansong et al. 2013).

Whereas K48-linked ubiquitin chains are well established as mediators of proteasomal degradation, K63-linked ubiquitin chains act in non-proteolytic events such as cell signalling, kinase activation, cytokine signalling, DNA damage response, endocytosis and autophagosomal degradation (Trempe 2011, Spasser and Brik 2012). So far, the roles of unconventional polyubiquitin chains linked through K6, K11, K27, K29, or K33 are not well understood. However, in 2009 Xu et al. found all non-K63 polyubiquitin linkage types to be accumulated upon proteasome inhibition. Therefore all of them may be able to mediate proteasomal protein degradation (Xu, Duong et al. 2009).

2.6.3 “Deubiquitylating enzymes” (DUBs)

The ubiquitylation of substrate proteins is a reversible process. The ubiquitin specific proteases which counteract the ubiquitylation are termed “deubiquitylating enzymes” (DUBs, also referred to as deubiquitinases) (Kimura and Tanaka 2010). Many DUBs exhibit a specificity for the topologies of their target ubiquitin chains and some DUBs are substrate-specific, such that a certain sequence of the ubiquitylated substrate is recognised (Wilkinson 2009, Clague, Coulson et al. 2012, Spasser and Brik 2012). The cleavage of the ubiquitin chains could either occur from the end of the chain, or within the ubiquitin chain (Wilkinson 2009, Spasser and Brik 2012). By trimming or removing the ubiquitin chains completely, DUBs influence or even reverse those processes which involve ubiquitin signalling such as: protein degradation, DNA repair, chromatin remodelling, cell cycle regulation, endocytosis, and kinase signalling pathways (Komander, Clague et al. 2009, Kimura and Tanaka 2010). Further, DUBs were shown to interact with ubiquitin E3 ligases, which themselves have a propensity to autoubiquitylate. Via controlling the stability of those E3 enzymes, DUBs indirectly control the stability of the corresponding E3 substrates (Clague, Coulson et al. 2012). Since DUBs cleave ubiquitin from its substrate proteins a prior they do enter the proteasomal lumen, ubiquitin is not degraded along

with its substrates. Thus, DUBs also contribute to the intracellular ubiquitin homeostasis (Komander, Clague et al. 2009, Kimura and Tanaka 2010).

2.6.4 What becomes degraded: the N-end rule

The half-lives of intracellular proteins range from a few seconds to many days. The features of proteins which confer their metabolic instability are called degradation signals or degrons (Varshavsky 1997). The N-end rule relates the *in vivo* half-life of a protein to the identity of its N-terminal amino acid (Varshavsky 2012).Therefore, the destabilising N-terminal amino acid of a protein is called the N-degron. N-degrons are recognised by components of E3 enzymes termed N-recognins (Sriram, Banerjee et al. 2009). In otherwise stable proteins, N-degrons can be generated through posttranslational modifications of pro-N-degrons. Through proteolytic cleavage for example, anciently embedded destabilising amino acids can be exposed at the N-terminus (Tasaki, Sriram et al. 2012).

2.7 Ubiquitin-like proteins (UBLs)

Ubiquitin-like proteins can be subdivided into two separate groups (fig.6). Since they function in a manner analogous to ubiquitin, the members of the first group are termed “ubiquitin-like modifiers” (UBLs) (Jentsch and Pyrowolakis 2000, Muller, Hoege et al. 2001). The proteins of the second class of ubiquitin -ike proteins are referred to as “ubiquitin-domain proteins” (UDPs). UDPs are characterised by domains which are sequence wise related to ubiquitin (fig.6) but are otherwise unrelated to each other. In contrast to UBLs, UDPs are not conjugated to other proteins (Jentsch and Pyrowolakis 2000, Muller, Hoege et al. 2001).

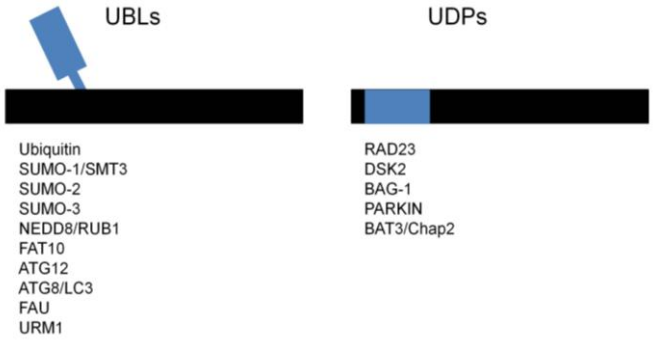

Figure 6: Two classes of ubiquitin-like proteins. Ubiquitin-like modifiers (UBLs) function as modifiers (blue) in a manner analogous to that of ubiquitin; ubiquitin-domain proteins (UDPs) bear ubiquitin-like domains (UDs; blue) but do not form conjugates with other proteins. A hallmark of UBLs is a C-terminal diglycine motif. Modified from (Jentsch and Pyrowolakis 2000).

UBLs do not necessarily share high sequence similarity, but they essentially do all possess the same three-dimensional structure, the ubiquitin- or β-grasp fold. Moreover, as with ubiquitin, the C-terminal residue of mature UBLs is a glycine and the carboxyl group of this glycine is the site of attachment to substrates (Kerscher, Felberbaum et al. 2006). Like ubiquitin, UBLs can be covalently attached to substrate proteins (or in one case, a phospholipid) via an isopeptide bond between the UBL's C-terminal α-carboxyl group and the ε-amino group of a lysine in the substrate protein (fig.6). Alternatively, UBLs can be ligated to the N-terminus, or to the serine, threonine, or cysteine residues of their substrate proteins (Hochstrasser 2009). All the UBLs seem to be attached to substrates via ubiquitin related enzymatic pathways. Most of the UBLs are synthesised as inactive precursors which need to be processed at their C-termini by specific proteases to expose the glycine carboxylate (Hochstrasser 2009, Schulman 2011).

2.7.1 "Neural precursor cell expressed developmentally down-regulated 8" (NEDD8)

The conjugation of "neural precursor cell expressed developmentally down-regulated 8" (NEDD8) to proteins can also lead to their proteasomal degradation. This is mediated by the adaptor proteins "NEDD8 ultimate buster 1" (NUB1) and "NUB1 Long" (NUB1L) (Herrmann, Lerman et al. 2007). NUB1 acts as a negative regulator of the NEDD8 conjugation system, since its interaction with NEDD8 leads to

a post-transcriptional down-regulation of the NEDD8 expression. Kamitani et al. suggested that NUB1 might have an adaptor function between RPN10 and NEDD8 (Kamitani, Kito et al. 2001). Apart from ubiquitylation, the neddylation pathway involves one E1, one E2, a few E3s and is only directed to a small number of targets (Huang, Miller et al. 2004).

2.7.1.1 "NEDD8 ultimate buster 1L" (NUB1L)

NUB1 is inducible with the antiviral cytokines IFNβ and IFNγ (Kito, Yeh et al. 2001, Tanaka, Kawashima et al. 2003). The original human NUB1 contains two UBA domains and was supposed to act as a negative regulator of the NEDD8 conjugation system. By interacting with NEDD8 and the proteasome subunit RPN10, NUB1 links NEDD8 and its conjugates to the proteasome for degradation (Kamitani, Kito et al. 2001, Tanaka, Kawashima et al. 2003). A splicing variant called NUB1L possesses a third UBA domain located between the two original UBA domains. NUB1 has a NEDD8-binding site at the C-terminus, whereas NUB1L has an additional site at the newly generated UBA domain. Therefore, NUB1L binds to NEDD8 much stronger than NUB1 (Tanaka, Kawashima et al. 2003). Like NUB1, also NUB1L possess the ability to down-regulate the expression of NEDD8 monomers and its conjugates (Tanaka, Kawashima et al. 2003). According to Hipp et al. ubiquitin and SUMO-1 do not bind to NUB1L at all (Hipp, Raasi et al. 2004).

2.7.2 "Small ubiquitin-related modifier" (SUMO)

In vertebrates three members of the "small ubiquitin-related modifier" (SUMO) family have been described (SUMO-1-3) (Muller, Hoege et al. 2001). All three SUMO isoforms differ in their localisation within the cells. In human, they are processed by SUMO-specific proteases to expose the C-terminal glycine residues (Herrmann, Lerman et al. 2007). SUMO is activated by a heterodimeric enzyme. SUMO has an unique E2 enzyme which is specific for SUMO and can directly recognise the substrates and transfer the activated SUMO to a lysine in the substrate protein without the need of an E3 enzyme (Herrmann, Lerman et al. 2007). In spite of the abilities of the E2 enzyme to directly detect substrates proteins and transfer SUMO, there are SUMO-related E3-like enzymes which mediate the modification of specific substrates (Herrmann, Lerman et al. 2007). The SUMOylation of substrate proteins

can also be influenced by phosphorylation- and acetylation (Herrmann, Lerman et al. 2007). SUMOylation seems to enhance the stability or modulate the subcellular compartmentalisation of the target proteins (Muller, Hoege et al. 2001).

2.7.3 The "autophagy-related" (ATG) proteins ATG8 and ATG12

During autophagic degradation, the cytoplasmic autophagy substrates are sequestered in *de novo* formed double-membrane vesicles and delivered to the lysosome for degradation via the lysosomal hydrolases (Mizushima 2007). Many of the ATG proteins are involved in two ubiquitin-like conjugation systems: ATG12-ATG5 and ATG8-phosphatidylethanolamine (PE). These two conjugation systems are well conserved among eukaryotes and can impact on each other (Yang, Liang et al. 2005).

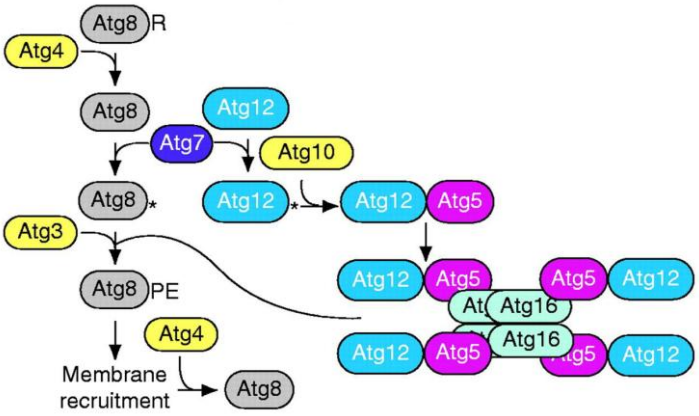

Figure 7: Two ubiquitin-like proteins participate in the formation of autophagic vesicles. ATG8 and ATG12 are ubiquitin-like proteins which both are activated by the E1-like enzyme ATG7. ATG8 and ATG12 are then transferred to the E2-like enzymes ATG3 and ATG10 and are conjugated to phosphatidylethanolamine (PE) and ATG5, respectively. ATG12 and ATG5 bind ATG16 non-covalently. A similar set of reactions occurs in mammalian cells (Klionsky 2005).

Since ATG12 is not expressed as a precursor molecule, its C-terminus does not have to be processed. ATG12 is conjugated to its unique target protein ATG5 by the action of the E1- and the E2-like enzyme ATG7 and ATG10, respectively (fig.7) (Yang, Liang et al. 2005, Herrmann, Lerman et al. 2007). There is no typical E3 enzyme involved in ATG12–ATG5 conjugation (Geng and Klionsky 2008). This conjugation process is constitutive since it is independent of starvation or other autophagy-inducing conditions. The conjugates are formed immediately after their synthesis and

so far no protease has been found which reverse this process (Yang, Liang et al. 2005). The ATG12-ATG5 conjugates bind to ATG16 non-covalently and positively affect the second autophagy relevant ubiquitin-like ATG system (fig.7) (Klionsky 2005, Herrmann, Lerman et al. 2007).

The second ubiquitin-like modifier essential for autophagy is called ATG8 (Herrmann, Lerman et al. 2007). ATG8 does not form a conjugate with other proteins, but interacts with the membrane phospholipid phosphatidylethanolamine (PE). This lipidation reaction is necessary for the membrane dynamics of autophagy (Yang, Liang et al. 2005, Herrmann, Lerman et al. 2007). As depicted in figure 7, ATG8 is expressed as a precursor molecule and the ATG4 protease has to cleave the C-terminus (Herrmann, Lerman et al. 2007). Afterwards, ATG8 can be activated by the E1 enzyme ATG7 and subsequently be transferred to the conjugating E2 enzyme ATG3 (Yang, Liang et al. 2005). Interestingly, ATG7 has the ability to activate the two different ubiquitin-like proteins, ATG12 and ATG8, and to further assign them to their proper E2 enzymes, ATG10 and ATG3, respectively (Yang, Liang et al. 2005).

It has been assumed that the E3 activity is not required for the ATG8 lipidation. However, it was recently reported that the ATG12–ATG5 conjugate may have an E3-like activity for the ATG8 lipidation (fig.7) (Geng and Klionsky 2008). Besides its function in the initial processing of ATG8, ATG4 has also been identified as its deconjugating enzyme (Herrmann, Lerman et al. 2007).

The microtubule-associated protein 1 “light chain 3” (LC3) is the mammalian orthologue of ATG8 (Yang, Liang et al. 2005). Like ATG8 in yeast, the C-terminus of newly synthesised LC3 has to be processed to become the active, unconjugated cytosolic form LC3-I. The mammalian orthologue of the yeast protease ATG4 is termed autophagin (Yang, Liang et al. 2005). Via the ATG7 and ATG3 conjugation machinery LC3-I finally is converted to LC3-II which means that it is covalently attached to PE (Yang, Liang et al. 2005). Additionally to LC3, more orthologues of yeast ATG8 have been identified in mammalian: the “γ-aminobutyric acid type A receptor-associated protein” (GABARAP), the “Golgi-associated ATPase enhancer” of 16 kDa (GATE-16) and ATG8L. All of these proteins can also be converted to their membrane bound forms (form II) by the action of ATG4, ATG3 and ATG7. But the

particular functions of these orthologues and their modified forms are not yet investigated (Geng and Klionsky 2008)

2.7.4 "Human leukocyte antigen (HLA)-F adjacent transcript 10" (FAT10)

The abbreviation FAT10 stands for "Human leukocyte antigen (HLA)-F adjacent transcript 10". By performing sequence analysis of the MHC class I region, the Weissman group discovered in 1996 seven new genes in the most telomeric end, around the HLA-F locus. Among this genes, one was found to be homologous to a diubiquitin and was expressed in a "Epstein Barr Virus" (EBV) transformed B-cell line only (Fan, Cai et al. 1996). Therefore, the18 kDa protein FAT10 initially was termed either diubiquitin or ubiquitin D. The two tandem arranged ubiquitin-like domains are 29 % and 36 % identical to ubiquitin, respectively, and are separated by five amino acids forming a short linker. The N-terminal domain has an initial extension of six amino acids (Bates, Ravel et al. 1997, Raasi, Schmidtke et al. 1999, Schmidtke, Aichem et al. 2013). Like all UBL modifiers, FAT10 has a C-terminal diglycine motif which is required for the conjugation to the substrate proteins (Raasi, Schmidtke et al. 2001). Since FAT10 is not expressed as a precursor, its C-terminus is not processed in advance of its activation (Schmidtke, Aichem et al. 2013).

Like ubiquitylation, FAT10ylation leads to the proteasomal degradation of otherwise long living substrate proteins. Also monomeric FAT10 molecules are efficiently degraded by the proteasome. Compared to FAT10, ubiquitin is much more stable. FAT10 is a short-lived and highly regulated protein with a half-life of 4 hours. (Raasi, Schmidtke et al. 2001, Hipp, Raasi et al. 2004, Hipp, Kalveram et al. 2005, Schliehe, Bitzer et al. 2012). Apart from ubiquitin, FAT10 is not recycled but degraded along with its substrates. So far there is no evidence for a FAT10-specific deconjugation enzyme (Hipp, Kalveram et al. 2005, Schmidtke, Aichem et al. 2013).

In humans, FAT10 is constitutively expressed in tissues associated with the immunological system, such as spleen and thymus (Lee, Ren et al. 2003). Further it was detected in tissue of the gastrointestinal, liver, kidney, lung, tonsils and at low levels in the cardiovascular and reproductive tissues, but is strikingly absent in the brain (Bates, Ravel et al. 1997, Lee, Ren et al. 2003). However in rats, besides in the

heart, kidney, liver, spleen, and lung, FAT10 mRNA and protein were also found to be expressed in the brain (Peng, Shao et al. 2013). In different mouse tissues, FAT10 was found to be most strongly expressed in the thymus, spleen, lymph nodes and intestine (Lukasiak, Schiller et al. 2008). Small amounts of FAT10 mRNA were also found in cell lines derived from colon, kidney, neuroblasts, liver and keratinocytes (Raasi, Schmidtke et al. 1999). In freshly isolated primary cells the FAT10 expression was restricted to mature DC and B cells (Bates, Ravel et al. 1997). Also certain cell lines, derived from DCs, B cells, kidney carcinoma and myeloid precursor cells, constitutively express FAT10. No expression however was detectable in a T-cell line (Raasi, Schmidtke et al. 1999).

There are contradictory data about the intracellular distribution of FAT10. In some publication it is reported that FAT10 is predominantly localised in the cytoplasm and only weakly in the nucleus (Liu, Pan et al. 1999, Raasi, Schmidtke et al. 1999). However other studies found FAT10 localised to the nucleus (Lee, Ren et al. 2003, Ji, Jin et al. 2009, Yuan, Tu et al. 2012) and Kalveram et al. found FAT10 in both, the cytosol and the nucleolus (Kalveram, Schmidtke et al. 2008). Since a C-terminal diglycine motif lacking FAT10 mutant [FAT10(ΔGG)] showed the same localisation pattern as wild-type FAT10, the intracellular localisation of FAT10 doesn't seem to depend on its conjugation capability (Raasi, Schmidtke et al. 2001).

The FAT10 expression is generally and synergistically inducible with the cytokines TNFα and IFNγ but not with the antiviral cytokines IFNα/β (Raasi, Schmidtke et al. 1999). Upon cytokine stimulation, the FAT10 expression is induced or up-regulated in most of the tested primary cultures of human cells as well as in cell lines, except for Jurkat T cells. The FAT10 mRNA expression is already induced within 2 hours after cytokine stimulation (Raasi, Schmidtke et al. 1999). The FAT10 protein becomes prominent after 12 hours IFNγ treatment and decreased progressively after 24 or 48 hours of treatment (Liu, Pan et al. 1999). Under sustained IFNγ/TNFα treatment for 72 hours, the mRNA and protein level of FAT10 in HEK293T cells was shown to further increase within 72 hours (Aichem, Kalveram et al. 2012).

The E1 enzyme UBA6 can activate ubiquitin and also seems to be necessary and sufficient to activate FAT10 (Chiu, Sun et al. 2007, Pelzer, Kassner et al. 2007). Under non-stimulated conditions the UBA6 pathway may be biased toward ubiquitin

conjugation. Upon TNFα/IFNγ-stimulation, the ratio of free ubiquitin to free FAT10 decreases remarkably and FAT10 was much more efficiently activated (Gavin, Chen et al. 2012). The E2 enzyme USE1 interacts exclusively with UBA6 and has been shown to accept both, activated ubiquitin and FAT10 from UBA6. Furthermore, USE1 is the major E2 enzyme in the FAT10 conjugation cascade because siRNA-mediated knockdown almost abolished FAT10 conjugate formation (Aichem, Pelzer et al. 2010). USE1 is not only a E2 enzyme but also a substrate of FAT10 conjugation, as it was efficiently auto-FAT10ylated in *cis* but not in *trans* (Aichem, Pelzer et al. 2010). So far, there is no E3-ligase published for FAT10. Interestingly, the ubiquitin E1 enzyme UBA1, despite not being able to activate FAT10, is a substrate for FAT10ylation. The FAT10ylation of UBA1 leads to its proteasomal degradation (Rani, Aichem et al. 2012).

In both UBL domains of FAT10, lysine residues corresponding to the positions 29, 48, and 63 of ubiquitin are conserved which could potentially serve as conjugation sites for the formation of FAT10 chains or the modification by other ubiquitin-like modifiers (Raasi, Schmidtke et al. 2001). Although, both ubiquitin-like domains of FAT10 were shown to be ubiquitylated (Hipp, Kalveram et al. 2005, Buchsbaum, Bercovich et al. 2012), FAT10 was shown to be an ubiquitin-independent degradation signal (Raasi, Schmidtke et al. 2001, Hipp, Raasi et al. 2004, Hipp, Kalveram et al. 2005, Schmidtke, Kalveram et al. 2009). The N-terminal FAT10-DHFR fusion protein was found to be degraded *in vitro* by purified 26S proteasomes in an ubiquitin independent manner (Schmidtke, Kalveram et al. 2009). After all, Buchsbaum et al. published in 2012 that the efficient degradation of FAT10 itself, as well as of the FAT10ylated substrates requires its prior ubiquitylation (Buchsbaum, Bercovich et al. 2012) which is in contradiction to the data of Hipp et al. 2005 and Schmidtke et al. 2009 (Hipp, Kalveram et al. 2005, Schmidtke, Kalveram et al. 2009).

Although being independent of ubiquitylation, the degradation of FAT10 was shown to be depending on the presence of NUB1L *in vivo* and *in vitro* (Schmidtke, Kalveram et al. 2009). NUB1 and NUB1L were found to interact non-covalently with FAT10 and to promote the proteasomal degradation of FAT10 and FAT10-modified proteins (Hipp, Raasi et al. 2004). The co-expression of NUB1L reduced the half-life of FAT10 to less than 30 minutes (Hipp, Raasi et al. 2004).

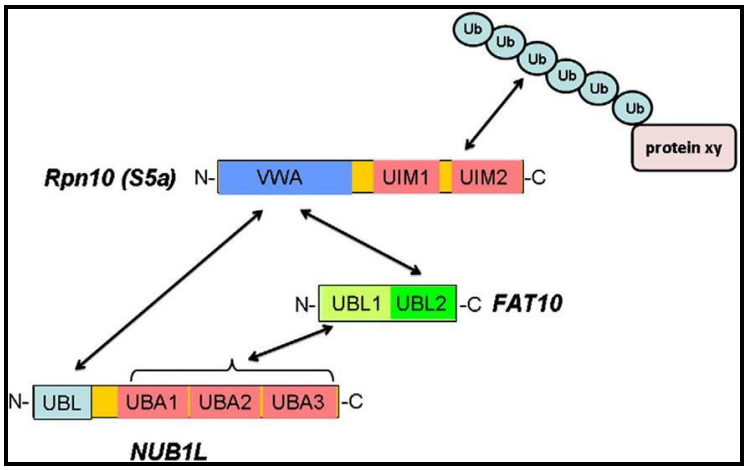

Figure 8: The 26S proteasome subunit RPN10 (S5a) can bind FAT10, NUB1L, and poly-ubiquitin. FAT10 can bind to the 26S proteasome either directly or via NUB1L. Via its C-terminal UBL domain FAT10 binds to RPN10 and with its N-terminal UBL domain to the UBA domains of NUB1L. NUB1L binds with is N-terminal UBL domain to RPN10 (Schmidtke, Aichem et al. 2013).

FAT10 can either bind to the proteasome directly or can become tied to the proteasome via NUB1L (fig.8) (Schmidtke, Kalveram et al. 2006, Rani, Aichem et al. 2012). Via its UBL domain, NUB1L mediates the interaction with the 26S proteasome and all three UBA domains of NUB1L are required for the interaction with FAT10 (Schmidtke, Kalveram et al. 2006, Rani, Aichem et al. 2012). Via its N-terminal UBL domain, FAT10 binds to NUB1L and via its C-terminal domain to the 26S proteasome subunit RPN10 (S5a) only (fig.8). Both, FAT10 and NUB1L were shown to interact with the “von Willebrand A” (VWA) domain of RPN10 which is a newly identified binding domain for FAT10 (Rani, Aichem et al. 2012). However, NUB1L can additionally bind to the RPN1 (S2) subunit of the 26S proteasome. FAT10 competes with NUB1L for binding to RPN10. With an excess of FAT10, NUB1L is unable to bind to RPN10 but can still bind to RPN1 (Rani, Aichem et al. 2012). Rani et al. suggested that FAT10, by binding with the N-terminal UBL domain to NUB1L and with the C-terminal UBL domain to RPN10, forms of a trimeric NUB1L–FAT10–RPN10 complex (Rani, Aichem et al. 2012). However, the direct interaction between FAT10 and NUB1L is not required for the accelerated degradation of FAT10. Probably, NUB1L, functions as a facilitator of proteasomal degradation of FAT10 without the necessity to serve as a linker (Schmidtke, Kalveram et al. 2006). The lysine 48-linked poly-ubiquitin chains, normally do bind to the UIM motifs of RPN10 (Schmidtke, Aichem et al. 2013).

According to Ebstein et al. there might be additional FAT10 binding domains in the 26S proteasome (Ebstein, Lehmann et al. 2012). FAT10 was also shown to co-precipitates the 20S proteasome subunits α6, and the 19S subunit RPT5 (Buchsbaum, Bercovich et al. 2012).

2.7.4.1 The biological relevance of FAT10

In the last six years, a great progress was achieved concerning the discovery of the mechanistic of the FAT10ylation process (Chiu, Sun et al. 2007, Pelzer, Kassner et al. 2007, Aichem, Pelzer et al. 2010, Gavin, Chen et al. 2012). However, despite many interesting findings and estimations, the biological function of FAT10 remains obscure.

The generation of a homozygote FAT10 knockout mouse was one approach to shed light on the dark, but these mice only showed minor phenotypes (Canaan, Yu et al. 2006). The $FAT10^{-/-}$ mice are viable and fertile and no obvious histological differences were found (Canaan, Yu et al. 2006). The lymphocyte populations from their spleens, thymuses and bone marrows did not reveal any abnormalities apart from an increased susceptibility to spontaneous apoptotic death. Interestingly, the $FAT10^{-/-}$ mice demonstrated a high level of sensitivity toward low doses of endotoxin challenge (LPS) (Canaan, Yu et al. 2006). The latter could implicate FAT10 in the defence mechanism against pathogens.

Many features of FAT10 do point to a function in antigen presentation, however neither the cell surface expression of MHC Class I molecules nor the MHC Class I-restricted antigen presentation was affected by the FAT10 induction in a murine fibroblast cell line (Raasi, Schmidtke et al. 2001). However, Ebstein et al. have shown that the FAT10 modification is a distinct and alternative signal for facilitated MHC class I antigen presentation. FAT10 was shown to accelerate the proteasomal degradation of pp65 and results in improved direct presentation and DC-mediated cross-presentation of the HLA-A2-restricted pp65495–503 epitope (Ebstein, Lehmann et al. 2012). They further show that the FAT10 derived pp65495–509 epitope presentation is less dependent on RPN10 than the presentation of Ub-pp65. In contrast to ubiquitin, the FAT10-dependent pp65 epitope presentation was not enhanced by immunoproteasomes or by PA28 (Ebstein, Lehmann et al. 2012).

Additionally, they found NUB1 to act FAT10-specific, while NUB1L seems to be positioned at the intersection of the ubiquitin and FAT10 pathways (Ebstein, Lehmann et al. 2012).

FAT10 was also implicated to apoptosis. However the data are ambiguous in so far, that there are studies which assume a pro-apoptotic function of FAT10 (Raasi, Schmidtke et al. 2001, Li, Santockyte et al. 2011) and studies which assume an anti-apoptotic function (Canaan, Yu et al. 2006, Buchsbaum, Bercovich et al. 2012).

Also a cell cycle related function for FAT10 was suggested. Lim et al. for example found in a human colon carcinoma cell line the FAT10 expression, to be cell cycle-regulated on both the protein and transcript level. The FAT10 protein expression peaks in the S-phase of the cell cycle and decreases when the cells were arrested at the G2/M border (Lim, Zhang et al. 2006). During mitosis, FAT10 was shown to bind to the mitotic spindle checkpoint protein “mitotic arrest deficient 2” (MAD2) (Liu, Pan et al. 1999). High levels of FAT10 protein in cells lead to increased mitotic nondisjunction and chromosome instability, during the prometaphase stage of the cell cycle (Ren, Kan et al. 2006, Ren, Wang et al. 2011). Liu et al. showed that the ectopic expression of FAT10 enhanced the cell proliferation, inhibited apoptosis and induced cell cycle progression, whereas silencing FAT10 expression suppressed cell proliferation and induced apoptosis (Liu, Dong et al. 2013). Recently, Merbl et all published that the inhibition of the FAT10 pathway leads to prolonged mitotic arrest and cell death (Merbl, Refour et al. 2013).

FAT10 is expressed in normal myocardial tissue of human, mouse and rat and is upregulated in the heart at the border zone of myocardial infarction and in cultured “neonatal rat cardiac myocytes” (NRCM) in response to hypoxia/reoxygenation (H/R) stress. The FAT10 overexpression in NRCM cells reduced the p53 level and reduced apoptosis, while a knock down of FAT10 had the opposite effects. Thus, FAT10 was suggested to be a cardioprotective protein (Peng, Shao et al. 2013).

The eukaryotic translational “elongation factor 1A1” (eEF1A1) was identified as a FAT10-specific binding protein. Endogenous FAT10 and endogenous eEF1A1 co-localise in the cytoplasm and a knockdown of FAT10 results in the downregulation of eEF1A1 expression in human HCC cells. (Yu, Liu et al. 2012).

Upon proteasomal inhibition, FAT10 non-covalently interacts with “histone deacetylase 6” (HDAC6) *in vivo* and localises to aggresome in a microtubule-dependent manner (Kalveram, Schmidtke et al. 2008). Since aggresomes contain, besides other proteins, also the autophagosomal receptor protein SQSTM1 (p62) and since they are suspected to be degraded by aggrephagy (Lamark and Johansen 2012, Li, Shin et al. 2013), Birte Kalveram tested whether FAT10 also interacts with p62 or the autophagosomal marker protein LC3. Whereas, there was no direct interaction with LC3 detectable (unpublished data), p62 was found to be mono-FAT10ylated at several lysines and also a non-covalent interaction between FAT10 and p62 was detectable (Aichem, Kalveram et al. 2012). The FAT10ylation of p62 leads to its proteasomal degradation. FAT10 co-localises with p62 in p62 bodies, however, there is no evidence that FAT10 serves as a signal for autophagosomal degradation (Aichem, Kalveram et al. 2012).

There are not so many FAT10 substrates and interacting proteins identified yet. In a mass spectrometry screen of endogenous FAT10 conjugates from IFNγ -and TNFα stimulated HEK293 cells, Aichem et al. identified 569 novel putative FAT10 interacting proteins (Aichem, Kalveram et al. 2012). They were involved in different functional pathways such as autophagy, cell cycle regulation, apoptosis and cancer. The biggest group comprised proteins involved in binding DNA or RNA with many transcription factors as well as DNA or RNA polymerases followed by the group of cancer-related proteins and the group of putative E3 ligases (Aichem, Kalveram et al. 2012). Among the twenty identified E3 ligases, ten were found to belong to the RING-finger family. In addition, two HECT domain-, two F-box containing- and two SUMO-specific ligases, one anaphase-promoting complex E3 ligase, and two zinc-finger and two cullin E3 ligases were identified (Aichem, Kalveram et al. 2012). However, it has not been confirmed yet, whether there are FAT10 specific E3 ligases among them.

Mutations in the “aryl hydrocarbon receptor-interacting protein-like 1” (AIPL1) protein, causes the inherited “leber congenital amaurosis” (LCA) blindness. AIPL1 was previously found to interact with NUB1 and to bind non-covalently to free FAT10 and FAT10ylated proteins. In line with this, it was shown that it can form a ternary complex with FAT10 and NUB1. A minor proportion of AIPL1 itself may also be modified by FAT10. Furthermore, it was shown that AIPL1 blocks the NUB1-

mediated degradation of FAT10ylated proteins. Interestingly, AIPL1 also co-immunoprecipitated UBA6, suggesting that AIPL1 may have a role in directly regulating the FAT10 conjugation machinery (Bett, Kanuga et al. 2012).

The inflammatory mediator “leucine-rich repeat Fli-I-interacting protein 2” LRRFIP2 and the endoplasmic reticulum membrane protein LULL1 (TOR1AIP2 “TORsin 1A-Interacting Protein 2”) were found to be covalently modified by FAT10 (Buchsbaum, Bercovich et al. 2012). Whereas the function of LULL1 is largely unknown, LRRFIP2 is involved in NF-κB activation following stimulation of TLR4. By leading to the translocation of LRRFIP2 to the cellular insoluble fraction, the FAT10ylation of LRRFIP2 inhibits NF-κB activation (Buchsbaum, Bercovich et al. 2012).

2.7.4.2 The pathological relevance of FAT10

There is also a lot of evidence for FAT10 to have a pathological meaning. An upregulated FAT10 expression was found to be a common feature of “hepatocellular carcinoma” (HCC) and other cancers of the gastrointestinal tract and of the female reproductive system (Lee, Ren et al. 2003). In tissue samples of HCC tumours with distinct aetiologies, the FAT10 expression level did correlate neither with the aetiologies nor with the histological tumour grade (Lukasiak, Schiller et al. 2008). However, in glioma tissues, FAT10 protein and mRNA was over-expressed with increased expression levels from grade I to grade IV glioma (Yuan, Tu et al. 2012). In the HCC samples tested by Sebastian Lukasiak, the FAT10 cDNA sequences were not mutated and intact FAT10 protein was detectable (Lukasiak, Schiller et al. 2008). Since the FAT10 expression in cancer tissues was shown to correlate with the expression of LMP2, (Lukasiak, Schiller et al. 2008, Bardag-Gorce, Oliva et al. 2010, French, Oliva et al. 2011, Qing, French et al. 2011) it seems to be likely that the joint overexpression of FAT10 and LMP2 was just a consequence of the increased cytokine induction during the proinflammatory immune response against these tumours (Lukasiak, Schiller et al. 2008). Since the tumour suppressor p53 negatively regulates the expression of FAT10 and p53 is the most commonly mutated gene known in human cancer, FAT10 is likely upregulated in those tumour cells with mutant p53 (loss of function) (Li, Santockyte et al. 2011).

FAT10 is one of the most upregulated genes in a renal tubular epithelial cell line (RTECs) from a patient with “HIV-associated nephropathy” (HIVAN) and the expression of FAT10 were found to induce apoptosis in RTEC (Ross, Wosnitzer et al. 2006, Snyder, Alsauskas et al. 2009). On the other hand, FAT10 deficiency in RTECs abrogated the TNFα induced IkBα degradation as well as the nuclear translocation of p65. Furthermore, the FAT10 deficiency was shown to reduce the expression of LMP2 (Gong, Canaan et al. 2010) which plays a key role in the degradation of phosphorylated IκBα and the subsequent activation of NF-κB (Hayashi and Faustman 2000). The IkBα degradation in FAT10$^{-/-}$ RTECs could be restored by the transfection of LMP2. FAT10 probably mediates the NF-κB activation and may promote tubulointerstitial inflammation in chronic kidney diseases (Gong, Canaan et al. 2010).

Besides cancer and renal diseases, FAT10 is also implicated to play a role in neuronal degeneration diseases such as Huntington disease (Nagashima, Kowa et al. 2011).

2.8 Autophagy

Autophagy is a general term for the degradation of cytoplasmic components within lysosomes. But this processes have to be distinguished from the endocytosis-mediated lysosomal degradation of extracellular and plasma membrane proteins (Mizushima 2007). Basically there are three types of autophagy: microautophagy, chaperone-mediated autophagy (CMA) and macroautophagy (Mizushima 2007). All contribute to lysosomal degradation, but differ in their regulation, the type of cargo preferentially degraded, and the mechanisms that contribute to targeting the cargo to the lysosomal compartment (Bejarano and Cuervo 2010).

2.8.1 Macroautophagy

Macroautophagy (hereafter referred to as autophagy), is conserved in eukaryotic organisms and mainly mediates the unselective bulk degradation of long-lived proteins (Mizushima 2007, Geng and Klionsky 2008). The characteristic feature of autophagy is the *de novo* formation of a double-membrane vesicle, termed the autophagosome which sequesters a part of the cytoplasm and delivers it to the

lysosome for degradation via the lysosomal hydrolases (Mizushima 2007, Geng and Klionsky 2008). Although autophagy is mainly considered to be an unselective degradation progress, some forms of macroautophagy selectively target macro-molecules, organelles and protein aggregates (Mehrpour, Esclatine et al. 2010).

Autophagy can be subclassified into “basal autophagy” and “induced autophagy”. The former is required for the constitutive turnover of cytosolic components, while the latter is used for the upregulation of the autophagic turnover upon certain intracellular and extracellular stimuli such as amino acid starvation, growth factor withdrawal, low cellular energy levels, endoplasmic reticulum (ER) stress, hypoxia, oxidative stress, pathogen infection, and organelle damage (Burman and Ktistakis 2010).

Autophagy is divided into seven steps: the initiation, the nucleation of a “pre autophagosomal structure” (PAS) in the mammalian system called omegasome, the expansion of the PAS into an isolation membrane or phagophore (the precursor of the autophagosome), the elongation of the isolation membrane, the closure of the autophagosome, the autophagosome-lysosome fusion, and the degradation of intra-autophagosomal contents by lysosomal hydrolases (Mehrpour, Esclatine et al. 2010, Polson, de Lartigue et al. 2010, Tanida 2011, Alers, Loffler et al. 2012).

Around thirty-two genes could have been identified whose products contribute to the autophagosome formation. Many of these “autophagy-related genes” (ATG) are well conserved from yeast to mammals (Mehrpour, Esclatine et al. 2010, Alers, Loffler et al. 2012). The mammalian ATG protein counterparts form complexes which are recruited in a hierarchical manner to the single site of autophagosome biogenesis (Itakura and Mizushima 2010). (1) The ULK1:ATG13:FIP200:ATG101 protein kinase complex functions at the most upstream position, followed by (2) the ATG14:Beclin 1:VPS34:p150 class III PI3-kinase complex, (3) its putative effectors WIPI-1, ATG9 and DFCP1, (4) the ATG12–ATG5:ATG16L1 conjugation system, and (5) the LC3–PE conjugation system (Itakura and Mizushima 2010, Tanida 2011).

2.8.1.1 The induction of autophagy

In mammalian cells autophagosomes can be generated anywhere in the cytoplasm (Longatti and Tooze 2009) in omegasomes which are directly connected to the endoplasmic reticulum (ER) (Axe, Walker et al. 2008).

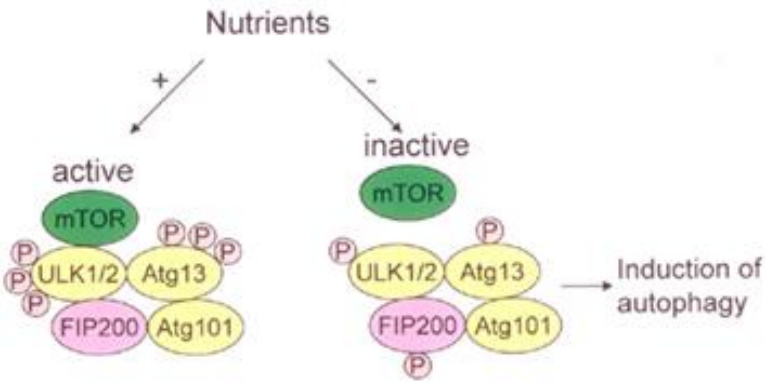

Figure 9: Autophagy induction by mTOR. In presence of nutrients, active mTOR inhibits ULK1/2–ATG13-FIP200-ATG101 complex. In response to nutrient deprivation, mTOR dissociates from the ULK complex, resulting in the induction of autophagy. Modified from (Zeng and Kinsella 2011).

Upstream of the autophagy machinery, the “unc-51-like kinase” (ULK) complex in combination with the mTOR kinase contribute to the induction of autophagy. Under optimal growth conditions, the active mTOR kinase negatively regulates autophagy by directly phosphorylating ATG13 and the serine/threonine protein kinases ULK1 and ULK2 (fig.9) (Mehrpour, Esclatine et al. 2010). Starvation or rapamycin treatment inactivates mTOR and therefore decreases the ATG13 and ULK1/2 phosphorylation. The subsequent increased activation of the ULKs results in the phosphorylation of ATG13 and FIP200 which might trigger the translocation of ULK1/2-ATG13-FIP200 to pre-autophagosomal structures and for autophagy initiation (fig.9) (Alers, Loffler et al. 2012).

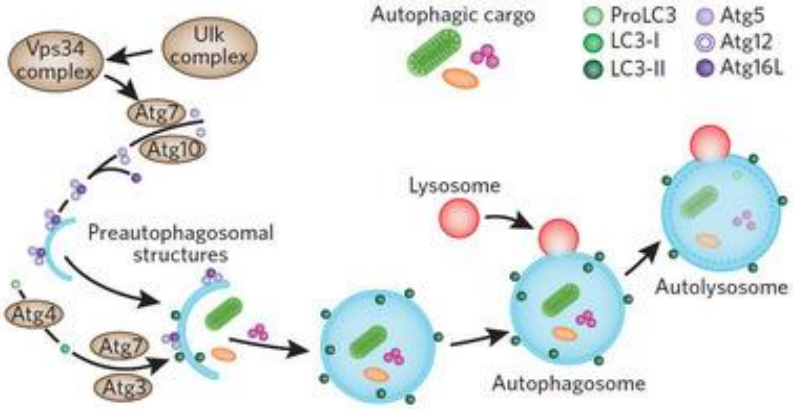

Figure 10: Macroautophagy in mammalian cells. A model of the molecular events involved in membrane initiation, elongation and completion of the autophagosome (Fleming, Noda et al. 2011).

After the induction of autophagy, the ULK1 complex (comprising ULK1/2:ATG13:FIP200:ATG101) translocates to the ER and activates the class III PI3K VPS34 complex (Beclin 1:VPS34:ATG14L) (fig.10) (Rubinsztein, Shpilka et al. 2012, Molejon, Ropolo et al. 2013). Together, both complexes regulate the initial events of autophagosome formation (Alemu, Lamark et al. 2012). The class III PI3K activity of the VPS34 complex is required for phagophore formation. The production of PI3P leads to the recruitment of PI3P-binding proteins such as the "WD-repeat domain phosphoinositide-interacting" (WIPI) family proteins 1 and 2 and "double FYVE-containing protein 1" (DFCP1) (Alers, Loffler et al. 2012). Next, the two conjugation systems ATG12-ATG5:ATG16L complex and LC3-II were added to the elongating membrane (fig.10). The membrane growths, engulfs the cytoplasmic components and finally closes to form the autophagosome (Molejon, Ropolo et al. 2013). In the final step of the process, lysosomes fuse with the autophagosome, releasing lysosomal hydrolases into the interior, resulting in degradation of the vesicle contents (fig.10) (Molejon, Ropolo et al. 2013).

Besides its function in maintaining cellular homeostasis by degrading cellular proteins and organelles, autophagy was also found to function in the adaptive and innate immune systems (Oh and Lee 2012). Autophagy regulates uncontrolled immune responses and protects host cells from invading pathogens. Various intracellular bacteria, viruses, and protozoans are removed from host cells by autophagy, and endogenous antigens are processed and presented to MHC class II via autophagy (Oh and Lee 2012).

2.9 The autophagic adaptor proteins

Autophagy receptors, such as p62, NBR1, NDP52 and optineurin (OPTN), which simultaneously bind both ubiquitin and autophagy-specific ubiquitin-like modifiers (LC3, GABARAP, ATG16L), have provided a molecular link between ubiquitylation and autophagy (fig.11).

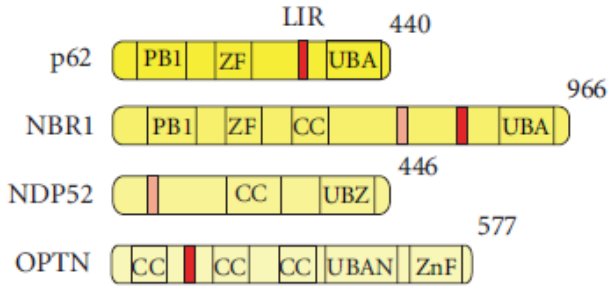

Figure 11: The domain architecture of the known, characterised autophagy receptors. Modified from (Behrends and Fulda 2012).

Macroautophagy often is described as a non-selective bulk degradation pathway. This was proven not to be always the case since through autophagic adapter proteins selectively ubiquitylated substrates are degraded in autophagosomes (Ichimura and Komatsu 2010, Komatsu and Ichimura 2010).

In the following chapter, the function of selective autophagic adaptors in the degradation of ubiquitylated substrates by autophagy will be described. Such substrates may include for example protein aggregates, soluble proteins and intracellular bacteria (Komatsu and Ichimura 2010, Johansen and Lamark 2011)

2.9.1 p62 (sequestosome 1/SQSTM1)

The 440–amino acid protein sequestosome 1(SQSTM1/p62) is not found in plants and fungi and seems to be confined to the metazoans (Johansen and Lamark 2011). p62 can interact with a large number of proteins and changes its face by altering the binding partner(s) (Komatsu, Kageyama et al. 2012).

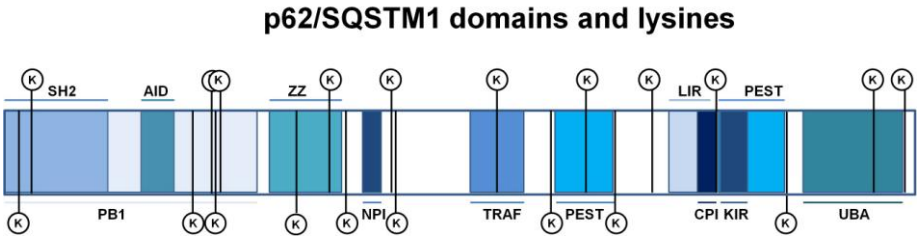

Figure 12: Schematic overview of the domains and lysines (K) in p62.

The N-terminal “Phox and Bem1” (PB1) domain (aa 1-122) of p62 is responsible for the self- and hetero-oligomerisation with other proteins containing PB1 domains such as aPKCs and NBR1 (Lamark, Perander et al. 2003, Seibenhener, Babu et al. 2004, Johansen and Lamark 2011). The “Src-homology 2“ (SH2) domain (aa 1-50) binds the tyrosine kinase $p56^{lck}$ in a phosphotyrosine-independent manner (Vadlamudi, Joung et al. 1996). The “acidic interaction domain” (AID, aa 66-82) of p62 interacts with aPKCs, recruits them to the receptor signaling complex and activates them (Moscat and Diaz-Meco 2000). The two “rich in proline (P), glutamate (E), serine (S), and threonine (T)” PEST motifs (aa 266-294 and aa 345-377) of p62 are expected to be targets for several kinases, including serine/threonine kinases like the “Casein kinase II” (CK2) (Joung, Strominger et al. 1996, Stumptner, Heid et al. 1999) For the interaction with the “receptor interacting protein” (RIP), the ZZ type zinc finger domain (aa 128-163) of p62 is required (Sanz, Sanchez et al. 1999, Sanz, Diaz-Meco et al. 2000). p62 associates with p38 using two domains. The “N-terminal p38 interaction” (NPI) domain (aa 173-182) binds to p38 directly, while the “C-terminal p38 interaction” (CPI) domain (aa 335-344) binds to p38 indirectly. While the indirect binding of p38 to the CPI domain may induce the formation of a conformation suitable for the association with p38, the NPI domain probably function as a regulator to p38 (Kawai, Saito et al. 2008) Via its “tumor necrosis factor (TNF) receptor-associate factor 6” (TRAF6) binding site (aa 228–254) p62 binds to the ubiquitin E3 ligase TRAF6 (Wooten, Geetha et al. 2005). The “Keap1-interacting region” (KIR) domain (aa 346-359) is involved in the NRF2 regulation (Komatsu, Kurokawa et al. 2010). Via its 22 amino acids “LC3-interacting region” (LIR) domain (aa321-342), human p62 interacts directly with both to LC3A and -B as well as other human ATG8 homologues such as GABARAP, GABARAPL1 and GABARAPL2 (Pankiv, Clausen et al. 2007). In accordance to Pankiv et al., Ichimura et al. simultaneously published the discovery of the “LC3 recognition sequence” (LRS) (334-344) in murine p62

(Ichimura, Kumanomidou et al. 2008). Ichimura et al. found the ATG8 homologues LC3, GABARAP and GATE-16 to have similar affinities for p62 under *in vitro* conditions (Ichimura, Kumanomidou et al. 2008). Via its “ubiquitin-associated” UBA domain (aa 386-434), p62 binds to polyubiquitin chains with a preference for binding to K63-polyubiquitylated substrates (Seibenhener, Babu et al. 2004).

2.9.1.1 The biological relevance of p62

Due to its large number of interaction partners, p62 is involved in many cellular processes (Komatsu, Kageyama et al. 2012).

Upon cellular stress, p62 is required for the formation of membrane free ubiquitylated protein aggregates (Isakson, Holland et al. 2013). Further, p62 is involved in the delivery of K63-polyubiquitinated substrates for proteolytic degradation (Seibenhener, Babu et al. 2004). By binding simultaneously to LC3 and ubiquitin p62 was found to act as a shuttling factor which links polyubiquitylated protein aggregates to the autophagy machinery (Bjorkoy, Lamark et al. 2006). Probably by directly binding to the proteasome, p62 can also target its polyubiquitylated substrates to the proteasome (Seibenhener, Babu et al. 2004).

Since the UBA domain of p62 preferentially binds to K63 linked ubiquitin and p62 is also known to interact with the E3 ubiquitin ligase TRAF6, which catalyses K63 polyubiquitylation it is likely that TRAF6 could contribute to the ubiquitylation of protein aggregates degraded by autophagy (Knaevelsrud and Simonsen 2010).

K63- polyubiquitin chains are generally known to also function in processes apart from degradation, such as in the activation of the NF-κB pathway and in the DNA damage tolerance (Seibenhener, Babu et al. 2004). By interacting with aPKC and TRAF6, p62 serves as a scaffold in both the TNFα and interleukin-1 (IL1) receptor signalling NF-κB pathways (Geetha and Wooten 2002). The interaction of p62 with TRAF6 results in the activation of NF-κB (Yin, Lin et al. 2009, Komatsu and Ichimura 2010). In the Th2 cell differentiation, p62 is involved in the control of the NF-kB stimulation during the late phases of the T-cell activation (Martin, Diaz-Meco et al. 2006). Further p62 was found to play a role in the maintenance of apoptosis (Bekes and Salvesen 2009, Jin, Li et al. 2009).

The intracellular level of p62 is tightly regulated by autophagy through the direct interaction of LC3 with p62 (Pankiv, Clausen et al. 2007, Ichimura, Kumanomidou et al. 2008). p62 itself is not covalently modified by ubiquitin (Seibenhener, Babu et al. 2004, Matsumoto, Wada et al. 2011) however, it is a substrate for FAT10ylation and the FAT10ylated p62 is degraded by the proteasome (Aichem, Kalveram et al. 2012).

2.9.1.2 The modification of p62

Matsumoto et al. found p62 to be phosphorylated constitutively at T269, S272, S282, S332 and S366 whereas the amount of S24-, S207-, or S403-phosphorylated p62 was increased in response to the MG132 treatment (Matsumoto, Wada et al. 2011). Under proteasomal inhibition, the CK2 kinase phosphorylates S403 of p62. The phosphorylation of p62 at S403 increases the affinity of its UBA domain for polyubiquitylated chains. This leads to an enhanced recruitment of polyubiquitylated proteins into the sequestosome which is a targeting unit for the autophagosome entry. The binding of the polyubiquitin chain to S403-phosphorylated p62 prevents its dephosphorylation (Matsumoto, Wada et al. 2011). Pili et al. could show that also the kinase “TANK-binding kinase 1” (TBK1) is able to directly phosphorylate the S403 of p62 (Pilli, Arko-Mensah et al. 2012).

Pankiv et al. published in 2009, that p62 shuttles continuously between nuclear and cytosolic compartments at a high rate (Pankiv, Lamark et al. 2010). They showed that p62 contains two “nuclear localisation signals” NLS (aa 186–189 NLS1 and aa 164–267 NLS2) and one “nuclear export signal” NES (aa 303-320). From their data, they suggested that the nucleocytoplasmic shuttling of p62 is modulated by phosphorylations at or near the most important nuclear localisation signal, NLS2. The phosphorylation of p62 at T269 and S272 can increase the nuclear import activity of NLS2, whereas the phosphorylation of S266 in the middle of NLS2 has an inhibitory effect on its nuclear import (Pankiv, Lamark et al. 2010). The transport of p62 between the compartments is also regulated by the aggregation of p62. The accumulation of ubiquitylated proteins or aggregates has an anchoring effect on p62, resulting in its accumulation in aggregates in the cytosol or in the nucleus (Pankiv, Lamark et al. 2010).

Other modifications, such as tyrosine phosphorylation, ubiquitylation, SUMOylation, or acetylation were not detected by Matusmoto et al. (Matsumoto, Wada et al. 2011).

2.9.1.3 "Nuclear factor erythroid 2-related factor 2" (NRF2)

The transcription factor "nuclear factor erythroid 2-related factor 2" (NRF2) is ubiquitously expressed in a wide range of tissue and cell types and regulates the basal and inducible expression of numerous detoxifying and antioxidant genes (Kaspar, Niture et al. 2009, Jain, Lamark et al. 2010). All target genes up regulated by NRF2 contain a DNA regulatory sequence called the "antioxidant response element" (ARE) in their promoters (Kaspar, Niture et al. 2009, Jain, Lamark et al. 2010). NRF2 is negatively regulated by the cytoplasmic protein "kelch-like ECH-associated protein 1" (KEAP1), also known as "inhibitor of NRF2" (INRF2) (fig.13) (Motohashi and Yamamoto 2004, Kaspar, Niture et al. 2009, Jain, Lamark et al. 2010).

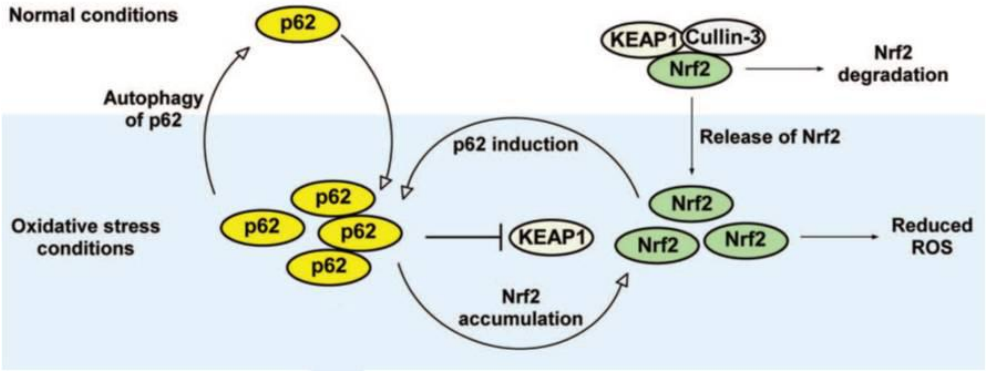

Figure 13: p62 and NRF2 as regulators of the oxidative stress response. Under normal conditions, there is a low level of p62 and NRF2 due to selective autophagy of p62 and KEAP1-mediated proteasomal degradation of NRF2. Under oxidative stress conditions, there is an elevated level of p62 and NRF2. This results in the establishment of a feedback loop where NRF2 induces expression of p62, and p62 inhibits KEAP1-mediated degradation of NRF2. Modified from (Johansen and Lamark 2011).

The simultaneous binding of KEAP1 to a Cullin3 E3 ubiquitin ligase complex and to NRF2 leads to the ubiquitylation and subsequent degradation of NRF2 through the 26S proteasome. Under basal cellular conditions, NRF2 is constantly degraded (fig.13) (Kaspar, Niture et al. 2009, Niture, Kaspar et al. 2010). However, in response to oxidative stress, NRF2 is released from the KEAP1 degradation. Once NRF2 is released from KEAP1 (fig.13), it stabilises and translocates into the nucleus where it activates the ARE-mediated gene expression (Kaspar, Niture et al. 2009, Jain,

Lamark et al. 2010, Komatsu, Kurokawa et al. 2010). Interestingly, via its KIR domain, also p62 can bind directly to KEAP1 and thereby blocking the binding between KEAP1 and NRF2. A model is proposed, in which p62 competes with NRF2 for interaction with KEAP1 (Jain, Lamark et al. 2010, Komatsu, Kurokawa et al. 2010). Since also the promoter/enhancer region of the p62 gene itself contains an ARE sequence which is responsible for its induction in response to oxidative stress, p62 is able to set up a positive feedback loop (Jain, Lamark et al. 2010). When the sustained activation of ARE response genes is no longer needed, the autophagic degradation of p62 will probably break the loop. The LIR and KIR motifs of p62 cannot interact with LC3 and KEAP1 simultaneously. But since p62 molecules can polymerise, the interaction between KEAP1 and p62 leads to the accumulation of KEAP1 in p62 bodies, which is followed by autophagic degradation of KEAP1 (Jain, Lamark et al. 2010).

2.9.1.4 p62 and aggregate formation

In antigen-presenting cells, such as dendritic cells and macrophages, “dendritic cell aggresome-like induced structures” (DALISs) are formed during immune cell maturation. Misfolded proteins such as “defective ribosomal products” (DRiPs) accumulate in DALIS and become ubiquitylated within these structures. The formation of DALIS is stress-induced and transient and does not depend on transport along microtubules (Lelouard, Gatti et al. 2002, Lamark and Johansen 2012).

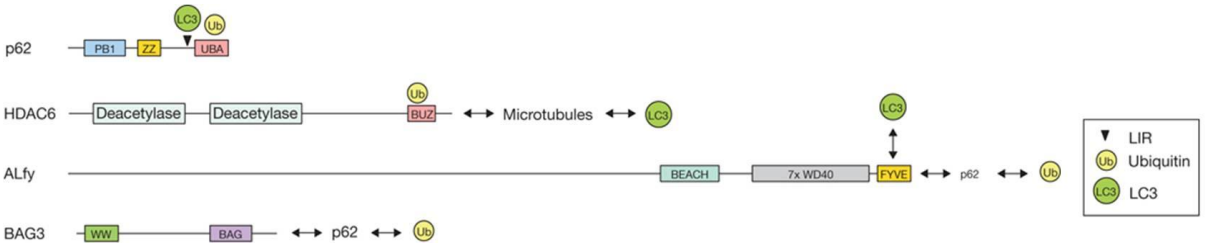

Figure 14: The domain architecture of different LC3 and/or ubiquitin-binding proteins that are involved in aggresome formation. Proximity indicates direct binding of the protein with ubiquitin and/or LC3, and arrows designate indirect binding. Modified from (Kraft, Peter et al. 2010).

Similar structures can be formed in many cell types in response to stressors like puromycin, oxidative stress, starvation, and transfection. Therefore they were termed aggresome-like induced structures (ALIS) (Szeto, Kaniuk et al. 2006). The term p62-

bodies comprise all aggregates, formed by p62 in response to various stressors that serve as substrates for selective autophagy. (Lamark and Johansen 2012). Bjorkoy et al. found p62 bodies to be either membrane-free protein aggregates (sequestosomes) or membrane-confined autophagosomal and lysosomal structures (Bjorkoy, Lamark et al. 2005). Aggresomes are formed in response to proteasomal inhibition or overexpression of aggregation prone proteins and are located close to the nuclear envelope at the "microtubule organizing centre" (MTOC). They are insoluble and metabolically stable and their proteins normally are ubiquitylated (Lamark and Johansen 2012). Upon proteasomal inhibition, in FAT10 overexpressing cells, also FAT10 is localised to aggresomes (Kalveram, Schmidtke et al. 2008). The formation of aggresomes depends on the microtubule-dependent transport of protein aggregates. Either HDAC6 or "BCL2-associated athanogene 3" (BAG3) mediate the transport of the aggregates to the aggresomen (Lamark and Johansen 2012).

"Autophagy-linked FYVE" (ALFY)

The "autophagy-linked FYVE" protein ALFY is ubiquitously expressed in mammalian tissues (Simonsen, Birkeland et al. 2004, Isakson, Holland et al. 2013). ALFY interacts with PI3P, ATG5 and p62 (Yamamoto and Simonsen 2011, Isakson, Holland et al. 2013). By its recruitment to intracellular inclusions ALFY is suggested to scaffold ubiquitylated proteins to the autophagic effectors ATG5, ATG12, ATG16L and LC3. When p62 binds to aggregation-prone ubiquitylated proteins, its PB1 domain facilitates the formation of microaggregates. Those can be combined and deposited into larger aggregates (p62 bodies) by ALFY and subsequently degraded by autophagy (Yamamoto and Simonsen 2011, Isakson, Holland et al. 2013).

ALFY is a regulator, however not a part of the basal machinery for autophagy (Simonsen, Birkeland et al. 2004, Clausen, Lamark et al. 2010). It is not required for the macroautophagic bulk degradation under starvation conditions. Via regulating the ALFY level or its localisation, cells can also regulate the starvation induced autophagy versus aggrephagy (Yamamoto and Simonsen 2011, Isakson, Holland et al. 2013).

p62 and ALFY undergo nucleocytoplasmic shuttling. p62 is mainly localised in the cytoplasm and its nuclear import is modulated by phosphorylation. ALFY under basal conditions is manly located in the nucleus and the translocation into the cytosol is

induced by cellular stress (Clausen, Lamark et al. 2010, Yamamoto and Simonsen 2011, Isakson, Holland et al. 2013). Since p62 was found to facilitate nuclear export of ALFY, p62 might work as a signal when aggrephagy needs to be activated. The degradation of ALFY by autophagy depends on p62, whereas p62 is turned over by autophagy independent of ubiquitylated proteins and ALFY. This might reflect the need for a tight control of the level of p62 (Clausen, Lamark et al. 2010, Isakson, Holland et al. 2013).

2.9.1.5 The pathological relevance of p62

p62 has a pathological relevance since it is a common component of protein aggregates found in protein aggregation diseases affecting both the brain and the liver. These include “Lewy bodies” in Parkinsons disease, “neurofibrillary tangles” in Alzheimer’s disease, “huntingtin aggregates” and “Mallory Denk bodies” in alcoholic liver disease and hepatocellular carcinoma (Kuusisto, Salminen et al. 2001, Zatloukal, Stumptner et al. 2002, Nagaoka, Kim et al. 2004). All of these aggregates also contain polyubiquitylated proteins (Komatsu, Kageyama et al. 2012).

Most of the mutations which are identified for being associated with the skeletal disorder “Paget's disease of bone” (PDB) are clustered within the UBA domain of p62 and impair the ability of p62 to bind ubiquitin (Long, Garner et al. 2010).

2.9.2 “Neighbour of Brca1 gene1” (NBR1)

Also the protein “neighbour of Brca1 gene1” (NBR1) is an autophagic cargo receptor which is selectively degraded by autophagy. NBR1 is found in plants, fungi and in metazoans, but the gene is lost in several animal lineages including the model organisms *Drosophila melanogaster* and *Caenorhabditis elegans* (Johansen and Lamark 2011). Like p62, NBR1 has PB1, ZZ, UBA and even two LIR domains. Although NBR1 cannot polymerise, via its PB1 domain, it binds to p62 via this domain. Thus it can either be a part of, or the terminator of a polymeric p62 molecule chain (Johansen and Lamark 2011). Oligomers of NBR1 are formed via its CC1 domain. The isolated UBA domain of NBR1 has a high affinity for both K48- and K63-linked diubiquitin. NBR1 directly interacts with LC3 and the LIR1 motif is most important for autophagic degradation of NBR1 (Kirkin, Lamark et al. 2009). It has

been shown *in vitro* and *in vivo* that NBR1 interacts non-covalently with all members of the ATG8 protein family (GABARAP, GABARAPL1, GABARAPL2, LC3A, LC3B, and LC3C). Further NBR1 was found to interact non-covalently with GST-ubiquitin and GST-4xubiquitin (Kirkin, Lamark et al. 2009). The NBR1 protein level is regulated by autophagy and seems not to be influenced by proteasomal degradation (Lamark, Kirkin et al. 2009).

Together with p62 and ubiquitylated proteins, NBR1 localises to inclusion bodies associated with human pathologies. In Mallory bodies of alcoholic steatohepatitis, endogenous NBR1 was found to co-localise with p62 and ubiquitin (Kirkin, Lamark et al. 2009). NBR1 has been shown to directly bind to the sarcomeric protein kinase titin and to p62 in the M-line of the sarcomere of skeletal muscles. Mutations in titin which disrupt the NBR1 binding cause hereditary muscle disease in humans (Johansen and Lamark 2011). Further, NBR1 was found to be necessary and sufficient for the degradation of peroxisomes (pexophagy) (Deosaran, Larsen et al. 2013).

Jorge Moscat's group found NBR1 to be a critical mediator of T cell activation and to act in the control of Th2 differentiation and allergic airway inflammation (Yang, Liu et al. 2010).

2.9.3 Optineurin (OPTN)

OPTN is a cytosolic protein of 67 kDa that contains several domains such as an UBD, a LIR motif, a zinc finger and binding site for the TBK1 kinase (Ying and Yue 2012). In adult mice, OPTN is ubiquitously present in various tissues including the heart, brain, placenta, skeletal muscle, kidney, pancreas, adrenal cortex, liver, and eye. The expression of OPTN is inducible by TNFα (Ying and Yue 2012). OPTN is ubiquitylated and the UPS probably seems to be the major pathway for endogenous OPTN processing, whereas autophagy and lysosomes seem to have a rather minor role (Ying and Yue 2012).

The UBD in OPTN resembles to the UBD found in ABIN proteins and "NF-κB essential modulator NEMO" and is therefore termed UBAN-domain. OPTN binds to ubiquitin-chains, but not to mono-ubiquitin or other UBL proteins. However, FAT10 was not tested in this study (Wild, Farhan et al. 2011). The UBAN domain of OPTN preferentially binds to K63-linked polyubiquitin-chains (Ying and Yue 2012). Via its

LIR motif OPTN binds to the autophagy modifier proteins LC3 and GABARAP (Wild, Farhan et al. 2011).

OPTN is involved in the NF-κB pathway as well as in the antiviral and antibacterial signalling. By competing with NEMO, OPTN negatively regulates the TNFα-induced NF-κB activation (Ying and Yue 2012). Interestingly, the promoter region of OPTN showed a NF-κB binding site located immediately upstream of the transcription start site (Ying and Yue 2012). OPTN was shown to be involved in the selective autophagy of ubiquitin-coated cytosolic *Salmonella enterica ssp. enterica ser. Typhimurium*. The phosphorylation of OPTN on serine 177 (S177) by the TBK1 kinase was found to enhance its LC3 binding capacity and to thereby promote the autophagic clearance of *Salmonella Typhimurium* (Wild, Farhan et al. 2011).

2.9.4 "Nuclear dot protein 52 kDa" (NDP52)

The "nuclear dot protein 52 kDa" (NDP52), is a mainly cytosolic protein. Two vertebrate paralogues exist, Tax1BP1 (also known as TXBP151 or T6BP) and COCOA (also known as CALCOCO1). NDP52 does not contain an UBA domain, but instead it binds ubiquitin through a zinc-finger belonging to the ubiquitin-binding zinc-finger (UBZ) class (Thurston, Ryzhakov et al. 2009, Kraft, Peter et al. 2010). Moreover, NDP52 contains a non-canonical LIR consensus motif (CLIR) which has been shown to interact selectively and preferentially with the LC3 isoform C (LC3C) (von Muhlinen, Akutsu et al. 2012). The galectin-8 binding domain of NDP52 is involved in the induction of autophagy upon *Salmonella Tymphimurium* infection (Thurston, Wandel et al. 2012, Boyle and Randow 2013). Felix Randow and colleagues showed that NDP52 is recruited to cytosolic ubiquitin positive bacteria. Since NDP52 directly binds to both ubiquitin and LC3, it functions as an adaptor protein which was shown to be needed for the efficient autophagic degradation of *Salmonella Tymphimurium* (Thurston, Ryzhakov et al. 2009, von Muhlinen, Akutsu et al. 2012). Both p62 and NDP52 restrict intracellular replication of *Salmonella Tymphimurium*. However, p62 and NDP52 are recruited independently to distinct microdomains surrounding the bacteria and cooperate for efficient autophagy of the intracellular bacteria (Cemma, Kim et al. 2011, Johansen and Lamark 2011). NDP52

also coordinates a signalling complex including TBK1, SINTBAD and NAP1 (Thurston, Ryzhakov et al. 2009).

2.10 “Chaperone-assisted degradation”

Three main pathways of chaperone-assisted degradation can be distinguished in higher eukaryotes. The “chaperone-assisted proteasomal degradation” (CAP) involves the ubiquitylation of a chaperone client and its subsequent sorting to the proteasome (Kettern, Dreiseidler et al. 2010). The “chaperone-assisted selective autophagy” (CASA) refers to the engulfment of a ubiquitylated chaperone client by an autophagic isolation membrane leading to lysosomal degradation whereas “chaperone-mediated autophagy” (CMA) relies on the ubiquitin-independent chaperone-assisted transport of a client molecule directly across the lysosomal membrane (Kettern, Dreiseidler et al. 2010). Since the “Heat shock protein 70 kDa” (HSP70) protein can mediate the delivery to all three degradation pathways, the same substrate can in principle be degraded by all three systems. Insufficient degradation by one degradation system is often compensated by increased degradation by another system (Lamark and Johansen 2012).

2.10.1 The heat shock proteins

The constitutively expressed chaperon is termed “Heat shock cognate protein 70 kDa” (HSC70), the stress inducible chaperones are called “Heat shock protein 70 kDa” (HSP70) and “Heat shock protein 90 kDa” (HSP90). HSP90 assures the stability of the HSP90 client proteins (Lanneau, Wettstein et al. 2010). HSP70/HSP90 chaperone complexes have an important role in the quality control of mature proteins. If the chaperones fail to refold a misfolded protein, this normally results in its degradation through the UPS and autophagy. HSP90 protects proteins from unfolding and aggregation, whereas HSP70 is responsible for their degradation in cases when unfolding or aggregation cannot be prevented (fig.15) (Kettern, Dreiseidler et al. 2010, Lamark and Johansen 2012).

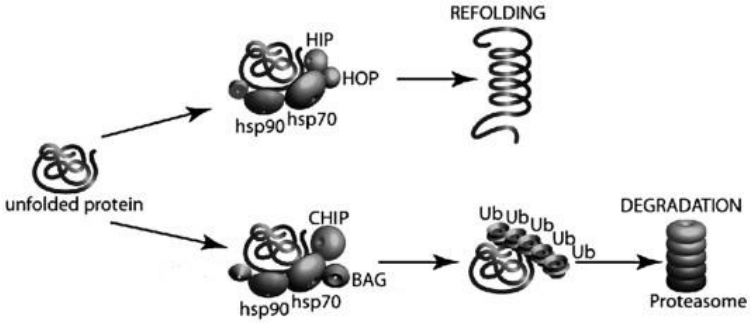

Figure 15: Heat shock proteins between refolding and degradation Protein misfolding is detected by HSP70, which then forms complexes with HSP90, as well as a number of co-chaperones. The HSP70/HSP90 chaperone folding complex is formed upon association with HIP and HOP. The HSP70 chaperone degradation complex includes association with the CHIP and BAG1 (Kalmar and Greensmith 2009).

Protein misfolding is detected by HSP70, which then forms complexes with HSP90, as well as a number of co-chaperones (Kalmar and Greensmith 2009). Depending on the regulatory co-chaperones this results either in the formation of a “folding” or a “degrading” chaperone complex (Kettern, Dreiseidler et al. 2010). The association of the HSP70/HSP90 complex with the co-chaperones “HSP70-interacting protein” (HIP) and “HSP70/HSP90 organizing protein” (HOP) result in the refolding of the client protein (fig.15) (Mayer and Bukau 2005, Kettern, Dreiseidler et al. 2010, Lanneau, Wettstein et al. 2010). Once the protein-HSP70/HSP90 complex associates with the E3 ligase “carboxyl terminus of constitutive HSC70-interacting protein” (CHIP) and the BAG family protein BAG1, the client protein will not be refolded, but ubiquitylated. The ubiquitylated protein will in turn be directed to the proteasome for degradation (fig.11) (Kalmar and Greensmith 2009, Lanneau, Wettstein et al. 2010).

2.10.2 “Chaperone-assisted proteasomal degradation” (CAP)

To be degraded by the UPS, the chaperone clients must be ubiquitylated with K48 linked poly-ubiquitin chains (Kettern, Dreiseidler et al. 2010, Lamark and Johansen 2012). CHIP promotes the proteasomal degradation of HSP70 and HSP90 substrate proteins by ubiquitylating them in a K48-linked mode. By interacting with S5a via its UBL domain, CHIP also participates in the delivery of ubiquitylated proteins to the proteasome (Kettern, Dreiseidler et al. 2010, Lanneau, Wettstein et al. 2010, Johansen and Lamark 2011). BAG1 can also interact with the 20S and the 19S subunit of the proteasome, favouring the proteasome recruitment (Kettern, Dreiseidler et al. 2010, Lanneau, Wettstein et al. 2010, Lamark and Johansen 2012).

However, CHIP is also able to generate K63 chains and target the substrate to the autophagic machinery (Shaid, Brandts et al. 2013).

2.10.3 “Chaperone-assisted selective autophagy” (CASA)

The dedicated chaperone in CASA is BAG3. A multichaperone complex with HSP70 and BAG3 induces selective degradation of misfolded proteins by autophagy (Kettern, Dreiseidler et al. 2010, Lamark and Johansen 2012). Interestingly, aggresome-targeting by BAG3 does not depend on substrate ubiquitylation and is therefore involved in the clearance of misfolded proteins which are not ubiquitylated (Behl 2011). BAG3 co-localises with p62-positive protein aggregates and autophagic markers and also interacts with p62 directly (fig.12). Further, BAG3 was assumed to stimulate the sequestering of proteins into inclusion bodies in concert with SQSTM1 (Gamerdinger, Hajieva et al. 2009, Willis, Townley-Tilson et al. 2010, Shaid, Brandts et al. 2013).

The BAG3:BAG1 ratio within the specific cell decides between CAP and CASA (Lamark and Johansen 2012). The autophagy inducer BAG3 and the proteasome interactor BAG1 compete for the interaction with the chaperone/CHIP complex and thus serve as a molecular switch between CASA and CAP (Kettern, Dreiseidler et al. 2010).

3 Aim of this study

Birte Kalveram found FAT10ylated proteins to be delivered to aggresomes under proteasomal inhibition (Kalveram, Schmidtke et al. 2008). Since aggresomes contain, besides other proteins, also the autophagic adaptor protein p62 (Lamark and Johansen 2012, Li, Shin et al. 2013), Birte Kalveram was interested whether FAT10 would also interact with p62 *in vitro* and found FAT10 to interact with p62 both, covalently and non-covalently. Furthermore she confirmed that the diglycine motif of FAT10 is required for the FAT10-p62 conjugate formation and that the UBA domain of p62 is dispensable for both, the covalent and non-covalent interaction. In addition she could show that p62 seems to be monoFAT10ylated rather than being modified by FAT10 chains (Aichem, Kalveram et al. 2012).

Since there were still many unanswered questions concerning the interactions between FAT10 and p62, the aim of this study was to further confirm and characterise the covalent and non-covalent interactions between FAT10 and p62 *in vitro*. First of all, it should be clarified whether the modification of p62 occurs on lysine residues or even on cysteines, serines or threonines. The next question was, which of the twenty lysines is or are modified and in which domains of p62 these lysines are localised. Furthermore, it should be clarified which domains of p62 are required for the non-covalent interaction with FAT10 and whether the polymerisation capability of p62 is required for the interaction with FAT10. Since the phosphorylation status of p62 at S403 was shown to influence its ubiquitin binding capacities (Matsumoto, Wada et al. 2011) it should be investigated whether the phosphorylation status would also influence the interaction with FAT10. Since FAT10 and its substrates normally become degraded by the proteasome and p62 is mainly turned over via autophagy, the question by which pathway the FAT10-p62 conjugate will be degraded should be answered. Finally it should be investigated whether other autophagy receptors are also able to interact with FAT10. Therefore NBR1, OPTN and NDP52 were tested for their FAT10 interaction capabilities.

4 Material and Methods

4.1 Materials and chemicals

The following chemical compounds were used for this study and the respective manufactures are listed.

Chemical	Company
Acetic Acid	VWR, Darmstadt
Acrylamide - Solution (30 %)	AppliChem, Darmstadt
Agar	Becton Dickinson (BD), Heidelberg
Agarose	SERVA, Heidelberg
Ampicillin	Sigma Aldrich, Steinheim
Ammonium persulfate (APS)	BioRad, München
Aprotinin	AppliChem, Darmstadt
β-Mercaptoethanol	Merck, Darmstadt
Bafilomycin A1	Sigma Aldrich, Steinheim
Bromophenol Blue	AppliChem, Darmstadt
BSA	Sigma Aldrich, Steinheim
BSA (non-acetylated)	Thermo Scientific, Rockford
Chloramphenicol	Roche, Penzberg
Coomassie Brilliant Blue	SERVA, Heidelberg
Cycloheximide	Sigma Aldrich, Steinheim
Dimethyl sulfoxide (DMSO)	Sigma Aldrich, Steinheim
DL-Dithiothreitol (DTT)	Sigma Aldrich, Steinheim
EDTA	Carl Roth, Karlsruhe
Ethanol (EtOH)	Riedel-de Haen, Seelze
Ethidium Bromide	Sigma Aldrich, Steinheim
Glucose	Sigma Aldrich, Steinheim

L-Glutathione reduced	Sigma Aldrich, Steinheim
Glycerol	VWR, Darmstadt
Glycine	Carl Roth, Karlsruhe
HCL, 37 %	VWR, Darmstadt
Isopropyl-β-D-thiogalactopyranosid (IPTG)	Sigma Aldrich, Steinheim
Kanamycin	Carl Roth, Karlsruhe
KCl	Merck, Darmstadt
KH_2PO_4	Carl Roth, Karlsruhe
Leupeptin	Roche, Penzberg
Methanol (MeOH)	Chemikalienlager
$MgCl_2$	Acros Organics, Geel
MG132 (Z-Leu-Leu-Leu-al)	Sigma Aldrich, Steinheim
NaCl	VWR, Darmstadt
NaOH	Sigma Aldrich, Steinheim
Na_2HPO_4	Sigma Aldrich, Steinheim
Na_2HPO_4 $2H_2O$	Sigma Aldrich, Steinheim
N,N,N',N'-Tetramethylethylendiamin (TEMED)	SERVA, Heidelberg
Pepstatin	Roche, Penzberg
Phenol red	Merck, Darmstadt
Phenylmethylsulfonyl fluoride (PMSF)	Sigma Aldrich, Steinheim
Ponceau S	Merck, Darmstadt
2-Propanol	Riedel-de Haen, Seelze
Sodium Dodecyl Sulfate (SDS)	SERVA, Heidelberg
TRIS	Invitrogen, Karlsruhe
Triton-X-100	Merck, Darmstadt
TRIZMA	Sigma Aldrich, Steinheim
Tween® 20 (Polysorbat)	Merck, Darmstadt

Tryptone	Becton Dickinson (BD), Heidelberg
Yeast extract	Becton Dickinson (BD), Heidelberg

The following technical equipment was used for this study and the respective manufactures are listed.

Equipment	Designation	Company
Centrifuge	Sorvall™ Evolution	Thermo scientific, Rockford
Centrifuge	Heraeus™ Multifuge™ X3 Centrifuge Series	Heraeus, Hanau
Centrifuge	Heraeus™ Pico™	Heraeus, Hanau
Centrifuge	Heraeus™ Fresco™	Heraeus, Hanau
Centrifugation tube	15 ml/50 ml, conical	TPP, Trasadingen
DNA gel electrophoresis	Mini-Sub® Cell GT System	BioRad, München
Flask 75 cm^2 (tissue culture) Flask 150 cm^2 (tissue culture)	75, Filter, 150 x 85 x 35, PS 150, Filter, 205 x 120 x 45, PS	TPP, Trasadingen
Fluorescence and Absorbance Microplate Reader	Tecan Spectrafluor Plus Plate Reader	Tecan Group, Männedorf
Gel dryer	Gel dryer, model 583	BioRad, München
Haemocytometer	Neubauer Chamber	
Imager	Molecular Imager® Gel Doc™	BioRad, München
Imager	ChemiDoc™	BioRad, München
Imaging Plate and Cassette	Storage Phosphor Screen BAS 2040	FujiFilm, Düsseldorf
laminar flow cabinet	Heraeus LaminAir HB2472	Heraeus, Hanau
laminar flow cabinet	HERAsafe HS12	Heraeus, Hanau
Nitrocellulose blotting membrane	Nitrocellulose blotting membrane; 0,45 µm pore size	GE Healthcare, München
Nitrocellulose blotting membrane; 0,2 µm pore size	Nitrocellulose blotting membrane; 0,2 µm pore size	GE Healthcare, München

PCR-thermocycler	Thermocycler T3	Biometra, Göttingen
Phospho-imager	Bio-Rad Personal Molecular Imager FX	BioRad, München
Pipettes	PIPETMAN Classic™ P20, P200, and P1000	Gilson International, Limburg
	Eppendorf Research® plus: 0,5–10 µl	Eppendorf, Hamburg
Pipette controller	PIPETBOY acu precision pipette	INTEGRA Biosciences GmbH (IBS), Fernwald
Plates 60x15 mm (tissue culture)	60x15 mm,STERIL	Greiner bio one, Frickenhausen
Powersupply:	PowerPac 100 PowerPac 300 PowerPac HC	BioRad, München
PVDF membrane	Amersham Hybond 0.2 µm PVDF	GE Healthcare, München
Reaction tubes (1,5/2 ml)		Eppendorf, Hamburg
Reaction tubes (0,5 ml)	Safe-Lock Tubes (0.5 ml)	Eppendorf, Hamburg
Scale	Mettler Toledo AG204 Delta Range Balance	Mettler Toledo, Greifensee
Screen Eraser	Bio-Rad Screen Eraser	BioRad, München
SDS-PAGE	Mini-PROTEAN® Tetra cell	BioRad, München
Shaker	Unimax 1010	Heidolph, Schwabach
Sonicator	Ultrasonic homogenizer, SONOPULS HD	Bandelin electronic, Berlin
Spectrophotometer	NanoVue™ Plus	GE Healthcare, München
Thermo mixer	Thermo mixer comfort	Eppendorf, Hamburg
Test Tube Rotator	Test Tube Rotator	Snijders, Tilburg
Vacuum pump	IBS VACUSAFE	IBS - INTEGRA Biosciences, Fernwald
Vortex mixer	Vortex Genie®2	scientific industries, Bohemia, New York
6-wells (tissue culture) 96-wells (tissue culture)	CELLSTAR® 6-wells CELLSTAR® 96-wells	Greiner bio one, Frickenhausen

Western blot (Semi-Dry)	Fastblot 34	Biometra, Göttingen
Western blot (Wet-blot)	Criterion™ Blotter	BioRad, München
Whatman paper		GE Healthcare, München

In table 1, the plasmids which were used in this study are listed. Further, the donor, the publication and the modifications which were performed in the course of this study are mentioned.

Table 1: DNA plasmids used in this study.

Name	Published	Source	Modifications for this study
GST-FAT10	(Hipp, Raasi et al. 2004)	our lab	
(GST) pGEX-4T-3		Amersham Biosciences	
His-3*Flag-FAT10	(Chiu, Sun et al. 2007)	Ph.D. Zhijian J. Chen, Dallas	
His-3*Flag-FAT10ΔGG	(Aichem, Pelzer et al. 2010)	our lab	
HA-FAT10	(Raasi, Schmidtke et al. 2001)	our lab	
HA-FAT10ΔGG	(Raasi, Schmidtke et al. 2001)	our lab	
HA-OPTN	(Wild, Farhan et al. 2011)	Prof. Dr. Ivan Dikic, Frankfurt	
HA-OPTN(5*A)	(Wild, Farhan et al. 2011)	Prof. Dr. Ivan Dikic, Frankfurt	
HA-OPTN(5*E)	(Wild, Farhan et al. 2011)	Prof. Dr. Ivan Dikic, Frankfurt	
EGFP-NDP52	(Cemma, Kim et al. 2011)	Dr. John Kendrick-Jones, Cambridge	
pENTR-p62Δ1-123		Prof. Dr. Terje Johansen, Tromsø	
pENTR-p62Δ123-170		Prof. Dr. Terje Johansen, Tromsø	
pENTR-p62Δ123-256		Prof. Dr. Terje Johansen, Tromsø	
pENTR-p62Δ123-319		Prof. Dr. Terje Johansen, Tromsø	
pENTR-p62Δ170-256		Prof. Dr. Terje Johansen, Tromsø	

pENTR-p62Δ257-370		Prof. Dr. Terje Johansen, Tromsø	
pENTR-p62Δ257-440		Prof. Dr. Terje Johansen, Tromsø	
pENTR-p62Δ321-348		Prof. Dr. Terje Johansen, Tromsø	
pENTR-p62Δ371-386		Prof. Dr. Terje Johansen, Tromsø	
pENTR-p62Δ386-440		Prof. Dr. Terje Johansen, Tromsø	
pDEST-HA	(Lamark, Perander et al. 2003)	Prof. Dr. Terje Johansen, Tromsø	
HA-p62Δ1-123		this study	
HA-p62Δ123-170		this study	
HA-p62Δ123-256		this study	
HA-p62Δ123-319		this study	
HA-p62Δ170-256		this study	
HA-p62Δ257-370		this study	
HA-p62Δ257-440		this study	
HA-p62Δ321-348		this study	
HA-p62Δ371-386		this study	
HA-p62Δ386-440		this study	
HA-NBR1	(Lamark, Perander et al. 2003)	Prof. Dr. Terje Johansen, Tromsø	HA-tag repaired with site-directed mutagenesis
HA-p62	(Lamark, Perander et al. 2003)	Prof. Dr. Terje Johansen, Tromsø	HA-tag repaired with site-directed mutagenesis
HA-p62(K0)		this study	
HA-p62(K7R/D69R)		this study	
HA-p62(S403A)		this study	
HA-p62(S403E)		this study	
p62-6*His	(Aichem, Kalveram et al. 2012)	our lab	
p62(K0)-6*His	(Aichem, Kalveram et al. 2012)	this study	
pcDNA6/myc-His-A		Invitrogen, Karlsruhe	
HA-p62(PB1 only)		this study	
HA-p62(PEST only)		this study	
HA-p62(TRAF only)		this study	
HA-p62(UBA only)		this study	

DNA sequencing and DNA oligonucleotide synthesis were carried out by commercial providers (tab.2).

Table 2: DNA sequencing and synthesis of DNA oligonucleotides.

Services	Company
Synthesis of DNA oligonucleotides	Microsynth AG, Balgach
DNA sequencing	GATC, Konstanz

The following antibodies were used for western blot analysis in this study. Further, their final concentrations and respective manufacturers are mentioned (tab.3).

Table 3: The antibodies used for this study.

Name	target species	source species	type	Company	final concentration
Anti-Actin	human	mouse	mAb	Sigma-Aldrich, Steinheim	1:2000
Anti-CALCOCO2 (ab68588)	human	rabbit	pAb	Abcam, Cambridge	1:1000
Anti-Flag (M2)		mouse	mAb	Sigma-Aldrich, Steinheim	1:2000
Anti-Flag-HRP (M2)		mouse	mAb	Sigma-Aldrich, Steinheim	1:2000
Anti-GAPDH-71.1	human	mouse	mAb	Sigma-Aldrich, Steinheim	1:5000
Anti-GFP G1544	human	rabbit	pAb	Sigma-Aldrich, Steinheim	1:1000
Anti-GST					
Anti-guinea pig-HRP	guinea pig	rabbit	pAb	Dako, Hamburg	1:2000
Anti-HA (7)		mouse	mAb	Sigma-Aldrich, Steinheim	1:2000
Anti-HA-HRP (HA-7)		mouse	mAb	Sigma-Aldrich, Steinheim	1:2000
Anti-HA (12CA5)		mouse	mAb	Roche, Penzberg	1:2000
Anti-HA -HRP (12CA5)		mouse	mAb	Roche, Penzberg	1:500
Anti-His_6		mouse	mAb	Roche, Penzberg	0,3 µg/ml
Anti-His_6-HRP		mouse	mAb	Roche, Penzberg	1:2000
Anti-mouse-HRP	mouse	goat	pAb	Dako, Hamburg	1:2000
Anti-NBR1	human	mouse	mAb	Abnova, Heidelberg	1:1000
Anti-p62/SQSTM1 (H290)	human	rabbit	pAb	Santa Cruz, Heidelberg	1:400
Anti-p62/SQSTM1 (GP62)	human	guinea pig	pAb	Progen, Heidelberg	1:500
Anti-rabbit-HRP	rabbit	swine	pAb	Dako, Hamburg	1:2000
Anti-Tubulin (B-5-1-2)	human	mouse	mAb	Sigma-Aldrich, Steinheim	1:2000

4.2 Methods

4.2.1 Gel electrophoresis

4.2.1.1 Agarose gel electrophoresis

For agarose gel electrophoresis, the following chemicals and compounds were used (tab.4-6).

Table 4: Tris-acetate-EDTA (TAE)-buffer.

Compounds	Concentration [mM]
TRIS	40
Acetic acid	20
EDTA	1
pH	7,5

Table 5: 6xDNA loading buffer.

Compounds	Concentration
Glycerol	12 %
EDTA	60 mM
Bromphenol blue	0,0003 %

Table 6: DNA ladders used for agarose gel electrophoresis.

Ladder	Company
SmartLadder – 200 – 10000 bp	Eurogentec, Köln
SmartLadder SF – 100 – 1000 bp	

Handcast 2 % agarose gels were prepared with TAE-buffer and 1 µl Ethidium Bromide per 50 ml gel. The gels were run in TAE-buffer at 90 V until the DNA is separated to the desired level. For analysis the Molecular Imager® Gel Doc™ was used.

4.2.1.2 SDS-Polyacrylamide gel electrophoresis (PAGE)

SDS-PAGE was performed with the Mini-PROTEAN® Tetra Handcast System and the handcast gels were prepared according to the protocols in table 7 and 8.

Table 7: Resolving gels for tris-glycine SDS-PAGE.

	Acrylamide concentration			
Compounds	10 %	12 %	15 %	18 %
ddH_2O [ml]	1,9	1,6	1,1	0,6
Acrylamide solution (30 %)	1,7	2,0	2,5	
1,5 M TRIS (pH 8,8) [ml]	1,3	1,3	1,3	1,3
10 % SDS [ml]	0,05	0,05	0,05	0,05
10 % ammonium persulfate [ml]	0,05	0,05	0,05	0,05
TEMED [ml]	0,002	0,002	0,002	0,002

Table 8: 5 % stacking gels for tris-glycine SDS-PAGE.

Compounds	Amount [µl]
ddH_2O	680
Acrylamide solution (30 %)	170
1,0 M TRIS (pH 6,8)	130
10 % SDS	10
10 % Ammonium persulfate	10
TEMED	1

SDS-PAGE was performed by using running buffer (tab.9). The utilised protein ladders are listed in table 10.

Table 9: SDS-PAGE running-buffer.

Compounds	Concentration
TRIZMA	25 mM
Glycine	200 mM
SDS	0,1 %
ddH_2O	Ad 1000 ml

Table 10: Protein ladders for SDS-PAGE.

Protein ladder	Company
PageRuler Prestained Protein Ladder, 10 - 170 kDa	Thermo Schientific, Rockford
PageRuler Plus Prestained Protein Ladder, 10 - 250 kDa	
Spectra Multicolor High Range Protein Ladder, 40 - 300 kDa	
Spectra Multicolor Low Range Protein Ladder, 1,7 - 40 kDa	

The gels were run for 30 minutes at 60 V and afterwards at 120 V until the desired protein separation is achieved.

4.2.2 Western blotting (protein immunoblot)

Two different blotting techniques were used for protein transfer: semi-dry and wet-blotting.

Semi-dry blotting

For semi-dry blotting the Fastblot B34 system was used for which Whatman-filter papers were soaked in semi-dry blotting buffer (tab.11).

Table 11: Semi-dry blotting buffer.

Compounds	Concentration
TRIZMA	25 mM
Glycine	200 mM
Methanol	10 %
ddH_2O	Ad 1000 ml

Semi dry blotting was conducted at 120 mA for 12 Vh.

Wet-blotting

For wet-blotting, the tank of the Criterion™ Blotter was filled with wet blotting buffer (tab.12).

Table 12: Wet blotting buffer.

Compounds	Concentration
TRIZMA	25 mM
Glycine	192 mM
Methanol	20 %
ddH_2O	Ad 1000 ml

Wet blotting was performed for 40 minutes at 950 mA.

4.2.2.1 Blocking, antibody staining and protein detection

Table 13: T-PBS.

Compounds	Concentration
PBS	1x
Tween® 20 (Polysorbat)	0,002%

Table 14: Blocking and stripping solutions and Chemiluminescent substrate.

Compounds	Concentration
Roti®-Block 10x	Carl Roth, Karlsruhe
Restore Western Blot Stripping Buffer	Thermo Schientific, Rockford
SuperSignal West Pico Chemiluminescent Substrate	

Table 15: Software used for autoradiogram and western blot analysis.

Software	Company
Quantity One 1-D Analysis Software 4.6.6	BioRad, München
Adobe Photoshop 7.0	Adobe, München

After western blotting, the blotting membranes were stained with Ponceau S in order to test for successful blotting. Subsequently, the membranes were destained by washing with T-PBS (tab.13). The destained membranes were blocked for 1 hour in 1xRoti®-Block (tab.14). The blocked membranes were incubated with the respective primary antibody for either 1 hour at room temperature or over night at 4 °C. In case of a not directly HRP-labelled primary antibody, the membranes were washed with

T-PBS and then incubated with the appropriate HRP-labelled secondary antibody for 1 hour at room temperature. Prior to western blot imaging, the antibody covered membranes were washed with T-PBS (tab.13). Imaging was performed according to the manufacturer's protocols for the SuperSignal West Pico Chemiluminescent substrate (tab.14) and the ChemiDoc™ imaging system. Final analysis of the images was done using the Quantity One 1-D Analysis Software and Photoshop (tab15).

4.2.3 Bacterial culture & DNA purification

In order to store and replicate plasmids, competent *E.coli* cells (tab.16) were heat shock transformed with plasmid DNA and cultivated with the appropriate selection antibiotic in either liquid LB medium or on LB plates (tab.17).

Table 16: Competent cells for storage and replication of plasmid DNA.

***E.coli* strain**	**Antibiotic resistance**	**Company**
XL10-Gold© Ultracompetent Cells	Tetracycline/Chloramphenicol	Agilent Technologies, Karlsruhe
XL1-Blue© Competent Cells	Tetracycline	

Table 17: liquid and solid Luria Bertani (LB) medium for bacterial cultures.

Compounds	**Liquid**	**Solid**
Tryptone	10 g	10 g
Yeast Extract	5 g	5 g
NaCl	10 g	10 g
Agar	-	15 g
ddH_2O	Ad 1000 ml	

Table 18: Super Optimal Broth (SOB) and Super Optimal Broth with Catabolite repression (SOC) for transformation.

Compounds	SOB	SOC
Tryptone	20 g	20 g
Yeast extract	5 g	5 g
NaCl	0,5 g	0,5 g
KCl	0,186 g	0,186 g
$MgCl_2$	0,95 g	0,95 g
Glucose	-	5 g
ddH_2O	Ad 1000 ml	

Table 19: Antibiotics used for bacterial selection.

Antibiotic	Final concentration [µg/ml]
Ampicillin (Amp)	100
Chloramphenico (Camp)l	35
Kanamycin (Kan)	25

Table 20: Plasmid purification kits used for isolation of plasmid DNA.

Plasmid purification kits	Company
NucleoSpin® Plasmid MiniPrep	Macherey & Nagel, Düren
NucleoBond® PC 500 MaxiPrep	Macherey & Nagel, Düren
QIAGEN Plasmid Maxi Kit MaxiPrep	QIAGEN, Hilden

4.2.3.1 Transformation of bacteria and plasmid purification

Heat shock transformation of chemically competent E.coli cells

100 µl competent cells were thawed on ice and 1 - 3 µl of the desired plasmid DNA, depending on the respective DNA concentration, was added. The mixture was incubated on ice for 30 minutes and afterwards heat shocked at 42 °C for 45 seconds. After the heat shock, the cells were incubated for 2 minutes on ice before 500 µl of pre-warmed SOC-medium (tab.18) (without antibiotic) was added. The mixture of transformed bacteria and SOC-medium was incubated for 1 hour at 37 °C. Subsequently, 10 µl, 50 µl, 100 µl and 500 µl of the transformed bacteria were

plated on LB-agar plates (tab.17) containing the appropriate selection antibiotic. The LB-agar plates were incubated overnight at 37 °C. Five millilitre of the likewise antibiotic containing liquid LB-medium (tab.17) were inoculated with single colonies which were picked from the plates. The 5 ml cultures were incubated overnight at 37 °C and 250 rpm. Glycerol stocks were prepared by exhaustively mixing 800 µl of the bacterial cultures with 200 µl of sterile glycerol and were stored at -80 °C. The remaining bacterial cultures were centrifuged at 4500 rpm for 15 minutes and the supernatants discarded. The bacterial pellets were used for plasmid DNA purification using the NucleoSpin® Plasmid MiniPrep kit (tab.20) according to the manufacturer's protocol.

4.2.4 Cloning and site-directed mutagenesis experiments

4.2.4.1 Traditional (restriction enzyme and ligase-based) cloning

In order to investigate the FAT10-p62 interaction, a His-tagged p62(k0) construct has been prepared (p62(k0)-6*His). Further the PB1, PEST, TRAF and UBA domains of HA-p62 were isolated from p62 and provided with a HA-tag [HA-p62(PB1 only), HA-p62(PEST only), HA-p62(TRAF only) and HA-p62(UBA only)].

Table 21: Kits and compounds used for cloning.

Kits/compunds	Company
GoTaq® DNA Polymerase	Promega, Mannheim
Phusion® High-Fidelity DNA Polymerase	NEB, Frankfurt
KAPAHiFi ™ DNA Polymerase	Peqlab, Erlangen
$MgCl_2$	Promega, Mannheim
Shrimp Alkaline Phosphatase (SAP)	Promega, Mannheim
T4 DNA ligase	Promega, Mannheim
NucleoSpin® Gel and PCR Clean-up	Macherey & Nagel, Düren
Gateway® LR Clonase® Enzyme mix	Invitrogen™, Karlsruhe

Table 22: Restriction enzymes used for cloning and control digests.

Restriction enzymes	Company
KpnI	Fermentas, Thermo Scientific, Schwerte
XbaI	
EcoRI	
BshTI	

*Cloning of p62(k0)-6*His*

For generation of p62(K0)-6*His, p62(K0) was PCR-amplified (tab.23, 24) from HA-p62(K0) (tab.1) and the cDNA inserted into the EcoRI and BshTI sites of pcDNA6/myc-His-A (tab.1). The PCR was run using the GoTaq®DNA polymerase (tab.21). The $MgCl_2$ concentration of 1,5 mM in the reaction mixture was increased by adding additionally 1 mM $MgCl_2$ (tab.21).

Table 23: PCR reaction mixture for p62(K0)-His cloning.

Compounds	Name	Sequence	Concentration/ amount
Upstream primer	p62-K0-1F EcoRI	5'-gtcggaattcatggcgtcgctcaccgtgagg-3'	0,5 µM
Downstream primer	P62-K0-440R BshTI	5'-tagcaccggtcaacggcgggggatgccttg-3'	0,5 µM
Template DNA	HA-p62-K0		0,5 µg
dNTPs			200 µM each
Polymerase	GoTaq Polymerase		2,75 U
$MgCl_2$			1 mM
Reaction Buffer	5x-colourless GoTaq Reaction buffer		1x
ddH_2O			Ad 25 µl

Table 24: PCR program for p62(K0)-His cloning.

Segment	Cycle	Temperature [°C]	Time [min]
1	1	94	2
2	35	94	0,5
		56	0,5
		72	1,5
3	1	72	5

The purified PCR product (NucleoSpin® Gel and PCR Clean-up, tab.21) was digested with the restriction enzymes EcoRI and BshTI (tab.22), separated by agarose gel electrophoresis and purified again (NucleoSpin® Gel and PCR Clean-up, tab.21).

The pcDNA6/myc-His-A plasmid (tab.1) was also digested with EcoRI and BshTI (tab.22) The enzymatically digested plasmid was separated by agarose gel electrophoresis, subsequently purified (NucleoSpin® Gel and PCR Clean-up, tab.21) and afterwards dephosphorylated with “shrimp alkaline phosphatise” (SAP) (tab.21) according to the manufactures protocol. For ligation 200 ng of the digested and dephosphorylated pcDNA6/myc-His-A plasmid and 600 ng of the digested and purified PCR p62(K0) product were used for ligation. Ligation was carried out with the T4 DNA ligase (tab.21) according to the manufacturer’s protocol. The ligation product was transformed into XL10-Gold (tab.16) and the cloning success confirmed by control restriction enzyme digests and by sequence analysis.

Cloning of the isolate p62 domains: HA-p62(PB1 only), HA-p62(PEST only) HA-p62(TRAF only) and HA-p62(UBA only)

The respective p62 domains were PCR amplified (tab.25-29) from HA-p62 (tab.1) using either the KAPAHiFi ™ DNA Polymerase (tab.21) [HA-p62(PB1 only)] or the Phusion® High-Fidelity DNA Polymerase (tab.21) [HA-p62(PEST only), HA-p62(TRAF only), HA-p62(UBA only)]. The pcDNA3-HA-FAT10 plasmid (tab.1) was digested enzymatically with KpnI and XbaI (tab.22) to remove FAT10. The PCR products were then inserted into the KpnI and XbaI sites of the HA-pcDNA3 vector.

Table 25: Primers for HA-p62(domains only) cloning.

Primers	Name	Sequence
Upstream primer	N-KpnI PB1	5'-gtaattggtaccactcaccgtgaagg-3'
Downstream primer	C-XbaI PB1	5'-actaattctagactatttctctttaatgtagattcgg-3'
Upstream primer	N-KpnI PEST	5'-gtaattggtaccaagccgcctgacccccg-3'
Downstream primer	C-XbaI PEST neu	5'-actaattctagactagctggggtcagagcagcagc-3'
Upstream primer	N-KpnI TRAF	5'-gtaattggtaccagcttctggtccatcgg-3'
Downstream primer	C-XbaI TRAF neu	5'-actaattctagactacagagggctaagggc-3'
Upstream primer	N-KpnI UBA	5'-gtaattggtaccactgattgagtccctctccc-3'
Downstream primer	C-XbaI UBA	5'-actaattctagactagatggtgtccagagccg-3'

Table 26: PCR reaction for HA-p62(PB1 only) cloning.

Compounds	Concentration/ amount
Upstream primer: N-KpnI PB1	300 nM
Downstream primer: C-XbaI PB1	300 nM
HA-p62 template DNA	100 ng
dNTP mix	300 nM each
KAPAHiFi ^{TM} DNA Polymerase	0,02 U/µl
DMSO	5 %
5x Reaction buffer fidelity	1x
ddH_2O	Ad 25 µl

Table 27: PCR program for HA-p62(PB1 only) cloning.

Segment	Cycle	Temperature [°C]	Time [sec]
1	1	95	300
2	30	98	20
		50	15
		72	40
3	1	72	300

Table 28: PCR reaction for HA-p62 (PEST only), HA-p62 (TRAF only) and HA-p62 (UBA only) cloning.

Compounds	Concentration
Upstream primer:	500 nM
Downstream primer:	500 nM
HA-p62 template DNA	25 ng
dNTP mix	200 µM each
Phusion® High-Fidelity DNA Polymerase	0,02 U/µl
DMSO	3 %
5X Phusion HF or GC Buffer	1x
ddH_2O	Ad 25 µl

Table 29: PCR program for HA-p62 (PEST only), HA-p62 (TRAF only) andHA-p62 (UBA only) cloning.

Segment	Cycle	Temperature [°C]	Time [sec]
1	1	98	30
2	30	98	10
		55	20
		72	20
3	1	72	300

The purified PCR product (NucleoSpin® Gel and PCR Clean-up) was digested with the restriction enzymes KpnI and XbaI (tab.22) and purified (NucleoSpin® Gel and PCR Clean-up, tab.21).

The pcDNA3-HA-FAT10 (tab.1) was digested with the restriction enzymes KpnI and XbaI (tab.22) in order to remove the FAT10 insert. The restriction digested plasmid was separated by agarose gel electrophoresis, subsequently purified (NucleoSpin® Gel and PCR Clean-up, tab.21) and afterwards dephosphorylated with “shrimp alkaline phosphatise” (SAP) (tab.21) according to the manufacturer’s protocol. For ligation 200 ng of digested and dephosphorylated pcDNA3-HA plasmid and 600 ng of digested and purified PCR product were used for ligation. The ligation was done using the T4 DNA ligase (tab.21) according to the manufacturer’s protocol. The ligation product was transformed into XL10-Gold (tab.16). In order to confirm the

successful cloning, control restriction enzyme digests and sequence analyses were performed.

4.2.4.2 Gateway® cloning

The Gateway® recombination cloning technology was used in order to clone the p62 insertions from the pENTR vectors: pENTR-p62Δ1-123, pENTR-p62Δ123-170, pENTR-p62Δ123-256, pENTR-p62Δ123-319, pENTR-p62Δ170-256, pENTR-p62Δ257-319, pENTR-p62Δ257-370, pENTR-p62Δ257-440, pENTR-p62Δ321-348, pENTR-p62Δ371-386 and pENTR-p62Δ386-440 into the pDEST-HA vector (tab.1). The Gateway cloning was carried out by means of the Gateway® LR Clonase® Enzyme mix (tab.21) according to the manufacturer's protocol, resulting in the following constructs: pDEST HA p62Δ1-123, pDEST-HA-p62Δ123-170, pDEST-HA-p62Δ123-256, pDEST-HA-p62Δ123-319, pDEST-HA-p62Δ170-256, pDEST-HA-p62Δ257-319, pDEST-HA-p62Δ257-370, pDEST-HA-p62Δ257-440, pDEST-HA-p62Δ321-348, pDEST-HA-p62Δ371-386, pDEST-HA-p62Δ386-440 (tab.1).

4.2.4.3 Site-directed mutagenesis

The site-directed mutagenesis was conducted in order to mutate all twenty lysines in p62, as well as the three lysines between the HA-tag and the p62 insert into arginines. Moreover, site-directed mutagenesis was used in order to obtain the HA-p62 mutants HA-p62(K7R/D69R), HA-p62(S403A), HA-p62(S403E) and to correct undesired random mutations in HA-p62. Different site-directed mutagenesis kits (tab.30) were used according to the respective manufacturer's protocols.

Table 30: Site-directed mutagenesis kits.

Kits	Company
QuikChange Multi Site-Directed Mutagenesis Kit	Agilent Technologies, Karlsruhe
QuikChange II XL Site-Directed Mutagenesis Kit	Agilent Technologies, Karlsruhe

The mutagenesis primers (tab.31) were designed with the QuikChange primer design tool provided by Agilent on their homepage.

Table 31: Summary of the primers used for the site-directed mutagenesis.

Primer name	Experiment	Sequence 5'-3'	Agilent Mutagenesis Kit
HA-p62(K7R)	HA-p62 lysine mutation	ggcgtcgctcaccgtgagggcctacct	QuikChange Multi Site-Directed Mutagenesis Kit
HA-p62(K13R)	HA-p62 lysine mutation	ctaccttctgggcagggaggacgcggc	QuikChange Multi Site-Directed Mutagenesis Kit
HA-p62(K91R)	HA-p62 lysine mutation	atggccatgtcctacgtgagggatgacatcttcc	QuikChange Multi Site-Directed Mutagenesis Kit
HA-p62(K100R)	HA-p62 lysine mutation	ggatgacatcttccgaatctacattagagagagaagagagtgcc	QuikChange Multi Site-Directed Mutagenesis Kit
HA-p62(K102R K103R)	HA-p62 lysine mutation	atcttccgaatctacattaaagagagaagagagtgccggcgg	QuikChange Multi Site-Directed Mutagenesis Kit
HA-p62(K141R)	HA-p62 lysine mutation	ggaacccgctacaggtgcagcgtctgc	QuikChange Multi Site-Directed Mutagenesis Kit
HA-p62(K157R)	HA-p62 lysine mutation	gcgtctgcgagggaaggggcttgcac	QuikChange Multi Site-Directed Mutagenesis Kit
HA-p62(K165R)	HA-p62 lysine mutation	cgggggcacaccaggctcgcattcc	QuikChange Multi Site-Directed Mutagenesis Kit
HA-p62(K187R K189R)	HA-p62 lysine mutation	cgctggctccggagggtgagacacggacact	QuikChange Multi Site-Directed Mutagenesis Kit
HA-p62(K238R)	HA-p62 lysine mutation	gagtgtgaatttcctgaggaacgttggggagagtg	QuikChange Multi Site-Directed Mutagenesis Kit
HA-p62(K264R)	HA-p62 lysine mutation	gagcacggagggagaagaagccgcctg	QuikChange Multi Site-Directed Mutagenesis Kit
HA-p62(K281R)	HA-p62 lysine mutation	cagcacagaggagaggagcagctcacagc	QuikChange Multi Site-Directed Mutagenesis Kit
HA-p62(K295R)	HA-p62 lysine mutation	gctctgaccccagcaggccgggtg	QuikChange Multi Site-Directed Mutagenesis Kit
HA-p62(K313R)	HA-p62 lysine mutation	cggagcagatgaggaggatcgccttggagtc	QuikChange Multi Site-Directed Mutagenesis Kit
HA-p62(K344R)	HA-p62 lysine mutation	ggacccatctgtcttcaagagaagtggacccgtc	QuikChange Multi Site-Directed Mutagenesis Kit
HA-p62(K378R)	HA-p62 lysine mutation	ggacccacagggctgagggaagctgc	QuikChange Multi Site-Directed Mutagenesis Kit
HA-p62(K420R)	HA-p62 lysine mutation	ggctcctgcagaccaggaactatgacatcgg	QuikChange Multi Site-Directed Mutagenesis Kit
HA-p62(K435R)	HA-p62 lysine mutation	ggacaccatccagtattcaaggcatcccccgc	QuikChange Multi Site-Directed Mutagenesis Kit
HA-(K1R K2R)p62	HA-p62 lysine mutation between tag and insert	gggaattatcaaacaagtttgtacagaagagcaggctttggccgctcg	QuikChange Multi Site-Directed Mutagenesis Kit
HA-(K3R)p62	HA-p62 lysine mutation between tag and insert	ggctttggccgctcgagattccgggccagctcg	QuikChange Multi Site-Directed Mutagenesis Kit

HA-p62(S247A)	correction of random mutations	gagagtgtggcagctgcccttagccctg	QuikChange Multi Site-Directed Mutagenesis Kit
HA-p62(V251L)	correction of random mutations	gcagctgcccttagccctttgggcattgaa	QuikChange Multi Site-Directed Mutagenesis Kit
HA-p62(K7R D69R) K7R	oligomerisation deficient p62 mutant	ggcgtcgctcaccgtgagggcctacct	QuikChange Multi Site-Directed Mutagenesis Kit
HA-p62(K7R D69R) D69R	oligomerisation deficient p62 mutant	ggcgcactaccgccgtgaggacgggg ac	QuikChange Multi Site-Directed Mutagenesis Kit
HA-p62(S403A)	non-phosphorylation p62 mutant	ctctcccagatgctggccatgggcttctct g	QuikChange Multi Site-Directed Mutagenesis Kit
HA-p62(S403E)	phospho-mimicing p62 mutant	gtccctctcccagatgctggagatgggct tctctgatgaag	QuikChange Multi Site-Directed Mutagenesis Kit
HArepairYPin sert	HA(repair)-p62 and HA(repair)-p62(K0)	cccaagcttgccgccaccatgtacccct atgatgttcctgattatgctagcc	QuikChange II XL Site-Directed Mutagenesis Kit
HArepairYPin s rwd	HA(repair)-p62 and HA(repair)-p62(K0)	ggctagcataatcaggaacatcatagg ggtacatggtggcggcaagcttggg	QuikChange II XL Site-Directed Mutagenesis Kit

4.2.5 HEK293T cell culture

4.2.5.1 Culturing HEK293T Cells

All experiments in this study were conducted using HEK293T cells. The tissue culture media and supplements used for cell cultivation and experiments are listed in table 32-33.

Table 32 Commercial tissue culture media and supplements.

Media and supplements	Company
Iscove's Modified Dulbecco's Media (IMDM)	Gibco/Life Technologies GmbH, Darmstadt
Fetal Bovine Serum (FBS)	Gibco/Life Technologies GmbH, Darmstadt
Penicillin/Streptomycin (Pen/Strep)	Gibco/Life Technologies GmbH, Darmstadt
0,25% Trypsin-EDTA (1X), Phenol Red	Gibco/Life Technologies GmbH, Darmstadt

Table 33: 1xPBS.

Compounds	Concentration [mM]
NaCl	136,9
KCl	2,7
Na_2HPO_4	10,2
KH_2PO_4	18
ddH_2O	Ad 1000 ml
	pH 7,4

HEK293T cells were cultured in IMDM medium supplemented with 10 % FBS and 0,1 mg/ml Penicillin/Streptomycin (complete IMDM) (tab.32) at 37 °C and 5 % CO_2. The cells were maintained in either 75 cm^2 or 150 cm^2 tissue culture flasks until they reached 70 - 80 % confluence. Prior to adding Trypsin/EDTA (tab.32), in order to detach the adherent cells from the culture flasks, the cells were washed once with 1xPBS (tab.33). Detached cells were diluted with FBS-containing complete IMDM in order to inactivate the Trypsin/EDTA and the cell suspension was centrifuged for 3 minutes at 800 rpm. The supernatant was removed and the cell pellet resuspended in complete IMDM medium. Cells numbers were determined using a Neubauer chamber. Afterwards, cells were either partially refilled into tissue culture flasks for culture maintenance or seeded for experiments. For long term storage liquid nitrogen stocks were prepared using 10 % DMSO and 90 % FBS.

4.2.6 Transient transfection experiments

The Mirus TransIT®-LT1-transfection reagent (tab.34) was used in order to transiently transfect HEK293T cells.

Table 34: Transient transfection reagent.

Transfection reagent	Company
Mirus TransIT®-LT1-transfection reagent	MoBiTec, Göttingen

Table 35: Proteasome-, autophagy- and protein biosynthesis inhibitors.

Compounds	Concentration
Bafilomycin A1	200 nM
Cycloheximide	50 µg/ml
Z-Leu-Leu-Leu-al (MG132)	5 µM

For transient transfection of 6-well plates, $3*10^5$ HEK293T cells per well were seeded and incubated with 2 ml culture medium overnight. Prior to transfection the medium was exchanged with fresh medium. For transfection 100 µl of serum-and-antibiotic-free IMDM medium (serum free medium = sfm) (tab.32) were mixed with 3 µl Mirus TransIT®-LT1 transfection reagent (tab.34). After 5 minutes incubation at room temperature, 1000 ng in total of plasmid DNA were added to the mixture, mixed again and incubated for 15 minutes at room temperature. Then, the transfection mixture was added to the cells and mixed carefully with the culture medium. After 18 hours incubation at 37 °C and 5 % CO_2, the cells could be harvested.

For transient transfection of 75 cm^2 flasks, $2,34*10^6$ cells per 75 cm^2 flask were seeded and incubated with 10 ml culture medium overnight. The culture medium was exchanged prior to transfection. For transfection 756 µl of sfm (tab.32) were mixed with 23,4 µl Mirus TransIT®-LT1 transfection reagent (tab.34). The mixture was incubated for 5 minutes at room temperature. Afterwards, 7800 ng plasmid DNA were added, carefully mixed and incubated for 15 minutes at room temperature. Finally, the transfection mixture was added to the cells, mixed carefully with the culture medium and incubated for 18 hours.

For inhibition of protein biosynthesis, cells were treated with 50 µg/ml cycloheximide (tab.35) for either 2,5 or 5 hours before harvesting. In order to inhibit proteasomal degradation, 5 µM MG132 (tab.35) was added to the cells for 6 hours. In order to inhibit autophagy the culture medium was supplemented with 200 nM Bafilomycin A1 (tab.35) for 8 hours prior harvesting.

4.2.6.1 Sample preparation

After harvesting, the transfected cells were lysed in a hypotonic, detergent-containing (Triton-X-100) lysisbuffer (tab.36) and by means of sonication.

Table 36: Hypotonic and isotonic lysis buffer.

Compounds	Hypotonic lysis buffer	Isotonic lysis buffer
TRIS	20 mM	20 mM
Triton-X-100	0,1 %	0,1 %
Pepstatin	1 µM	1 µM
Leupeptin	10 µM	10 µM
Aprotinin	5 µg/ml	5 µg/ml
PMSF	100 µM	100 µM
MG132	10 µM	10 µM
NaCl	-	150 µM

Table 37: Protein concentration determination.

Kit	Company
DC^{TM}Protein Assay Kit II	BioRad, München

Table 38: 4xSDS-sample buffer.

Compounds	Concentration
Glycerol	40 %
TRIS	240 mM
SDS	8 %
Bromophenol blue	0,04 %
Add freshly before usage:	
β-Mercaptoethanol	10 %

The harvested cells were centrifuged at 1200 rpm for 5 minutes and the supernatant was discarded. The remaining cell pellet was dissolved in either 100 µl (6-well) or 220 µl (75 cm^2 flask) hypotonic lysis-buffer (tab.36) and incubated for 30 minutes on

ice. Afterwards, the cell lysate was sonicated three times for 10 seconds at 70 % intensity and five intervals. After sonication, the NaCl content of the cell lysate was set to 150 mM and the cell lysate centrifuged for 20 minutes at 4 °C and 14000 rpm. The supernatant (cleared cell lysate) was transferred into a fresh vessel and the pellet discarded. The protein concentration was determined using the DC^{TM}Protein assay kit (tab.37) and adjusted equally.

The 100 µl lysate, obtained from a 6-well, were mixed with 25 µl of 10 % ß-mercaptoethanol-containing 4xSDS-sample buffer (tab.38). From the 220 µl lysate, resulting from 75 cm^2 flasks, a 40 µl aliquot was taken and mixed with 15 µl 10 % ß-mercaptoethanol-containing 4xSDS-sample-buffer (tab.38). The remaining 180 µl lysate was used for immunoprecipitation experiments. The sample buffer-containing samples were boiled at 95 °C for 5 minutes.

4.2.6.2 Immunoprecipitation experiments

Immunoprecipitation experiments were performed with antibody-coupled agarose beads (tab.39) in order to separate either FAT10 and FAT10ylated proteins or p62. The detection of either co-immunoprecipitated p62 or FAT10 revealed the non-covalent interaction between FAT10 and p62.

Table 39: Antibody-coupled agarose used for co-immunoprecipitation.

Affinity gel	Company
EZview™ Red ANTI-FLAG® M2 Affinity Gel	Sigma-Aldrich, Steinheim
EZview™ Red Anti-HA Affinity Gel	

Table 40: Isotonic TRIS buffer.

Compounds	Concentration
TRIS	20 mM
NaCl	150 mM

Thirty microlitre 30 µl of either α-Flag or α-HA coupled agarose beads (EZview™ Red ANTI-FLAG® M2 or EZview™ Red Anti-HA Affinity Gel) (tab.39) were washed three times with isotonic lysis buffer (tab.36). In order to reduce unspecific binding, the washed beads were blocked with 1 mg/ml non-acetylated BSA for 1 hour at room

temperature. After blocking, the beads were washed again twice with isotonic lysis buffer (tab.36).

The remaining 180 µl of the 220 µl cleared cell lysates were added to the blocked beads and incubated for 1 hour at 4 °C.

After this incubation, the supernatant was removed and the beads were washed four times with isotonic lysis buffer (tab.36) and once with isotonic TRIS-buffer (tab.39). After the last washing step, the supernatant was removed completely and 60 µl of 10 % ß-mercaptoethanol-containing 4xSDS-sample buffer (tab.38) were added. Finally, the sample-buffer/beads mixture was boiled for 5 minutes at 95 °C.

4.2.7 Recombinant protein expression

Recombinant GST and GST-FAT10 were produced by Birte Kalveram and me in BL21(DE3)pLysS competent cells (tab.41), according to the following protocol.

Table 41: Competent cells used for recombinant expression of GST and GST-FAT10.

***E.coli* strain**	**Antibiotic resistance**	**Company**
BL21(DE3)pLysS	Chloramphenicol	Promega, Mannheim

Table 42: 2xYT medium.

Compounds	**Amount [g/l]**
Tryptone	16
Yeast	10
NaCl	5
ddH_2O	Ad 1000 ml

Table 43: Lysis buffer for bacterial lysates.

Compounds	Concentration
PBS	1x
Lysozyme	1 mg/ml
Pepstatin	1 µM
Leupeptin	10 µM
Aprotinin	5 µg/ml
PMSF	100 µM
NaCl	150 mM
DNAse	0,1 mg/ml

Table 44: Protein purification columns.

Purification columns	Company
GSTrapFF	GE healthcare, München
HiTrap Desalting column	GE healthcare, München

Table 45: Elution buffer.

Compounds	Concentration [mM]
TRIS	100
NaCl	150
GSH (reduced form)	20
DTT	5

BL21(DE3)pLysS cells (tab.41) were transformed with either pGEX-4T-3 (tab.1) in order to express GST or a GST-FAT10 encoding pGEX-4T-3 plasmid (tab.1) in order to express GST-FAT10. The transformation mixtures were plated on 35 µg/µl chloramphenicol (Camp) (tab.19) and 100 µg/µl ampicillin (Amp) (tab.19) containing LB-plates (tab.17). Single colonies were used in order to inoculate 5 ml LB (35 µg/µl Camp and 100 µg/µl Amp) precultures which subsequently were incubated overnight at 37 °C and 250 rpm. The precultures were again used to inoculate 500 ml 2xYT (tab.42) (35 µg/µl Camp and 100 µg/µl Amp) cultures which were raised at 37°C 250 rpm until the OD_{600} reached 0,5 - 0,8. The expression of GST and GST-FAT10 was induced with 100 µM IPTG after which the cultures were incubated for another

3 hours at 37°C and 250 rpm. Afterwards, the cultures were harvested and centrifuged for 15 minutes at 10000 rpm and 4°C. The bacterial pellets were resuspended in 20 ml lysis buffer (tab.43) and incubated for 1 hour on ice. After this incubation the suspensions were sonicated five times for 20 seconds with five cycles at 70 % and subsequently centrifuged at 4 °C and 15000 rpm for 15 minutes. GSTrap FF columns (tab.44) were used to purify GST or GST-FAT10 from the cleared lysates according to the manufacturer's protocol. In order to reduce precipitation of GST-FAT, the elution buffer (tab.45) was exchanged to 1xPBS by using a HiTrap Desalting column (tab.44). Subsequently, the protein content was determined either photometrically or by using the DC^{TM}Protein assay kit (tab.37).

Further, the purity of the protein was determined by gel electrophoresis and Coomassie brilliant blue-staining as well as western blotting and anti-GST antibody detection.

Furthermore, recombinant GST-FAT10 was obtained from the BIT*g* (Nicola Catone).

4.2.8 *In vitro* transcription and translation

Table 46: Kits and compounds used for the *in vitro* transcription/ translation assay.

Kits/Compounds	Company
Promega TNT® T7 Quick Coupled Transcription/ Translation Systems	Promega, Mannheim
EasyTag™ L-[^{35}S]-Methionine, 500µCi (18.5MBq), Stabilised Aqueous Solution	PerkinElmer, Rodgau

The *in vitro* transcription and translation of HA-p62 or the HA-p62 deletion constructs as well as the isolated HA-p62 domains was performed with Promega TNT® T7 Quick Coupled Transcription/Translation Systems (tab.46), according to the manufacturer's protocol.

Table 47: *In vitro* transcription/translation reaction mixture.

Compounds	Amount
Rabbit reticulocyte lysate	12,5 µl
TNT reaction buffer	1 µl
T7 polymerase	0,5 µl
Amino acid mixture (-)Methionine	0,5 µl
RNAsin	0,5 µl
DNA template	500 ng
[^{35}S] methionine(1,000Ci/mmol at 10mCi/ml)	1 µl
Nuclease-free water	Ad 25 µl

The *in vitro* transcription/translation reaction mixture was incubated for 1,5 hours at 37 °C. After the incubation 200 µl of isotonic lysis-buffer (tab.36) were added. A 25 µl aliquot was taken and mixed with 6 µl of 10 % β-mercaptoethanol-containing 4xSDS-sample buffer (tab.38) and boiled for 5 minutes at 95 °C. The remaining 200 µl were used for the GST pulldown assay.

4.2.9 GST pulldown assay

Table 48: GSH coupled Sepharose.

Compound	Company
Gluthation Sepharose 4B	GE Healthcare, München

Preclearance

In order to remove those molecules from the 200 µl *in vitro* transcription/translation mixture which are prone to stick to the GSH Sepharose unspecifically, a preclearance was performed. Thirty microlitre GSH Sepharose (tab.48) per sample were washed three times with isotonic lysis buffer and subsequently incubated with the *in vitro* transcription/translation mixture for 1 hour at 4 C. Afterwards, the precleared supernatant of the GSH Sepharose (tab.48) was removed and used for the GST pulldown.

GSH Sepharose blocking

Two times 30 µl GSH Sepharose (tab.48) per sample were washed three times with isotonic lysis buffer (tab.36) and incubated for 1 hour at room temperature with 1 mg/ml non-acetylated BSA in order to reduce unspecific binding. After blocking, the GSH Sepharose was washed twice with isotonic lysis buffer (tab.36).

GST pulldown

For the GST pulldown assay, 90 µl of the precleared *in vitro* transcription/translation mixture were incubated with 30 µl blocked GSH Sepharose and 25 µg recombinant GST. The other 90 µl were incubated with 30 µl blocked GSH Sepahrose and 25 µl GST-FAT10. The pulldown mixtures were incubated for 1 hour at 4 °C. After incubation, the supernatants were removed and the GSH-Sepharose was washed four times with isotonic lysis buffer (tab.36) and once with isotonic TRIS-buffer (tab.40). Afterwards, the supernatants were removed completely from the GSH-Sepahrose and 40 µl of 10 % β-mercaptoethanol-containing 4xSDS-sample buffer (tab.38) were added. The samples were subsequently boiled for 5 minutes at 95 °C.

The samples were analysed by SDS-PAGE. GST as well as GST-FAT10 were detected by Coomassie brilliant blue-staining and the *in vitro* transcribed and translated proteins by western blotting and autoradiography. The autoradiography was performed by using the Personal Molecular Imager FX phospho-imager. The obtained images were analysed using Quantity One 1-D Analysis Software and Photoshop (tab.15).

5 Results

5.1 The characterisation of the FAT10 p62 interaction

In 2008, Birte Kalveram found in 2008 that FAT10 interacts covalently and non-covalently with p62 in HEK293T cells which were transiently co-transfected with FAT10 and p62 constructs. In western blot experiments, a single FAT10-p62 conjugate of approximately 130 kDa was detectable. According to the molecular weight it seems to consist out of one single p62 molecule, decorated with up to three FAT10 molecules and/or additional unknown components. The characteristic FAT10-p62 conjugate of 130 kDa is specific, since it is never detectable in the mock controls or in those cells which are transfected with FAT10 or p62 only. The FAT10-p62 conjugate is also absent in those samples which co-express a diglycine mutant of FAT10 [FAT10(ΔGG)] and p62. Interestingly, in cytokine induced cells a ladder of FAT10-p62 conjugates is detectable (Aichem, Kalveram et al. 2012) which is never the case in overexpression experiments.

5.1.1 The amount of the FAT10-p62 conjugate was not increased upon MG132 treatment

Since FAT10ylated proteins are targeted to proteasomal degradation (Raasi, Schmidtke et al. 2001, Hipp, Raasi et al. 2004), it was investigated whether this is also true for the FAT10-p62 conjugate. The proteasome inhibitor MG132 was used in order to compare the amount of the FAT10-p62 conjugate in MG132 treated cells with untreated cells. Therefore HEK293T cells were transiently co-transfected with Flag-FAT10 and HA-p62 and either kept untreated (fig.16, lane 4) or were treated with 5 µM MG132 for 6 hours (fig.16, lane 5). Since MG132 is dissolved in DMSO, as a negative control in one sample the cells were treated with 0,05 % DMSO for 6 hours (fig.16, lane 6). In the mock control, cells were treated with the transfection reagent only (fig.16, lane 1) and as additional negative controls cells were transfected with either Flag-FAT10 or HA-p62 only (fig.16, lanes 2, 3). After harvesting, the cleared cell lysates were analysed by western blot experiments. In order to detect either the monomeric Flag-FAT10 and Flag-FAT10 conjugates or the

monomeric HA-p62 protein, the western blots were stained with either anti-Flag or anti-HA reactive antibodies respectively (fig.16).

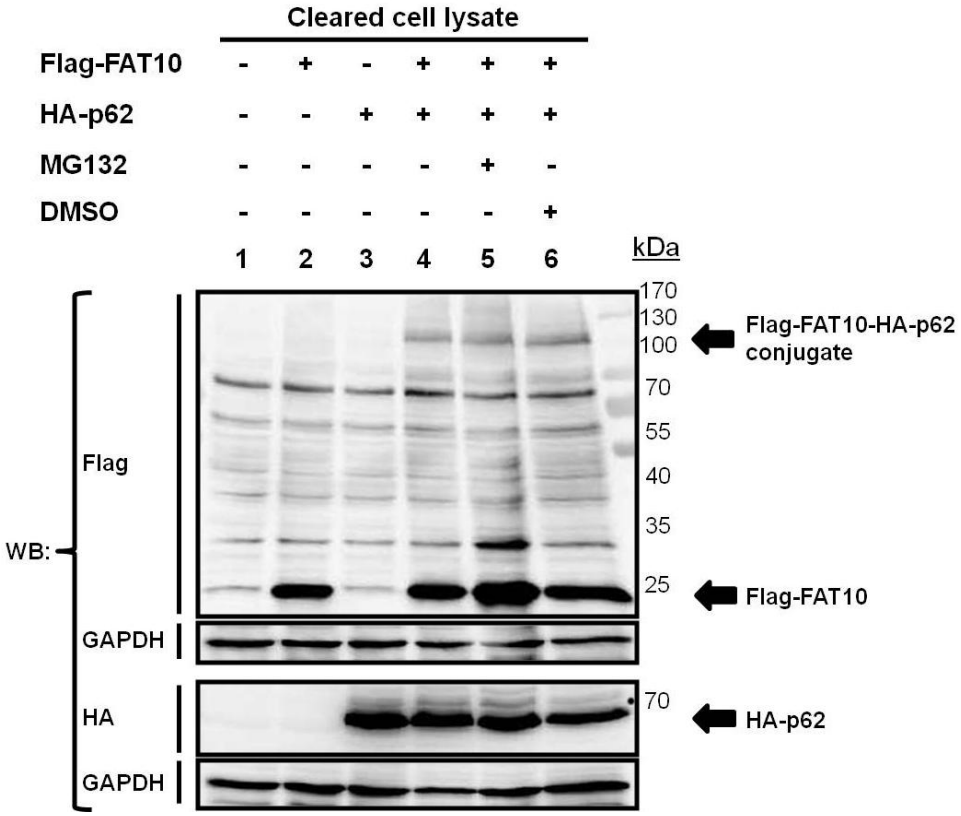

Figure 16: The inhibition of the proteasome did not increase the amount of the FAT10-p62 conjugate. HEK293T cells were transiently transfected with Flag-FAT10 and HA-p62 expression plasmids. As indicated, in some samples previous to the harvesting, the cells were treated with either 5 µM MG132 or 0,05 % DMSO respectively. After harvesting, the cells were lysed in a hypotonic lysis buffer. The cleared cell lysates were boiled with a 10 % β-mercaptoethanol containing SDS-sample buffer and separated by SDS PAGE on 12 % gels. After wet-blotting, the blots were probed with either anti-Flag, or anti-HA reactive antibodies. One experiment out of three independent experiments with similar outcome is shown.

In the anti-HA and anti-Flag western blots, the monomeric HA-p62 (fig.16, lanes 3, 4, 5, 6) and Flag-FAT10 proteins as well as the Flag-FAT10 conjugates (fig.16, lanes 2, 4, 5, 6) were detectable in all samples which were transfected with the respective constructs. In the anti-Flag western blot, a characteristic FAT10-p62 conjugate of 130 kDa was detectable in all cells which were co-transfected with Flag-FAT10 and HA-p62 (fig.16, lanes 4-6) but not in the mock-control (fig.16, lane 1) or in the Flag-FAT10 or HA-p62 only transfected cells

(fig.16, lanes 2, 3). Interestingly, upon the MG132 treatment only the amount of the monomeric Flag-FAT10 and the amount of the background band at 30 kDa were markedly increased, while the general conjugate smear and the characteristic FAT10-p62 conjugate of 130 kDa were not altered (fig.16, lane 5). In the DMSO treated cells (fig.16, lane 6), like in the untreated cells (fig.16, lane 4), there was no increase of monomeric Flag-FAT10 and the 30 kDa conjugate detectable. Hence, it was confirmed that this increase indeed is due to the inhibition of the proteasome and not to the DMSO.

5.1.2 The FAT10ylation of the lysineless p62 mutant is not always abolished completely

In total, p62 contains twenty lysines which could be potential FAT10ylation targets (K7, K13, K91, K100, K102, K103, K187, K189, K141, K157, K165, K238, K264, K281, K295, K313, K344, K378, K420 and K435). Beside lysines, also the N-terminus, cysteines, threonines and serines can be conjugated with ubiquitin-like modifiers (Hochstrasser 2009, Kravtsova-Ivantsiv and Ciechanover 2012). In the following chapter it should be investigated whether in fact the lysines of p62 become FAT10ylated and if so, the respective lysine(s) should be identified.

In order to confirm that p62 actually becomes FAT10ylated at the ε-amino-groups of its lysines, all twenty lysines of p62 were mutated to arginines [HA-p62(K0)]. HEK293T cells were transiently transfected either with the lysineless HA-p62(K0) construct alone (fig.17, lanes 5, 14), or co-transfected with Flag-FAT10 (fig.17, lanes 7, 16). As a positive control, the HA-p62 construct was co-transfected together with Flag-FAT10 in order to confirm that the experimental setup in principal would have been suitable for the conjugate formation (fig.17, lanes 6, 15). As negative controls, the non-conjugating Flag-FAT10(ΔGG) was co-transfected with either HA-p62 (fig.17, lanes 8, 17) or HA-p62(K0) (fig.17, lanes 9, 18). Further cells were also transfected with either Flag-FAT10 (fig.17, lanes 2, 11), Flag-FAT10(ΔGG) (fig.17, lanes 3, 12) or HA-p62 only (fig.17 lanes 4, 13). In the mock control (fig.17 lanes 1, 10), cells were treated with the transfection reagent only. In order to investigate the non-covalent interaction capabilities of the HA-p62 proteins with FAT10, anti-Flag immunoprecipitation experiments were performed with the cleared cell lysates (fig.17, lanes 10-18). The samples were analysed by western blot

experiments. The western blots with the cleared cell lysates (load) were stained with anti-HA an anti-Flag antibodies, in order to detect the monomeric HA-p62 and Flag-FAT10 proteins as well as conjugates. The western blots of the anti-Flag immunoprecipitation experiments were stained with either anti-Flag or anti-HA antibodies in order to detect either the immunoprecipitated monomeric Flag-FAT10 and the FAT10-conjugates, or the co-immunoprecipitated HA-p62 proteins respectively. In the anti-HA western blot of the anti-Flag immunoprecipitation experiments only those HA-p62 proteins should be detectable which are covalently attached to Flag-FAT10 or which formerly were bound to Flag-FAT10 non-covalently.

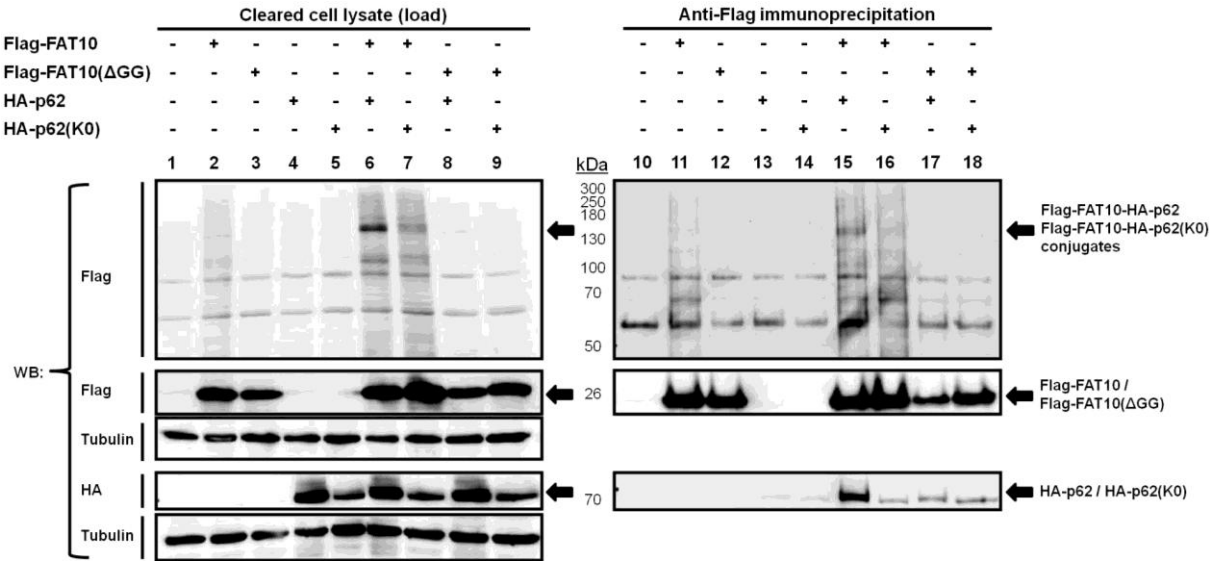

Figure 17: The FAT10ylation of the lysineless p62 mutant is not always abolished completely. HEK293T cells were transiently transfected with Flag-FAT10, Flag-FAT10(ΔGG), HA-p62 and HA-p62(K0), as indicated. After harvesting, the cells were lysed in a hypotonic lysis buffer. The cleared supernatants were used for immunoprecipitation experiments with anti-FLAG-M2-conjugated agarose. The samples were boiled with a 10 % β-mercaptoethanol containing SDS-sample buffer and separated by SDS PAGE on 10 % or 12 % gels. After wet-blotting, blots were probed with either anti-Flag, or anti-HA reactive antibodies. One experiment out of four independent experiments with similar outcome is shown.

In the anti-HA and anti-Flag western blots of the cleared cell lysates (fig.17, lanes 1-9), the monomeric HA-p62 (fig.17, lanes 4, 6, 8), HA-p62(K0) (fig.17, lanes 5, 7, 9), Flag-FAT10(ΔGG) (fig.17, lanes 3, 8, 9) and Flag-FAT10 proteins as well as the Flag-FAT10 conjugates (fig.17, lanes 2, 6, 7) were detectable in all samples which were transfected with the respective constructs. In the anti-Flag

western blots, in the Flag-FAT10 and HA-p62 co-expressing HEK293T cells, the characteristic Flag-FAT10-HA-p62 conjugate band of 130 kDa was highly pronounced in the cell lysate (fig.17, lane 6) and also detectable in the corresponding anti-Flag immunoprecipitation experiment (fig.17, lane 15). Concerning the Flag-FAT10 and HA-p62(K0) co-expressing cells, only in the western blot of the cell lysates (fig.17, lane 7), but not in the corresponding immunoprecipitation experiment (fig.17, lane 16) a faint band was visible at 130 kDa. Therefore, the FAT10ylation of p62(K0) seems to be not completely abolished. As expected, the FAT10-p62 conjugate neither was detectable in the mock control (fig.17, lanes 1, 10) nor in cells expressing either Flag-FAT10 (fig.17, lanes 2, 11), HA-p62 (fig.17, lanes 4, 13) or HA-p62(K0) (fig.17, lanes 5, 14) alone. In cells expressing either the non-conjugating Flag-FAT10(ΔGG) mutant only (fig.17, lane 3, 12) or together with HA-p62 (fig.17, lanes 8, 17) or HA-p62(K0) (fig.17, lanes 9, 18), all Flag-FAT10 conjugates disappeared, as expected.

In the anti-Flag western blots of the corresponding anti-Flag immunoprecipitation experiments (fig.17, lanes 10-18), the immunoprecipitated monomeric Flag-FAT10(ΔGG) (fig.17, lanes 12, 17, 18) and Flag-FAT10 as well as the Flag-FAT10 conjugates (fig.17, lanes 11, 15, 16) were detectable. According to the anti-HA western blots of the anti-Flag immunoprecipitation experiments, the non-covalent interaction between Flag-FAT10 and HA-p62(K0) (fig.17, lane16) as well as Flag-FAT10(ΔGG) and HA-p62 (fig.17, lane 17) or HA-p62(K0) (fig.17, lane 18) was markedly alleviated compared to the Flag-FAT10 and HA-p62 expressing samples (fig.17, lane 15). While the detection of the non-covalent interaction between wild-type FAT10 and wild-type p62 was reproducible, the results for the non-covalent interactions between wild-type FAT10 and p62(K0) were inconsistent as will be further documented in the course of this thesis. Interestingly, in the predominant part of experiments which were performed for this study, the FAT10(ΔGG) mutant was found to fail in the co-immunoprecipitation of p62.

In this experiment the protein amount of the HA-p62(K0) mutant (fig.17, lane 7) was less compared to the HA-p62 protein amount (fig.17, lane 6). This was observed in several experiments (fig.19, lane 8) and was also true for the His-tagged p62 construct (data not shown). However, in order to make a clear statement concerning

the FAT10 interaction capabilities of p62 and p62(K0), the protein amounts have to be equal. The attempt to adjust the p62(K0) protein amount by loading a higher volume of the sample onto the gel failed since the simultaneous increase of the overall FAT10 conjugate smear in the FAT10 and p62(K0) co-expressing samples impedes the detection of single conjugate bands (data not shown). Also the usage of a higher amount of p62(K0) DNA for the transfection did not solve the problem of unequal p62 protein amounts (data not shown). Therefore, the effective dependency between the amount of p62 protein and the detectability of the FAT10-p62 conjugate was investigated.

5.1.2.1 The protein amount of p62 may influences the detectability of the FAT10-p62 conjugate

In order to estimate the influence of the p62 protein amount on the conjugate detectability, HA-FAT10 was transiently co-transfected together with either an equal DNA amount of p62(K0)-His (fig.18, lanes 9), or with declining amounts of p62-His DNA which, as aspired, resulted in declining amounts of the expressed p62-His protein (fig.18, lanes 5-7). As negative controls cells were transfected with either HA-FAT10 (fig.18, lane 1), p62(K0)-His (fig.18, lane 8) or the declining amounts of p62-His (fig.18, lanes 2-4) DNA only. After harvesting, anti-HA immunoprecipitation experiments were performed with the cleared cell lysates in order to investigate the non-covalent interaction capabilities of p62-His and p62(K0)-His with HA-FAT10. The samples were analysed by western blot experiments. The western blots with the cleared cell lysates (load) were stained with either anti-His or anti-HA antibodies, in order to detect the monomeric p62-His and HA-FAT10 proteins as well as conjugates. The western blots of the anti-HA immunoprecipitation experiments were stained with either anti-HA or anti-His antibodies in order to detect the immunoprecipitated HA-FAT10 and the HA-FAT10-conjugates, or the co-immunoprecipitated p62-His proteins respectively. In the anti-His western blot of the immunoprecipitation experiments only those p62-His deletion proteins should be detectable which are covalently attached to HA-FAT10 or which formerly were interacting with HA-FAT10 non-covalently.

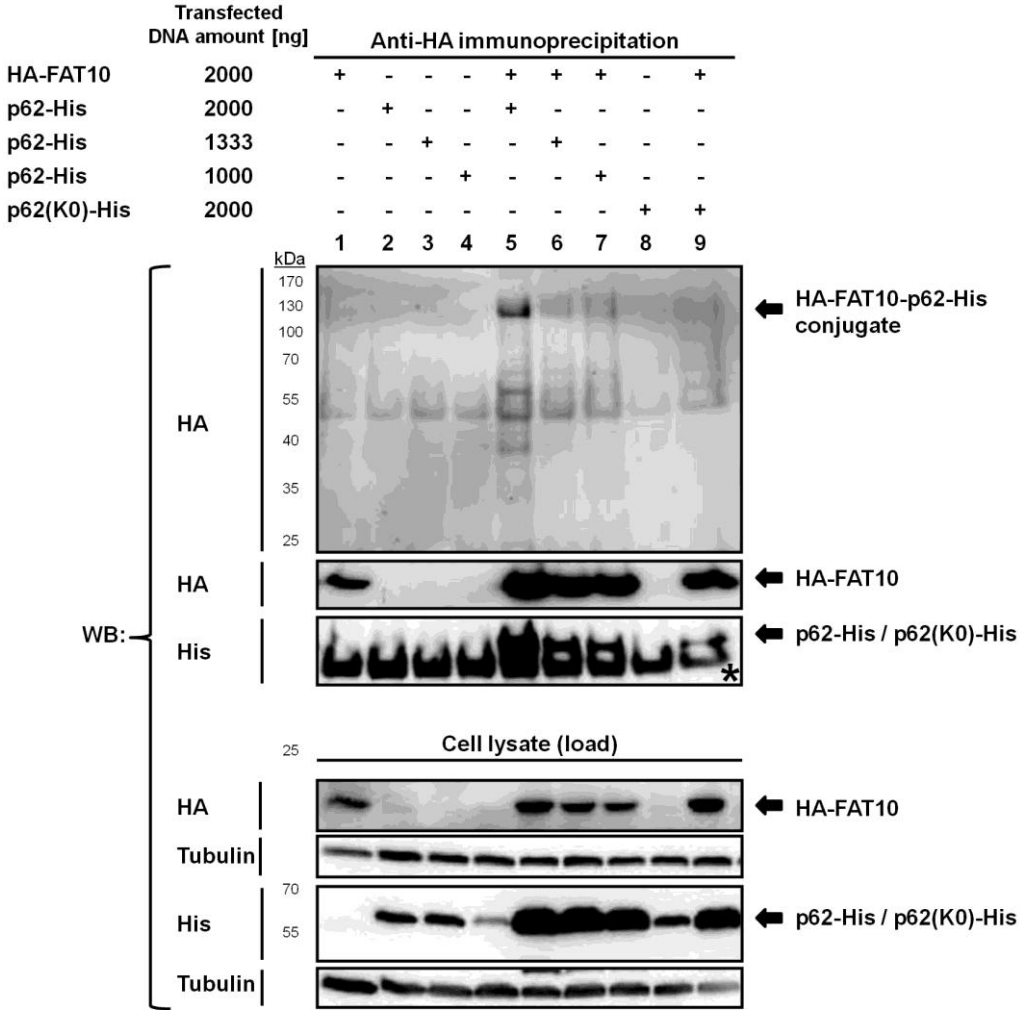

Figure 18: The p62 protein amount may influence the FAT10-p62 conjugate detectability. HEK293T cells were transiently transfected with either 2000 ng HA-FAT10 DNA and 2000 ng p62(K0)-His DNA or with 2000 ng HA-FAT10 DNA and either 2000 ng, 1333 ng or 1000 ng p62-His encoding plasmid as indicated. After harvesting, the cells were lysed in a hypotonic lysis buffer. The cleared supernatants were used for immunoprecipitation experiments with anti-HA-7-conjugated agarose. The samples were boiled with a 10 % β-mercaptoethanol containing SDS-sample buffer and separated by SDS PAGE on 10 % or 12 % gels. After the semi-dry-blotting, the blots were probed with either anti-HA or anti-His reactive antibodies. The asterisk indicates the heavy chain of the anti-HA reactive anti-body used for the immunoprecipitation experiment. This experiment was only performed once.

In the anti-His and anti-HA western blots of the cleared cell lysates(load) in the lower panels of figure 18, the monomeric p62-His (lanes 2-7), p62(K0)-His (lanes 8-9) and HA-FAT10 proteins (fig.18, lanes 1, 5-7, 9) were detectable in all samples which were transfected with the respective constructs. In this experiment, the HA-FAT10-p62-His conjugate of 130 kDa was not detectable in the anti-HA western blots of the cleared cell lysates (load) (data not shown).

In the corresponding anti-HA immunoprecipitation experiments, shown in the upper panel of figure 18, the immunoprecipitated monomeric HA-FAT10 is detectable (fig.18, lanes 1, 5-7, 9) in the anti-HA western blots. In this western blot, also the HA-FAT10-p62-His conjugate of 130 kDa was prominently detectable in cells which were co-transfected with HA-FAT10 and the highest amount of the p62-His DNA (fig.18, lane 5). In those cells, according to the anti-His western blot of the load, also the expressed p62-His amount was at highest (fig.18, lane 5). In cells which were co-transfected with the same amounts of either p62(K0)-His DNA and HA-FAT10, no HA-FAT10-p62(K0)-His conjugate was visible (fig.18, lane 9). However, besides using the same amounts of p62 DNA for both transfections, the resulting p62 protein amount in the p62(K0)-His and HA-FAT10 co-expressing cells (fig.18, lane 9) again was not as high as in the wild-type p62-His and HA-FAT10 co-expressing cells (fig.18, lane 5). Also no FAT10-p62 conjugate was detectable in those cells which were co-transfected with FAT10 and declining amounts of the p62-His encoding plasmid (fig.18, lanes 6, 7). Since in these cells, also the resulting p62 amounts were decreased one could assume that the protein amount of p62 may influences the detectability of the FAT10-p62 conjugate. In the negative controls which express either HA-FAT10 (fig.18, lane 1), p62-His (fig.18, lanes 2-4) or p62(K0)-His (fig.18, lane 8) only, there were also no conjugate bands visible.

According to the anti-His western blot of the immunoprecipitation experiment, shown in the upper panel of figure 18, in this experiment also p62(K0)-His was successfully co-immunoprecipitated with HA-FAT10 (fig.18, lane 9). However, the amount of the p62(K0)-His protein which was co-immunoprecipitated together with HA-FAT10 (fig,18, lane 9) was less compared to all the co-immunoprecipitated amounts of p62-His in the HA-FAT10 and p62-His co-expressing samples (fig.18, lanes 5-7). In those cells which were transfected with either p62-His or p62(K0)-His DNA only, neither p62-His (fig.18, lanes 2-4) nor p62(K0)-His proteins (fig.18, lane 8) were detectable in the anti-HA immunoprecipitation experiments, indicating that the non-covalent interaction was specific for FAT10 and p62.

5.1.3 The oligomerisation capability of p62 doesn't seem to be a prerequisite for its interaction with FAT10

Since it has been shown that the oligomerisation capability of p62 is essential for some of its functions (Lamark, Perander et al. 2003, Seibenhener, Babu et al. 2004), the meaning of this oligomerisation capability for the interaction with FAT10 was investigated. Therefore, a PB1 defective mutant of p62 which cannot form oligomers anymore [p62(K7R/D69R)] was prepared (Ichimura, Kumanomidou et al. 2008). HEK293T cells were transiently co-transfected with the HA-p62(K7R/D69R) mutant and Flag-FAT10 (fig.19, lanes 9, 19). As a positive control, HA-p62 was co-expressed with Flag-FAT10 (fig.19, lanes 7, 17). As negative controls HA-p62(K0) was co-transfected with Flag-FAT10 (fig.19, lane 8, 18) and HA-p62 was co-transfected with Flag-FAT10(ΔGG) (lanes 10, 20). Further cells were transfected with either Flag-FAT10 (fig.19, lane 2), Flag-FAT10(ΔGG) (fig.19, lane 3), HA-p62 (fig.19, lane 4), HA-p62(K0) (fig.19, lane 5) or HA-p62(K7R/D69R) (fig.19, lane 6) only. In the mock control, cells were treated with the transfection reagent only (fig.19, lane 1). The samples were analysed by western blot experiments. The western blots with the cleared cell lysates (load) were stained with anti-HA and anti-Flag antibodies, in order to detect the monomeric HA-p62 and Flag-FAT10 proteins as well as conjugates. The western blots of the anti-Flag immunoprecipitation experiments were stained with either anti-Flag or anti-HA antibodies in order to detect either the immunoprecipitated Flag-FAT10(ΔGG) and Flag-FAT10 proteins as well as the Flag-FAT10-conjugates, or the co-immunoprecipitated HA-p62, HA-p62(K0) and HA-p62(K7R/D69R) proteins respectively. In the anti-HA western blot of the anti-Flag immunoprecipitation experiments only those HA-p62 proteins should be detectable which are covalently attached to Flag-FAT10 or which previously were interacting with Flag-FAT10 non-covalently.

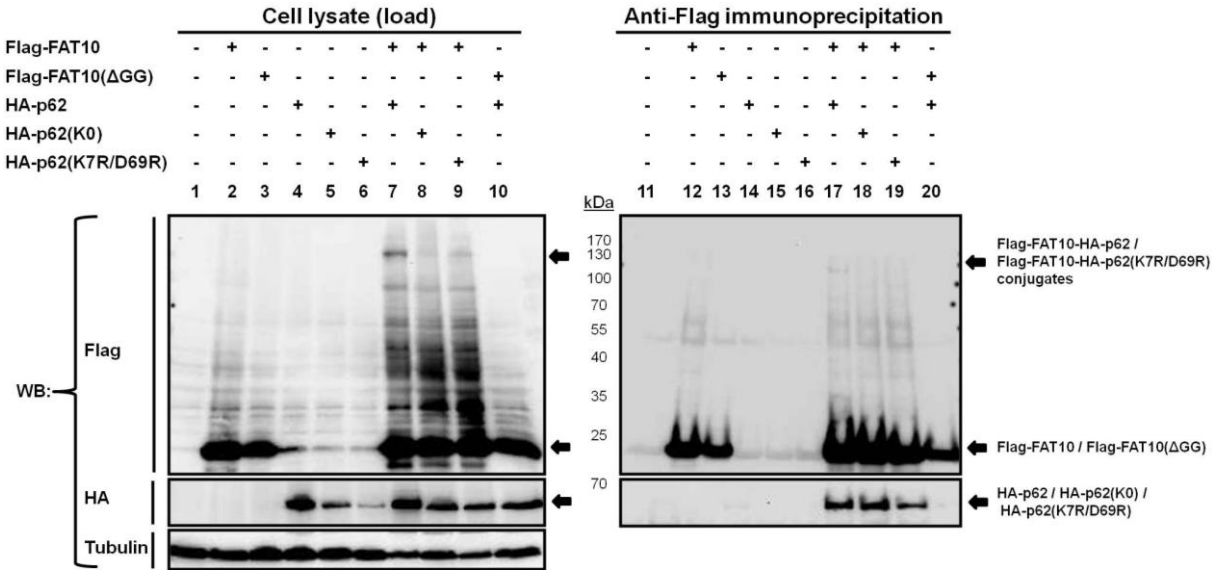

Figure 19: For the interaction with FAT10, the oligomerisation capability of p62 doesn't seem to be a prerequisite. HEK293T cells were transiently transfected with Flag-FAT10, Flag-FAT10(ΔGG), HA-p62, HA-p62(K0) or HA-p62(K7R/D69R) as indicated. The cleared supernatants were used for the immunoprecipitation experiments with anti-Flag M2-conjugated agarose. The samples were boiled with a 10 % β-mercaptoethanol containing SDS-sample buffer and separated by SDS PAGE on 10 % or 12 % gels. After wet-blotting, blots were probed with either anti-Flag, or anti-HA reactive antibodies. For the cell lysates one experiment out of three independent experiments with inconsistent results is shown. For the co-immunoprecipitation one out of two independent experiments with inconsistent results is shown.

In the anti-HA and anti-Flag western blots of the cleared cell lysates (load) (fig.19, lanes 1-10), the monomeric HA-p62 (fig.19, lanes 4, 7, 10), HA-p62(K0) (fig.19, lanes 5, 8), Flag-FAT10(ΔGG) (fig.19, lanes 3, 10) and Flag-FAT10 proteins as well as the Flag-FAT10 conjugates (fig.19, lanes 2, 7-9) were detectable in all samples which were transfected with the respective constructs. The FAT10-p62 conjugate was prominently detectable in the lysate of cells which were transiently transfected with Flag-FAT10 and HA-p62 (fig.19, lane 7). In cells which express Flag-FAT10 and HA-p62(K7R/D69R) the amount of the FAT10-p62(K7R/D69R) conjugate was markedly reduced (fig.19, lane 9) compared to the cells co-transfected with Flag-FAT10 and HA-p62 (fig.19, lane 7). However, in these samples, also the protein amount of the HA-p62(K7R/D69R) mutant (fig.19, lane 9) was less, compared to HA-p62 (fig.19, lane 7).

In the Flag-FAT10 and HA-p62(K0) co-expressing cells (fig.19, lane 8), despite having a p62 protein amount comparable to the Flag-FAT10 and HA-p62(K7R/D69R) co-expressing cells (fig.19, lane 9), the effect was even severe and no FAT10-p62

conjugate was detectable anymore. This is in contrast to the experiment show in figure 17, where in the cell lysates of Flag-FAT10 and HA-p62(K0) expressing cells a faint FAT10-p62(K0) band was detectable (fig.17. lane 7).

As expected, no 130 kDa band was detectable in the either Flag-FAT10 (fig.19, lane 2), HA-p62 (fig.19 lane 4), HA-p62(K0) (fig.19, lane 5) or HA-p62(K7R/D69R) (fig.19, lane 6) only expressing cells, as well as in the mock control (fig.19, lane 1). As expected, no FAT10-conjugates at all were formed in cells which do express the Flag-FAT10(ΔGG) mutant (fig.19, lanes 3, 10, 13, 20).

Despite being markedly diminished, the FAT10-p62(K7R/D69R) conjugate was detectable in two out of three experiments (fig.19, lane 9). Only in one experiment it was completely absent (data not shown). Therefore, the oligomerisation capability of p62 at least doesn't seem to be a basic prerequisite for the covalent FAT10 and p62 interaction.

In the corresponding anti-Flag immunoprecipitation experiments (fig.19, lanes 11-20), only in the HA-p62 and Flag-FAT10 expressing cells the characteristic FAT10-p62 conjugate of 130 kDa was detectable (fig.19, lane 17). However, compared to the corresponding cell lysate sample (fig.19, lane 7), the FAT10-p62 conjugate band in the immunoprecipitation experiment was not very prominent (fig.19, lane 17). Interestingly, while the amount of the monomeric Flag-FAT10 was strongly enriched in the immunoprecipitation experiments as expected (fig.19, lanes 12, 13, 17-20) the amount of the FAT10-p62 conjugate was markedly diminished (fig.19, lane 17). The comparatively poor immunoprecipitation capability of the FAT10-p62 conjugate will be further documented in the course of this thesis. This may also be the reason why the faint FAT10-p62(K7R/D69R) conjugate which was detected in the cell lysates (fig.19, lane 9), was not detectable in the corresponding immunoprecipitation experiment (fig.19, lane 19).

In a second data set, HA-p62(K0) as well as HA-p62(K7R/D69R) were not co-immunoprecipitated with Flag-FAT10 (data not shown). However, since in the experiment shown in figure 19, HA-p62 as well as HA-p62(K0) and HA-p62(k7R/D69R) were co-immunoprecipitated with Flag-FAT10 (fig.19, lanes 17-19), the oligomerisation capability of p62 at least doesn't seem to be a basic prerequisite

for a successful non-covalent FAT10 and p62 interaction. Otherwise, the non-covalent interaction capability might be absent in all experiments.

Also in this experiment the Flag-FAT10(ΔGG) mutant failed to co-immunoprecipitate HA-p62 (fig.19, lane 20).

5.1.4 Which domain(s) and lysine(s) of p62 is/are required for the covalent interaction with FAT10

5.1.4.1 No FAT10-p62 conjugate was detectable with PB1, NPI, TRAF and N-terminal PEST domain deleted p62 mutants

For the identification of the domains and lysines of p62 which are involved in the covalent FAT10 interaction, eleven HA-tagged p62 deletion proteins were used (Pankiv, Clausen et al. 2007). All together their deleted areas comprise all domains of p62: HA-p62(Δ1-123), HA-p62(Δ123-170), HA-p62(Δ123-256), HA-p62(Δ123-319), HA-p62(Δ170-256), HA-p62(Δ257-319), HA-p62(Δ257-370), HA-p62(Δ257-440), HA-p62(Δ321-348), HA-p62(Δ371-386) and HA-p62(Δ386-440).

HEK293T cells were transiently co-transfected with Flag-FAT10 and each of these eleven deletion proteins (fig.20). As a positive control, the wild-type HA-p62 construct was co-transfected with Flag-FAT10 (fig.20, lane 4) and as a negative control, HA-p62(K0) was co-transfected with Flag-FAT10 (fig.20, lane 28). Further, as additional negative controls, Flag-FAT10 (fig.20, lane 2) as well as all eleven HA-p62 deletion constructs (fig.20), wild-type HA-p62 (fig.20, lane 3) and HA-p62(K0) (fig.20, lane 27) only were expressed. In the mock control, cells were treated with the transfection reagent only (fig.20, lane 1). The samples were analysed by western blot experiments and the western blots were stained with anti-HA and anti-Flag antibodies, in order to detect the monomeric HA-p62 and HA-p62 deletion proteins or Flag-FAT10 proteins as well as conjugates respectively.

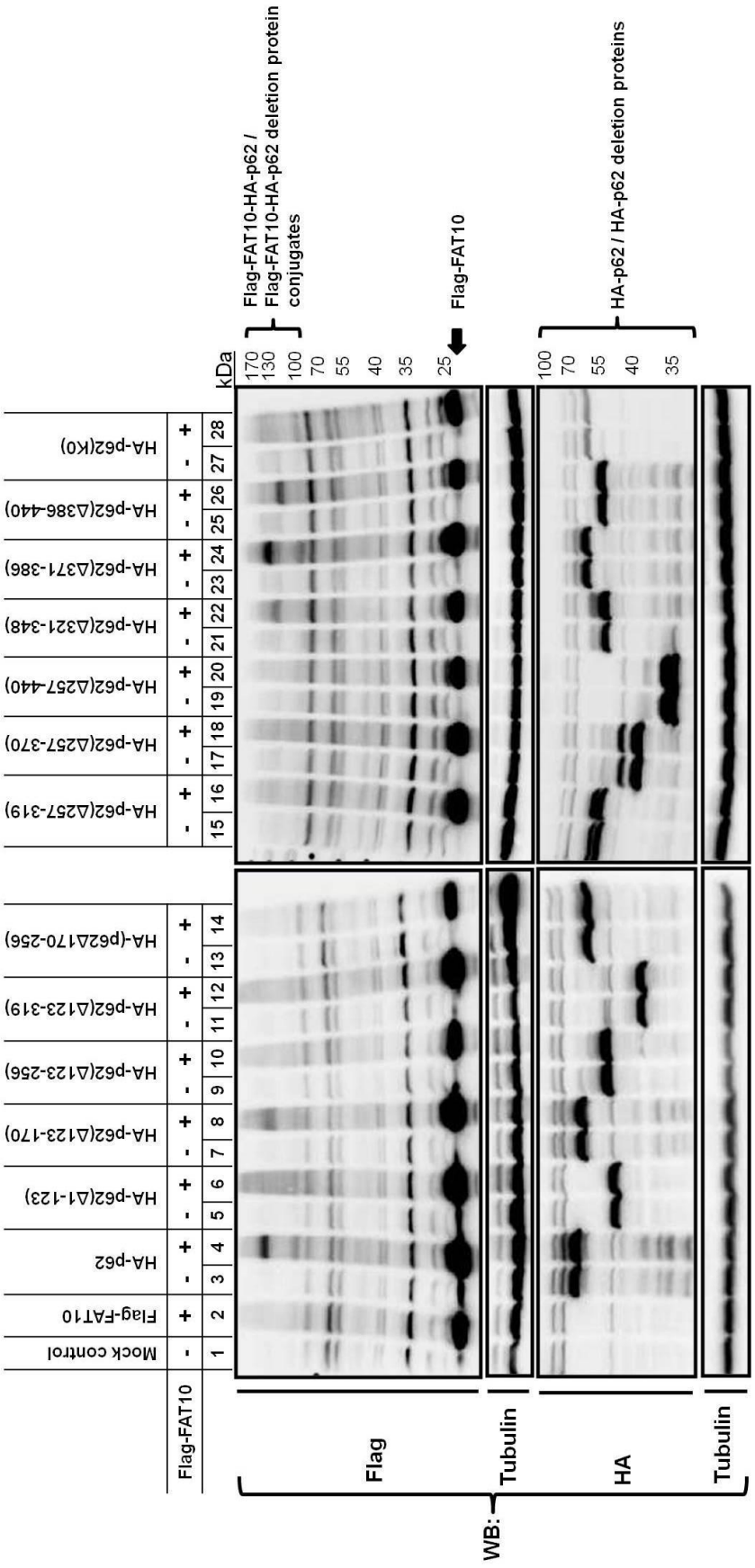
Flag-FAT10
Mock control
Flag-FAT10
HA-p62
HA-p62(Δ1-123)
HA-p62(Δ123-170)
HA-p62(Δ123-256)
HA-p62(Δ123-319)
HA-(p62Δ170-256)
HA-p62(Δ257-319)
HA-p62(Δ257-370)
HA-p62(Δ257-440)
HA-p62(Δ321-348)
HA-p62(Δ371-386)
HA-p62(Δ386-440)
HA-p62(K0)
kDa
170
130
100
70
55
40
35
25
Flag-FAT10-HA-p62 / Flag-FAT10-HA-p62 deletion protein conjugates
Flag-FAT10
HA-p62 / HA-p62 deletion proteins
WB:
Flag
Tubulin
HA
Tubulin

Figure 20: The deletion of the N-terminus (aa 1-123) as well as deletions between the amino acids 170-319 of p62 impede FAT10ylation of p62. HEK293T cells were transiently transfected with expression plasmids for Flag-FAT10, HA-p62, HA-p62(K0) and eleven different HA-p62 deletion constructs as indicated. In the mock control, cells were treated with the transfection reagent only. The cleared cell lysates were boiled with a 10 % β-mercaptoethanol containing SDS-sample buffer and separated by SDS PAGE on 10 % or 12 % gels. After wet-blotting, blots were probed with either anti-Flag, or anti-HA reactive antibodies. One out of four independent experiments with the same outcome is shown.

Except the HA-p62(K0) protein (fig.20, lanes 27-28), all HA-p62 deletion proteins (fig.20, lanes 5-26) as well as the wild-type p62 (fig.20, lanes 3-4) were expressed at comparable amounts. Also the Flag-FAT10 protein amounts were equally expressed in all samples. The characteristic FAT10-p62 conjugate was only detectable in cells which were co-transfected with Flag-FAT10 and HA-p62(Δ123-170) (fig.20, lane 8), HA-p62(Δ321-348) (fig.20, lane 22), HA-p62(Δ371-386) (fig.20, lane 24) or HA-p62(Δ386-440) (fig.20, lane 26). The molecular weights of these FAT10-p62 conjugates were decreased in accordance to the sizes of the deletions in the respective HA-p62 deletion constructs. In the samples of cells which co-express Flag-FAT10 and HA-p62(Δ1-123) (fig.20, lane 6), HA-p62(Δ123-256) (fig.20, lane 10), HA-p62(Δ123-319) (fig.20, lane 12), HA-p62(Δ170-256) (fig.20, lane 14), HA-p62(Δ257-319) (fig.20, lane 16), HA-p62(Δ257-370) (fig.20, lane 18) or HA-p62(Δ257-440) (fig.20, lane 20), no conjugate band could be detected.

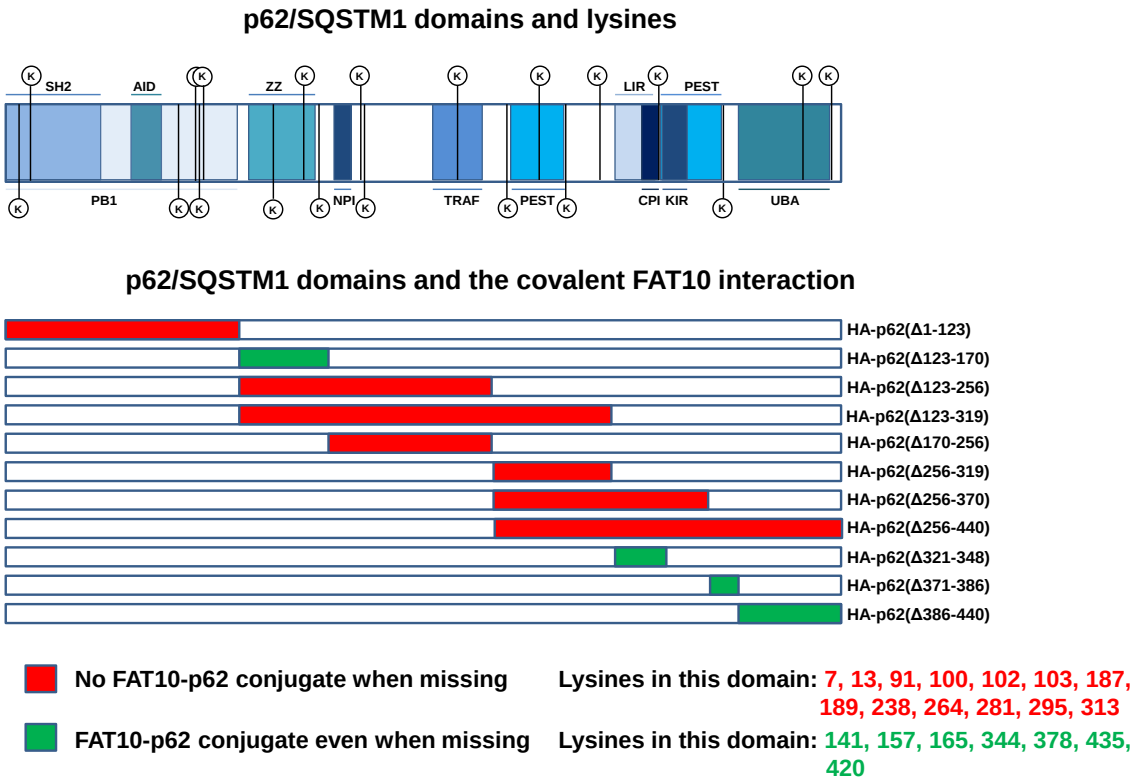

Figure 21: Overview over the domains and lysines of p62 which may be required for the covalent interaction with FAT10. In the upper part of the figure a schematic of p62, including all domains and lysines, is depicted. The schematic on the lower part of the figure summarises the results obtained for the covalent interactions between the HA-p62 truncations and the wild-type Flag-FAT10 (fig.20). In the HA-p62 deletion constructs, where the deletions impede the FAT10ylation the deleted areas are coloured in red. The deleted areas of p62 deletion constructs which are FAT10ylated irrespectively of their deletions are coloured in green. Those lysines of p62 which are potential FAT10ylation sites are listed in green while those which are not FAT10ylated are listed in red.

Concerning the PB1, SH2 and AID deficient HA-p62(Δ1-123) proteins, no FAT10-p62 conjugate formation was detectable anymore (fig.20, 21). The formation of detectable FAT10-p62 conjugates was also impeded with those HA-p62 deletion constructs in which the deletions encompassed amino acids 170-319. This region harbours the NPI domain, the TRAF domain and the N-terminal PEST domain (fig.20, 21). Therefore, these p62 domains might be involved in FAT10ylation. In this region, the following thirteen lysines are located: K7, K13, K91, K100, K102, K103, K187, K189, K238, K264, K281, K295, and K313. Therefore, these lysines could be potential FAT10ylation sites (fig.21).

Also for the HA-p62(Δ256-370) deletion construct which, in addition to the N-terminal PEST domain also lacks the LIR, the CIP, the KIR as well as the N-terminus of the C-

terminal PEST domain, no FAT10-p62 conjugate was detectable. The same was true for the HA-p62(Δ256-440) construct, where the whole N-terminus, including the N-terminal PEST domain was missing (fig.20, 21). However, in case of the HA-p62 deletion proteins where only the LIR domain, the CPI domain and the UBA domain were missing, the FAT10-p62 conjugates were detectable. Also the zinkfinger (ZZ) deleted HA-p62 construct became FAT10ylated (fig. 20, 21). Thus, these p62 domains are dispensable for the FAT10ylation. Those deleted domains do harbour the following lysines: K141, K157, K165, K344, K378, K420 and K435. Therefore these seven lysines are at least non essential FAT10ylation sites (fig.21).

The KIR domain and the C-terminus of the C-terminal PEST domain are only missing in the HA-p62(Δ256-440) construct where the N-terminal PEST domain is missing too. However, those domains do not contain lysines anyway (fig. 21).

5.1.4.2 No lysine of p62 which is indispensable for the FAT10ylation could be identified

In order to investigate which of the thirteen potential FAT10ylation site lysines in HA-p62 become FAT10ylated, site directed mutagenesis was used to successively mutate them to arginine (fig.22). The thirteen lysines were mutated one after the other and HEK293T cells were subsequently co-transfected with Flag-FAT10 and each single mutant. In each experiment, as a positive control, wild-type HA-p62 and Flag-FAT10 were co-transfected (fig.22). The samples were analysed by western blot experiments. The western blots with the cleared cell lysates were stained with anti-HA and anti-Flag antibodies, in order to detect the monomeric HA-p62, the HA-p62 deletion proteins or the monomeric Flag-FAT10 proteins as well as the Flag-FAT10 conjugates respectively.

According to the molecular weight of wild-type FAT10-p62 conjugate (130 kDa), up to three FAT10 molecules may be covalently attached to one p62 molecule. Therefore, the absence of one Flag-FAT10 molecule might lead either to a downshift of the molecular weight of around 25 kDa, which is the molecular weight of one Flag-FAT10 molecule, or to the disappearance of the entire conjugate. The initial idea was to take the first lysine mutant of p62, which shows the expected 25 kDa downshift, as the basis for adding the next mutation. This was supposed to be continued until a further

25 kDa downshift of the FAT10-p62 conjugate would appear and/or finally the entire conjugate would be gone.

For the sake of conciseness, in the following figure only those samples are displayed in which the wild-type HA-p62 or the respective lysine HA-p62 mutant are co-transfected with Flag-FAT10 (fig.22) to observe the potential molecular weight shifts of the FAT10-p62 conjugates. For every experiment the mock control, the wild-type Flag-FAT10 only, the wild-type HA-p62 only and the respective lysine mutants of p62 only controls were performed as well. The respective western blots, showing the whole experiments, are displayed in the appendix (fig.40).

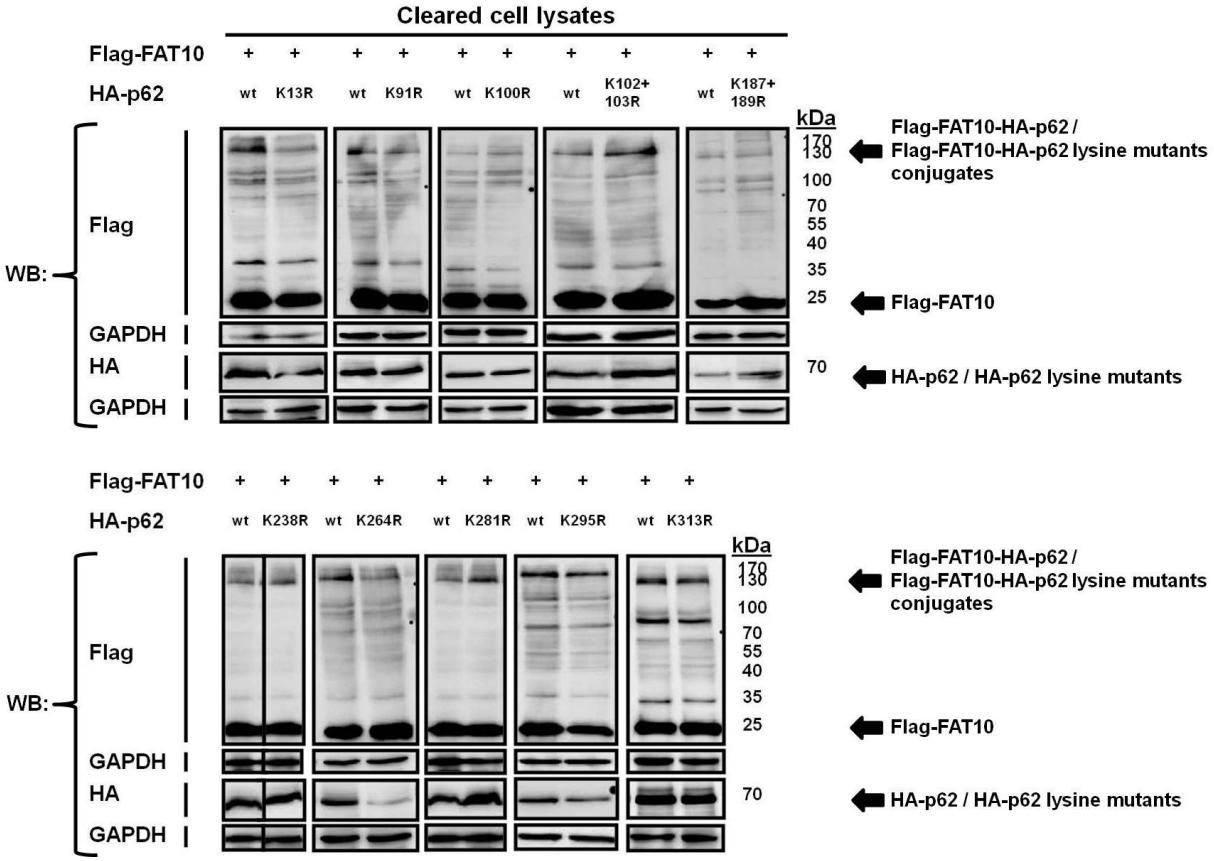

Figure 22: No lysine of p62 which is indispensable for the FAT10ylation could be identified. HEK293T cells were transiently transfected with expression plasmids for Flag-FAT10, HA-p62, and the respective lysine mutants of HA-p62, as indicated. The cleared cell lysates were boiled with a 10 % β-mercaptoethanol containing SDS-sample buffer and separated by SDS PAGE on 10 % or 12 % gels. After wet-blotting, blots were probed with either anti-Flag, or anti-HA reactive antibodies. The experiment was only performed once.

In all experiments shown in figure 22, the monomeric wild-type HA-p62 proteins as well as the respective HA-p62 lysine mutants were detectable in the anti-HA western blots. Also the monomeric Flag-FAT10 and the characteristic FAT10-p62 conjugate

of 130 kDa could be identified in each sample (fig.22). None of the lysine mutants did show a downshift in the molecular weight of the FAT10-p62 conjugate (fig.22). Only the 130 kDa FAT10-p62 conjugate band of the HA-p62(K13R) mutant was fainter compared to the wild-type control (fig.22). Therefore, one can conclude that none of these lysines are indispensable for the formation of the covalent FAT10-p62 conjugate and possibly the lysines of p62 which become FAT10ylated are redundant. In this experiment, the HA-p62(K7R) mutant is missing because the expression construct wasn't available (fig.22). The HA-p62(K7R/D69R) mutant, which was tested for its FAT10-p62 interaction capability in earlier experiments (fig.19 lane 9) in principal comprise this mutation already. However, due to the poor reproducibility of the results obtained in the experiments with the p62(K7R/D69R) constructs, it would be worthwhile to test a HA-p62(K7R) only mutant as well in the near future.

5.1.5 Which domain(s) of p62 is/are required for the non-covalent interaction with FAT10

In order to investigate which domains of p62 are involved in the non-covalent interaction with FAT10, two different methods were used: GST pulldown assays and co-immunoprecipitation experiments. For both experimental set ups the eleven HA-p62 deletion proteins mentioned in the experiment before, in combination with wild-type FAT10 were used.

5.1.5.1 *In vitro* transcription/translation and GST pulldown experiments

In order to test the non-covalent interaction between FAT10 and the HA-p62 deletion constructs, recombinantly expressed and affinity purified GST-FAT10 and *in vitro* transcribed and translated, [^{35}S] methionine labelled HA-p62 deletion proteins were used in a GST pulldown experiment (fig.23). To verify that the experimental conditions were prone to show the non-covalent interaction, in each assay the wild-type HA-p62 construct was taken along as a positive control. As negative control, besides the GST-FAT10 pulldown, also a GST pulldown was performed. The HA-p62 constructs were detected by autoradiography and the GST fusion proteins were visualised by Coomassie Brilliant Blue-staining (fig.23).

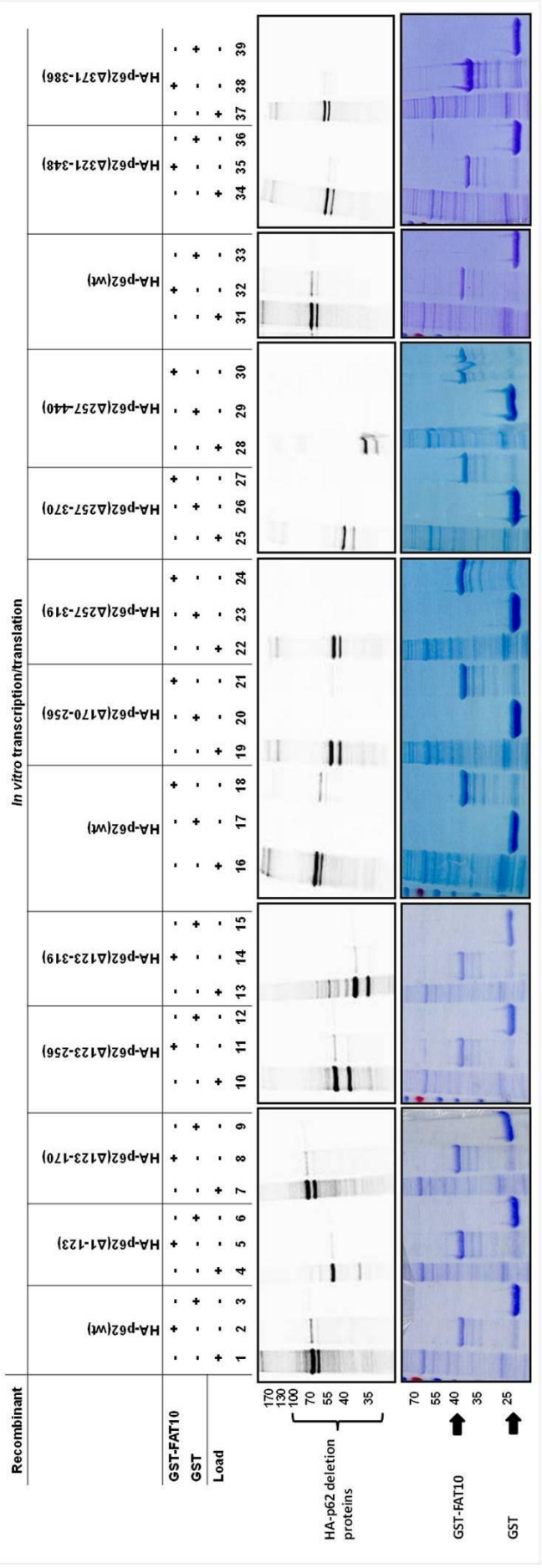
Recombinant
In vitro transcription/translation
GST-FAT10
GST
Load
HA-p62(wt)
HA-p62(Δ1-123)
HA-p62(Δ123-170)
HA-p62(Δ123-256)
HA-p62(Δ123-319)
HA-p62(wt)
HA-p62(Δ170-256)
HA-p62(Δ257-319)
HA-p62(Δ257-370)
HA-p62(Δ257-440)
HA-p62(wt)
HA-p62(Δ321-348)
HA-p62(Δ371-386)
1 2 3 4 5 6 7 8 9 10 11 12 13 14 15 16 17 18 19 20 21 22 23 24 25 26 27 28 29 30 31 32 33 34 35 36 37 38 39
170
130
100
70
55
40
35
HA-p62 deletion proteins
70
55
40
35
25
GST-FAT10
GST

Figure 23: One exemplified GST pulldown experiment for the non-covalent interaction of FAT10 and p62. Wild-type HA-p62 and HA-p62 deletion constructs were *in vitro* transcribed and translated and labelled with [^{35}S]-Methionine. Recombinant GST and GST-FAT10 were bound to a glutathione-Sepharose matrix and incubated with the respective *in vitro* translated [^{35}S]-labelled HA-p62 deletion proteins. The samples were boiled with a 10 % β-mercaptoethanol containing SDS-sample buffer and separated by SDS-PAGE on 12 % gels. The HA-p62 constructs were detected by autoradiography and the GST fusion proteins were visualised by Coomassie Brilliant Blue-staining. One out of several independent experiments with different outcomes is shown. The number of repeats for each p62 construct, as well as its FAT10 interaction results are summarised in table 49.

According to the Coomassie Brilliant Blue-staining, the amounts of the recombinant GST-FAT10 or GST protein which were used for the pulldown assay were comparable. Also the amounts of the *in vitro* transcribed and translated, [^{35}S] labelled HA-p62 deletion proteins were expressed at comparable amounts, according to the autoradiogram. The wild-type HA-p62 protein was successfully pulled down together with GST-FAT10 (fig.23, lane 2, 18, 32). According to the autoradiogram of the experiment which is exemplified in figure 23, also the HA-p62(Δ1-123) (fig.23, lane 5), HA-p62(Δ123-170) (fig.23, lane 8), HA-p62(Δ123-256) (fig.23, lane 11), HA-p62(Δ123-319) (fig.23, lane 14), HA-p62(170-256) (fig.23, lane 21), HA-p62(Δ321-348) (fig.23, lane 35) and HA-p62(Δ371-386) (fig.23, lane 38) did interact with GST-FAT10. The HA-p62 deletion constructs HA p62(Δ257-319) (fig.23, lane 24), HA-p62(Δ257-370) (fig.23, lane 27) and HA p62(Δ257-440) (fig.23, lane 30) did not interact with GST-FAT10.

Among the HA-p62 proteins which were pulled down together with the GST-FAT10, the intensity of the bands differed. The bands of the wild-type p62 (fig.23, lanes 2, 18, 32) or HA-p62(Δ123-170) (fig.23, lane 8), HA-p62(123-256) (fig.23, lane 11), HA-p62(Δ123-319) (fig.23, lane 14) which were pulled down together with GST-FAT10 were more prominent compared to the amounts of HA-p62(Δ170-256) (fig.23, lane 21), HA-p62(Δ321-348) (fig.23, lane 35) or HA-p62(Δ371-386) (fig.23, lane 38). This could be due to differences among the HA-p62 deletion proteins concerning their affinities towards GST-FAT10. In this experiment there was no interaction detectable between the HA-p62 constructs and the recombinant GST only protein.

Since when the experiment was repeated, for some of the HA-p62 deletion proteins the results were inconsistent, a table was prepared which summarises the results for all HA-p62 deletion proteins (tab.49).

Table 49: Overview of the interaction results and the number of replicates for the GST pulldown assays with the HA-p62 deletion proteins and GST-FAT10 (fig.23). Only those experiments were considered in which the GST only negative controls were actually negative.

p62 deletion proteins	total number of repeats	non-covalent interaction		
		+	-	?
HA-p62(wt)	6	6		
HA-p62(Δ1-123)	2	1	1	
HA-p62(Δ123-170)	2	2		
HA-p62(Δ123-256)	2	2		
HA-p62(Δ123-319)	2	2		
HA-p62(Δ170-256)	2	1		1
HA-p62(Δ257-319)	2		1	1
HA-p62(Δ257-370)	4		4	
HA-p62(Δ257-440)	4	1	3	
HA-p62(Δ321-348)	2	2		
HA-p62(Δ371-386)	2	2		
HA-p62(Δ386-440)	0			

According to this summary, it can be suggested that HA-p62(Δ123-170), HA-p62(Δ123-256), HA-p62(Δ123-319) HA-p62(Δ321-348) and (HA-p62Δ371-386) may still interact with GST-FAT10 while HA-p62(Δ257-370) and probably HA-p62(Δ257-440) do not (tab.49). Despite using equal amounts of the recombinant GST-FAT10 and GST protein and despite having equal expression rates for the *in vitro* transcribed and translated HA-p62 protein in each assay, the data for the interaction of HA-p62(Δ1-123), HA-p62(Δ170-256) and HA-p62(Δ257-319) with FAT10 interaction were inconsistent (tab.49). In the following figure, the results which are summarised in table 49 are depicted as a schematic (fig.24).

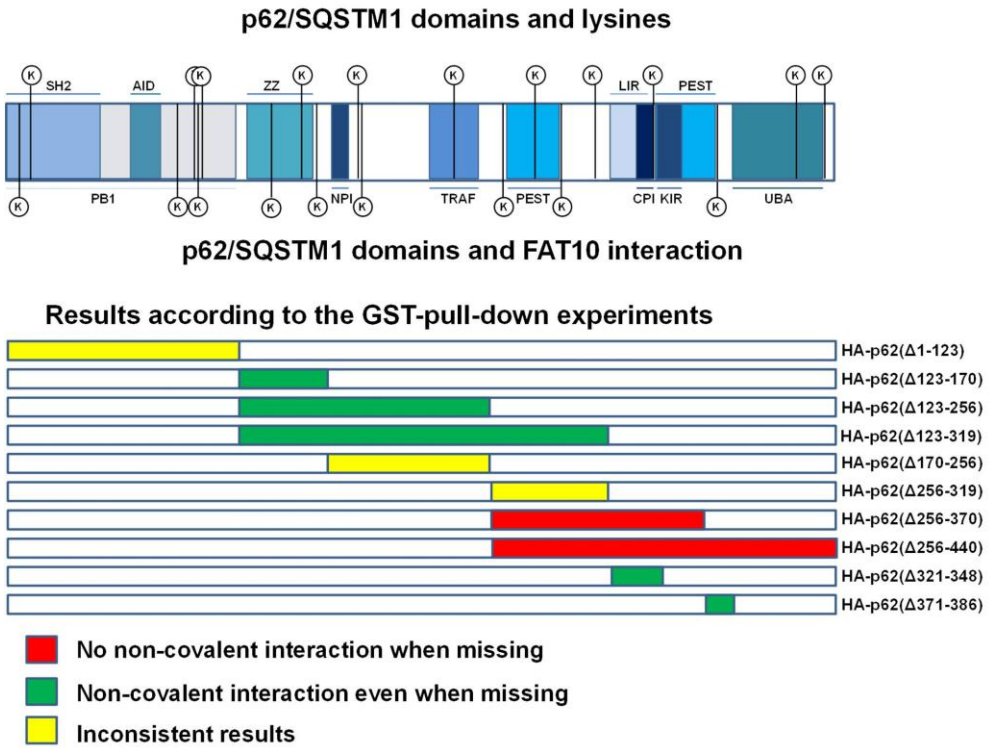

Figure 24: Overview over the domains of p62 which, according to the GST pulldown experiments (tab.49), may be required for the non-covalent interaction with FAT10. In the upper part of the figure a schematic of p62, including all domains and lysines, is depicted. The schematic on the lower part of the figure summarises the results obtained for the non-covalent interactions between the HA-p62 deletion proteins and Flag-FAT10 (fig.23, tab.49). HA-p62 deletion proteins, where the deletions impeded the non-covalent interaction with FAT10 the deleted areas are coloured in red. The deleted areas of p62 deletion proteins which did interact non-covalently with FAT10 irrespectively of their deletions are coloured in green. Deletions with inconsistent results were coloured in yellow.

According to the schematic in figure 24, deletions in HA-p62 between the amino acids 123 and 348 as well as 371 and 386 do not impede the interaction with FAT10. These deletions comprise the ZZ domain, the NPI domain, the TRAF domain, the N-terminal PEST domain, the LIR domain and the CPI domain of p62 (fig.24). Theses area overlaps with those deletions of p62 which do impede the interaction with FAT10 when missing: HA-p62(Δ256-440). Therefore, the areas between the amino acids 348 and 371 or 386 and 440 of p62 seem to be required for the non-covalent interaction with FAT10. Those areas comprise the KIR domain, the C-terminus of the C-terminal PEST domain and the UBA domain (fig.24). The results for HA-p62(Δ170-256), HA-p62(256-319) and the PB1 deleted HA-p62(Δ1-123) were inconsistent. However, the area between the amino acids 170 and 319 was also comprised in other truncations (fig.24). For the PB1 domain one could, according to the results for

the amino acids 256-440 deleted HA-p62 proteins at least suggest, that its presence alone doesn't suffice for the non-covalent interaction with FAT10.

In order to repeat and complement the existing data set shown in figure 23-24 and table 49, a fresh batch of recombinant GST-FAT10 was prepared. In the first experiment that was performed with the freshly prepared GST-FAT10 stock, all *in vitro* transcribed and translated HA-p62 constructs which were utilises for this experiment were pulled down with the recombinant GST-FAT10 (fig.25, upper panel, lanes 3, 6, 9, 12, 15, 18, 21). This was in contradiction to the results shown before (fig.23-24, tab.49). This for example could be due to the precipitation of proteins. The FAT10 protein in general is prone for precipitation (Buchsbaum, Bercovich et al. 2012) and the GST-FAT0 protein, despite being much more soluble than untagged FAT10, still has a tendency to precipitate (unpublished data). Although there was no obvious protein precipitation visible by eye, a second experiment with the new GST-FAT10 batch and the same HA-p62 deletion constructs was performed. In order to spin down the potentially precipitated GST-FAT10 or GST only proteins the reaction mixtures, which contain the respective *in vitro* transcribed and translated HA-p62 deletion constructs with either the recombinant GST-FAT10 or GST, were incubated for 3 hours at 4 °C and afterwards centrifuged with 15000 rpm at 4 °C for 15 minutes. Only the supernatants were used in the subsequent GST pulldown experiments (fig.25, lower panel).

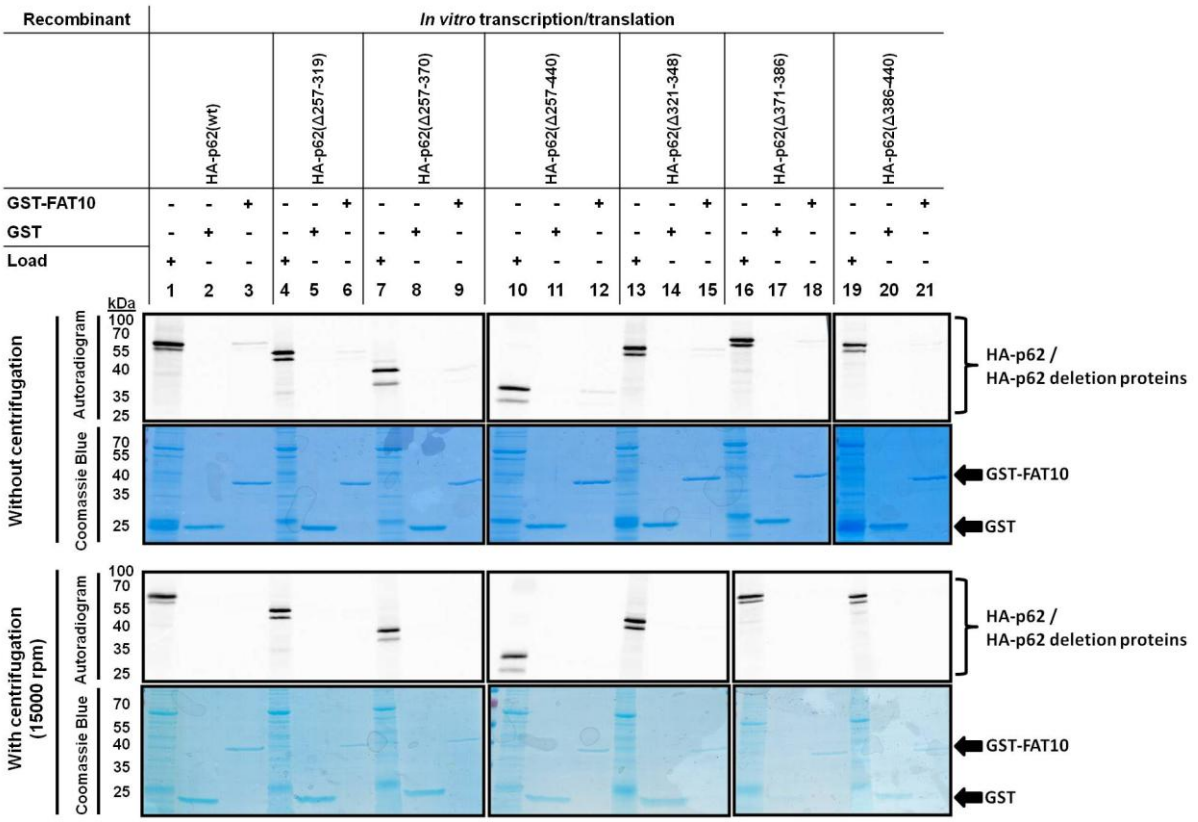

Figure 25: The GST-FAT10 protein has a tendency to precipitate which may lead to inconsistent results in the GST pulldown experiments. A freshly prepared GST-FAT10 batch was used to complete and verify the dataset shown in figure 23 and table 49. The wild-type HA-p62 and HA-p62 truncations were *in vitro* transcribed and translated and labelled with [^{35}S]-methionine. Recombinant GST and GST-FAT10 were bound to glutathione-Sepharose matrix and incubated with the *in vitro* transcribed and translated [^{35}S]-labelled HA-p62 deletion proteins. The samples were boiled with a 10 % β-mercaptoethanol containing SDS-sample buffer and separated by SDS PAGE on 12 % gels. The HA-p62 deletion proteins were detected by autoradiography and the GST fusion proteins were visualised by Coomassie Brilliant Blue-staining. In the experiment shown in the upper panel, the GST-FAT10 or GST proteins and the respective *in vitro* transcribed and translated HA-p62 proteins were directly loaded on the GSH-Sepharose. In the experiments shown in the lower panel, the GST-FAT10 or GST proteins were incubated together with the *in vitro* transcribed and translated HA-p62 proteins and in order to remove the precipitated proteins, the mixtures were centrifuged and only the supernatants were loaded on the GSH-Sepharose.

In the experiment shown in the upper panel, according to the Coomassie Brilliant Blue-staining, in all samples equal amounts of the GST-FAT10 or GST protein were used. Also the amounts of HA-p62, HA-p62(Δ257-319), HA-p62(Δ257-370), HA-p62(Δ257-440), HA-p62(321-348), HA-p62(Δ371-386) and HA-p62(Δ386-440) were equally expressed. All these p62 deletion proteins were pulled down together with GST-FAT10, but not with GST. This is in contrast to the results of the experiments

summarised in figure 24 and table 49 in which HA-p62(Δ257-370) and HA-p62(Δ257-440) were found not to interact with GST-FAT10.

In the pulldown experiment which is shown in figure 25 in the lower panel, after the centrifugation step the recombinant GST-FAT10 and GST protein were still detectable in the Coomassie staining. However in this experiment, none of the *in vitro* transcribed and translated HA-p62 deletion proteins were pulled down anymore, not even the wild-type HA-p62 which was never the case in the former experiments (tab.49). Therefore, one cannot rule out that the recombinant GST-FAT10 precipitates and that the p62 deletion constructs precipitate along with FAT10, leading to inconsistent data in the pulldown experiments.

5.1.5.2 Transient transfection and co-immunoprecipitation experiments

Because of the mentioned inconsistencies in the result obtained with the *in vitro* transcription/translation assay (tab.49, fig.23-25), another experimental setup was used to further characterise the non-covalent interaction between FAT10 and p62.

HEK293T cells were transiently transfected with either the HA-p62 deletion constructs alone, or co-transfected with Flag-FAT10 and the HA-p62 deletion constructs (fig.26). Additionally cells were co-transfected with wild-type HA-p62 and Flag-FAT10 (fig.26, lane 4) and transfected with either Flag-FAT10 or HA-p62 only (fig.26, lanes 2, 3). For the mock control, cells were treated with the transfection reagent only (fig.26, lane 1). With the cleared cell lysates, anti-Flag immunoprecipitation experiments were performed. The samples were analysed by western blot experiments. In order to detect the monomeric HA-p62 and the monomeric HA-p62 deletion proteins or the monomeric Flag-FAT10 as well as the Flag-FAT10 conjugates which were utilised for the anti-Flag immunoprecipitation experiments, the western blots with the cleared cell lysates (load) were stained with either anti-HA or anti-Flag antibodies, respectively. The western blots of the anti-Flag-immunoprecipitation experiment were stained with either anti-Flag or anti-HA antibodies in order to detect either the immunoprecipitated monomeric Flag-FAT10 and the Flag-FAT10-conjugates, or the co-immunoprecipitated HA-p62 as well as the HA-p62 deletion proteins. In the anti-HA western blot of the immunoprecipitation experiments only those HA-p62 proteins should be detectable which are covalently

attached to Flag-FAT10 or which formerly did interact with Flag-FAT10 non-covalently.

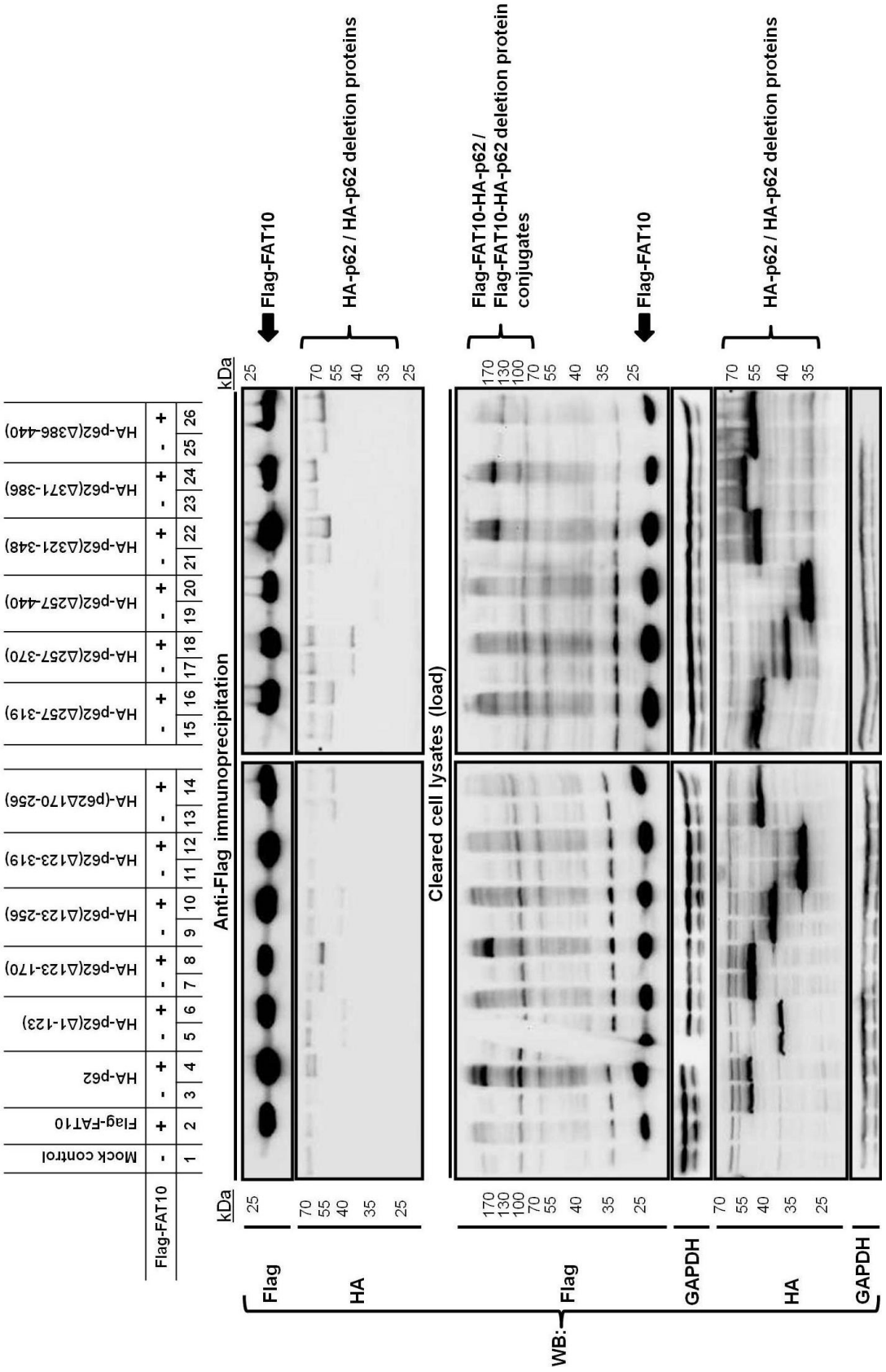

Figure 26: In order to test the non-covalent interaction between FAT10 and p62, co-immunoprecipitation experiments with Flag-FAT10 and HA-p62 deletion proteins were performed. HEK293T cells were transiently transfected with Flag-FAT10 and wild-type HA-p62 or the HA-p62 deletion proteins, as indicated. After harvesting, cells were lysed and supernatants were used for the co-immunoprecipitation experiments with anti-FLAG-M2-conjugated agarose. The samples were boiled with a 10 % β-mercaptoethanol containing SDS-sample buffer and separated by SDS PAGE on 12 % gels. After wet-blotting, blots were probed with either anti-Flag, or anti-HA reactive antibodies. One experiment out of two independent experiments is shown.

According to the anti-HA western blots of the cell lysates (load), HA-p62 (fig.26, lanes 3, 4) as well as the eleven HA-p62 deletion proteins were detectable in all cells which were transfected with the respective DNA constructs (fig.26, lanes 5-26). The same was true for the monomeric Flag-FAT10 proteins as well as for the Flag-FAT10 conjugates in the corresponding anti-Flag western blots (fig.26). As shown in figure 22, the Flag-FAT10-HA-p62 conjugates were detectable in the anti-Flag western blots of the cell lysates in cells which co-express either HA-p62, HA-p62(Δ123-170), HA p62(Δ321-348), HA-p62(Δ371-386) or HA-p62(Δ386-440) together with Flag FAT10 (fig.26, lanes 4, 8, 22, 24, 26).

In the anti-Flag western blot of the anti-Flag immunoprecipitation experiments, the monomeric Flag-FAT10 was detectable in all samples (fig.26). Besides the wild-type HA-p62 (fig.26, lane 4), also HA-p62(Δ123-170) (fig.26, lane 8), HA-p62(Δ170-256) (fig.26, lane 14), HA p62(Δ257-319) (fig.26, lane 16), HA-p62(Δ257-370) (fig.26, lane 18), HA p62(Δ321-348) (fig.26, lane 22), HA-p62(Δ371-386) (fig.26, lane 24) and HA-p62(Δ386-440) (fig.26, lane 26) were co-immunoprecipitated together with Flag-FAT10. Despite the stringent washing conditions, also in those samples which were transfected with the HA-p62 deletion constructs only, these deletion proteins were co-immunoprecipitated with the anti-Flag coupled agarose. However, besides for the HA-p62(Δ170-256) deletion protein (fig.26, lanes 13, 14), the signals were stronger in samples in which the deletion protein was pulled down together with Flag-FAT10. No co-immunoprecipitation at all was detectable for the HA-p62(Δ1-123) (fig.26, lane 6), HA-p62(Δ123-256) (fig.26, lane 10), HA-p62(Δ123-319) (fig.26, lane 12) and HA-p62(Δ257-440) (fig.26, lane 20) deletion proteins.

The experiment shown in figure 26 was repeated in exactly the same way and is shown in figure 27.

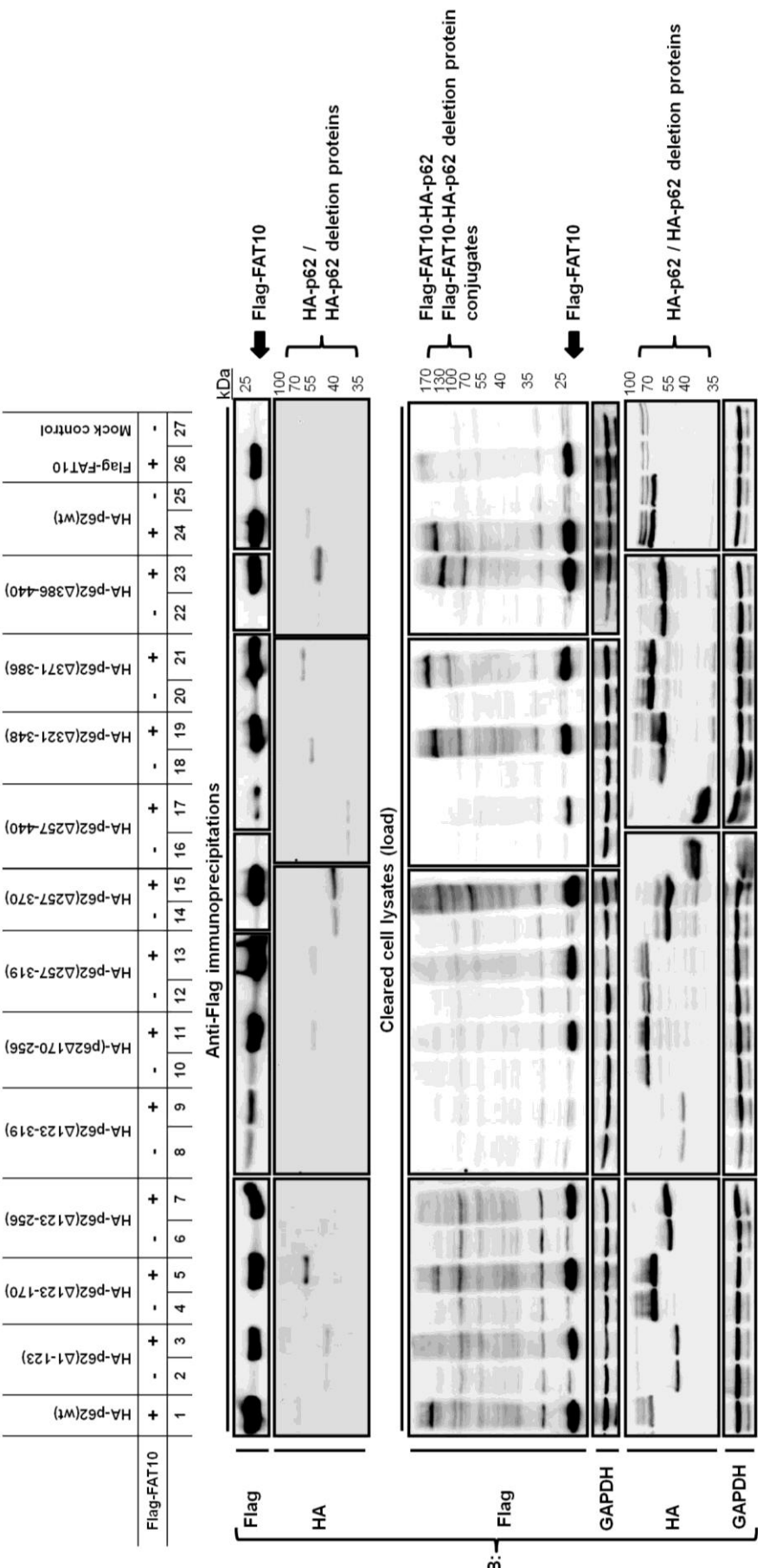
Flag-FAT10
HA-p62(wt)
HA-p62(Δ1-123)
HA-p62(Δ123-170)
HA-p62(Δ123-256)
HA-p62(Δ123-319)
HA-(p62Δ170-256)
HA-p62(Δ257-319)
HA-p62(Δ257-370)
HA-p62(Δ257-440)
HA-p62(Δ321-348)
HA-p62(Δ371-386)
HA-p62(Δ386-440)
HA-p62(wt)
Flag-FAT10
Mock control
1 2 3 4 5 6 7 8 9 10 11 12 13 14 15 16 17 18 19 20 21 22 23 24 25 26 27
Anti-Flag immunoprecipitations
Cleared cell lysates (load)
kDa
Flag-FAT10
HA-p62 / HA-p62 deletion proteins
Flag-FAT10-HA-p62
Flag-FAT10-HA-p62 deletion protein conjugates
Flag-FAT10
HA-p62 / HA-p62 deletion proteins
WB:
Flag
HA
Flag
GAPDH
HA
GAPDH

Figure 27: Repetition of the co-immunoprecipitation experiments as shown in figure 26, to test non-covalent interaction between Flag-FAT10 and HA-p62 deletion constructs. HEK293T cells were transiently transfected with wild-type Flag-FAT10 and wild-type HA-p62 or the HA-p62 deletion constructs as indicated. After harvesting, the cells were lysed and the supernatants were used for co-immunoprecipitation experiments with anti-FLAG-M2-conjugated agarose. The samples were boiled with a 10 % β-mercaptoethanol containing SDS.-sample buffer and separated by SDS PAGE on 12 % gels. After wet-blotting, blots were probed with either anti-Flag, or anti-HA reactive antibodies. One experiment out of two independent experiments is shown.

In the anti-Flag western blots for the cell lysates (load), the monomeric FLAG-FAT10 as well as the Flag-FAT10 conjugates were detectable in all cells which were transfected with the respective DNA constructs (fig.27). However in the Flag-FAT10 and HA-p62(Δ123-319) (fig.27, lane 9) or HA-p62(Δ257-440) (fig.27, lane 17) co-transfected cells the Flag-FAT10 protein amounts were very low. As shown in the figures 20 and 26, the Flag-FAT10-HA-p62 conjugates were detectable in the anti-Flag western blots of the cell lysates in cells which co-express either HA-p62 (fig.27, lanes 1, 24), HA-p62(Δ123-170) (fig.27, lane 5), HA-p62(Δ321-348) (fig.27, lane 19), HA p62(Δ371-386) (fig.27, lane 21) or HA-p62(Δ386-440) (fig.27, lane 23) together with Flag-FAT10. Possibly in this experiment there is also a Flag-FAT10-HA-p62(Δ257-370) conjugate detectable in the HA-p62(Δ257-370) and Flag-FAT10 co-expressing cells (fig.27, lane 15). In this sample also the general Flag-FAT10 conjugate smear was more intensive compared to the other Flag-FAT10 containing samples in this experiment. However this potential Flag-FAT10-HA-p62(Δ257-370) conjugate was detected in one experiment (fig.27) out of four independent experiments (fig.20 + replicate, 26 and 27) only. The monomeric HA-p62 (fig.27, lanes 1, 24-25) as well as the eleven HA-p62 deletion proteins (fig.27, lanes 2-23) were detectable in all cells which were transfected with the respective DNA constructs. However, the protein amounts of HA-p62(Δ123-319) (fig.27, lanes 8-9) were less compared to the protein amounts of the other ten HA-p62 deletion proteins (fig.27, lanes 2-7, 10-23) and the wild-type HA-p62 (fig.27, lanes 1, 24, 25).

As shown in the anti-Flag western blot of the immunoprecipitation experiments, in all samples which express Flag-FAT10, the monomeric Flag-FAT10 was successfully immunoprecipitated (fig.27). In the anti-HA western blots of the immunoprecipitation experiments, the HA-p62(Δ123-170) (fig.27, lane 5), HA-p62(Δ257-370)

(fig.27, lane 15) and HA-p62(Δ386-440) (fig.27, lane 23) deletion proteins were co-immunoprecipitated most successfully. Like in the experiment shown in figure 26 lane 4, the bands of the co-immunoprecipitated wild-type HA-p62 (fig.27, 1, 24) were very faint in this experiment, too. Comparable faint signals were also detectable for the co-immunoprecipitated HA-p62(Δ1-123) (fig.27, lane 3), HA-p62(Δ170-256) (fig.27, lane 11), HA-p62(Δ257-319) (fig.27, lane 13), HA-p62(Δ257-440) (fig.27, lane 17), HA-p62(Δ321-348) (fig.27, lane 19) and HA-p62(Δ371-386) (fig.27, lane 21) deletion proteins. Compared to the experiment in figure 26, in this experiment the signals of the co-immunoprecipitated HA-p62 deletion proteins were much fainter (fig.27). However, in this experiment only two of the HA-p62 deletion proteins were found to bind to the anti-Flag coupled agarose directly. In the HA-p62(Δ257-370) only expressing sample (fig.27, lane 14), HA-p62(Δ257-370) was also found to bind to the anti-Flag coupled agarose unspecifically, however to a less extend compare to the amount which was co-immunoprecipitated together with Flag-FAT10 (fig.27, lane 15). For HA-p62(Δ257-440) the signal of the co-immunoprecipitated protein was very faint (fig.27, lane 17) and a comparable signal was found in the HA-p62(Δ257-440) only expressing sample (fig.27, lane 16).

No co-immunoprecipitation was detectable for HA-p62(Δ123-256) (fig.27, lane 7) and HA-p62(Δ123-319) (fig.27, lane 9). However, the protein amounts of Flag-FAT10 and HA-p62(Δ123-319) were very low in this sample.

The results of the experiments shown in the figures 26 and 27 for the non-covalent interaction capability of the HA-p62 deletion constructs are summarised in the following table (tab.50).

Table 50: Overview of the results and the number of replicates for co-immunoprecipitation experiments with the HA-p62 deletion proteins and wild-type Flag-FAT10 (fig.26-27).

p62 contructs	total number of repeats	non-covalent interaction		
		+	-	?
HA-p62(wt)	2	2		
HA-p62(Δ1-123)	2	1	1	
HA-p62(Δ123-170)	2	2		
HA-p62(Δ123-256)	2		2	
HA-p62(Δ123-319)	2		2	
HA-p62(Δ170-256)	2	1		1
HA-p62(Δ257-319)	2	2		
HA-p62(Δ257-370)	2	2		
HA-p62(Δ257-440)	2		1	1
HA-p62(Δ321-348)	2	2		
HA-p62(Δ371-386)	2	2		
HA-p62(Δ386-440)	2	2		

According to this results (fig.26-27, tab.50) it can be suggested that probably the following HA-p62 deletion constructs may interact with Flag-FAT10 non-covalently: HA-p62(Δ123-170), HA-p62(Δ257-319), HA-p62(Δ257-370), HA-p62(Δ321-348), HA-p62(Δ371-386) and HA-p62(Δ386-440) (tab.50, fig.28). The deletion constructs HA-p62(Δ123-256) and HA-p62(Δ123-319) possibly do not interact non-covalently with Flag-FAT10. For HA-p62(Δ1-123), HA-p62(Δ170-256) and HA-p62(Δ257-440) the current data do not afford any assessments (tab.50, fig.28).

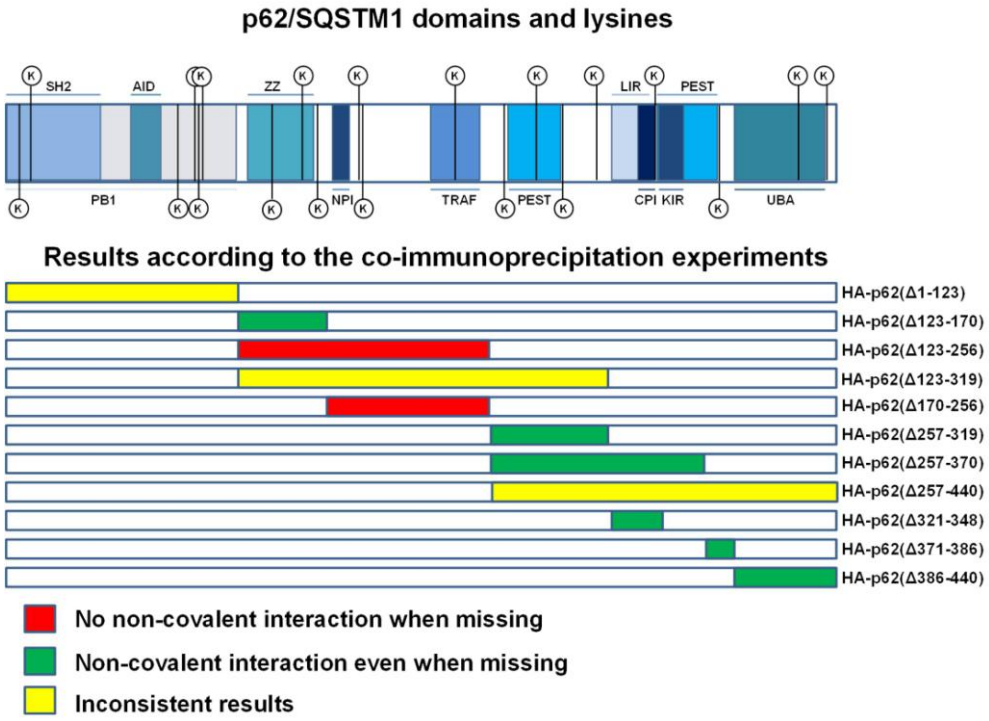

Figure 28: Overview over the domains of p62 which according to the anti-Flag co-immunoprecipitation experiments (tab.50), may be required for the non-covalent interaction with FAT10. In the upper part of the figure a schematic of p62, including all domains and lysines, is depicted. The schematic on the lower part of the figure summarises the results obtained for the non-covalent interactions between the HA-p62 deletion proteins and the Flag-FAT10 (fig.26-27, tab.50). In the HA-p62 deletion proteins, where the deletions impede the non-covalent interaction with FAT10, the deleted areas are coloured in red. The deleted areas of p62 deletion proteins which do interact with Flag-FAT10 irrespectively of their deletions are coloured in green. Deletions that, due to inconsistent results, could not have been assessed were coloured yellow.

According to the results of the co-immunoprecipitation experiments, one could conclude, that deletions between the amino acids 170 and 256 of HA-p62 might impede the non-covalent interaction with Flag-FAT10. This area comprises the NPI and the TRAF domains (fig.28).

In contrast to the data obtained with the co-transfection and co-immunoprecipitation experiment (tab.50, fig.28), the data collected in the GST pulldown assay, HA-p62(Δ123-256) would still interact with GST-FAT10 while HA-p62(Δ257-370) does not (tab.491, fig.24). Only for four of the eleven p62 deletion constructs, the results that were obtained with both experimental set ups were not contradicting (fig.29).

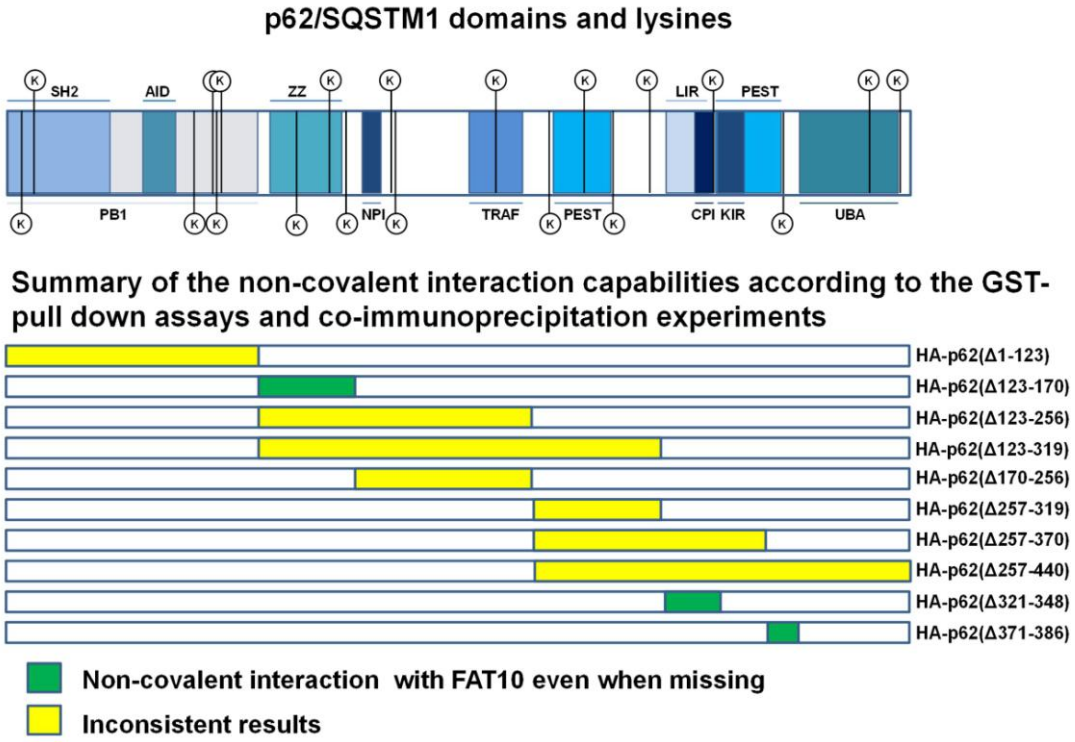

Figure 29: Summary of the domains of p62 that, according to the GST pulldown (tab.49) and anti-Flag co-immunoprecipitation experiments (tab.50), may be required for the non-covalent interaction with FAT10. In the upper part of the figure a schematic of p62 with all its domains and lysines is depicted. In the lower part of the figure a schematic overview for the non-covalent interaction result that were obtained with the GST pulldown (fig.23, 24, tab.1) and anti-Flag-co-immunoprecipitation experiments (fig.26-28, tab.2). The deleted areas of p62 deletion proteins which do interact with FAT10 irrespectively of their deletions are coloured in green. Deletions that, due to inconsistent results, could not have been assessed are coloured in yellow.

With both experimental systems, the deletion constructs HA-p62(Δ123-170), HA-p62(Δ321-348) and HA-p62(Δ371-386) were tested positive for the non-covalent interaction with FAT10 (tab.49, 50 and fig.24, 28, 29). Therefore, one could suggest, that the ZZ domain, the LIR domain, the CPI domain and the C-terminus of the C-terminal PEST domain of HA-p62 are dispensable for the non-covalent interaction with Flag-FAT10. According to the summarised results which were obtained with the two different experimental setups, no deleted area of p62 could be detected which impedes the non-covalent interaction with FAT10 completely in both systems (fig.29).

5.1.6 The isolated PB1 domain of HA-p62 doesn't suffice to bind to Flag-FAT10 neither covalently, nor non-covalently

5.1.6.1 Transient transfection and co-immunoprecipitation experiments

Since those HA-p62 deletion constructs in which the deletion encompass the PB1 domain, the TRAF domain, or the N-terminal PEST domain were not FAT10ylated anymore (fig.20-21), it was tested whether these isolated p62 domains would suffice to become FAT10ylated. Therefore, HEK293T cells were transiently co-transfected with the HA-tagged constructs encoding for the respective isolated p62 domains and Flag-FAT10 (fig.30, lanes 9, 10, 11). As positive control, a sample of cells which co-expressed both Flag-FAT10 and HA-p62 was taken along (fig.30, lanes 8). Since the depletion of the UBA domain did not influence the FAT10ylation of HA-p62 (Aichem, Kalveram et al. 2012), the isolated UBA domain of p62 was taken along as a negative control (fig.30, lanes 7, 12). Further, Flag-FAT10 (fig.30, lanes 2, 14), HA-p62 (fig.30, lanes 3, 15), HA-p62(PB1 only) (fig.30, lanes 4, 16), HA-p62(TRAF only) (fig.30, lanes 5, 17), HA-p62(PEST only) (fig.30, lanes 6, 18) and HA-p62(UBA only) (fig.30, lanes 7, 19) were transfected alone as negative controls. As a mock control, cells were treated with the transfection reagent only (fig.30, lane 1, 13). An anti-Flag immunoprecipitation was performed in order to investigate whether the isolated p62 domains would be co-immunoprecipitated with FAT10 (fig.30, lanes 13-24). The samples were analysed by western blot experiments. In order to detect the monomeric HA-p62 and the isolated HA-p62 domains or the monomeric Flag-FAT10 as well as the Flag-FAT10 conjugates which were utilised for the anti-Flag immunoprecipitation experiments, the western blots with the cleared cell lysates (load) were stained with either anti-HA or anti-Flag antibodies respectively. The western blots of the anti-Flag-immunoprecipitation experiment were stained with either anti-Flag or anti-HA antibodies in order to detect either the immunoprecipitated monomeric Flag-FAT10 and the Flag-FAT10-conjugates, or the co-immunoprecipitated HA-p62 as well as the isolated HA-p62 domains. In the anti-HA western blot of the immunoprecipitation experiments only those HA-p62 proteins should be detectable which are covalently attached to Flag-FAT10 or which formerly did interact non-covalently with Flag-FAT10.

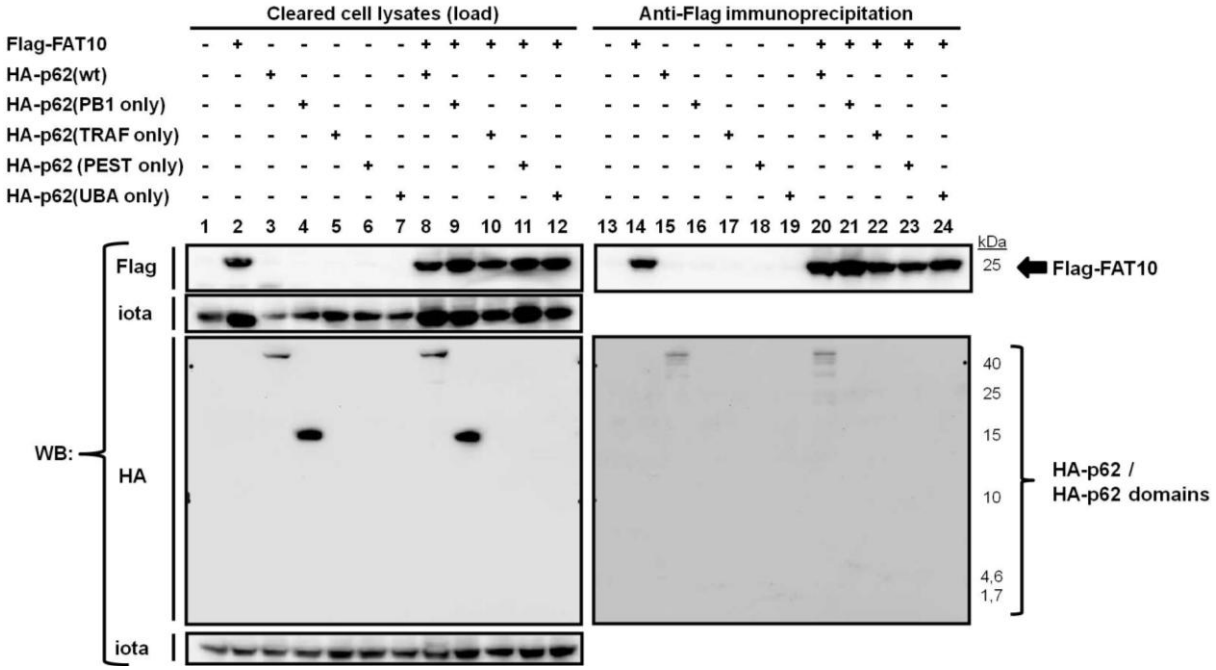

Figure 30: The isolated PB1 domain of p62 doesn't seem to interact with Flag-FAT10, neither covalently nor non-covalently. HEK293T cells were transiently transfected with Flag-FAT10 and HA-p62 or the isolated HA-tagged p62 domains (PB1, TRAF, PEST, UBA) as indicated. After harvesting, the cleared supernatants were used for the co-immunoprecipitation experiments with anti-FLAG-M2-conjugated agarose. The samples were boiled with a 10 % β-mercaptoethanol containing SDS-sample buffer and separated by TRIS-Tricin gel electrophoresis (Schagger and von Jagow 1987). After the wet-blotting on PVDF membranes, the blots were probed with either anti-Flag, or anti-HA reactive antibodies. The monomeric wild-type HA-p62 has a molecular weight of 70 kDa, the HA-PB1 domain of 12,5 kDa, the HA-TRAF domain of 4,5 kDa, the N-terminal PEST domain as well as the HA-UBA domain of 6 kDa and the monomeric FAT10 of 25 kDa. One experiment out of two independent experiments is shown.

In the anti-Flag and anti-HA stained western blots of the cleared cell lysates, Flag-FAT10 (fig.30, lanes 2, 8-12) and HA-p62 (fig.30, lanes 3, 8) were detectable in the samples which were transfected with the respective DNA constructs. Although being cloned into the same backbone plasmid and besides the verification of the cloning success by sequencing, out of the four isolated p62 domains only the HA-PB1 domain of p62 was detectable in the anti-HA western blot (fig.30, lanes 4, 9). In the anti-Flag western blots, of the corresponding anti-Flag immunoprecipitation experiment, the immunoprecipitated Flag-FAT10 was detectable for all Flag-FAT10 containing samples (fig.30, lanes 14, 20-24). In the anti-HA western blot of the immunoprecipitation experiments, the isolated PB1 domain was not co-immunoprecipitated with Flag-FAT10 (fig.30, lane 21), indicating, that it doesn't interact with FAT10. HA-p62 in contrast was detectable in the anti-Flag

immunoprecipitation experiments of the Flag-FAT10 and HA-p62 co-expressing sample (fig.30, lanes 21) as well as in the HA-p62 only containing sample (fig.30, lanes 15), indicating that it stacked to the anti-Flag coupled agarose unspecifically.

5.1.6.2 *In vitro* transcription/translation and GST pulldown experiments

Since, besides the HA tagged PB1 domain of p62 (fig.30, lane 4, 9), the isolated HA-p62 domains were not detectable in the total cell lysates of the transfected HEK293T cells (fig.30), the *in vitro* transcription and translation system was used in order to express HA-p62 (fig.31, lane 1) and the isolated HA-p62 domains (fig.31, lanes 4, 7, 10, 13) in the next experiment. In the subsequent GST pulldown with GST-FAT10, their non-covalent interaction capabilities with FAT10 were tested. As negative controls, the GST pulldowns for HA-p62 and all isolated HA-p62 domains were additionally performed with recombinant GST protein instead of GST-FAT10. The samples were separated in western blot experiments and the [^{35}S] methionine labelled HA-p62 domains were detected by autoradiography and the GST-fusion proteins were visualised by Coomassie Brilliant Blue-staining.

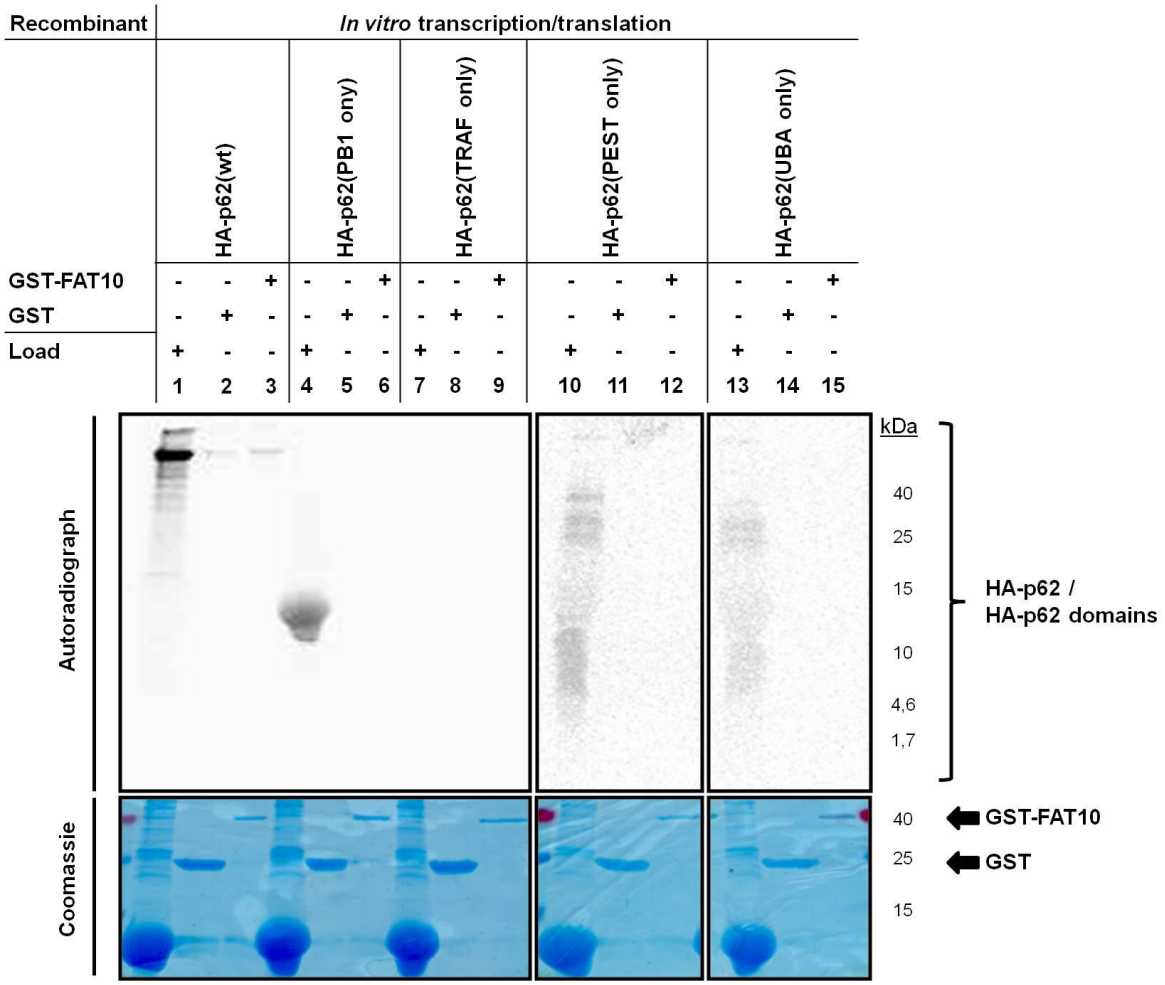

Figure 31: The isolated PB1 domain of p62 doesn't seem to interact with Flag-FAT10 non-covalently. The wild-type HA-p62 and the isolated HA-tagged p62 domains were *in vitro* transcribed/translated and labelled with [^{35}S]-methionine. Recombinant GST and GST-FAT10 were bound to glutathione-Sepharose matrix and incubated with the *in vitro* translated [^{35}S]-labelled HA-p62 constructs. The samples were boiled with a 10 % β-mercaptoethanol containing SDS-sample buffer and separated by SDS PAGE on 18 % gels. The HA-p62 constructs were detected by autoradiography and the GST fusion proteins were visualised by Coomassie Blue-staining. The monomeric wild-type HA-p62 protein has a molecular weight of 70 kDa, the HA-PB1 domain of 12,5 kDa, the HA-TRAF domain of 4,5 kDa, the N-terminal PEST domain as well as the HA-UBA domain of 6 kDa and the monomeric GST-FAT10 of 40 kDa. This experiment was only repeated once.

In the Coomassie Blue-staining, the recombinant GST (fig.31, lanes 2, 5, 8, 11, 14) and GST-FAT10 (fig.31, lanes 3, 6, 9, 12, 15) were detectable. In the autoradiogram, only the HA-p62 (fig.31, lane 1) and HA-p62(PB1 only) (fig.31, lane 4) were detectable. No signal was detectable for HA-p62(TRAF only), HA-p62(PEST only) or HA-p62(UBA only) (fig.31, lanes 7, 10, 13). In the corresponding GST pulldown experiment however, the PB1 was not pulled down together with GST-FAT10 (fig.31, lane 6), indicating that they do not interact. In the HA-p62 positive control

experiment however HA-p62 was pulled down with GST-FAT10 (fig.31, lane 3), but also with GST (fig.31, lane 2), indicating that it also binds to either the GSH-coupled agarose or to GST unspecifically.

Like in the transfection experiments (fig.30), also with the *in vitro* transcription and translation assay, only the wild-type HA-p62 and the isolated HA-PB1 domain were detectable (fig.31). Besides the start methionine, with the exception of the HA-p62(TRAF only) peptide, all isolated p62 domain peptides contain additional methionines and/or cysteines. Therefore, theoretically at least the HA-p62(PEST only) and HA-p62(UBA only) peptides should be easily detectable in the autoradiogram.

5.1.7 The phosphorylation status of p62 at S403 does not seem to have a severe impact on its interaction capability

Under proteasomal inhibition, the phosphorylation of p62 at S403 by a kinase called CK2 increases the affinity of the p62 UBA domain for K48- and K63-linked ubiquitin chains. This leads to an enhanced recruitment of polyubiquitylated proteins into the sequestosomes (Matsumoto, Wada et al. 2011). Proteasomal inhibition also leads to a non-covalent interaction between FAT10 and HDAC6, resulting in the microtubule-dependent localisation of FAT10 into aggresomes (Kalveram, Schmidtke et al. 2008). Furthermore, endogenous p62 and FAT10 were found to co-localise in p62 bodies in TNFα and IFNγ treated cells (Aichem, Kalveram et al. 2012). Therefore, it was interesting to investigate, whether the phosphorylation status of p62 at S403 also influences the interaction with FAT10. The phospho-mimicking p62(S403E) mutant and the non-phosphorylated p62(S403A) mutant were used in order to investigate the influence of the phosphorylation status of p62 on its FAT10 interaction capabilities.

For this, HEK293T cells were co-transfected with Flag-FAT10 and either HA-p62(S403A) (fig.32, lanes 8, 20) or HA-p62(S403E) (fig.32, lanes 9, 21). As a positive control, Flag-FAT10 and wild-type HA-p62 were co-transfected (fig.32, lanes 7, 19) and as negative controls, Flag-FAT10(ΔGG) was co-transfected with all three HA-p62 constructs (fig.32, lanes 10-12, 22-24). As additional negative controls, cells were transfected with either Flag-FAT10 (fig.32, lanes 2, 14), Flag-FAT10(ΔGG)

(fig.32, lanes 3, 15), HA-p62 (fig.32, lanes 4, 16), HA-p62(S403A) (fig.32, lanes 5, 17) or HA-p62(S403E) (fig.32, lanes 6, 18) only and as a mock control, cells were treated with the transfection reagent only (fig.32, lanes 1, 13). By an anti-Flag immunoprecipitation experiment, the non-covalent interactions between Flag-FAT10 and HA-p62(S403A) or HA-p62(S403E) were investigated. The samples were analysed by western blot experiments. In the anti-HA and anti-Flag western blots of the cleared cell lysates, the protein amounts of monomeric HA-p62, HA-p62(S403A), HA-p62(S403E) or Flag-FAT10(ΔGG) and Flag-FAT10 as well as the Flag-FAT10 conjugates were detected. The western blots of the anti-Flag-immunoprecipitation experiment were stained with either anti-Flag or anti-HA antibodies respectively in order to detect either the immunoprecipitated monomeric Flag-FAT10 and the Flag-FAT10-conjugates, or the co-immunoprecipitated HA-p62, HA-p62(S403E) and HA-p62(S403A) proteins. In the anti-HA western blot of the immunoprecipitation experiments only those HA-p62 proteins should be detectable which are covalently attached to Flag-FAT10 or which formerly did interact non-covalently with Flag-FAT10.

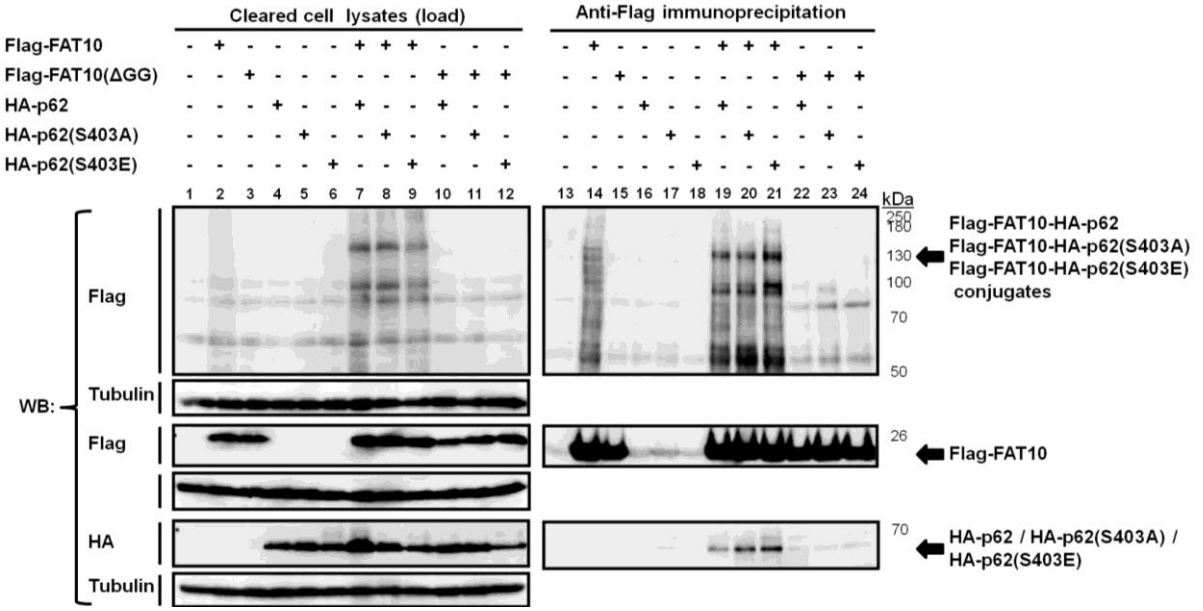

Figure 32: The phosphorylation status of p62 at S403 does not seem to have a severe impact on its interaction capability with FAT10. HEK293T cells were transiently transfected with expression plasmids for Flag-FAT10, Flag-FAT10(ΔGG), HA-p62, HA-p62(S403E) and HA-p62(S403A) as indicated. After harvesting, the cleared cell lysates were used for the co-immunoprecipitation experiments with anti-FLAG-M2-conjugated agarose. The samples were boiled with a 10 % β-mercaptoethanol containing SDS-sample buffer and separated by SDS PAGE on 10 % or 12 % gels. After wet-blotting, blots were probed with either anti Flag, or anti HA reactive antibodies. One experiment out of three independent experiments with similar outcome is shown.

In the anti-Flag western blots of the cleared cell lysates Flag-FAT10 and the FAT10ylated conjugates (fig.32, lanes 2, 7-9) as well as the monomeric Flag-FAT10(ΔGG) (fig.32, lanes 3, 10-12) were detectable in all cells which were transfected with the respective constructs. The same was true for HA-p62 (fig.32, lanes 4, 7, 10), HA-p62(S403A) (fig.32, lanes 5, 8, 11) and HA-p62(S403E) (fig.32, lanes 6, 9, 12) in the anti-HA western blots. In the anti-Flag western blots of the cell lysates, the characteristic FAT10-p62 conjugate of 130 kDa was visible in the positive control with Flag-FAT10 and HA-p62 (fig.32, lane 7) and in those samples which were co-transfected with Flag-FAT10 and either HA-p62(S403A) or HA-p62(S403E) (fig.32 lanes 8-9). The conjugate was absent in the mock control (fig.32, lane 1) as well as in the either Flag-FAT10, HA-p62, HA-p62(S403A), HA-p62(S403E) only expressing samples (fig.32, lanes 2, 4-6). As expected, no FAT10-conjugates at all were formed in cells expressing Flag-FAT10(ΔGG) (fig.32, lanes 3, 10-12).

According to the anti-Flag western blot of the immunoprecipitation experiments, monomeric Flag-FAT10(ΔGG) (fig.32, lanes 15, 22-24) and Flag-FAT10 as well as the FAT10-conjugates (fig.32, lanes 14, 19-21) were successfully immunoprecipitated in all samples expressing these proteins. In the corresponding anti-HA western blot of the immunoprecipitation experiment, all three HA-p62 constructs were also co-immunoprecipitated with Flag-FAT10 (fig.32, lanes 19-21), indicating that both mutants do interact non-covalently with FAT10. Interestingly, the Flag-FAT10(ΔGG) mutant again failed to co-immunoprecipitate HA-p62 and also HA-p62(S403A) and (S403E) (fig.32, lanes 22-24).

Taken together, the phosphorylation status of p62 on serine S403 had no influence on the interaction with FAT10 *per se*. Still it would be possible that the phosphorylation influence the amount of FAT10 interacting with p62. Unfortunately, like in figure 32 in the lanes 7-9, in all experiments the proteins amounts of the different p62 proteins were slightly different. Therefore, no clear conclusion about the quantity of the interacting FAT10 can be performed.

5.1.8 Is the FAT10-p62 conjugate of 130 kDa degraded via the proteasome or via autophagy

Annette Aichem found endogenous FAT10-p62 conjugates as well as endogenous p62 to be degraded by the proteasome (Aichem, Kalveram et al. 2012). Since FAT10 and the FAT10ylated proteins in general are degraded by the proteasome (Raasi, Schmidtke et al. 2001, Hipp, Raasi et al. 2004), but p62 mainly becomes degraded by autophagy (Pankiv, Clausen et al. 2007, Ichimura, Kumanomidou et al. 2008), it would be interesting to investigate whether the FAT10-p62 conjugate of 130kDa also is degraded via autophagy. Therefore, HEK293T cells were co-transfected with Flag-FAT10 and HA-p62 and treated either with 200 nM Bafilomycin A1 for 8 hours (fig. 33, lanes 7-12) to inhibit the autophagic degradation, or additionally with 5 µM MG132 for 6 hours (fig.33, lanes 10-12) to inhibit the proteasomal degradation, too. In order to inhibit the protein biosynthesis simultaneously, the cells were treated with 50 µg/ml cycloheximide for 2,5 hours (lanes 8, 11) or 5 hours (lanes 9, 12). Subsequently, the samples were analysed by western blot experiments. As negative control, Flag-FAT10 and HA-p62 co-transfected cells were either kept untreated (fig.33, lane 4), or were treated with cycloheximide for either 2,5 or 5 hours

(fig.33, lanes 5-6). Furthermore cells were transfected with either Flag-FAT10 or HA-p62 only (fig.33, lanes 2, 3) or were treated with transfection reagent only as a mock control (fig.33, lane 1). The samples were analysed in western blot experiments. The western blots were stained with either anti-Flag reactive antibodies in order to detect the monomeric Flag-FAT10 as well as the Flag-FAT10-conjugates, or with anti-HA reactive anti-bodies in order to detect the monomeric HA-p62.

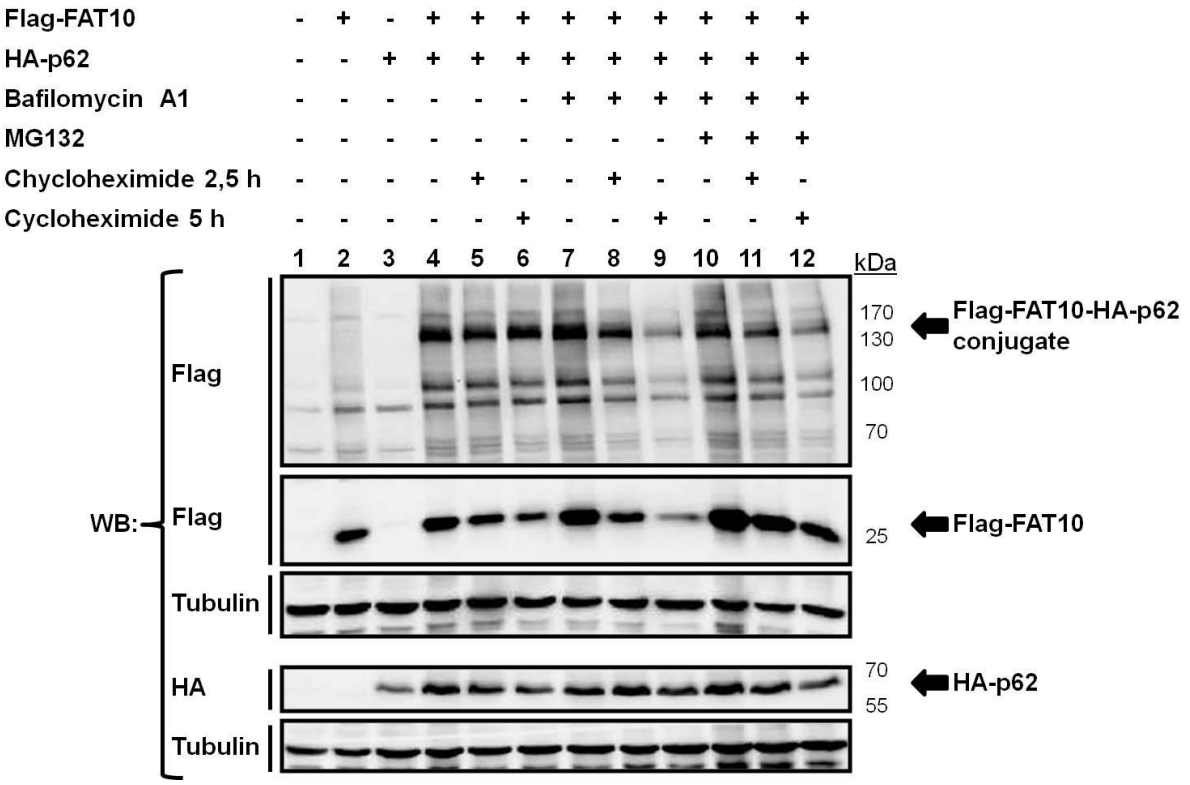

Figure 33: In transiently transfected cells, cycloheximide or simultaneous cycloheximide and Bafilomycin A1 treatment leads to a gradual decrease of the monomeric FAT10 protein amount during the cycloheximide treatment. HEK293T cells were transiently transfected with Flag-FAT10 and HA-p62 and treated with 50 µg/ml cycloheximide for 2,5 or 5 hours, 200 nM bafilomycin A1 for 8 hours and 5 µM MG132 for 6 hours as indicated. After harvesting, the cleared cell lysates were boiled with a 10 % β-mercaptoethanol containing SDS-sample buffer and separated by SDS PAGE on 10 % or 12 % gels. After wet-blotting, blots were probed with either anti-Flag, or anti-HA reactive antibodies. One experiment out of three independent experiments is shown.

According to the anti-Flag western blot, in all samples which were transfected with the respective DNA construct, monomeric HA-p62 was detectable (fig.33, lanes 3-12). In the anti-Flag western blots in all samples which were transfected with the expression construct, the monomeric Flag-FAT10 and the Flag-FAT10-conjugates were detectable (fig.33, lanes 2, 4-12). The characteristic

Flag-FAT10-HA-p62 conjugate of 130 kDa was detectable in all cells which co-expressed Flag-FAT10 and HA-p62 (fig.33, lanes 4-12) and was absent in those cells which expressed either Flag-FAT10 or HA-p62 only (fig.33, lanes 2, 3) and in the mock control (fig.33, lane 1).

According to the anti-Flag western blot, in the Flag-FAT10 and HA-p62 co-expressing cells which were treated with either cycloheximid only or together with Bafilomycin A1, the protein amount of the monomeric Flag-FAT10 markedly decreases during the cycloheximide treatment (fig.33, lanes 4-9). In those cells which were simultaneously treated with both, MG132 and Bafilomycin A1, this effect was alleviated (fig.33 lanes 10-12) indicting that the monomeric FAT10 is degraded by the proteasome. In the cycloheximide only treated samples the amounts of the characteristic FAT10-p62 conjugates did not alter markedly (fig.33, lanes 4-6). In those cells however which additionally were treated with either Bafilomycin A1 alone (fig.33, lanes 7-9) or together with MG132 (fig,33, lanes 10-12), the amounts of the characteristic FAT10-p62 conjugate markedly decrease. However, in the MG132 this effect was alleviated considerably (fig.33, lanes 10-12). Since, also the characteristic conjugate smear decreases, this effect is not specific for the FAT10-p62 conjugate. All together these findings indicate, that proteasomal degradation, rather than autophagosomal degradation is involved in the degradation of the characteristic FAT10-p62 conjugate as also shown for endogenous p62-FAT10 conjugate (Aichem, Kalveram et al. 2012). This is in line with the published property of monomeric FAT10 and other FAT10-conjugates to be degraded by the proteasome (Raasi, Schmidtke et al. 2001, Hipp, Raasi et al. 2004).

According to the anti-HA western blot, the HA-p62 protein amount did not change upon the different treatments (fig.33, lanes 4-12).

5.2 There was no interaction detectable between FAT10 and other published autophagic adaptor proteins

Despite p62 there are other autophagic adaptor proteins published, such as NBR1, NDP52 and OPTN (Komatsu and Ichimura 2010, Johansen and Lamark 2011, Behrends and Fulda 2012). Since some of these adaptor proteins do not differ in their function and since it is not yet fully clarified how their commitments are

regulated, it was interesting to investigate whether p62 exclusively would interact with FAT10. Therefore co-transfection and co-immunoprecipitation experiments with subsequent western blot analysis were performed with FAT10 and the respective adaptor proteins.

NBR1

Since NBR1 has many structural and functional similarities with p62, and since they can both interact with each other non-covalently (Johansen and Lamark 2011), it was interesting to investigate whether FAT10 does also interact with NBR1. Therefore, HEK293T cells were co-transfected with expression constructs for HA-NBR1 and Flag-FAT10 (fig.34, lane 5). As positive control, HA-p62 and Flag-FAT10 were taken along (fig.34, lane 6). As negative controls beside a mock control, Flag-FAT10, as well as HA-p62 and HA-NBR1 were expressed alone (fig.34, lanes 1-4). In order to investigate the non-covalent interaction between Flag-FAT10 and HA-NBR1, an immunoprecipitation experiment against Flag-FAT10 was performed (fig.34, lanes 7-12).

The western blots of the cleared cell lysates used for the immunoprecipitation experiments were stained with either with anti-HA or anti-NBR1 reactive antibodies in order to detect HA-p62 or HA-NBR1. Since the HA-NBR1 construct is not detectable with the HA7 antibody from Sigma-Aldrich, NBR1 was detected with a NBR1-specific antibody from Abnova. Anti-Flag reactive antibodies were used to detect monomeric Flag-FAT10 as well as Flag-FAT10 conjugates. For the immunoprecipitation experiments, anti-Flag western blots were used in order to detect the immunoprecipitated monomeric Flag-FAT10 as well as the Flag-FAT10 conjugates. In the anti-HA or anti-NBR1 western blots the co-immunoprecipitated HA-p62 and HA-NBR1 respectively should be detectable. In the anti-HA and anti-NBR1 western blot only those HA-p62 and HA-NBR1 proteins should be detectable which are covalently attached to Flag-FAT10 or which formerly did interact non-covalently with Flag-FAT10.

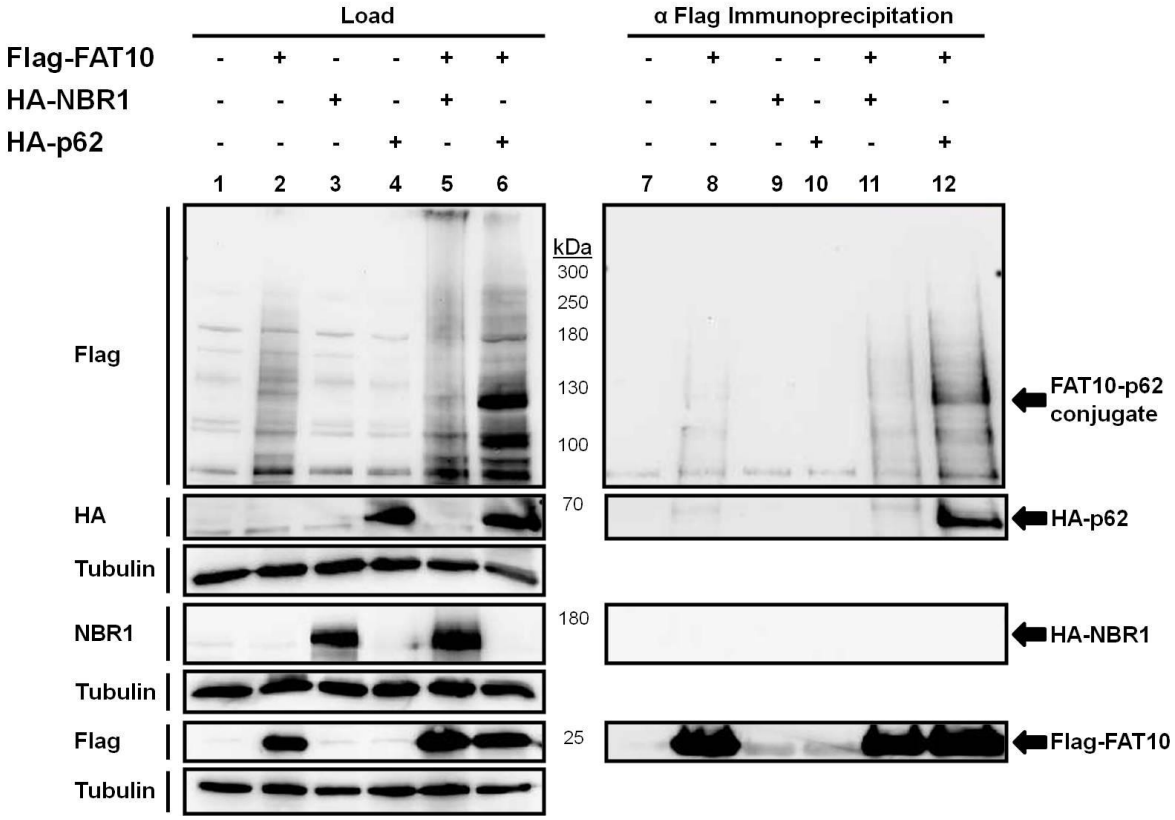

Figure 34: HA-NBR1 does not interact with Flag-FAT10. HEK293T cells were transiently transfected with Flag-FAT10, HA-p62 and HA-NBR1 as indicated. After harvesting, the cleared cell lysates were used for co-immunoprecipitation experiments with anti-FLAG-M2-conjugated agarose. The samples were boiled with a 10 % β-mercaptoethanol containing SDS-sample buffer and separated by SDS PAGE on 10 % or 12 % gels. After wet-blotting, blots were probed with either anti-Flag, anti-HA or anti-NBR1 reactive antibodies. One out of five independent experiments is shown.

In the anti-Flag western blots of the cleared cell lysates monomeric Flag-FAT10 as well as the Flag-FAT10-conjugates were detectable in all cells which were transfected with the respective DNA constructs (fig.34, lanes 2, 5, 6). In the anti-HA and anti-NBR1 western blots, also HA-p62 (fig.34, lanes 4, 6) and HA-NBR1 (fig.34, lanes 3, 5) were detectable in the respective samples. In the Flag-FAT10 and HA-NBR1 co-expressing cells no Flag-FAT10-HA-NBR1 conjugate band was detectable, neither in the anti-Flag, nor in the anti-HA or anti-NBR1 western blots (fig.34, lane 5). However, the characteristic Flag-FAT10-HA-p62 conjugate of 130 kDa was detectable in the cleared cell lysates of cells which were co-transfected with Flag-FAT10 and HA-p62.

In the corresponding anti-Flag immunoprecipitation experiments, the immunoprecipitated Flag-FAT10 and Flag-FAT10 conjugates were detectable in all

Flag-FAT10 expressing cells in the anti-Flag western blot (fig.34 lanes 8, 11, 12). Also the characteristic Flag-FAT10-HA-p62 conjugate of 130 kDa was detectable in the immunoprecipitation experiment of the Flag-FAT10 and HA-p62 co-expressing cells (fig.34, lane 12). In the immunoprecipitation experiment of the Flag-FAT10 and HA-NBR1 co-expressing cells no such a prominent conjugate was detectable, neither in the anti-Flag, nor in the anti-HA or anti-NBR1 western blots (fig.34, lane 11), indicating that Flag-FAT10 and HA-NBR1 do not interact covalently. In the anti-HA western blot, HA-p62 was found to be co-immunoprecipitated along with Flag-FAT10 in the Flag-FAT10 and HA-p62 co-expressing sample (fig.34, lane 12). No HA-NBR1 was found to be co-immunoprecipitated with Flag-FAT10, neither in the anti-HA, nor in the anti-NBR1 western blots (fig.34, lane 11), indicating that there is also no non-covalent interaction between Flag-FAT10 and HA-NBR1.

Only in one out of five experiments a band of more than 130 kDa was detectable in HEK293T cells that were co-transfected with HA-NBR1 and Flag-FAT10 (data not shown), but this result was not reproducible.

In none of these experiments a non-covalent interaction between Flag-FAT10 and HA-NBR1 was detectable. In order to investigate, whether the non-covalent interaction between p62 and NBR1 (Lamark, Perander et al. 2003) influences the interaction with FAT10, in one sample HA-p62 and HA-NBR1 were both co-transfected together with Flag-FAT10. However, in this sample only Flag-FAT10 and HA-p62 were found to interact covalently and non-covalently (data not shown).

NDP52

NDP52 binds ubiquitin through an ubiquitin-binding zinc-finger (UBZ) and contains a non-canonical LIR consensus motif (CLIR) (Thurston, Ryzhakov et al. 2009, Kraft, Peter et al. 2010). NDP52 functions as a p62 independent adaptor protein and was shown to be required for the efficient autophagic degradation of *Salmonella typhimurium* (Thurston, Ryzhakov et al. 2009, Cemma, Kim et al. 2011, Johansen and Lamark 2011). Since FAT10 was shown to co-localise with cytosolic *Salmonella* in HUVECs (Valentina Spinnenhirn, unpublished data), it was interesting to investigate whether NDP52 would also interact with FAT10. Therefore HEK293T cells were co-transfected with EGFP tagged wild-type NDP52 and Flag-FAT10 (fig.35, lane 7, 19). As a positive control, cells were co-transfected with Flag-FAT10

and HA-p62 (fig.35, lane 8, 20) and as a negative control Flag-FAT10(ΔGG) was co-transfected with EGFP-NDP52 (fig.35, lane 9, 21). Since the EGFP tag contains lysines too, as an additional negative control, EGFP only was co-transfected with Flag-FAT10 (fig.35 lane 11, 23). Thus it could be tested whether it is actually NDP52 itself, or the EGFP tag which interacts with FAT10. In order to investigate whether the presence of p62 influences a potential FAT10-NDP52 interaction, HA-p62 was co-expressed together with EGFP-NDP52 and Flag-FAT10 (fig.35, lanes 12, 24). As negative controls Flag-FAT10 (fig.35, lanes 2, 14), Flag-FAT10(ΔGG) (fig.35, lanes 3, 15), EGFP-NDP52 (fig.35, lanes 4, 16), HA-p62 (fig.35, lanes 5, 17) and EGFP (fig.35, lanes 6, 18) were transfected alone. As a mock control cells were treated with the transfection reagent only (fig.35, lane 1, 13). Subsequently, an anti-Flag immunoprecipitation was performed. The samples were analysed by western blot experiments. The western blots of the cleared cell lysates and the anti-Flag immunoprecipitation were stained with either anti-HA, anti-EGFP or anti-Flag reactive antibodies in order to detect HA-p62, EGFP, EGFP-NDP52, Flag-FAT10(ΔGG), Flag-FAT10 as well as the respective conjugates.

In the anti-Flag western blots the immunoprecipitated monomeric Flag-FAT10 as well as the Flag-FAT10 conjugates were detectable. In the anti-HA or anti-GFP western blots the co-immunoprecipitated HA-p62, EGFP and EGFP-NDP52 respectively should be detectable which are covalently attached to Flag-FAT10 or which formerly did interact non-covalently with Flag-FAT10.

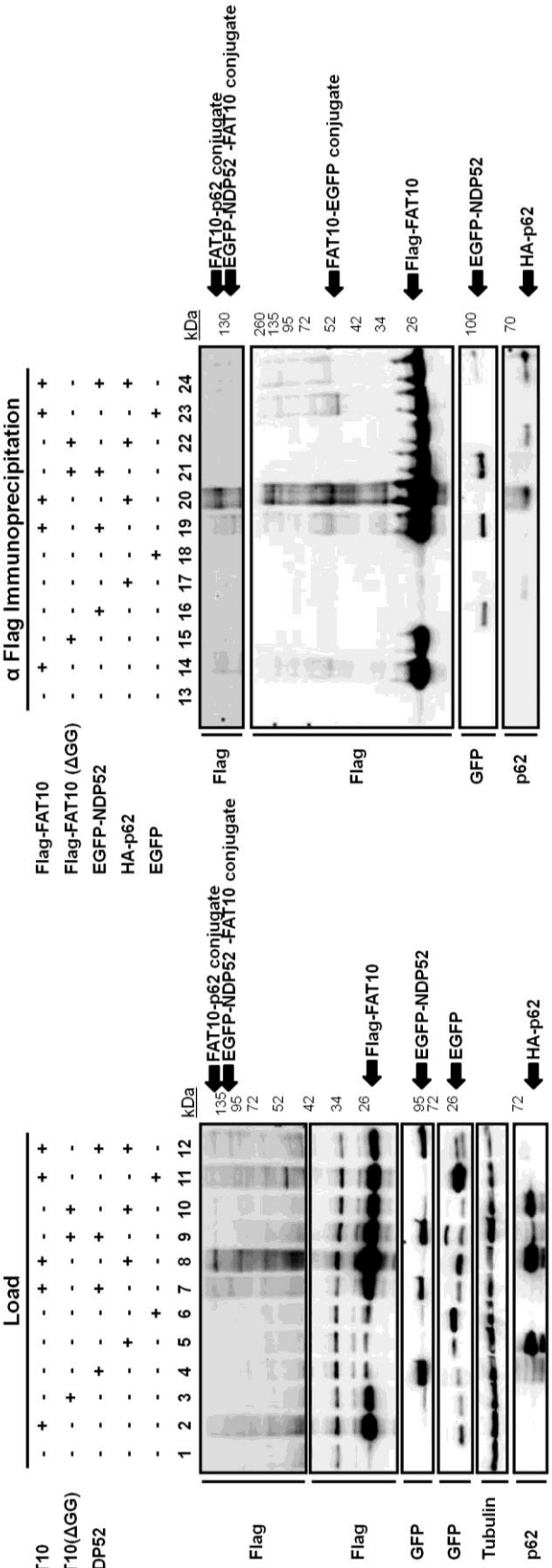
Load
α Flag Immunoprecipitation
Flag-FAT10
Flag-FAT10(ΔGG)
EGFP-NDP52
HA-p62
EGFP
1 2 3 4 5 6 7 8 9 10 11 12
13 14 15 16 17 18 19 20 21 22 23 24
kDa
FAT10-p62 conjugate
EGFP-NDP52 -FAT10 conjugate
Flag-FAT10
EGFP-NDP52
EGFP
HA-p62
FAT10-EGFP conjugate
Flag
GFP
p62
Tubulin

Figure 35: EGFP-NDP52 and EGFP are FAT10ylated. HEK293T cells were transiently transfected with Flag-FAT10, Flag-FAT10(ΔGG), HA-p62, EGFP-NDP52 and EGFP expression plasmids, as indicated. After harvesting, the cleared cell lysates were used for the co-immunoprecipitation experiments with anti-FLAG-M2-conjugated agarose. The samples were boiled with a 10 % β-mercaptoethanol containing SDS-sample buffer and separated by SDS PAGE on 10 % or 12 % gels. After wet-blotting, blots were probed with either anti-Flag, anti-HA and anti-EGFP reactive antibodies. This experiment was only performed once.

In the anti-HA and anti-EGFP western blots of the cleared cell lysates, HA-p62 (fig.35, lanes 5, 8, 10, 12), EGFP-NDP52 (fig.35, lanes 4, 7, 9, 12) as well as EGFP (fig.35, lanes 6, 11) were detectable in all samples which were transfected with the respective DNA constructs. The same was true for the Flag-FAT10 proteins and the Flag-FAT10-conjugates (fig.35, lanes 2, 7, 8, 11, 12) as well as Flag-FAT10(ΔGG) proteins (fig.35, lanes 3, 9, 10) in the anti-Flag western blots.

Besides the characteristic Flag-FAT10-HA-p62 of 130 kDa in the Flag-FAT10 and HA-p62 co-expressing cells (fig.35, lanes 8, 12), a faint band of around 115 kDa was detectable in the sample co-expressing Flag-FAT10 and EGFP-NDP52 (fig.35, lanes 7, 12). According to the size, this could be a conjugate consisting out of one Flag-FAT10 molecule (25 kDa) bound to one EGFP-NDP52 molecule (95 kDa). However also in the sample of Flag-FAT10 and EGFP, a band of 50 kDa was detectable (fig.35, lane 11). According to the size, this conjugate consists of one EGFP molecule (25 kDa) decorated with one FAT10 molecule. Therefore, the Flag-FAT10-EGFP-NDP52 conjugate, most probably is due to the covalent interaction between FAT10 and EGFP rather than to the interaction between FAT10 and NDP52 itself. In order to really investigate the FAT10 NDP52 interaction, one would require either an untagged NDP52 construct or a NDP52 construct tagged with a lysineless tag such as a His- or HA-tag.

No such conjugates were detectable in the mock-control (fig.35, lane 1) and in cells which expressed Flag-FAT10, EGFP-NDP52, HA-p62 or EGFP only (fig.35, 2, 4, 5, 6) and, as expected, no conjugates at all were detectable in cells expressing Flag-FAT10(ΔGG) (fig.35, lanes 3, 9, 10).

In the corresponding anti-Flag immunoprecipitation experiments (fig.35, lanes 13-24) in the anti-Flag western blots the immunoprecipitated Flag-FAT10(ΔGG) (fig.35, lanes 15, 21-22), Flag-FAT10 and its conjugates (fig.35, lanes 14, 19, 20, 23, 24) were detectable. Also the Flag-FAT10-HA-p62 (fig.35, lanes 20, 24), Flag-FAT10-

EGFP-NDP52 (fig.35, lanes 19, 24) and Flag-FAT10-EGFP (fig.35, lane 23) conjugates were detectable in the immunoprecipitation. According to the anti-EGFP western blot of the anti-Flag immunoprecipitation, EGFP-NDP52 was co-immunoprecipitated with Flag-FAT10 (fig.35, lanes 19, 24) and Flag-FAT10(ΔGG) (fig.35, lane 21). This may indicate a non-covalent interaction. However, EGFP-NDP52 was also detectable in the EGFP-NDP52 only expressing cells (fig.35, lane 16), indicating that EGFP-NDP52 binds unspecifically to the anti-Flag coupled agarose. Thus no assessment concerning the non-covalent interaction between Flag-FAT10 and EGFP-NDP52 can be made. HA-p62 in contrast was only co-immunoprecipitated in those samples which co-expressed either Flag-FAT10 (fig.35, lanes 20, 24) or Flag-FAT10(ΔGG) (fig.35 lanes 22).

OPTN

By binding simultaneously to LC3 and to ubiquitin (Ying and Yue 2012), OPTN is involved in the selective autophagic clearance of ubiquitin coated cytosolic *Salmonella enterica*. The phosphorylation of OPTN on serine 177, enhances the LC3 binding by OPTN and thus promotes the autophagic clearance of *Salmonella* (Wild, Farhan et al. 2011). A phospho-mimicking OPTN mutant, with all five serines in the LIR domain mutated to glutamic acid (5xE) binds to LC3B with a higher affinity than the wild-type OPTN, while the non-phosphorylatable mutant, with all serines mutated to alanines (5xA) was strongly impaired in its ability to bind LC3B (Wild, Farhan et al. 2011). Since Valentina Spinnenhirn found FAT10 to be localised to cytosolic *Salmonella* in HUVECs (unpublished data) and since OPTN is also inducible with TNFα (Ying and Yue 2012), it was interesting to investigate, whether OPTN would interact with FAT10. Therefore HEK293T cells were co-transfected with both HA-OPTN and Flag-FAT10 (fig.36, lanes 6, 14). Further HEK293T cells were co-transfected with Flag-FAT10 and the non-phosphorylatable (5xA) (fig.36, lane 7, 15) or the phosphor-mimicking mutants of OPTN (5xE) (fig.36, lane 8, 16) in order to investigated whether the phosphorylation status or the ability to interact with LC3 does influence a potential interaction between Flag-FAT10 and HA-OPTN. As negative controls cells were transfected with either Flag-FAT10, HA-OPTN, HA-OPTN(5xA) and HA-OPTN(5xE) only (fig.35, lanes 2-5, 10-13) and as a mock control cells were treated with transfection reagent only (fig.35, lanes 1, 9). In an anti-Flag

immunoprecipitation experiment the non-covalent interaction capability of HA-OPTN with Flag-FAT10 was investigated. Subsequently, the samples were analysed by western blot experiments.

For the immunoprecipitation experiments, anti-Flag western blots were used in order to detect the immunoprecipitated monomeric Flag-FAT10 as well as the Flag-FAT10 conjugates. In the anti-HA western blots the co-immunoprecipitated only those HA-OPTN proteins should be detectable which are covalently attached to Flag-FAT10 or which formerly did interact non-covalently with Flag-FAT10.

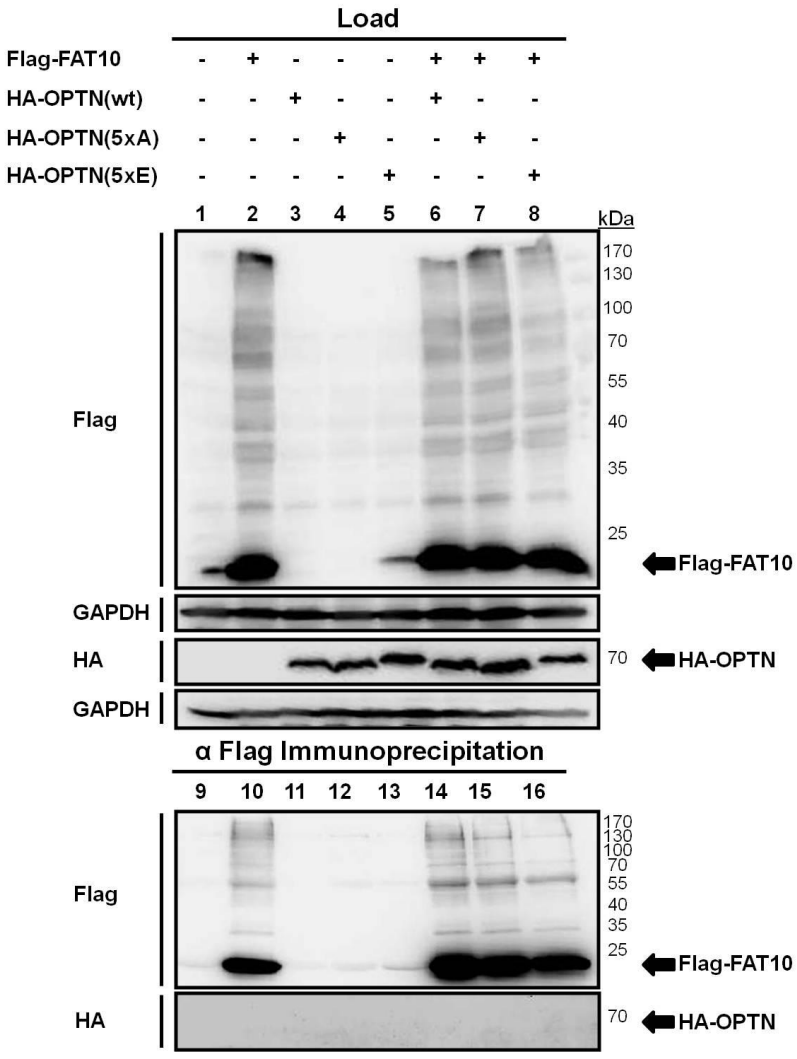

Figure 36: OPTN and FAT10 do not interact with each other, neither covalently nor non-covalently. HEK293T cells were transiently transfected with Flag-FAT10, HA-OPTN, HA-OPTN(5xE) and HA-OPTN(5xA) expressing plasmids as indicated. After harvesting, the cleared cell lysates were used for the co-immunoprecipitation experiments with anti-FLAG-M2-conjugated agarose. The samples were boiled with a 10 % β-mercaptoethanol containing SDS-sample buffer and separated by SDS PAGE on 12 % gels. After wet-blotting, blots were

probed with either anti Flag, or anti HA reactive antibodies. One experiment out of two independent experiments is shown.

In the cleared cell lysates, in all samples which were transfected with the respective DNA plasmid, Flag-FAT10 as well as the Flag-FAT10 conjugates were detectable in the anti-Flag western blots (fig.36, lanes 2, 6-8). Also in all HA-OPTN (fig.36, lane 3, 6), HA-OPTN(5xA) (fig.36, lanes 4, 7) and HA-OPTN(5xE) (fig.36, lanes 5, 8) transfected cells, the proteins were detectable in the anti-HA western blots. In the corresponding anti-Flag immunoprecipitation, the immunoprecipitated Flag-FAT10 as well as the Flag-FAT10 conjugates were detectable in the anti-Flag western blot (fig.36, lanes 10, 14-16). In the anti-HA-western blot neither co-immunoprecipitated HA-OPTN, nor HA-OPTN(5xA) or HA-OPTN(5xE) was detectable (fig.36, lanes 14-16). No covalent or non-covalent interactions between Flag-FAT10 and the wild-type HA-OPTN or the HA-OPTN(5xA) and HA-OPTN(5xE) mutants were detectable. According to these results, OPTN is not a substrate for FAT10ylation and also doesn't interact with FAT10 non-covalently.

Taken together, FAT10 seems to interact only specifically with p62 but not with other autophagic adaptor proteins such as NBR1, NDP51 or OPTN.

6 Discussion

In the following chapters the result of this study will be discussed and finally, possible consequences of the FAT10-p62 interaction will be contemplated.

6.1 The characterisation of the FAT10 p62 interaction

Wild-type FAT10 and wild-type p62 were shown to interact with each other covalently and non-covalently. These interactions were detectable either endogenously in TNFα and IFNγ stimulated HEK293 cells as well as in transiently transfected HEK293T cells (Aichem, Kalveram et al. 2012). However, there are some aberrations between the results collected with the endogenous experiments and the results with the transient transfection experiments. These differences will be mentioned and discussed in the first part of the discussion.

In the transient co-transfection experiments there is only one prominent FAT10-p62 conjugate band of 130 kDa detectable. Like ubiquitin, FAT10 also has conserved lysines which theoretically would allow the formation of either FAT10 chains or mixed chains with other ubiquitin-like modifiers (Raasi, Schmidtke et al. 2001). According to the size of the FAT10-p62 conjugate, more than one FAT10 molecule has to be attached to p62. Because of this the question arises whether FAT10 is either multi-monoFAT10ylated or whether it is decorated by a chain, containing FAT10. To answer this question, Birte Kalveram co-transfected p62 with a lysineless FAT10 mutant [FAT10(K0)], which cannot form a chain anymore (Aichem, Kalveram et al. 2012). The corresponding FAT10(K0)-p62 conjugate runs at the same sizes as the wild-type FAT10 and p62 containing conjugate, concluding that p62 rather becomes multi-monoFAT10ylated (Aichem, Kalveram et al. 2012). In line with this, Buchsbaum et al. found evidence for a multi-monoFAT10ylation rather than a chain formation. They found the FAT10ylation profile for LRRFIP2 to be the same using either wild-type FAT10 or a lysineless FAT10 mutant FAT10(K0) (Buchsbaum, Bercovich et al. 2012).

Curiously, while in cells which were transiently co-transfected with FAT10 and p62 one FAT10-p62 conjugate is detectable only (e.g. fig.16, lanes 4-6; fig.17, lane 6), in

cytokine stimulated cells, a ladder of four endogenous FAT10-p62 conjugates is visible (fig.37, lanes 2, 4).

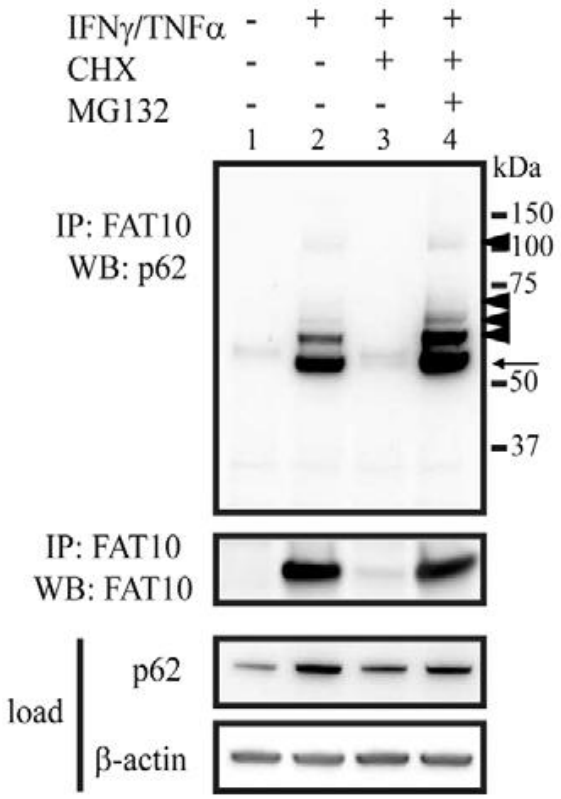

Figure 37: Detection of endogenous p62-FAT10 conjugates in cytokine treated HEK293 cells, by Annette Aichem (Aichem, Kalveram et al. 2012). Total cell extracts of untreated or IFNγ and TNFα stimulated HEK293 cells were used to immunoprecipitate endogenous FAT10 conjugates with the monoclonal FAT10 antibody 4F1. Western blot analysis was then performed using a polyclonal FAT10 antibody or a polyclonal p62 antibody to detect endogenous p62-FAT10 conjugate formation under reducing conditions (10% β-mercaptoethanol). Where indicated, cells were treated for 6 hours with proteasomal inhibitor MG132 and/or for five hours with cycloheximide (CHX). An arrow indicates endogenous p62 non-covalently interacting with FAT10, arrowheads indicate covalent p62-FAT10 conjugates (Aichem, Kalveram et al. 2012).

These conjugates probably do consist of out of one p62 molecule, decorated with either one or up to four FAT10 molecules, respectively. Interestingly, out of these four FAT10-p62 conjugates, the lowest molecular weight FAT10-p62 conjugate band, which most likely contains monoFAT10ylated p62, is the most prominent one (fig.37, lanes 2, 4) (Aichem, Kalveram et al. 2012). In the transient co-transfected cells however, the only detectable FAT10-p62 conjugate is, according to its size of 130 kDa, probably more than mono-FAT10ylated (e.g. fig.16, lanes 4-6; fig.17, lane 6). It is unclear, why in contrast to the endogenous data, in the FAT10

and p62 transient co-transfection experiments only one FAT10-p62 conjugate band is detectable at all. One possible explanation could be that due to the high protein amounts of p62 and FAT10 in over-expressing cells, the FAT10-p62 conjugate of 130 kDa is the favoured form.

In cells which were transiently co-transfected with FAT10 and p62, compared to the provided FAT10 and p62 amounts, the characteristic FAT10-p62 conjugate band of 130 kDa is quite faint (e.g. fig.16, lanes 4-6). Thus, only a low portion of the expressed p62 molecules seems to be FAT10ylated contemporaneously. This seems to be a common feature of FAT10ylated proteins because we see this also in case of other FAT10 substrates such as USE1 (Aichem, Pelzer et al. 2010), PHD14, JunB, UBE1, VCP/p97 (our lab, all unpublished), AIPL1 (Bett, Kanuga et al. 2012) or LRRFIP2 (Buchsbaum, Bercovich et al. 2012). This could either be caused by a short half-life of the conjugates due to degradation and/or due to a deFAT10ylation processes. Since there are no evidences for the existence of FAT10 reactive proteases so far (Schmidtke, Aichem, & Groettrup, 2013), deFAT10ylation might not be the reason for a tentatively supposed ephemeral nature of the FAT10-p62 conjugate. However, in a cycloheximide chase, Annette Aichem found endogenous monomeric FAT10 as well as the FAT10-p62 conjugates to be degraded rapidly (fig.37, lane 3). Since this effect was diminished in those cells treated with the proteasome inhibitor MG132, the proteasome was found to be the main degradation pathway for the monomeric FAT10 as well as for the FAT10-p62 conjugates (fig.37, lane 4). Therefore, it is very likely, that the FAT10-p62 conjugate of 130 kDa is also degraded constantly by the proteasome.

However, upon proteasomal inhibition with MG132 of cells which were transiently co-transfected with Flag-FAT10 and HA-p62, only the amount of monomeric FAT10 increased but not the amount of the 130 kDa FAT10-p62 conjugate (fig.16, lanes 4, 5). However, the inhibition of the protein biosynthesis with cycloheximide in presence of the autophagy inhibitor Bafilomycin A1, led to a decrease of the FAT10-p62 conjugate amount (fig.33, lanes 7-9). Since this effect at least was diminished when the proteasome simultaneously was inhibited with MG132 (fig.33, lanes 10-12), the proteasomal degradation of the FAT10-p62 conjugate of 130 kDa was confirmed. The effect of the cycloheximide and MG132 treatment on

the amounts of monomeric FAT10 and the FAT10 conjugates is more drastic visible in cytokine treated cells [fig.37, (Aichem, Kalveram et al. 2012)], compared to transiently transfected cells (fig.33). This probably is due to the much stronger increase of the p62 and FAT10 protein amounts with transient transfection (e.g. fig.16, 17, 33) compared to the induction with cytokines [fig.37, (Aichem, Kalveram et al. 2012)].

Besides the degradation of the FAT10-p62 conjugate, also the formation of FAT10-p62 conjugates may be restricted. For example, the fraction of the p62 protein which is prone to be FAT10ylated at all might be limited. This could either be due to the localisation of FAT10, p62 and the FAT10ylation machinery, or to other prerequisites which have to be fulfilled prior to FAT10ylation. p62 for example was shown to shuttle between the nucleus and the cytoplasm (Pankiv, Lamark et al. 2010) and also FAT10 has been detected in both compartments (Liu, Pan et al. 1999, Raasi, Schmidtke et al. 1999, Lee, Ren et al. 2003, Kalveram, Schmidtke et al. 2008, Ji, Jin et al. 2009). Other possible prerequisites which may have to be fulfilled in order to enable or prevent the FAT10ylation of p62 could be for example other modifications of p62 such as phosphorylation (Matsumoto, Wada et al. 2011). Also limitations in the FAT10ylation machinery capacity may restrict the formation of FAT10 conjugates in general.

Interestingly, the amount of the monomeric p62 protein in cells which were co-transfected with FAT10 and p62 (fig.18, lanes 5-7), was always higher, compared to the samples of cells which were transfected with p62 alone (fig.18, lanes 2-4). This is in contradiction to the endogenous data of Annette Aichem (Aichem, Kalveram et al. 2012). Annette Aichem could show that upon the stimulation of HEK293 cells with IFNγ and TNFα, the expression of both endogenous FAT10 and p62 on mRNA as well as protein level was increased. Within 24 hours after the induction, before detectable amounts of FAT10 were visible, the p62 protein accumulated. Due to the proteasomal degradation of the FAT10ylated p62, the amount of endogenous p62 declined, as soon as high amounts of FAT10 were expressed (Aichem, Kalveram et al. 2012). This finding raises the question why the p62 protein amount in cells which were transiently co-transfected with p62 and FAT10 is higher as compared to cells transfected with p62 only instead of the other way around. Possibly, with transient

transfection, the increase in the expression rate of p62 is higher than its degradation rate. This of course still doesn't answer the question why in the presence of the transiently co-transfected FAT10 the protein level of the transiently transfected p62 is increased at all, compared to those cells expressing p62 only. If there is no functional or physiological explanation for the increased p62 protein amount in p62 and FAT10 co-transfected cells, it still could be a transfection artefact such as an increased transfection efficiency or expression rate of the p62 encoding plasmid in the presence of the FAT10 encoding plasmid.

6.1.1 The lysineless p62 mutant p62(K0)

In some of the experiments, cells which were co-transfected with wild-type Flag-FAT10 and a lysineless HA-p62 mutant [HA-p62(K0)], the characteristic Flag-FAT10-HA-p62 conjugate of 130 kDa was gone completely. But in some experiments, there was still a faint band visible at 130 kDa (fig.17, lane 7). This band however was markedly diminished compared to the conjugate band in cells co-transfected with both wild-type p62 and FAT10 (fig.17, lane 6). Annette Aichem has observed a similar phenomenon for the FAT10-USE1 conjugate, where by using a lysineless USE1 mutant also a faint conjugate band remained (Aichem, Pelzer et al. 2010). This, for example could be due to the FAT10ylation of the N-termini of p62 and USE1. However, according to the molecular weight of the wild-type FAT10-p62 conjugate there might be more than one FAT10 molecule attached to p62. If the remaining faint conjugate band would result from an N-terminus only FAT10ylation and if we assume that p62 is either mono-, or multi-mono-FAT10ylated, than this would mean that probably also the wild-type p62 is mono-FAT10ylated only and probably contains additionally lysine independent posttranslational modifications. Another explanation could be that the FAT10ylation is not only restricted to the lysines of its substrate proteins, but also includes serines, cysteines and threonines (Kravtsova-Ivantsiv and Ciechanover 2012). However, in this case it would be striking why the remaining conjugate band in cells which do co-express wild-type Flag-FAT10 and HA-p62(K0) (fig.17, lane 7) is so strongly diminished compared to the wild-type conjugate band (fig.17, lane 6).

6.1.2 The self oligomerisation capability of p62

The PB1 domain of p62 plays a critical role in p62 recruitment to the autophagosome formation site (Itakura and Mizushima 2011). It was shown that the autophagic degradation of the non-polymerising mutant p62(K7R/D69R) was delayed but not completely abolished. Thus, the self-oligomerisation capability of p62 is required for the effective degradation of p62 via autophagy (Ichimura, Kumanomidou et al. 2008). However the dimerisation/oligomerisation of p62 alone doesn't suffice for the formation of p62 positive puncta, they were only formed when autophagy was induced (Itakura and Mizushima 2011). Since the covalent interaction between FAT10 and p62(K7R/D69R) was detectable in one out of two experiments (fig.19, lane 9) and the non-covalent interaction in two out of three experiments (fig.19, lane 19), the polymerisation capability at least doesn't seem to be a basic requirement for those interactions. Otherwise the results might have been always negative. Further it would be worthwhile to test, whether a PB1 deficient mutant would also be degraded by the proteasome in the presence of FAT10.

6.1.3 The identification of the FAT10ylation sites of p62

In order to identify the p62 domains which are required for the interaction with FAT10, HEK293T cells were co-transfected with several deletion constructs of HA-p62 together with wild-type Flag-FAT10 (fig.20). Theses p62 deletion constructs comprise different domains of p62 and overall do cover the whole protein. In western blot experiments the molecular weights of the HA-p62 deletion proteins were reduced, compared to wild-type HA-p62, in accordance to the sizes of the respective deletions. The molecular weights of the HA-p62 proteins range, from 65 kDa for wild-type HA-p62 to 35 kDa for HA-p62(Δ257-440) deletion construct (fig.20). Usually, these downshifts are visible in case of the corresponding FAT10-p62 conjugates, as well (fig.20). Since p62 possibly becomes multi-monoFAT10ylated, or additionally carries other modifications such as phosphorylation, a single deletion may not comprise all potential FAT10ylation or modification sites of p62. In this case, the molecular weight of the resulting FAT10-p62 conjugate would be further decreased in accordance to the missing modifications. In case of a missing Flag-FAT10 molecule, a size reduction of 25 kDa in addition to the deletion prone molecular weight shift might

occur in the remaining FAT10-p62 conjugate. If the FAT10-p62 conjugate of 130 kDa consists out of monoFAT10ylated p62 only, the conjugate would be gone completely. With this method it was tested which deletions in p62 do result in an additional downshift of the molecular weights of the corresponding FAT10-p62 conjugates or even impede the FAT10-p62 conjugate formation completely (fig.20). The FAT10-p62 conjugate was still visible in those cells co-expressing either HA-p62(Δ123-170) (fig.20, lane 8), HA-p62(Δ321-348) (fig.20, lane 22), HA-p62(Δ371-386) (fig.20, lane 24) or HA-p62(Δ386-440) (fig.20, lane 26) together with wild-type Flag-FAT10 (fig.21). However, according to the molecular weight shifts of the remaining FAT10-p62(ΔXY) conjugates (fig.20, lanes 8, 22, 24, 26) compared to the wild-type FAT10-p62 (fig.20, lane 4) conjugate, there was no FAT10 modification missing in none of these conjugates.

In the lower molecular weight part up to 70 kDa of a 12 % mini gel size differences of 5 kDa and more are precisely distinguishable. Therefore, in the anti-HA western blot there was no size shift distinguishable between the HA-p62(Δ371-386) deletion protein (fig.20, lane 24) and the wild-type HA-p62 (fig.20, lane 4). The molecular weights of the HA-p62(Δ321-348) deletion protein (fig.20, lane 22) however is declined by around 5 kDa and the molecular weights of the HA-p62(Δ123-170) (fig.20, lane 8) and the HA-p62(Δ386-440) deletion constructs (fig20, lane 26), are reduced between 10 and 15 kDa compared to the wild-type HA-p62 (fig.20, lane 4).

In contrast, in the higher molecular weight region, up from 70 kDa of a 12 % mini gel, the resolution is not that high anymore. Also the marker ladder is getting more imprecise in this area (100, 130 and 170 kDa). While a molecular weight shift of around 5 kDa in the FAT10-p62 conjugate of around 130 kDa is not distinguishable, according to the marker ladder, molecular weight shifts of 10 kDa or more are detectable. However, a precise estimation of the exact dimension of molecular weight shifts between 10 and 25 kDa might be difficult. Therefore, in the FAT10-p62 conjugates a molecular weight shift of 25 kDa, due to a missing FAT10 molecule would have been clearly detectable.

Thus, in the anti-Flag western blot compared to the wild-type FAT10-p62 conjugate, there is no molecular weight difference at all detectable for the FAT10-p62(Δ371-386) (fig.20, lane 24) and the FAT10-p62(Δ321-348) (fig.20, lane 22) conjugate. Although

the molecular weight shifts of the FAT10-p62(Δ123-170) (fig.20, lane 8) and the FAT10-p62(Δ386-440) (fig.20, lane 26) conjugates *per se* were clearly distinguishable, due to the imprecise marker ladder and to the low resolution in the high molecular weight area of the 12 % mini gels, the exact dimensions of theses shifts were hard to estimate. Therefore, one cannot rule out completely that the detected molecular weight shifts in the FAT10-p62(Δ123-170) (fig.20, lane 8) and FAT10-p62(Δ386-440) (fig.20, lane 26) conjugate bands are not only caused by the deletion itself, but may comprise additionally the absence of otherwise covalently attached small molecule/s such as phosphorylation, acetylation or glycosylation. p62 for example has been shown to be phosphorylated at various serines and threonines (S24, S207, T269, S272, S282, S332, S366, S403) whereas other modifications, such as tyrosine phosphorylation, ubiquitylation, SUMOylation, or acetylation were not detected (Matsumoto, Wada et al. 2011). FAT10 has been shown to become ubiquitylated (Hipp, Kalveram et al. 2005, Buchsbaum, Bercovich et al. 2012) and acetylated (Kalveram, Schmidtke et al. 2008) at its lysine residues. Since the FAT10(K0)-p62 conjugate which contains a lysineless FAT10 mutant and the wild-type FAT10-p62 conjugate both have the same molecular weights (Kalveram, Schmidtke et al. 2008), the ubiquitylation might not contribute to the molecular weight of the 130 kDa FAT10-p62 conjugate.

In order to estimate the molecular weight differences of the conjugates more precisely, one could increase the resolution in the higher molecular weight region by using either lower percentage gels, longer running times, longer gels or even gradient gels in combination with an adequate marker ladder for high molecular weights. Because of the huge size difference between Flag-FAT10 (25 kDa) and the FAT10-p62 conjugates (~130 kDa) it is worthwhile to use either longer gels, gradient gels or two different gel types for the detection of the monomeric FAT10 or the FAT10-p62 conjugate at the same time.

According to these results it appears that the p62 deletion constructs either become FAT10ylated completely or not at all. Maybe the FAT10ylation sites are variable to a certain extend and the deletion of potential FAT10ylation sites can be compensated in some cases by handing over FAT10 to lysine residues of other domains. This is also true for other FAT10 substrates such as the E2 conjugating USE1 which

undergoes self-FAT10ylation mainly at lysine 232. Mutation of this lysine to an arginine did not abolish FAT10ylation and instead of lysine 232, another lysine was FAT10ylated (Aichem et al, manuscript submitted). Interestingly and in line with this, Buchsbaum et al. found LRRFIP2 to be multi mono-FAT10ylated by two single FAT10 moieties; one is attached at the N-terminus and one at the C-terminus of LRRFIP2 (Buchsbaum, Bercovich et al. 2012). Interestingly, they found the second FAT10ylation to be depending on the first modification as well as on the structure of FAT10. While the gradual truncation of FAT10 from its N-terminus had no impact on the first modification of LRRFIP2, the second FAT10ylation was inhibited progressively. They suggested that the N-terminal domain of FAT10 may serve as a sensor for the second FAT10 molecule to modify LRRFIP2 (Buchsbaum, Bercovich et al. 2012). This could also be true in case of the p62-FAT10 conjugate and the dependency of a second FAT10ylation process from an antecedent FAT10 modification could also be the reason why some HA-p62 deletion proteins did not show a conjugate at all when co-expressed with Flag-FAT10 rather than a dramatic downshift in the molecular weight.

According to these results, the zinkfinger domain (ZZ), the LIR domain, the CPI domain, the UBA domain and the N-terminus of the C-terminal PEST domain of p62 are not required for FAT10ylation. Therefore, the seven lysines harboured in these domains, at least seem not to be indispensable FAT10ylation targets: K141, K157, K165, K344, K378, K435 and K420 (fig.21). The deleted domains which impede the formation of detectable FAT10-p62 conjugates, harbour the PB1 domain, the SH2 domain, the AID domain, the NPI domain, the TRAF domain and the N-terminal PEST domain. The following thirteen lysines are located in this domain: K7, K13, K91, K100, K102, K103, K187, K189, K238, K264, K281, K295, and K313. Therefore, these lysines are potential FAT10ylation sites (fig.21). The KIR domain and the C-terminus of the C-terminal PEST domain are only missing in the p62(Δ256-440) construct. But those regions anyway do not contain any lysines. Twelve out of thirteen lysines of wild-type p62 which are located in the deleted domains of truncations which were not FAT10ylated anymore became mutated one by one into arginine (fig.22). However none of these p62 mutations resulted in the downshift of the molecular weight of the corresponding FAT10-p62 conjugate, shown by one missing FAT10 molecule or by the disappearance of the FAT10-p62 conjugate

(fig.22). These results further support the notion that the lysines which become FAT10ylated are arbitrary, at least to a certain extend. Alternatively, p62 may also become FAT10ylated at its serines, cysteines, threonines and/or its N-terminus (Kravtsova-Ivantsiv and Ciechanover 2012). This assumption is further supported by the findings that the lysineless mutants of two FAT10ylation substrates p62(K0) (fig.17, lane 7) and USE1(K0) (Aichem, Pelzer et al. 2010) both still do form slight but detectable FAT10 conjugates.

6.1.4 The non-covalent FAT10 p62 interaction

GST pulldown experiments with *in vitro* transcribed and translated wild-type HA-p62 and HA-p62 deletion proteins and recombinant GST-FAT10 were performed in order to investigate which p62 domains are involved in the non-covalent interaction of p62 and FAT10 (fig.23). As negative control, for each sample also recombinant GST was used for the pulldown.

According to the GST pulldown experiments, deletions in HA-p62 between the amino acids 348 and 371 or 386 and 440 of p62 seem to be required for the non-covalent interaction with FAT10. Those areas comprise the KIR domain, the C-terminus of the C-terminal PEST domain and the UBA domain (fig.24). The presence of the PB1 domain alone doesn't seem to be sufficient for the non-covalent interaction with FAT10 (fig.24). Birte Kalveram found the *in vitro* transcribed and translated UBA deficient HA-p62(Δ386-440) protein to be pulled down with GST-FAT10 (unpublished data). Therefore the UBA domain of p62 does not seem to be required for the non-covalent interaction with FAT10.

However, the results which were obtained by using the *in vitro* transcribed and translated HA-p62 deletions were quite inconsistent. By repeating the assay, most of the HA-p62 deletions were tested alternating either positive or negative for the interaction with FAT10 (tab.49). In many experiments, also in the GST negative controls, a pull down of the HA-p62 proteins was detectable, however to a lesser extent than with GST-FAT10 (data not shown). This could be due to the stickiness of p62 (Terje Johansen, personal communication) and/ or to the precipitation of FAT10 which is – even when fused to GST - not completely in solution. For this study only

those experiments were considered where the “GST only” negative controls were clearly negative.

Strangely, when the experiment was repeated and completed with a new batch of GST-FAT10, all tested HA-p62 deletion proteins were pulled down, however only to a low extend (fig.25, upper panel). When in a second experiment, using the same HA-p62 proteins, the samples were centrifuged in advance to remove precipitated protein and only the soluble fraction in the supernatant was used for the pulldown, the interactions for all samples were negative (fig.25, lower panel). This finding may indicate that the HA-p62 deletion constructs may be prone to precipitate together with GST-FAT10. For this reason, under these experimental conditions it is hard to distinguish whether the interaction is indeed specific. In order to circumvent these problems and to avoid the usage of GST and the GST pulldown, as an alternative method a tag-less recombinant FAT10 in combination with *in vitro* transcribed and translated HA-p62 truncations and an anti-FAT10 immunoprecipitation was performed. In an additional approach immobilised recombinant FAT10 (FAT10 covalently coupled to agarose, Enzo Lifesience) in combination with *in vitro* transcribed and translated HA-p62 deletions were used. However in both approaches unspecific binding and inconsistent results occurred too (data not shown).

In order to avoid the usage of any recombinant FAT10 protein and thus in order to avoid unspecific binding to the beads as well as protein precipitation, co-immunoprecipitation assays (anti-Flag) with lysates of transiently co-transfected (Flag-FAT10 & HA-p62 deletion proteins) HEK293T cells were performed. As a negative control, the anti-Flag immunoprecipitation was performed with cell lysates of HEK293T cells which were transfected with the respective HA-p62 deletion construct only (fig.26, 27). According to the two co-immunoprecipitation experiments, deletions between the amino acids 170 and 256 of HA-p62 seem to impede the non-covalent interaction with Flag-FAT10 (tab.50, fig.28). This area comprises the NPI and the TRAF domains. However, the results of the immunoprecipitation experiments for the deletion proteins were also very inconsistent (tab.50) and the negative controls were also often not negative.

Besides the contradiction FAT10 interaction results for the eleven HA-p62 deletion proteins within the respective experimental setups, the results for the eleven HA-p62

deletion proteins were largely contradicting for the GST pulldown (fig.24) and the co-immunoprecipitation experiments (fig.28). However, since in both assays the HA-p62(Δ123-170), HA-p62(Δ321-348) and HA-p62(Δ371-386) deletion proteins were tested positive for the FAT10 interaction the ZZ domain, the LIR domain, the CPI domain and the C-terminus of the C-terminal PEST domain seem not to be required for the interaction with FAT10 (fig.29).

According to the existing data one cannot make any reliable assessment concerning the specificity of the interaction in general and the domains of p62 which are required for the non-covalent interaction with FAT10. Further investigations with optimised experimental setups concerning the washing conditions, tag combinations, immunoprecipitation or pulldown systems would be required. In the following, the advantages and disadvantages of each of the two systems will be discussed.

In transfection experiments, differences in the transfection or expression efficiencies, often lead to unequal protein amounts among the samples. In contrast, the transcription and translation efficiencies in the *in vitro* transcription and translation system as well as the resulting protein amounts are very consistent. Therefore it is much easier to create equal and thus comparable protein amounts in all experiments. Also the usage of recombinant proteins further facilitates the adjustment of the protein amounts. The possibility that some unknown intracellular factors, such as enzymes or other proteins might influence the investigated protein interaction is also lower with the *in vitro* transcription and translation system. Since, FAT10 is a very insoluble protein which tends to precipitated easily and the GST-tag enhances the solubility of FAT10 at least to a certain extent, GST-FAT10 was preferentially used to keep FAT10 in solution. However, in the past, the GST-tag has been shown to influence the binding capacity and maybe also the functionality of FAT10 (Hipp, Raasi et al. 2004, Chiu, Sun et al. 2007, Pelzer, Kassner et al. 2007) and NEDD8 (Tanaka, Kawashima et al. 2003). Chiu et al. for example could show that UBA6 activates untagged or Flag tagged FAT10 *in vitro* and *in vivo* respectively. However like Pelzer et al. and Jin et al. (Jin, Li et al. 2007, Pelzer, Kassner et al. 2007) they also failed to activate GST-FAT10 with UBA6. Therefore, they suggested that the large GST tag may interfere with the activation of FAT10 by UBA6 (Chiu, Sun et al. 2007). Further, Tanaka et al. found GST-NEDD8 to interact with NUB1L (Tanaka,

Kawashima et al. 2003). However, this interaction was not reproducible by Hipp et al. by using untagged NEDD8 and slightly different washing conditions (Hipp, Raasi et al. 2004).

Since Nicola Catone has recently established a system to create untagged recombinant FAT10 which is highly soluble (Aichem et al, manuscript submitted), it could be worthwhile to establish an improved co-immunoprecipitation experiment with this untagged recombinant FAT10 in combination with the monoclonal FAT10 antibody instead of the GST-FAT10 pulldown as a future perspective.

A further approach would be the investigation of the non-covalent interaction between wild-type FAT10 and the p62 deletion constructs fully *in vitro*. The usage of both, recombinant expressed wild-type FAT10 and p62 deletion proteins would fully exclude that any unknown intracellular components might participate in the FAT10 and p62 interaction. However it is not clear whether the folding of the recombinant expressed proteins coincides with the folding in mammalian cells.

Finally it would be interesting to have established both systems, the complete *in vitro* system and as well as the transfection and co-immunoprecipitation system. If both systems would show the same outcome, one could be quite sure that no technical factors affect the results.

6.1.5 The isolated PB1, TRAF, PEST and UBA domains of p62

According to the transfection experiments (fig.20), HA-p62 mutants where the deletions encompass, among others, the PB1 domain (122 aa), the TRAF domain (26 aa), or the N-terminal PEST domain (28 aa), were not FAT10ylated anymore (fig.21). Therefore it was tested whether the isolated domains suffice for the FAT10ylation and whether they are involved in the non-covalent interaction FAT10 (fig.30, 31). Since the UBA domain is not required for the FAT10ylation (fig.20) and according to the data of Birte Kalveram (unpublished data) also not for the non-covalent interaction, the isolated UBA domain was additionally taken along as a negative control. The wild-type p62 protein served as a positive control (fig.30, 31). Due to the low molecular weight of the peptides, gel electrophoresis according to Schagger (Schagger and von Jagow 1987) was performed and for the blotting, a 0,2 µm PVCF membrane was used.

When HEK293T cells were co-transfected with wild-type Flag-FAT10 and HA-p62 or the isolated HA-tagged p62 domains (fig.30, lanes 8-12) and an anti-Flag co-immunoprecipitation experiment was performed (fig.30, lanes 20-24). The wild-type p62 (fig.30, lanes 3, 8) and FAT10 (fig.30, lanes 2, 8-12) were both expressed properly. However, despite using the same pcDNA3.1-HA plasmid, the same cloning strategy and performing final sequencing for all four isolated p62 domains, only the isolated HA-PB1 domain was detectable in the western blot (fig.30, lanes, 4, 9). However there was no covalent (fig.30 lanes 9, 21) or non-covalent (fig.30, lane 21) interaction detectable between Flag-FAT10 and the HA-PB1 domain of p62. In this experiment, the wild-type HA-p62 was co-immunoprecipitated in the FAT10 co-expressing sample (fig.30, lane 20) and to the same extent also in the sample which only expresses HA-p62 (fig.30, lane 15). But since this was not the case in the other experiments which were performed for this study, (e.g. fig.17, lane 13; fig.18, lanes 2-4) this does not challenge the specificity of the non-covalent interaction between FAT10 and p62 in general.

There are many potential reasons why from all isolated p62 domains, only the HA-PB1 domain was detectable in the western blots. Either the other p62 domain constructs were not expressed properly, or the peptides were rapidly degraded. However, in a second experiment, the inhibition of the proteasome with MG132 5 µM for 6 hours did not improve the detection (data not shown). Of course, due to their low molecular weights, one cannot rule out, that the peptides are degraded by cytosolic proteases. Also by using the *in vitro* translation/transcription system for the expression of the isolated p62 domains (fig.31), only the wild-type HA-p62 (fig.31, lane 1) and the isolated HA-PB1 domain (fig.31, lane 4) were detectable. In the corresponding GST pulldown experiment, only the wild-type HA-p62 was pulled down together with GST-FAT10 (fig.31, lane 6). With both experimental setups, the isolated PB1 domain of p62 did not interact with FAT10, neither covalently or non-covalently (fig.30, lane 21; fig.31, lane 6), indicating that the isolated PB1 domain does not suffice for the interaction with Flag-FAT10.

An isolated domain of course doesn't necessarily reflect the situation in a full-length protein. The folding as well as the domains in the neighbourhood of an important domain may also be very crucial for the interaction with other proteins. While

Seibenhener et al. successfully used a recombinant expressed GST-UBA domain of p62 in order to pull down polyubiquitylated proteins from lysates of HA-tagged ubiquitin expressing HEK cells (Seibenhener, Babu et al. 2004), Kirkin et al. for example have shown that full-length and in particular wild-type, polymeric p62 binds much better to recombinant GST-ubiquitin and GST-4x-ubiquitin than its isolated UBA domain. Therefore they suggested that this finding supports the *in vivo* relevance of p62 polymerisation for targeting ubiquitylated cargo for autophagy (Kirkin, Lamark et al. 2009). According to the co-immunoprecipitation data which were obtained with Flag-FAT10 and HA-p62(K7R/D69R) (fig.19) the polymerisation capability of HA-p62 at least does not seemed to be an essential requirement for the non-covalent interaction with Flag-FAT10.

To prevent the degradation and to improve the detectability in the western blot, one could combine the constructs with bigger tags like GST or MBP. However these tags do contain lysines and are huger than the domains itself. The EGFP-tag for example has been shown to be FAT10ylated (fig.35, lanes 11, 23), while the GST-tag can influence the binding capability of its partner, as shown for GST-FAT10 and UBA6 (Chiu, Sun et al. 2007, Jin, Li et al. 2007, Pelzer, Kassner et al. 2007) as well as for GST-NEDD8 and NUB1L (Tanaka, Kawashima et al. 2003, Hipp, Raasi et al. 2004).

6.1.6 The phosphorylation status of p62 at S403

In the p62 chapter of the introduction in this thesis, many cellular functions of p62 were summarised. If one protein is involved in so many different signal transduction pathways and distinct degradation processes it raises the question how these fields of duty are separated or how their interference is prevented. Besides the compartmentalisation of p62 in the cytosol and in the nucleolus (Filimonenko, Isakson et al. 2010, Pankiv, Lamark et al. 2010), its variable interaction partners such as TRAF6 or LC3 (Komatsu, Kageyama et al. 2012), the transcriptional control of other mediators involved in the respective pathway, also the posttranscriptional modification of p62 itself could play a role (Matsumoto, Wada et al. 2011).

Matsumoto et al. focused on the function of p62 in mediating different degradation pathways. Since proteasomes cannot digest stable protein complexes or aggregates but autophagy can remove protein aggregates, p62 -mediated selective

macroautophagy (autophagy) has been implicated as a compensatory pathway for proteasomal protein degradation. However, it remains unclear how p62 controls the autophagic degradation of ubiquitylated proteins. (Matsumoto, Wada et al. 2011). As p62 is itself degraded during selective autophagy, Matsumoto et al. suggested that the p62 mediating signal transduction should be distinct from the p62 managing selective autophagy. They report that posttranslational modification of p62 specifies the p62 property for selective autophagy (Matsumoto, Wada et al. 2011). In cell extracts from Neuro2a cells, p62 was found to be multi phosphorylated at its serine and threonine residues (Matsumoto, Wada et al. 2011). While the phosphorylation at T269, S272, S282, S332, and S366 was constitutive, the amount of S24-, S207-, or S403-phosphorylated p62 was increased in response to proteasome inhibition via MG132 in a time-dependent manner (Matsumoto, Wada et al. 2011).

The phosphorylation of p62 at T269 and S272 has been shown to increase the nuclear import activity of NLS2, whereas the phosphorylation of S266 in the middle of NLS2 has an inhibitory effect on nuclear import (Pankiv, Lamark et al. 2010). The UBA domain of p62 preferentially binds to K63 polyubiquitylated substrates (Seibenhener, Babu et al. 2004). The phosphorylation of p62 at S403 by CK2 increases the affinity of the p62 UBA domain for K48 and K63 linked ubiquitin chains, leading to an enhanced recruitment of polyubiquitylated proteins into sequestosomes, followed by engulfment in the autophagosome through p62-LC3 interaction (Matsumoto, Wada et al. 2011). Matsumoto et al. suggests a model, where CK2 directly phosphorylates S403 constantly, but on a low level and these homeostatic low levels of S403-phos-p62 molecules can monitor the accumulation of polyubiquitylated proteins. Since S403-phos-p62 has a higher affinity to polyubiquitin chains and polyubiquitin binding prevents the dephosphorylation of S403, the S403-phosphorylation balance is shifted to the phosphorylated state when the polyubiquitylated protein level is increased. Thus, S403-phosphorylated p62 enhances autophagic degradation of ubiquitylated proteins, when the proteasome is malfunctioning or ubiquitylated proteins are accumulating (Matsumoto, Wada et al. 2011).

The phospho-mimic mutant p62(S403E) binds more K48-linked and K63-linked ubiquitin chains than the wild-type p62 while the non-phosphorylated p62(S403A)

mutant does not bind to K48 linked ubiquitin chains but significantly binds to K63-linked chains (Matsumoto, Wada et al. 2011). S403 is located in the UBA-domain of p62 which is not required for the covalent interaction with FAT10 (fig.20, lane 26) (Aichem, Kalveram et al. 2012) and the non-covalent interaction with FAT10 (Birte Kalveram, unpublished data). However, it could be possible that binding of ubiquitin to the UBA-domain of p62 might influence the binding capability of FAT10 at some other regions of p62 due to conformational changes or sterical hindrances. In contrast to the non-covalent interaction between the non-phosphorylated HA-p62(S403A) mutant and K48-linked ubiquitin, for FAT10 there is at least no clear negative result detectable, suggesting that both the phospho-mimicking and the non-phosphorylation p62 mutants do interact with Flag-FAT10, both covalently (fig.32, lanes 7-9) and non-covalently (fig.32, lanes 19-21).

However, due to unequal p62 protein amounts in the samples which were co-transfected with Flag-FAT10 and either wild-type HA-p62, HA-p62(S403A) or HA-p62(S403E) (fig.32, lanes 7-9), it was not possible to quantify possible variances in either the non-covalent (fig.32, lanes 19-21) or covalent interaction (fig.33, lanes 7-9). Since S403 is localised in the UBA domain of p62 which is anyway not required for the covalent (fig.20, lane 26) (Aichem, Kalveram et al. 2012) or non-covalent interaction with FAT10 (Birte Kalveram, unpublished data), one could further test the other six published phosphorylation sites of p62. According to Matsumoto et al, they did not show an apparent role in its autophagic degradation (Matsumoto, Wada et al. 2011). They are localised in the PB1 domain (aa 1-123: S24), the PEST domains (aa 266-294 and aa 345-377: T269, S272, S282, S366) and the LIR domain (aa 321-342: S332). S207 is not localised in a functional domain. By mutating also these serines and the threonine into either alanine or glutamic acid one could test their impact on the interaction with FAT10. Since the PB1 and PEST domains were shown to be required for the covalent interaction, the serines and threonines in these domains could possibly influence the interaction between FAT10 and p62.

6.1.7 The degradation of the 130 kDa p62-FAT10 conjugate (CHX chases)

Annette Aichem had shown that upon cycloheximide treatment the endogenous p62-FAT10 conjugates are degraded completely and also the unconjugated p62 in the

lysate was slightly degraded (Aichem, Kalveram et al. 2012). The FAT10-p62 conjugates were degraded by the proteasome since this effect could be rescued by MG132 treatment. The overexpression of HA-FAT10, but not HA-FAT10(ΔGG) lead to the degradation of endogenous unconjugated p62, indicating that the conjugating capability of FAT10 is required for the p62 degradation (Aichem, Kalveram et al. 2012). Valentina Spinnenhirn and Birte Kalveram both could show, that FAT10 and p62 co-localise on p62 bodies and aggresomes (Kalveram, Schmidtke et al. 2008, Aichem, Kalveram et al. 2012). Valentina Spinnenhirn was further using a mCherry-EGFP-FAT10 construct in order to investigate whether FAT10 subsequently also localises to the lysosomes. However, this was not the case (Aichem, Kalveram et al. 2012).

In order to investigate whether the characteristic FAT10-p62 conjugate of 130 kDa behaves the same as the endogenous FAT10-p62 conjugates, the cycloheximide chase was repeated with HEK293T cells transiently transfected with Flag-FAT10 and HA-p62 (fig.33, lanes 4-12). However, in order to measure the effect of the autophagic degradation on the level of the characteristic FLAG-FAT10-HA-p62 conjugate and the monomeric HA-p62, in this experiment the cells were additionally treated with Bafilomycin A1 (fig.33, lanes 7-12). In accordance to the data of Annette Aichem (Aichem, Kalveram et al. 2012), the amount of monomeric FLAG-FAT10 decreased during the cycloheximide treatment (fig.33, 4-6, 7-9, 10-12). This effect was mostly rescued by proteasomal inhibition (fig.33, lanes 10-12) while the inhibition of autophagic degradation by Bafilomycin A1 alone did not show such an effect (fig.33, lanes 7-9). This is in line with the finding of Valentina Spinnenhirn, that mCherry-EGFP-FAT10 is not localises to lysosomes (Aichem, Kalveram et al. 2012). For the characteristic FAT10-p62 conjugate of 130 kDa the degradation effect is clearly detectable only in the samples treated either with Bafilomycin A1 only (fig.33, lanes 7-9) or with Bafilomycin A1 and MG132 (fig.33, lanes 10-12). Paradoxically in this experiment, there was no effect on the conjugate amount visible in cells which were treated with cycloheximide only (fig.33, lanes 4-6). In a second experiment however, the FAT10-conjugate amount also decreased in those cells which were treated with cycloheximide only (data not shown). The degradation effects in the cycloheximide chases for the transient transfected cells were never as dramatic as shown by Annette Aichem for the endogenous p62-FAT10 conjugates

(fig.37) (Aichem, Kalveram et al. 2012). While for the endogenous situation upon cycloheximide treatment nearly all FAT10 conjugates as well as the monomeric FAT10 disappeared (fig.37, lane 3) (Aichem, Kalveram et al. 2012), in the transiently transfected cells there was only a reduction detectable (fig.33). Also the “rescue effect” of MG132 was not that strong in the transiently transfected cells (fig.33, lanes 10-12), compared to the endogenous data (fig.37, lane 4) (Aichem, Kalveram et al. 2012). Even if the effects in these experiments (fig.33) were not as dramatic as in the endogenous cycloheximide chase by Annette Aichem (fig.37) (Aichem, Kalveram et al. 2012), these data also confirm that FAT10, as well as its substrate proteins, become degraded by the proteasome. The extenuated and less consistent effects probably could be due to the immense protein amount which is achieved by transient transfection compared to the endogenous situation. Further, one has to admit, that for the endogenous data TNFα and IFNγ stimulated cells were used, in which also NUB1L is upregulated due to the IFNγ stimulation (Kito, Yeh et al. 2001, Schmidtke, Kalveram et al. 2006). Since NUB1L has been shown to accelerate the proteasomal degradation of FAT10 and FAT10ylated substrates (Hipp, Raasi et al. 2004, Schmidtke, Kalveram et al. 2009), this would explain why the degradation effects of the cycloheximide chase [fig.37, (Aichem, Kalveram et al. 2012)] were more dramatic in the cytokine stimulated cells, compared to the transiently transfected cells (fig.33). Bett et al. for example could show that when FAT10 was co-transfected together with NUB1L neither monomeric FAT10 nor FAT10 conjugates were detectable anymore which was not the case when only FAT10 was transfected (Bett, Kanuga et al. 2012).

According to these data, despite the interaction of FAT10 and p62, the autophagosomal degradation doesn’t seem to have an influence on the degradation of either the monomeric FAT10 or the characteristic 130 kDa p62-FAT10 conjugate (fig.33, lanes 7-9). Strikingly, in the transiently transfected cells also the monomeric p62 did not accumulate upon the inhibition of autophagy by Bafilomycin A1 (fig.33, lanes 7-9). Since in the cytokine induced cells the degradation and proteasome inhibition effects were more dramatic, it would be worthwhile to repeat the Bafilomycin A1 treatment in an endogenous cycloheximide chase. Further, it could also be interesting to use different autophagy inhibitors (for example

3-methyladenine) and autophagy inducing agents or treatments like rapamycin or starvation in order to investigate the effects on the FAT10-p62 conjugates.

6.2 p62 is the only autophagic adaptor protein which interacts with FAT10 covalently and non-covalently

Neither NBR1, nor OPTN or NDP52 were found to interact with FAT10 under the tested conditions. However, taken under consideration that also the detection of the FAT10-p62 conjugate requires certain requirements, it would be worthwhile to further try different tag, immunoprecipitation and antibody combinations.

NBR1

Like p62, NBR1 can interact with LC3 and function in autophagosomal clearance independently of p62. Both proteins were shown to be degraded by autophagy (Kirkin, Lamark et al. 2009). It is not clarified yet what the differences in the cognisance and function of these two proteins are. Since FAT10 has been shown to interact covalently and non-covalently with p62 and since the FAT10-p62 conjugates as well as monomeric p62 have been shown to be degraded by the proteasome, it would be interesting to test, whether FAT10 also interacts with NBR1. Interestingly, NBR1 was found in a mass spectrometry screen performed by Annette Aichem as a putative non-covalent interaction partner of FAT10 (Aichem, Kalveram et al. 2012). However in none of the co-immunoprecipitation experiments performed with the lysates of transiently co-transfected HEK293T cells a non-covalent interaction between Flag-FAT10 and HA-NBR1 was visible (fig.34, lane 11). Only in one out six experiments a potential FLAG-FAT10-HA-NBR1 conjugate was detectable, but this was not reproducible (fig34, lanes 5, 11). However, since also the interactions between FAT10 and p62 are sometimes hard to detect one could, in order to completely rule out any interactions between FAT10 and NBR1 further try more different tag, co-immunoprecipitation and antibody combinations as well as investigate the interaction under completely endogenous conditions. In order to find out whether NBR1 also becomes degraded by the proteasome in the presence of FAT10, one could perform a cycloheximide chase with both endogenous FAT10 and NBR1 as well as transfected HA-FAT10 or HA-FAT10(ΔGG) and endogenous NBR1, as shown for p62 by Aichem et al. (Aichem, Kalveram et al. 2012).

NDP52

NDP52 functions as a p62 independent adaptor protein (Thurston, Ryzhakov et al. 2009, Kraft, Peter et al. 2010). Since NDP52 has been shown to be required for the efficient autophagic degradation of *S. typhimurium* (Thurston, Ryzhakov et al. 2009, Cemma, Kim et al. 2011, Johansen and Lamark 2011) and since FAT10 was shown to co-localise with cytosolic *Salmonella* in HUVECs (Valentina Spinnenhirn, unpublished data), it was interesting to investigate whether NDP52 would also interact with FAT10. Surprisingly, in the Flag-FAT10 and EGFP-NDP52 co-transfected cells, a conjugate band was showing up at around 100-something kDa (fig.35, lanes 7, 19). However, in the EGFP and Flag-FAT10 co-transfected negative control a conjugate band of around 45 kDa was detectable (fig.35, lanes 11, 23), indicating that the EGFP-tag became FAT10ylated. A non-covalent interaction was not detectable. But to really make sure whether there is an interaction between NDP52 and FAT0, the experiment should be repeated by using a tag for NDP52 that doesn't contain any lysines such as a 6xHis-, or a HA-tag.

OPTN

OPTN expression is inducible by TNFα, and it mainly becomes degraded by the proteasome rather than by autophagy (Ying and Yue 2012). OPTN is also localised to intracellular *Salmonella* and has been shown to be involved in the selective autophagy of ubiquitin-coated cytosolic *S. typhimurium* (Wild, Farhan et al. 2011). The TBK1 kinase has been shown to promote the autophagic clearance of *Salmonella* by phosphorylating OPTN on S177 and thereby enhancing the LC3 binding affinity of OPTN (Wild, Farhan et al. 2011). Also FAT10 was shown to localise to cytosolic Salmonella (Valentina Spinnenhirn, unpublished data). Altogether, OPTN would be a good candidate to be a potential FAT10 interacting partner. Wild et al. tested the interaction capacity of OPTN for ubiquitin and ubiquitin-like proteins, except FAT10. They found OPTN to bind ubiquitin-chains, but not mono-ubiquitin or other UBL proteins (Wild, Farhan et al. 2011). In order to investigate whether OPTN would be a substrate for FAT10ylation, HEK293T cells were co-transfected with Flag-FAT10 and either HA-OPTN (fig.36, lanes 6, 14), the HA-OPTN(5xA) non-phosphorylated mutant (fig.36, lanes 7, 15) or the HA-OPTN(5xE) phospho-mimicking mutant (fig.36, lanes 8, 16). Co-immunoprecipitation

experiments were performed in order to investigate the non-covalent interaction between Flag-FAT10 and HA-OPTN. There were no covalent or non-covalent interactions detectable between Flag-FAT10 and either HA-OPTN (fig.36, lanes 6, 14) or the HA-OPTN mutants (fig.36, lanes 7, 8, 15, 16).

As already discussed for the investigation of the FAT10 and NBR1 interaction also for the further investigation of the FAT10 and NDP52 or OPTN interaction it would be interesting to use different tag co-immunoprecipitation and antibody combinations, or completely endogenous conditions.

6.3 Possible consequences of the FAT10 p62 interaction

In the following section some biological functions of p62 are summarised and possible consequences of the FAT10ylation of p62 are discussed.

6.3.1 The role of p62 and FAT10 in NF-κB signalling

Both, p62 (Geetha and Wooten 2002, Yin, Lin et al. 2009, Komatsu and Ichimura 2010) and FAT10 (Buchsbaum, Bercovich et al. 2012) were found to be involved in the NF-κB signalling.

6.3.1.1 The NF-κB pathway

The transcription factor “nuclear factor kappa B” (NF-κB) controls the cytokine production of cells (Napetschnig and Wu 2013). The activation of the classical NF-κB pathway is required for a successful immune response and to amplify the survival and proliferation of cells (Demchenko, Glebov et al. 2010).

By recognising specific patterns of microbial components, signalling via Toll-like receptors (TLRs) induce the production of inflammatory cytokines via NF-κB (Volz, Kaesler et al. 2012). Adaptors, such as “myeloid differentiation factor 88” (MyD88) modulate the TLR signalling pathways and transform the receptor ligation into intracellular signalling cascades (fig.38) (Volz, Kaesler et al. 2012). The signalling via MyD88 pathway induces the transcription factor NF-κB via several steps involving TRAF6 and finally initiates the production of pro-inflammatory cytokines such as TNFα. The MyD88 pathway can be activated by all TLRs, with the exception of TLR3 (fig.38) (Volz, Kaesler et al. 2012).

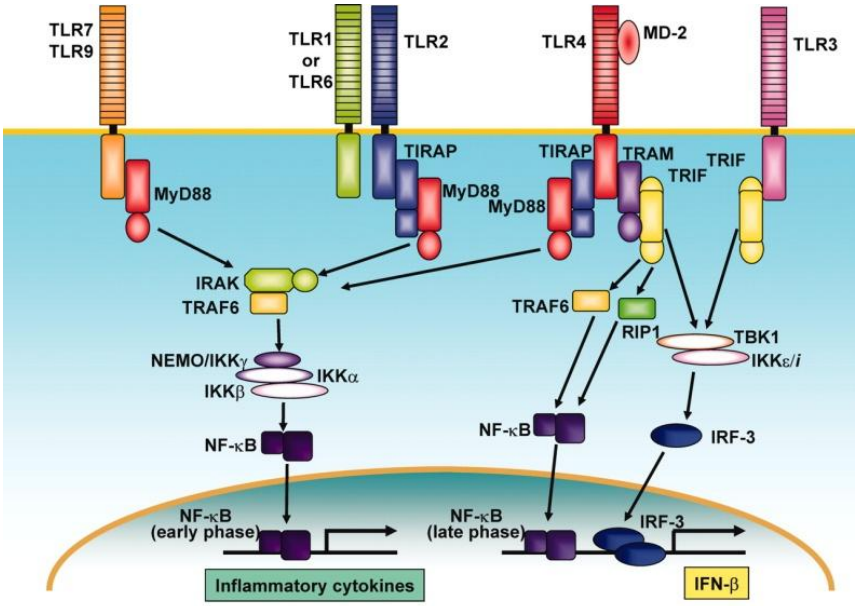

Figure 38: Toll-like receptors in innate immunity. TLRs activate the innate immunity by recognising specific patterns of microbial components**.** Adaptors, such as MyD88, TIRAP, and TRIF modulate the TLR signalling pathways. MyD88 is essential for the induction of inflammatory cytokines via NF-κB. The IKK complex consists of IKKα, IKKβ and NEMO/IKKγ and upon its activation it phosphorylates IκB, resulting in the nuclear translocation of NF-κB. The Non-typical IKKs IKKε and TBK1, mediate the activation of IRF-3 (Takeda and Akira 2005).

NF-kB is a heterodimer of p50 and Rel A (p65) (Demchenko, Glebov et al. 2010). In unstimulated cells, the inhibitory protein IκB-α is bound to NF-κB and prevents the nuclear translocation of NF-κB (Jaffray, Wood et al. 1995, Napetschnig and Wu 2013). The NF-κB activity can be induced by inflammatory and immunmodulatory molecules including: “reactive oxygen species” (ROS), TNFα, IL-1β or LPS (Liu, Xia et al. 2012, Napetschnig and Wu 2013). The recognition of these extracellular stimuli by receptors, finally leads to the activation of the “IκB kinase” (IKK) complex via a intracellular signalling cascade (Napetschnig and Wu 2013). The activated KKs phosphoryate the IκBα subunit of the NF-κB:IκB complex (Liu, Xia et al. 2012). The phosphorylated IκBα subunit is degraded by the proteasome and the NF-κB proteins are released. The freed NF-κB proteins travel into the nucleus, bind to their target sequences and activate the transcription of their target genes (Liu, Xia et al. 2012, Napetschnig and Wu 2013).

The IKK complex is composed of the catalytic subunits IKKα and IKKβ and the regulatory subunit IKKγ also known as NEMO (Demchenko, Glebov et al. 2010, Napetschnig and Wu 2013). The activation of IKK complex is dependent on the phosphorylation of IKKα/β and the ubiquitylation of NEMO (Shambharkar, Blonska et al. 2007). NEMO specifically recognize K63-linked polyubiquitin chains and becomes itself K63-linked ubiquitylated upon the activation of the NF-kB cascade (Israel 2010). Also the ubiquitylation of TRAF6 is required for NF-κB activation (Israel 2010, Komatsu and Ichimura 2010). This modification is catalysed by the TRAF6 ubiquitin ligase itself (Komatsu and Ichimura 2010). The DUBs CylD and A20 have been described as negative regulators of NF-kB (Israel 2010).

6.3.1.2 p62 serves as a scaffold for the NF-κB pathway

“Atypical protein kinase C” (aPKCs) selectively bind to the IKKs and activate them via phosphorylation. The interaction of p62 with aPKC and TRAF6 provides as a scaffold in both the TNFα and interleukin-1 (IL-1) receptor signalling NF-κB pathways (fig.39) (Geetha and Wooten 2002).

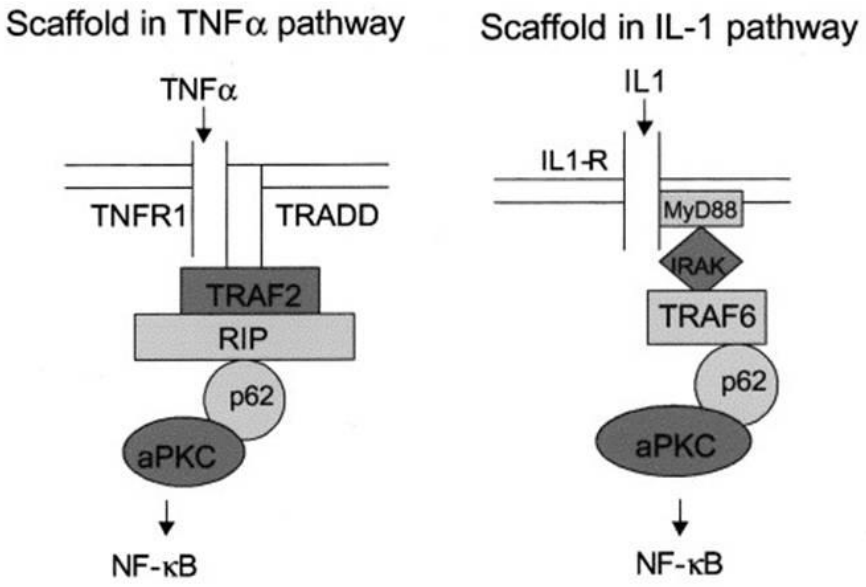

Figure 39: p62 in NF-κB signalling. Upon stimulation with TNFα, p62 links RIP and aPKC thereby leading to phosphorylation of IKK and subsequent activation of NF-κB. Upon IL-1 stimulation, p62 forms a ternary complex with TRAF6 and IRAK leading to recruitment of aPKC with subsequent phosphorylation of IKK and activation of NF-κB. Modified from (Geetha and Wooten 2002)

The interaction of p62 with TRAF6 promotes its oligomerisation and the subsequent activation, which leads to the K63 autopolyubiquitylation of TRAF6 resulting in the activation of NF-κB activation (Yin, Lin et al. 2009, Komatsu and Ichimura 2010).

Upon FAT10ylation, the proteasomal degradation of p62 would prevent its scaffolding function and therefore could theoretically lead to an inhibition of the NF-κB activation. This would be in accordance to the finding of Buchsbaum et al., in which the FAT10ylation of LRRFIP2 leads to the inhibition of the NF-κB activation (Buchsbaum, Bercovich et al. 2012).

6.3.1.3 The FAT10ylation of LRRFIP2 inhibits the NF-κB activation

Buchsbaum et al. have described that the FAT10ylation of LRRFIP2 results in the inhibition of the NF-κB activation (Buchsbaum, Bercovich et al. 2012). LRRFIP2 is involved in NF-κB activation following stimulation of TLR4. LRRFIP2 is recruited along with MYD88 to the cytosolic tail of the receptor, and thereby it mediates the activation of the downstream signalling cascade (Buchsbaum, Bercovich et al. 2012). Buchsbaum et al. found the FAT10ylation of LRRFIP2 to inhibit its recruitment to the membrane by translocating it to the cellular insoluble fraction. As a consequence, the NF-κB activation is inhibited (Buchsbaum, Bercovich et al. 2012). Probably also the proteasomal degradation of LRRFIP2 upon the FAT10ylation leads to the inhibition of the NF-κB activation. However this aspect was only discussed very vague by the authors.

One could imagine that the FAT10ylation of p62 and of other substrate proteins may also have a regulatory function for processes involving these substrates. The FAT10ylation of a certain domain in p62 for example may inhibit its function either sterically or by the proteasomal degradation of p62. Maybe not all substrates of FAT10ylation do have the same fate such as proteasomal degradation.

6.3.2 p62 is involved in IL-4 synthesis and FAT10 may also play a role

6.3.2.1 IL-4 synthesis

$CD8^+$ Th1 cells mainly produce IFNγ and IL-2, and play an essential role in cell-mediated immune responses against intracellular pathogens. $CD4^+$ Th2 cells secrete

the characteristic cytokines IL-4, IL-5, and IL-13 (Martin, Diaz-Meco et al. 2006). Th2 cells are required for providing host defence against extracellular parasitic infections and for the control of humoral immunity. Th2 differentiation is triggered by signals of the TCR and the cytokines generated during polarisation, particularly IL-4. IL-4 is important for the induction and maintenance of differentiated Th2 cells (Martin, Diaz-Meco et al. 2006).

The binding of IL-4 to its receptor (IL-4R) induces a signal cascade including the atypical PKC isoform PKCζ, Jak1/Jak3, STAT6 and GATA3 and STAT5 STAT6 and GATA3 together with STAT5 induce the secretion of copious amounts of IL-4, IL-5, and IL-13 by activated Th2 cells (Moscat, Rennert et al. 2006, Chapoval, Dasgupta et al. 2010). NF-kB has been shown to be essential for the GATA3 synthesis. The Inhibition of NF-κB activity prevented GATA3 expression and Th2 cytokine production in developing, but not committed Th2 cells (Das, Chen et al. 2001).

6.3.2.2 p62 is involved in IL-4 synthesis in the late phases of T cell activation

In $p62^{-/-}$ Th2 cells, the IL-4, IL-5, IL-10 and IL-13 secretion is significantly reduced. In Th2 cell differentiation, p62 has been shown to participate in the activation of NF-kB, by forming a part of the signalling complex that regulates the IKK activation. MALT1, p62 and TRAF6 build a p62/TRAF6/MALT1 complex. MALT1 most likely controls the IKK activation by inducing the K63 ubiquitylation of NEMO through the E3 ubiquitin ligase activity of TRAF6 (Martin, Diaz-Meco et al. 2006). Therefore, p62 is involved in the control of the NF-kB stimulation and IL-4 synthesis, at the level of GATA3 production, in the late phases of T cell activation, which are important for Th2 differentiation events (Martin, Diaz-Meco et al. 2006).

6.3.2.3 The transcription factor JunB is a substrate of FAT10ylation

The transcription factor JunB is expressed in Th2 cells and induces the IL-4 expression during T cell development and directs thereby Th2 differentiation (Li, Tournier et al. 1999). Interestingly, JunB is also a substrate of FAT10ylation and the FAT10-JunB conjugate is degraded by the proteasome. Additional data from luciferase assays further show that upon co-expression of FAT10 JunB shows a decreased transcriptional activity towards reporter constructs containing JunB binding

sites such as IL4 promoter sequences (Stella Ryu, 2012, unpublished, PhD thesis 2012, University of Konstanz). The outcome of FAT10-mediated JunB degradation on Th1/Th2 CD4+ T helper cell differentiation in naive versus *Listeria monocytogenes* infected wild-type C57BL/6 and FAT10$^{-/-}$ is therefore under current investigation.

With p62 and JunB there are already two FAT10 substrates which are involved in the IL4 secretion during the Th2 differentiation. This could indicate that FAT10 might play a role in the down regulation of the Th2 differentiation.

In freshly isolated T cells however, according to Bates et al., there was no FAT10 expression detectable at all (Bates, Ravel et al. 1997). But the cells which were used by Bates et al. were not stimulated with TNFα or IFNγ (Bates, Ravel et al. 1997). However, in Jurkat T cells FAT10 was not even detectable after TNFα and IFNγ stimulation (Raasi, Schmidtke et al. 1999).

If the FAT10 induction would be absent in certain cells types, in those cells the NF-κB production would be protected from a potential inhibition due to the FAT10ylation of either p62 or LRRFIP2 upon LPS or cytokine stimulation. In those cells also the degradation of JunB upon FAT10ylation would be prevented.

6.3.3 FAT10 and p62 in apoptosis

While p62 has been shown to participate in apoptosis (Bekes and Salvesen 2009, Jin, Li et al. 2009), for FAT10 the data are ambiguous.

6.3.3.1 Apoptosis

Apoptosis is a highly regulated process of cell suicide that helps multicellular animals to eliminate unneeded, damaged, or infected cells. There are several morphologically distinct apoptotic processes with different triggers. In the extrinsic pathway, cells are stimulated from the cells outside by specific pro-apoptotic ligands. Among other proteins cysteinylaspartate proteases called caspases are involved in the apoptotic process (Jin, Li et al. 2009). TNFR1 is the major signalling receptor for TNFα. It triggers distinct signalling pathways leading to either the activation of NF-κB transcription factors or apoptosis (He and Ting 2002). NF-κB activation results in the expression of anti-apoptotic genes which inhibit the apoptosis pathway that is activated in parallel. The binding of TNFα to TNFR1 leads to the recruitment of

"TNFR1-associated death domain" (TRADD) and "receptor-interacting protein" (RIP) (He and Ting 2002). Both, TRADD and RIP are required for signalling to NF-κB, as well as the apoptosis pathway. TRADD and RIP associate with TRAF2 and another death domain protein called "FAS-associated death domain protein" (FADD). At this step the NF-κB and apoptotic signals are thought to bifurcate: TRAF2 recruitment leads to the activation of downstream kinases and NF-κB activation, whereas FADD recruitment leads to the activation of caspase 8 and apoptosis (He and Ting 2002).

6.3.3.2 p62 participates in the maintenance apoptosis

p62 was shown to play a role in the maintenance of apoptosis (Bekes and Salvesen 2009, Jin, Li et al. 2009). The binding of the pro-apoptotic ligand "TNF-related apoptosis inducing ligand" (TRAIL) to the cell-surface death receptors DR4 and DR5 leads to receptor clustering and subsequently to the recruitment of the adaptor protein "Fas-associated death domain" (FADD) and thereby initiates the recruitment and activation of the apical initiator protease caspase-8 to form the "death-inducing signalling complex" (DISC) (Bekes and Salvesen 2009, Jin, Li et al. 2009). While the DISC recruitment initiates caspase-8 stimulation, the full activation of the protease depends on further molecular aggregation events. Caspase-8 is polyubiquitylated at the DISC complex by a neddylated form of a cullin3 (CUL3)-based E3 ligase. The polyubiquitylated caspase-8 recruits p62 in a CUL3-dependent manner. By autoprocessing the catalytic active caspase-8 domains are separated from those required for the recruitment. The catalytic component is transported by p62 to ubiquitin-rich aggresomes in the cytosol (Bekes and Salvesen 2009, Jin, Li et al. 2009). It is proposed that the caspase-8 maintains its catalytic activity through the stabilisation of its dimeric conformation. p62 might be involved in the maintenance of the caspase-8 activity by remaining the cleaved caspase-8 dimer, due to its aggregation within the cytosol. These results identify a mechanism that positively controls apoptosis signalling by polyubiquitylation and aggregation of a key initiator caspase (Bekes and Salvesen 2009, Jin, Li et al. 2009).

6.3.3.3 FAT10 and apoptosis

The data for the role of FAT10 in apoptosis are ambiguous. The overexpression of wild-type FAT10 in mouse fibroblasts was found to causes apoptosis in a caspase-

dependent manner (Raasi, Schmidtke et al. 2001). Li et al. found the overexpression of FAT10 in HEK 293 cells to induce apoptosis by activating the tumour suppressor p53 (Li, Santockyte et al. 2011). According to these data, one would assume a pro-apoptotic function of FAT10. However, in contradiction to this observations, Caanan et al. found the lymphocyte populations from spleens, thymuses and bone marrows from the FAT10$^{-/-}$ mice to be more prone to spontaneous apoptosis (Canaan, Yu et al. 2006). Further, Buchsbaum et al. found FAT10 to be rapidly ubiquitylated and degraded in response to the induction of apoptosis, suggesting that it plays a role in prosurvival pathways (Buchsbaum, Bercovich et al. 2012). These data rather support an anti-apoptotic or pro-survival function of FAT10.

The FAT10ylation of p62 and its subsequent proteasomal degradation may have an anti-apoptotic function. The proteasomal degradation of p62 upon the FAT10ylation would in this case prevent the recruitment of the catalytic active domains of the caspase-8 into the insoluble aggregates and thus the maintenance of their activity. This would be in line with the data obtained for the FAT10 knockout mice, in which lymphocytes show an increased susceptibility to spontaneous apoptotic death (Canaan, Yu et al. 2006).

Buchsbaum et al. reported that FAT10ylated LRRFIP2 is translocated to the cellular insoluble fraction. However in this case the consequence was not the maintenance, but the inhibition of the LRRFIP2 activity (Buchsbaum, Bercovich et al. 2012).

In summary this would mean, that p62 on the one hand is involved in the maintenance of the anti-apoptotic NF-κB signalling and on the other hand in the maintenance of apoptosis. Therefore, the consequences of the FAT10ylation of p62 and its subsequent proteasomal degradation may be either pro or anti-apoptotic.

Komatsu et al. have already proposed that p62-positive aggregates are signalling hubs that could decide whether cells survive by activating the TRAF6-NF-κB pathway, or die by facilitating the aggregation of caspase-8 and the downstream effector caspases (Komatsu and Ichimura 2010). Because the level of p62 protein is strictly regulated by autophagy, autophagy can control NF-κB pathway, activation of apoptosis and response to environmental stress (Komatsu and Ichimura 2010). With FAT10, there would be an additional, cytokine inducible regulator of the p62 content and activity.

6.3.4 The role of p62 and FAT10 in protein aggregation

Interestingly, FAT10 was found to interact with p62 (Aichem, Kalveram et al. 2012), HDAC6 (Kalveram, Schmidtke et al. 2008) and VCP/p97 (unpublished data, Ricarda Schwab). All three proteins participate in aggregation and degradation processes.

6.3.4.1 Protein aggregation

"Histone deacetylase 6" (HDAC6)

Unlike other deacetylases, HDAC6 has unique substrate specificity for nonhistone proteins (Li, Shin et al. 2013). It directly binds free ubiquitin as well as mono- and polyubiquitylated proteins but preferentially interacts with K63-linked polyubiquitin chains. By binding simultaneously to ubiquitin and to dynein, HDAC6 transports ubiquitylated protein aggregates along the microtubules to the aggresomes (Kraft, Peter et al. 2010). This role of HDAC6 especially is important under conditions of impaired proteasomal degradation, when misfolded proteins are preferentially degraded by autophagy. Since autophagy, unlike proteasomal degradation, capture mainly larger structures rather than single proteins HDAC6 could be involved in the bundling of ubiquitylated target proteins in aggresomes (Kraft, Peter et al. 2010). The ability of HDAC6 to form and clear aggresomes is regulated by phosphorylation. The protein kinase CK2 directly phosphorylates HDAC6 and unphosphorylated HDAC6 mutants failed to form and remove aggresomes. Therefore, CK2 can modulate the HDAC6 activity in respect of aggresome formation and clearance in response to stress (Li, Shin et al. 2013). HDAC6 has been implicated in the mediation of aggregation and autophagic clearance. It might function as a master regulator of the protective response to cytotoxic protein aggregates (Li, Shin et al. 2013).

Further, under proteasomal inhibition, the CK2 kinase also phosphorylates S403 of p62 and thus increases the affinity of its UBA domain for polyubiquitylated chains, leading to an enhanced recruitment of polyubiquitylated protein into the sequestosome.

"Valosin-containing protein" (VCP)/p97

The AAA-ATPase family protein VCP is a molecular chaperone with an important role in protein degradation. Its ATP hydrolysis is used to segregate ubiquitylated

substrates from nuclear or cytoplasmic protein complexes, followed by their degradation by the ubiquitin-proteasome system (Lamark and Johansen 2012). The loss of VCP in mammalian cells results in the accumulation of insoluble ubiquitylated proteins (Lamark and Johansen 2012). Further, VCP is also proposed to be involved in aggresome formation. Therefore, the aggregate has to be ubiquitylated by an E3 ligase such as parkin and VCP delivers the ubiquitylated aggregates to HDAC6 (Lamark and Johansen 2012). Subsequently, HDAC6 transports the protein aggregates to the aggresome. The contents of aggresomes subsequently may be degraded by aggrephagy (Lamark and Johansen 2012). Since the knockdown of VCP leads to the accumulation of ubiquitylated substrates containing autophagosomes, VCP also seems to be involved in the maturation of autophagosomes (Lamark and Johansen 2012).

By binding to their ubiquitin residues HDAC6 can sense misfolded proteins. The fate of these polyubiquitylated misfolded proteins is depending on the HDAC6:VCP ratio. While VCP favours degradation by the proteasome, HDAC6 promotes the transport of these proteins to the aggresomes (Li, Shin et al. 2013). An excess of VCP over HDAC6 facilitates the dissociation of the complex between HDAC6 and the polyubiquitylated proteins and therefore averts the delivery of polyubiquitylated protein to the proteasome (Li, Shin et al. 2013). Upon sensing ubiquitylated cellular aggregates, HDAC6 induces the expression of major cellular chaperones such as HSP90 by triggering the dissociation of a repressive HDAC6/HSF1/HSP90 complex and subsequent HSF1 activation (Li, Shin et al. 2013). No crosstalk between VCP and the HSP70/HSP90 molecular chaperones is reported, and cellular roles mediated by VCP may therefore be distinct from those displayed by the other group of molecular chaperones (Lamark and Johansen 2012).

6.3.4.2 The role of p62 in aggregate formation

By binding simultaneously to LC3 and ubiquitin, p62 act as a shuttling factor that links polyubiquitylated protein aggregates to the autophagy machinery (Bjorkoy, Lamark et al. 2006). The inhibition of autophagy leads to an increase in the size and number of p62 positive bodies and the p62 protein level. Those p62 constructs lacking the UBA domain, failed to form aggregates (Bjorkoy, Lamark et al. 2005) and also the

self-oligomerisation capability via the PB1 domain of p62 was shown to be required for the formation of the cytoplasmic bodies (Pankiv, Clausen et al. 2007, Ichimura, Kumanomidou et al. 2008).

6.3.4.3 FAT10 and aggregate formation

Upon proteasomal inhibition, FAT10 non-covalently interacts with HDAC6 *in vivo* and localises to aggresome in a microtubule-dependent manner (Kalveram, Schmidtke et al. 2008). Both UBL domains of FAT10 can interact independently with HDAC6 while the diglycine motif of FAT10 is not required for the interaction. The interaction is independent of the catalytic activity of HDAC6 (Kalveram, Schmidtke et al. 2008). The C-terminus of FAT10 binds to the BUZ domain of HDAC6 (Hard, Liu et al. 2010).

Interestingly, Ricarda Schwab found VCP to interact with FAT10 (unpublished data). Since the interaction of FAT10 and HDAC6 leads to the localisation of FAT10 and FAT10ylated substrates to the aggresome (Kalveram, Schmidtke et al. 2008) and since FAT10ylated p62 becomes degraded by the proteasome (Aichem, Kalveram et al. 2012) FAT10 might, by interacting with VCP, HDAC6 and p62, also be involved in the regulation of the aggregation and degradation processes upon cytokine stimulation.

6.3.5 p62 and FAT10 in Huntington's disease

Both FAT10 and p62 are present in cells expressing mutant huntingtin protein (HTT) (Nagaoka, Kim et al. 2004) (Neha Rani, 2012, unpublished, PhD thesis 2011, University of Konstanz).

6.3.5.1 Huntington's disease

The exact function of the HTT protein is unknown. However, it appears to play an important role in neurons in the brain and is essential for normal embryonic development (Nasir, Floresco et al. 1995). The HTT gene contains a particular DNA segment known as a cytosine, adenine, and guanine (CAG) trinucleotide repeat. This segment appears multiple times in a row and thus is translated into a polyglutamine (polyQ) stretch. Normally, under non-pathological conditions, the CAG segment is repeated up to thirty-five times within the gene (Nasir, Floresco et al. 1995,

Finkbeiner 2011). The dominantly inherited neurodegeneration disease “Huntington’s disease” is caused by the expression of mutant forms of the HTT protein in which the expanded CAG repeat leads to a polyQ chain with more than thirty-five repeats. These mutated HTT proteins are cytotoxic, they do have an increased susceptibility to aggregate and their expression causes the induction of apoptosis in cells (Nasir, Floresco et al. 1995, Finkbeiner 2011). In those cells expressing the mutant form of the HTT, the protein displayed both diffuse and aggregated localisation (Arrasate, Mitra et al. 2004). The aggregated proteins in the diseased brain suggest insufficient degradation by the UPS machinery (Finkbeiner 2011) and the aggregation seems to be a mechanism for cell survival (Arrasate, Mitra et al. 2004).

6.3.5.2 The role of p62 in Huntington’s disease

Interestingly, p62 is induced as a response to the expression of mutant HTT (Nagaoka, Kim et al. 2004). However, only cells which contain HTT aggregates seemed to express high levels of p62, whereas cells containing diffuse HTT mutant did not show an increase in the p62 level (Bjorkoy, Lamark et al. 2005). The protein inclusions formed by aggregate-prone proteins are degraded by macroautophagy. Confocal microscopy revealed that p62 and LC3 apparently formed a shell surrounding the HTT-containing aggregates. The reduction of endogenous p62 levels by expression of p62 antisense RNA increased apoptosis of HTT-expressing apoptotic cells (Bjorkoy, Lamark et al. 2005). Thus, p62 has a protective effect against cell death that is induced by overexpression of polyQ-expanded HTT (Bjorkoy, Lamark et al. 2005). Steffan et al. found that the ubiquitylation of mutant HTT is an important way to detoxify the protein, whereas SUMOylation of the same residues prevents aggregation and leads to cell death (Steffan, Agrawal et al. 2004).

6.3.5.3 The role of FAT10 in Huntington’s disease

Interestingly, during her PhD thesis, Neha Rani found FAT10 protein in aggregates from the brains of Huntington’s disease transgenic mice (Neha Rani, 2011, unpublished, PhD thesis 2012, University of Konstanz).

By using a Huntington’s disease cellular model, Nagashima et al. could show that HTT with a short polyQ chain was show to be preferentially FAT10ylated while

completely aggregated HTT was FAT10-negative (Nagashima, Kowa et al. 2011). The FAT10ylation of HTT facilitated its proteasomal degradation and knockdown of FAT10 enhanced the aggregation of HTT. For these studies HEK293 and Neuro2A cells were transfected with FAT10 and the respective HTT constructs (Nagashima, Kowa et al. 2011). By stabilising HTT, FAT10 probably provides protection from its toxicity. Since the overexpression or inhibition of FAT10 did not alter the ubiquitylation level of HTT, FAT10 seems to modify HTT in a non-competitive manner (Nagashima, Kowa et al. 2011). HTT-exon-1-GFP was shown to be mono- and/or polyubiquitylated at any lysine residue. FAT10ylation in contrast, seems to be achieved by a single molecule only (Nagashima, Kowa et al. 2011).

Lu et al. found the degradation of mutant HTT (mHTT) to be dependent on its lysine residues and that NUB1 suppresses the toxicity of mHTT (Lu, Al-Ramahi et al. 2013). Therefore, they used mouse neuroblastoma cells which expressed NEDD8 but no detectable FAT10 in order to assess whether FAT10 and/or NEDD8 are required for NUB1 effects on the mHTT abundance. They found only NEDD8 but not FAT10 to be required for the NUB1-mediated clearance (Lu, Al-Ramahi et al. 2013).

Both FAT10 and p62 are present in cells expressing mutant HTT (Nagaoka, Kim et al. 2004) (Neha Rani, 2012, unpublished, PhD thesis 2011, University of Konstanz). Since p62 has been shown to protect mutant HTT expressing cells from apoptosis and since the FAT10ylation of p62 was shown to decrease the endogenous p62 level (Aichem, Kalveram et al. 2012), the presence of FAT10 may inhibit the cytoprotective effect of p62 which is in contrast to the finding that FAT10 by stabilising HTT, itself was considered to provide protection.

6.3.6 The regulatory function of p62 in autophagy

In 2011, Itakura and Mizushima found p62 to localise to the autophagosome formation site, independently of downstream factors (Itakura and Mizushima 2011). They proposed that the localisation of p62 to the autophagosomal formation site might even determine where autophagosomes are nucleated (Itakura and Mizushima 2011). p62 is degraded along with its polyubiquitylated cargo by the autophagy–lysosome system (Komatsu and Ichimura 2010).

In order to maintain metabolic homeostasis, cells have to respond to changes in nutrient availability. In mammalian, the “target of rapamycin complex 1” (mTORC1) is the central kinase complex in this process. p62 binds to the mTOR kinase raptor and is an integral component of the mTORC1 pathway (Duran, Amanchy et al. 2011, Linares, Duran et al. 2013). In amino acid-stimulated cells, p62 negatively regulates autophagy by recruiting TRAF6 which in turn activates mTORC1. TRAF6 is necessary for the translocation of mTORC1 to the lysosomes and the TRAF6-catalysed K63 ubiquitylation of mTOR regulates mTORC1 activation by amino acids (Linares, Duran et al. 2013). Without p62 function, autophagy is upregulated in mammalian cells. While the p62 protein could negatively regulate autophagy via the activation of mTORC1 (Duran, Amanchy et al. 2011, Linares, Duran et al. 2013), its protein level is strictly regulated by autophagy (Pankiv, Clausen et al. 2007, Ichimura, Kumanomidou et al. 2008). Therefore, p62 regulates autophagy by creating a feedforward loop by which p62 activation of mTORC1 results in higher p62 levels. These increased levels of p62 thereby promote even more mTORC1 activity (Moscat and Diaz-Meco 2011). The physiological significance of this loop is not completely clear, but it suggests that when amino acids levels are low, mTORC1 activity is reduced and autophagy is upregulated (Moscat and Diaz-Meco 2011).

The cytokine induced proteasomal degradation of FAT10ylated p62 (Aichem, Kalveram et al. 2012) might influence the initiation of autophagy.

7 References

Aichem, A., B. Kalveram, V. Spinnenhirn, K. Kluge, N. Catone, T. Johansen and M. Groettrup (2012). "The proteomic analysis of endogenous FAT10 substrates identifies p62/SQSTM1 as a substrate of FAT10ylation." J Cell Sci 125(Pt 19): 4576-4585.

Aichem, A., C. Pelzer, S. Lukasiak, B. Kalveram, P. W. Sheppard, N. Rani, G. Schmidtke and M. Groettrup (2010). "USE1 is a bispecific conjugating enzyme for ubiquitin and FAT10, which FAT10ylates itself in cis." Nat Commun 1: 13.

Alemu, E. A., T. Lamark, K. M. Torgersen, A. B. Birgisdottir, K. B. Larsen, A. Jain, H. Olsvik, A. Overvatn, V. Kirkin and T. Johansen (2012). "ATG8 family proteins act as scaffolds for assembly of the ULK complex: sequence requirements for LC3-interacting region (LIR) motifs." J Biol Chem 287(47): 39275-39290.

Alers, S., A. S. Loffler, S. Wesselborg and B. Stork (2012). "The incredible ULKs." Cell Commun Signal 10(1): 7.

Arrasate, M., S. Mitra, E. S. Schweitzer, M. R. Segal and S. Finkbeiner (2004). "Inclusion body formation reduces levels of mutant huntingtin and the risk of neuronal death." Nature 431(7010): 805-810.

Axe, E. L., S. A. Walker, M. Manifava, P. Chandra, H. L. Roderick, A. Habermann, G. Griffiths and N. T. Ktistakis (2008). "Autophagosome formation from membrane compartments enriched in phosphatidylinositol 3-phosphate and dynamically connected to the endoplasmic reticulum." J Cell Biol 182(4): 685-701.

Bardag-Gorce, F., J. Oliva, J. Li, B. A. French and S. W. French (2010). "SAMe prevents the induction of the immunoproteasome and preserves the 26S proteasome in the DDC-induced MDB mouse model." Exp Mol Pathol 88(3): 353-362.

Basler, M., C. J. Kirk and M. Groettrup (2013). "The immunoproteasome in antigen processing and other immunological functions." Curr Opin Immunol 25(1): 74-80.

Bates, E. E., O. Ravel, M. C. Dieu, S. Ho, C. Guret, J. M. Bridon, S. Ait-Yahia, F. Briere, C. Caux, J. Banchereau and S. Lebecque (1997). "Identification and analysis of a novel member of the ubiquitin family expressed in dendritic cells and mature B cells." Eur J Immunol 27(10): 2471-2477.

Behl, C. (2011). "BAG3 and friends: co-chaperones in selective autophagy during aging and disease." Autophagy 7(7): 795-798.

Behrends, C. and S. Fulda (2012). "Receptor proteins in selective autophagy." Int J Cell Biol 2012: 673290.

Bejarano, E. and A. M. Cuervo (2010). "Chaperone-mediated autophagy." Proc Am Thorac Soc 7(1): 29-39.

Bekes, M. and G. S. Salvesen (2009). "The CULt of caspase-8 ubiquitination." Cell 137(4): 604-606.

Besche, H. C., A. Peth and A. L. Goldberg (2009). "Getting to first base in proteasome assembly." Cell 138(1): 25-28.

Bett, J. S., N. Kanuga, E. Richet, G. Schmidtke, M. Groettrup, M. E. Cheetham and J. van der Spuy (2012). "The inherited blindness protein AIPL1 regulates the ubiquitin-like FAT10 pathway." PLoS One 7(2): e30866.

Bjorkoy, G., T. Lamark, A. Brech, H. Outzen, M. Perander, A. Overvatn, H. Stenmark and T. Johansen (2005). "p62/SQSTM1 forms protein aggregates degraded by autophagy and has a protective effect on huntingtin-induced cell death." J Cell Biol 171(4): 603-614.

Bjorkoy, G., T. Lamark and T. Johansen (2006). "p62/SQSTM1: a missing link between protein aggregates and the autophagy machinery." Autophagy 2(2): 138-139.

Boyle, K. B. and F. Randow (2013). "The role of 'eat-me' signals and autophagy cargo receptors in innate immunity." Curr Opin Microbiol.

Buchsbaum, S., B. Bercovich and A. Ciechanover (2012). "FAT10 is a proteasomal degradation signal that is itself regulated by ubiquitination." Mol Biol Cell 23(1): 225-232.

Buchsbaum, S., B. Bercovich, T. Ziv and A. Ciechanover (2012). "Modification of the inflammatory mediator LRRFIP2 by the ubiquitin-like protein FAT10 inhibits its activity during cellular response to LPS." Biochem Biophys Res Commun 428(1): 11-16.

Burman, C. and N. T. Ktistakis (2010). "Autophagosome formation in mammalian cells." Semin Immunopathol 32(4): 397-413.

Canaan, A., X. Yu, C. J. Booth, J. Lian, I. Lazar, S. L. Gamfi, K. Castille, N. Kohya, Y. Nakayama, Y. C. Liu, E. Eynon, R. Flavell and S. M. Weissman (2006). "FAT10/diubiquitin-like protein-deficient mice exhibit minimal phenotypic differences." Mol Cell Biol 26(13): 5180-5189.

Cemma, M., P. K. Kim and J. H. Brumell (2011). "The ubiquitin-binding adaptor proteins p62/SQSTM1 and NDP52 are recruited independently to bacteria-associated microdomains to target Salmonella to the autophagy pathway." Autophagy 7(3): 341-345.

Chapoval, S., P. Dasgupta, N. J. Dorsey and A. D. Keegan (2010). "Regulation of the T helper cell type 2 (Th2)/T regulatory cell (Treg) balance by IL-4 and STAT6." J Leukoc Biol 87(6): 1011-1018.

Chiu, Y. H., Q. Sun and Z. J. Chen (2007). "E1-L2 activates both ubiquitin and FAT10." Mol Cell 27(6): 1014-1023.

Ciechanover, A., S. Elias, H. Heller, S. Ferber and A. Hershko (1980). "Characterization of the heat-stable polypeptide of the ATP-dependent proteolytic system from reticulocytes." J Biol Chem 255(16): 7525-7528.

Clague, M. J., J. M. Coulson and S. Urbe (2012). "Cellular functions of the DUBs." J Cell Sci 125(Pt 2): 277-286.

Clausen, T. H., T. Lamark, P. Isakson, K. Finley, K. B. Larsen, A. Brech, A. Overvatn, H. Stenmark, G. Bjorkoy, A. Simonsen and T. Johansen (2010). "p62/SQSTM1 and ALFY interact to facilitate the formation of p62 bodies/ALIS and their degradation by autophagy." Autophagy 6(3): 330-344.

Dahlmann, B., T. Ruppert, L. Kuehn, S. Merforth and P. M. Kloetzel (2000). "Different proteasome subtypes in a single tissue exhibit different enzymatic properties." J Mol Biol 303(5): 643-653.

Dantuma, N. P. and K. Lindsten (2010). "Stressing the ubiquitin-proteasome system." Cardiovasc Res 85(2): 263-271.

Das, J., C. H. Chen, L. Yang, L. Cohn, P. Ray and A. Ray (2001). "A critical role for NF-kappa B in GATA3 expression and TH2 differentiation in allergic airway inflammation." Nat Immunol 2(1): 45-50.

Demchenko, Y. N., O. K. Glebov, A. Zingone, J. J. Keats, P. L. Bergsagel and W. M. Kuehl (2010). "Classical and/or alternative NF-kappaB pathway activation in multiple myeloma." Blood 115(17): 3541-3552.

Deosaran, E., K. B. Larsen, R. Hua, G. Sargent, Y. Wang, S. Kim, T. Lamark, M. Jauregui, K. Law, J. Lippincott-Schwartz, A. Brech, T. Johansen and P. K. Kim (2013). "NBR1 acts as an autophagy receptor for peroxisomes." J Cell Sci 126(Pt 4): 939-952.

Deshaies, R. J. and C. A. Joazeiro (2009). "RING domain E3 ubiquitin ligases." Annu Rev Biochem 78: 399-434.

Duran, A., R. Amanchy, J. F. Linares, J. Joshi, S. Abu-Baker, A. Porollo, M. Hansen, J. Moscat and M. T. Diaz-Meco (2011). "p62 is a key regulator of nutrient sensing in the mTORC1 pathway." Mol Cell 44(1): 134-146.

Ebstein, F., A. Lehmann and P. M. Kloetzel (2012). "The FAT10- and ubiquitin-dependent degradation machineries exhibit common and distinct requirements for MHC class I antigen presentation." Cell Mol Life Sci 69(14): 2443-2454.

Ebstein, F., A. Voigt, N. Lange, A. Warnatsch, F. Schroter, T. Prozorovski, U. Kuckelkorn, O. Aktas, U. Seifert, P. M. Kloetzel and E. Kruger (2013). "Immunoproteasomes are important for proteostasis in immune responses." Cell 152(5): 935-937.

Fan, W., W. Cai, S. Parimoo, D. C. Schwarz, G. G. Lennon and S. M. Weissman (1996). "Identification of seven new human MHC class I region genes around the HLA-F locus." Immunogenetics 44(2): 97-103.

Fang, S. and A. M. Weissman (2004). "A field guide to ubiquitylation." Cell Mol Life Sci 61(13): 1546-1561.

Filimonenko, M., P. Isakson, K. D. Finley, M. Anderson, H. Jeong, T. J. Melia, B. J. Bartlett, K. M. Myers, H. C. Birkeland, T. Lamark, D. Krainc, A. Brech, H. Stenmark, A. Simonsen and A. Yamamoto (2010). "The selective macroautophagic degradation of aggregated proteins requires the PI3P-binding protein Alfy." Mol Cell 38(2): 265-279.

Finkbeiner, S. (2011). "Huntington's Disease." Cold Spring Harb Perspect Biol 3(6).

Finley, D. (2009). "Recognition and processing of ubiquitin-protein conjugates by the proteasome." Annu Rev Biochem 78: 477-513.

Fleming, A., T. Noda, T. Yoshimori and D. C. Rubinsztein (2011). "Chemical modulators of autophagy as biological probes and potential therapeutics." Nat Chem Biol 7(1): 9-17.

French, B. A., J. Oliva, F. Bardag-Gorce and S. W. French (2011). "The immunoproteasome in steatohepatitis: its role in Mallory-Denk body formation." Exp Mol Pathol 90(3): 252-256.

Gallastegui, N. and M. Groll (2010). "The 26S proteasome: assembly and function of a destructive machine." Trends Biochem Sci 35(11): 634-642.

Gamerdinger, M., P. Hajieva, A. M. Kaya, U. Wolfrum, F. U. Hartl and C. Behl (2009). "Protein quality control during aging involves recruitment of the macroautophagy pathway by BAG3." EMBO J 28(7): 889-901.

Gavin, J. M., J. J. Chen, H. Liao, N. Rollins, X. Yang, Q. Xu, J. Ma, H. K. Loke, T. Lingaraj, J. E. Brownell, W. D. Mallender, A. E. Gould, B. S. Amidon and L. R. Dick (2012). "Mechanistic studies on activation of ubiquitin and di-ubiquitin-like protein, FAT10, by ubiquitin-like modifier activating enzyme 6, Uba6." J Biol Chem 287(19): 15512-15522.

Gebauer, F. and M. W. Hentze (2004). "Molecular mechanisms of translational control." Nat Rev Mol Cell Biol 5(10): 827-835.

Geetha, T. and M. W. Wooten (2002). "Structure and functional properties of the ubiquitin binding protein p62." FEBS Lett 512(1-3): 19-24.

Geng, J. and D. J. Klionsky (2008). "The Atg8 and Atg12 ubiquitin-like conjugation systems in macroautophagy. 'Protein modifications: beyond the usual suspects' review series." EMBO Rep 9(9): 859-864.

Glickman, M. H. and A. Ciechanover (2002). "The ubiquitin-proteasome proteolytic pathway: destruction for the sake of construction." Physiol Rev 82(2): 373-428.

Gong, P., A. Canaan, B. Wang, J. Leventhal, A. Snyder, V. Nair, C. D. Cohen, M. Kretzler, V. D'Agati, S. Weissman and M. J. Ross (2010). "The ubiquitin-like protein FAT10 mediates NF-kappaB activation." J Am Soc Nephrol 21(2): 316-326.

Grabbe, C. and I. Dikic (2009). "Functional roles of ubiquitin-like domain (ULD) and ubiquitin-binding domain (UBD) containing proteins." Chem Rev 109(4): 1481-1494.

Groettrup, M., C. J. Kirk and M. Basler (2010). "Proteasomes in immune cells: more than peptide producers?" Nat Rev Immunol 10(1): 73-78.

Groettrup, M., C. Pelzer, G. Schmidtke and K. Hofmann (2008). "Activating the ubiquitin family: UBA6 challenges the field." Trends Biochem Sci 33(5): 230-237.

Groll, M., M. Bajorek, A. Kohler, L. Moroder, D. M. Rubin, R. Huber, M. H. Glickman and D. Finley (2000). "A gated channel into the proteasome core particle." Nat Struct Biol 7(11): 1062-1067.

Groll, M., M. Bochtler, H. Brandstetter, T. Clausen and R. Huber (2005). "Molecular machines for protein degradation." Chembiochem 6(2): 222-256.

Hard, R. L., J. Liu, J. Shen, P. Zhou and D. Pei (2010). "HDAC6 and Ubp-M BUZ domains recognize specific C-terminal sequences of proteins." Biochemistry 49(50): 10737-10746.

Hayashi, T. and D. Faustman (2000). "Essential role of human leukocyte antigen-encoded proteasome subunits in NF-kappaB activation and prevention of tumor necrosis factor-alpha-induced apoptosis." J Biol Chem 275(7): 5238-5247.

He, K. L. and A. T. Ting (2002). "A20 inhibits tumor necrosis factor (TNF) alpha-induced apoptosis by disrupting recruitment of TRADD and RIP to the TNF receptor 1 complex in Jurkat T cells." Mol Cell Biol 22(17): 6034-6045.

Herrmann, J., L. O. Lerman and A. Lerman (2007). "Ubiquitin and ubiquitin-like proteins in protein regulation." Circ Res 100(9): 1276-1291.

Hershko, A., A. Ciechanover, H. Heller, A. L. Haas and I. A. Rose (1980). "Proposed role of ATP in protein breakdown: conjugation of protein with multiple chains of the polypeptide of ATP-dependent proteolysis." Proc Natl Acad Sci U S A 77(4): 1783-1786.

Hipp, M. S., B. Kalveram, S. Raasi, M. Groettrup and G. Schmidtke (2005). "FAT10, a ubiquitin-independent signal for proteasomal degradation." Mol Cell Biol 25(9): 3483-3491.

Hipp, M. S., S. Raasi, M. Groettrup and G. Schmidtke (2004). "NEDD8 ultimate buster-1L interacts with the ubiquitin-like protein FAT10 and accelerates its degradation." J Biol Chem 279(16): 16503-16510.

Hochstrasser, M. (2006). "Lingering mysteries of ubiquitin-chain assembly." Cell 124(1): 27-34.

Hochstrasser, M. (2009). "Origin and function of ubiquitin-like proteins." Nature 458(7237): 422-429.

Hoppe, T. (2005). "Multiubiquitylation by E4 enzymes: 'one size' doesn't fit all." Trends Biochem Sci 30(4): 183-187.

Huang, D. T., D. W. Miller, R. Mathew, R. Cassell, J. M. Holton, M. F. Roussel and B. A. Schulman (2004). "A unique E1-E2 interaction required for optimal conjugation of the ubiquitin-like protein NEDD8." Nat Struct Mol Biol 11(10): 927-935.

Ichimura, Y. and M. Komatsu (2010). "Selective degradation of p62 by autophagy." Semin Immunopathol 32(4): 431-436.

Ichimura, Y., T. Kumanomidou, Y. S. Sou, T. Mizushima, J. Ezaki, T. Ueno, E. Kominami, T. Yamane, K. Tanaka and M. Komatsu (2008). "Structural basis for sorting mechanism of p62 in selective autophagy." J Biol Chem 283(33): 22847-22857.

Isakson, P., P. Holland and A. Simonsen (2013). "The role of ALFY in selective autophagy." Cell Death Differ 20(1): 12-20.

Israel, A. (2010). "The IKK complex, a central regulator of NF-kappaB activation." Cold Spring Harb Perspect Biol 2(3): a000158.

Itakura, E. and N. Mizushima (2010). "Characterization of autophagosome formation site by a hierarchical analysis of mammalian Atg proteins." Autophagy 6(6): 764-776.

Itakura, E. and N. Mizushima (2011). "p62 Targeting to the autophagosome formation site requires self-oligomerization but not LC3 binding." J Cell Biol 192(1): 17-27.

Jaffray, E., K. M. Wood and R. T. Hay (1995). "Domain organization of I kappa B alpha and sites of interaction with NF-kappa B p65." Mol Cell Biol 15(4): 2166-2172.

Jain, A., T. Lamark, E. Sjottem, K. B. Larsen, J. A. Awuh, A. Overvatn, M. McMahon, J. D. Hayes and T. Johansen (2010). "p62/SQSTM1 is a target gene for transcription factor NRF2 and creates a positive feedback loop by inducing antioxidant response element-driven gene transcription." J Biol Chem 285(29): 22576-22591.

Jentsch, S. and G. Pyrowolakis (2000). "Ubiquitin and its kin: how close are the family ties?" Trends Cell Biol 10(8): 335-342.

Ji, F., X. Jin, C. H. Jiao, Q. W. Xu, Z. W. Wang and Y. L. Chen (2009). "FAT10 level in human gastric cancer and its relation with mutant p53 level, lymph node metastasis and TNM staging." World J Gastroenterol 15(18): 2228-2233.

Jin, J., X. Li, S. P. Gygi and J. W. Harper (2007). "Dual E1 activation systems for ubiquitin differentially regulate E2 enzyme charging." Nature 447(7148): 1135-1138.

Jin, Z., Y. Li, R. Pitti, D. Lawrence, V. C. Pham, J. R. Lill and A. Ashkenazi (2009). "Cullin3-based polyubiquitination and p62-dependent aggregation of caspase-8 mediate extrinsic apoptosis signaling." Cell 137(4): 721-735.

Johansen, T. and T. Lamark (2011). "Selective autophagy mediated by autophagic adapter proteins." Autophagy 7(3): 279-296.

Joung, I., J. L. Strominger and J. Shin (1996). "Molecular cloning of a phosphotyrosine-independent ligand of the p56lck SH2 domain." Proc Natl Acad Sci U S A 93(12): 5991-5995.

Jung, T. and T. Grune (2012). "Structure of the proteasome." Prog Mol Biol Transl Sci 109: 1-39.

Kalmar, B. and L. Greensmith (2009). "Induction of heat shock proteins for protection against oxidative stress." Adv Drug Deliv Rev 61(4): 310-318.

Kalveram, B., G. Schmidtke and M. Groettrup (2008). "The ubiquitin-like modifier FAT10 interacts with HDAC6 and localizes to aggresomes under proteasome inhibition." J Cell Sci 121(Pt 24): 4079-4088.

Kamitani, T., K. Kito, T. Fukuda-Kamitani and E. T. Yeh (2001). "Targeting of NEDD8 and its conjugates for proteasomal degradation by NUB1." J Biol Chem 276(49): 46655-46660.

Kaneko, T., J. Hamazaki, S. Iemura, K. Sasaki, K. Furuyama, T. Natsume, K. Tanaka and S. Murata (2009). "Assembly pathway of the Mammalian proteasome base subcomplex is mediated by multiple specific chaperones." Cell 137(5): 914-925.

Kaspar, J. W., S. K. Niture and A. K. Jaiswal (2009). "Nrf2:INrf2 (Keap1) signaling in oxidative stress." Free Radic Biol Med 47(9): 1304-1309.

Kawai, K., A. Saito, T. Sudo and H. Osada (2008). "Specific regulation of cytokine-dependent p38 MAP kinase activation by p62/SQSTM1." J Biochem 143(6): 765-772.

Kerscher, O., R. Felberbaum and M. Hochstrasser (2006). "Modification of proteins by ubiquitin and ubiquitin-like proteins." Annu Rev Cell Dev Biol 22: 159-180.

Kettern, N., M. Dreiseidler, R. Tawo and J. Hohfeld (2010). "Chaperone-assisted degradation: multiple paths to destruction." Biol Chem 391(5): 481-489.

Kimura, Y. and K. Tanaka (2010). "Regulatory mechanisms involved in the control of ubiquitin homeostasis." J Biochem 147(6): 793-798.

Kincaid, E. Z., J. W. Che, I. York, H. Escobar, E. Reyes-Vargas, J. C. Delgado, R. M. Welsh, M. L. Karow, A. J. Murphy, D. M. Valenzuela, G. D. Yancopoulos and K. L. Rock (2012). "Mice completely lacking immunoproteasomes show major changes in antigen presentation." Nat Immunol 13(2): 129-135.

Kirkin, V., T. Lamark, Y. S. Sou, G. Bjorkoy, J. L. Nunn, J. A. Bruun, E. Shvets, D. G. McEwan, T. H. Clausen, P. Wild, I. Bilusic, J. P. Theurillat, A. Overvatn, T. Ishii, Z. Elazar, M. Komatsu, I. Dikic and T. Johansen (2009). "A role for NBR1 in autophagosomal degradation of ubiquitinated substrates." Mol Cell 33(4): 505-516.

Kisselev, A. F., M. Garcia-Calvo, H. S. Overkleeft, E. Peterson, M. W. Pennington, H. L. Ploegh, N. A. Thornberry and A. L. Goldberg (2003). "The caspase-like sites of proteasomes, their substrate specificity, new inhibitors and substrates, and allosteric interactions with the trypsin-like sites." J Biol Chem 278(38): 35869-35877.

Kito, K., E. T. Yeh and T. Kamitani (2001). "NUB1, a NEDD8-interacting protein, is induced by interferon and down-regulates the NEDD8 expression." J Biol Chem 276(23): 20603-20609.

Klionsky, D. J. (2005). "The molecular machinery of autophagy: unanswered questions." J Cell Sci 118(Pt 1): 7-18.

Kloetzel, P. M. (2004). "The proteasome and MHC class I antigen processing." Biochim Biophys Acta 1695(1-3): 225-233.

Knaevelsrud, H. and A. Simonsen (2010). "Fighting disease by selective autophagy of aggregate-prone proteins." FEBS Lett 584(12): 2635-2645.

Komander, D., M. J. Clague and S. Urbe (2009). "Breaking the chains: structure and function of the deubiquitinases." Nat Rev Mol Cell Biol 10(8): 550-563.

Komatsu, M. and Y. Ichimura (2010). "Physiological significance of selective degradation of p62 by autophagy." FEBS Lett 584(7): 1374-1378.

Komatsu, M. and Y. Ichimura (2010). "Selective autophagy regulates various cellular functions." Genes Cells 15(9): 923-933.

Komatsu, M., S. Kageyama and Y. Ichimura (2012). "p62/SQSTM1/A170: physiology and pathology." Pharmacol Res 66(6): 457-462.

Komatsu, M., H. Kurokawa, S. Waguri, K. Taguchi, A. Kobayashi, Y. Ichimura, Y. S. Sou, I. Ueno, A. Sakamoto, K. I. Tong, M. Kim, Y. Nishito, S. Iemura, T. Natsume, T. Ueno, E. Kominami, H. Motohashi, K. Tanaka and M. Yamamoto (2010). "The selective autophagy substrate p62 activates the stress responsive transcription factor Nrf2 through inactivation of Keap1." Nat Cell Biol 12(3): 213-223.

Kraft, C., M. Peter and K. Hofmann (2010). "Selective autophagy: ubiquitin-mediated recognition and beyond." Nat Cell Biol 12(9): 836-841.

Kravtsova-Ivantsiv, Y. and A. Ciechanover (2012). "Non-canonical ubiquitin-based signals for proteasomal degradation." J Cell Sci 125(Pt 3): 539-548.

Kulathu, Y. and D. Komander (2012). "Atypical ubiquitylation - the unexplored world of polyubiquitin beyond Lys48 and Lys63 linkages." Nat Rev Mol Cell Biol 13(8): 508-523.

Kuusisto, E., A. Salminen and I. Alafuzoff (2001). "Ubiquitin-binding protein p62 is present in neuronal and glial inclusions in human tauopathies and synucleinopathies." Neuroreport 12(10): 2085-2090.

Lamark, T. and T. Johansen (2012). "Aggrephagy: selective disposal of protein aggregates by macroautophagy." Int J Cell Biol 2012: 736905.

Lamark, T., V. Kirkin, I. Dikic and T. Johansen (2009). "NBR1 and p62 as cargo receptors for selective autophagy of ubiquitinated targets." Cell Cycle 8(13): 1986-1990.

Lamark, T., M. Perander, H. Outzen, K. Kristiansen, A. Overvatn, E. Michaelsen, G. Bjorkoy and T. Johansen (2003). "Interaction codes within the family of mammalian Phox and Bem1p domain-containing proteins." J Biol Chem 278(36): 34568-34581.

Lander, G. C., E. Estrin, M. E. Matyskiela, C. Bashore, E. Nogales and A. Martin (2012). "Complete subunit architecture of the proteasome regulatory particle." Nature 482(7384): 186-191.

Lanneau, D., G. Wettstein, P. Bonniaud and C. Garrido (2010). "Heat shock proteins: cell protection through protein triage." ScientificWorldJournal 10: 1543-1552.

Lasker, K., F. Forster, S. Bohn, T. Walzthoeni, E. Villa, P. Unverdorben, F. Beck, R. Aebersold, A. Sali and W. Baumeister (2012). "Molecular architecture of the 26S proteasome holocomplex determined by an integrative approach." Proc Natl Acad Sci U S A 109(5): 1380-1387.

Lecker, S. H., A. L. Goldberg and W. E. Mitch (2006). "Protein degradation by the ubiquitin-proteasome pathway in normal and disease states." J Am Soc Nephrol 17(7): 1807-1819.

Lee, C. G., J. Ren, I. S. Cheong, K. H. Ban, L. L. Ooi, S. Yong Tan, A. Kan, I. Nuchprayoon, R. Jin, K. H. Lee, M. Choti and L. A. Lee (2003). "Expression of the FAT10 gene is highly upregulated in hepatocellular carcinoma and other gastrointestinal and gynecological cancers." Oncogene 22(17): 2592-2603.

Lelouard, H., E. Gatti, F. Cappello, O. Gresser, V. Camosseto and P. Pierre (2002). "Transient aggregation of ubiquitinated proteins during dendritic cell maturation." Nature 417(6885): 177-182.

Li, B., C. Tournier, R. J. Davis and R. A. Flavell (1999). "Regulation of IL-4 expression by the transcription factor JunB during T helper cell differentiation." EMBO J 18(2): 420-432.

Li, T., R. Santockyte, S. Yu, R. F. Shen, E. Tekle, C. G. Lee, D. C. Yang and P. B. Chock (2011). "FAT10 modifies p53 and upregulates its transcriptional activity." Arch Biochem Biophys 509(2): 164-169.

Li, Y., D. Shin and S. H. Kwon (2013). "Histone deacetylase 6 plays a role as a distinct regulator of diverse cellular processes." FEBS J 280(3): 775-793.

Lim, C. B., D. Zhang and C. G. Lee (2006). "FAT10, a gene up-regulated in various cancers, is cell-cycle regulated." Cell Div 1: 20.

Linares, J. F., A. Duran, T. Yajima, M. Pasparakis, J. Moscat and M. T. Diaz-Meco (2013). "K63 polyubiquitination and activation of mTOR by the p62-TRAF6 complex in nutrient-activated cells." Mol Cell 51(3): 283-296.

Liu, F., Y. Xia, A. S. Parker and I. M. Verma (2012). "IKK biology." Immunol Rev 246(1): 239-253.

Liu, L., Z. Dong, J. Liang, C. Cao, J. Sun, Y. Ding and D. Wu (2013). "As an independent prognostic factor, FAT10 promotes hepatitis B virus-related hepatocellular carcinoma progression via Akt/GSK3beta pathway." Oncogene.

Liu, Y. C., J. Pan, C. Zhang, W. Fan, M. Collinge, J. R. Bender and S. M. Weissman (1999). "A MHC-encoded ubiquitin-like protein (FAT10) binds noncovalently to the spindle assembly checkpoint protein MAD2." Proc Natl Acad Sci U S A 96(8): 4313-4318.

Long, J., T. P. Garner, M. J. Pandya, C. J. Craven, P. Chen, B. Shaw, M. P. Williamson, R. Layfield and M. S. Searle (2010). "Dimerisation of the UBA domain of p62 inhibits ubiquitin binding and regulates NF-kappaB signalling." J Mol Biol 396(1): 178-194.

Longatti, A. and S. A. Tooze (2009). "Vesicular trafficking and autophagosome formation." Cell Death Differ 16(7): 956-965.

Lu, B., I. Al-Ramahi, A. Valencia, Q. Wang, F. Berenshteyn, H. Yang, T. Gallego-Flores, S. Ichcho, A. Lacoste, M. Hild, M. Difiglia, J. Botas and J. Palacino (2013). "Identification of NUB1 as a suppressor of mutant Huntington toxicity via enhanced protein clearance." Nat Neurosci 16(5): 562-570.

Lukasiak, S., C. Schiller, P. Oehlschlaeger, G. Schmidtke, P. Krause, D. F. Legler, F. Autschbach, P. Schirmacher, K. Breuhahn and M. Groettrup (2008). "Proinflammatory cytokines cause FAT10 upregulation in cancers of liver and colon." Oncogene 27(46): 6068-6074.

Macagno, A., M. Gilliet, F. Sallusto, A. Lanzavecchia, F. O. Nestle and M. Groettrup (1999). "Dendritic cells up-regulate immunoproteasomes and the proteasome regulator PA28 during maturation." Eur J Immunol 29(12): 4037-4042.

Martin, P., M. T. Diaz-Meco and J. Moscat (2006). "The signaling adapter p62 is an important mediator of T helper 2 cell function and allergic airway inflammation." EMBO J 25(15): 3524-3533.

Matsumoto, G., K. Wada, M. Okuno, M. Kurosawa and N. Nukina (2011). "Serine 403 phosphorylation of p62/SQSTM1 regulates selective autophagic clearance of ubiquitinated proteins." Mol Cell 44(2): 279-289.

Matyskiela, M. E. and A. Martin (2013). "Design principles of a universal protein degradation machine." J Mol Biol 425(2): 199-213.

Mayer, M. P. and B. Bukau (2005). "Hsp70 chaperones: cellular functions and molecular mechanism." Cell Mol Life Sci 62(6): 670-684.

Mehrpour, M., A. Esclatine, I. Beau and P. Codogno (2010). "Autophagy in health and disease. 1. Regulation and significance of autophagy: an overview." Am J Physiol Cell Physiol 298(4): C776-785.

Mehrpour, M., A. Esclatine, I. Beau and P. Codogno (2010). "Overview of macroautophagy regulation in mammalian cells." Cell Res 20(7): 748-762.

Merbl, Y., P. Refour, H. Patel, M. Springer and M. W. Kirschner (2013). "Profiling of ubiquitin-like modifications reveals features of mitotic control." Cell 152(5): 1160-1172.

Metzger, M. B., V. A. Hristova and A. M. Weissman (2012). "HECT and RING finger families of E3 ubiquitin ligases at a glance." J Cell Sci 125(Pt 3): 531-537.

Mizushima, N. (2007). "Autophagy: process and function." Genes Dev 21(22): 2861-2873.

Molejon, M. I., A. Ropolo, A. L. Re, V. Boggio and M. I. Vaccaro (2013). "The VMP1-Beclin 1 interaction regulates autophagy induction." Sci Rep 3: 1055.

Morel, S., F. Levy, O. Burlet-Schiltz, F. Brasseur, M. Probst-Kepper, A. L. Peitrequin, B. Monsarrat, R. Van Velthoven, J. C. Cerottini, T. Boon, J. E. Gairin and B. J. Van den Eynde

(2000). "Processing of some antigens by the standard proteasome but not by the immunoproteasome results in poor presentation by dendritic cells." Immunity 12(1): 107-117.

Moscat, J. and M. T. Diaz-Meco (2000). "The atypical protein kinase Cs. Functional specificity mediated by specific protein adapters." EMBO Rep 1(5): 399-403.

Moscat, J. and M. T. Diaz-Meco (2011). "Feedback on fat: p62-mTORC1-autophagy connections." Cell 147(4): 724-727.

Moscat, J., P. Rennert and M. T. Diaz-Meco (2006). "PKCzeta at the crossroad of NF-kappaB and Jak1/Stat6 signaling pathways." Cell Death Differ 13(5): 702-711.

Motohashi, H. and M. Yamamoto (2004). "Nrf2-Keap1 defines a physiologically important stress response mechanism." Trends Mol Med 10(11): 549-557.

Muller, S., C. Hoege, G. Pyrowolakis and S. Jentsch (2001). "SUMO, ubiquitin's mysterious cousin." Nat Rev Mol Cell Biol 2(3): 202-210.

Murata, S., K. Sasaki, T. Kishimoto, S. Niwa, H. Hayashi, Y. Takahama and K. Tanaka (2007). "Regulation of CD8+ T cell development by thymus-specific proteasomes." Science 316(5829): 1349-1353.

Murata, S., H. Yashiroda and K. Tanaka (2009). "Molecular mechanisms of proteasome assembly." Nat Rev Mol Cell Biol 10(2): 104-115.

Nagaoka, U., K. Kim, N. R. Jana, H. Doi, M. Maruyama, K. Mitsui, F. Oyama and N. Nukina (2004). "Increased expression of p62 in expanded polyglutamine-expressing cells and its association with polyglutamine inclusions." J Neurochem 91(1): 57-68.

Nagashima, Y., H. Kowa, S. Tsuji and A. Iwata (2011). "FAT10 protein binds to polyglutamine proteins and modulates their solubility." J Biol Chem 286(34): 29594-29600.

Nakayasu, E. S., C. Ansong, J. N. Brown, F. Yang, D. Lopez-Ferrer, W. J. Qian, R. D. Smith and J. N. Adkins (2013). "Evaluation of Selected Binding Domains for the Analysis of Ubiquitinated Proteomes." J Am Soc Mass Spectrom.

Napetschnig, J. and H. Wu (2013). "Molecular basis of NF-kappaB signaling." Annu Rev Biophys 42: 443-468.

Nasir, J., S. B. Floresco, J. R. O'Kusky, V. M. Diewert, J. M. Richman, J. Zeisler, A. Borowski, J. D. Marth, A. G. Phillips and M. R. Hayden (1995). "Targeted disruption of the Huntington's disease gene results in embryonic lethality and behavioral and morphological changes in heterozygotes." Cell 81(5): 811-823.

Nathan, J. A., V. Spinnenhirn, G. Schmidtke, M. Basler, M. Groettrup and A. L. Goldberg (2013). "Immuno- and constitutive proteasomes do not differ in their abilities to degrade ubiquitinated proteins." Cell 152(5): 1184-1194.

Niture, S. K., J. W. Kaspar, J. Shen and A. K. Jaiswal (2010). "Nrf2 signaling and cell survival." Toxicol Appl Pharmacol 244(1): 37-42.

Oh, J. E. and H. K. Lee (2012). "Autophagy in innate recognition of pathogens and adaptive immunity." Yonsei Med J 53(2): 241-247.

Pankiv, S., T. H. Clausen, T. Lamark, A. Brech, J. A. Bruun, H. Outzen, A. Overvatn, G. Bjorkoy and T. Johansen (2007). "p62/SQSTM1 binds directly to Atg8/LC3 to facilitate degradation of ubiquitinated protein aggregates by autophagy." J Biol Chem 282(33): 24131-24145.

Pankiv, S., T. Lamark, J. A. Bruun, A. Overvatn, G. Bjorkoy and T. Johansen (2010). "Nucleocytoplasmic shuttling of p62/SQSTM1 and its role in recruitment of nuclear polyubiquitinated proteins to promyelocytic leukemia bodies." J Biol Chem 285(8): 5941-5953.

Pelzer, C., I. Kassner, K. Matentzoglu, R. K. Singh, H. P. Wollscheid, M. Scheffner, G. Schmidtke and M. Groettrup (2007). "UBE1L2, a novel E1 enzyme specific for ubiquitin." J Biol Chem 282(32): 23010-23014.

Peng, X., J. Shao, Y. Shen, Y. Zhou, Q. Cao, J. Hu, W. He, X. Yu, X. Liu, A. J. Marian and K. Hong (2013). "FAT10 protects cardiac myocytes against apoptosis." J Mol Cell Cardiol 59: 1-10.

Pickart, C. M. (2001). "Ubiquitin enters the new millennium." Mol Cell 8(3): 499-504.

Pilli, M., J. Arko-Mensah, M. Ponpuak, E. Roberts, S. Master, M. A. Mandell, N. Dupont, W. Ornatowski, S. Jiang, S. B. Bradfute, J. A. Bruun, T. E. Hansen, T. Johansen and V. Deretic (2012). "TBK-1 promotes autophagy-mediated antimicrobial defense by controlling autophagosome maturation." Immunity 37(2): 223-234.

Polson, H. E., J. de Lartigue, D. J. Rigden, M. Reedijk, S. Urbe, M. J. Clague and S. A. Tooze (2010). "Mammalian Atg18 (WIPI2) localizes to omegasome-anchored phagophores and positively regulates LC3 lipidation." Autophagy 6(4): 506-522.

Qing, X., B. A. French, J. Oliva and S. W. French (2011). "Increased expression of FAT10 in colon benign, premalignant and malignant epithelial neoplasms." Exp Mol Pathol 90(1): 51-54.

Raasi, S., G. Schmidtke, R. de Giuli and M. Groettrup (1999). "A ubiquitin-like protein which is synergistically inducible by interferon-gamma and tumor necrosis factor-alpha." Eur J Immunol 29(12): 4030-4036.

Raasi, S., G. Schmidtke and M. Groettrup (2001). "The ubiquitin-like protein FAT10 forms covalent conjugates and induces apoptosis." J Biol Chem 276(38): 35334-35343.

Rani, N., A. Aichem, G. Schmidtke, S. G. Kreft and M. Groettrup (2012). "FAT10 and NUB1L bind to the VWA domain of Rpn10 and Rpn1 to enable proteasome-mediated proteolysis." Nat Commun 3: 749.

Ren, J., A. Kan, S. H. Leong, L. L. Ooi, K. T. Jeang, S. S. Chong, O. L. Kon and C. G. Lee (2006). "FAT10 plays a role in the regulation of chromosomal stability." J Biol Chem 281(16): 11413-11421.

Ren, J., Y. Wang, Y. Gao, S. B. Mehta and C. G. Lee (2011). "FAT10 mediates the effect of TNF-alpha in inducing chromosomal instability." J Cell Sci 124(Pt 21): 3665-3675.

Ross, M. J., M. S. Wosnitzer, M. D. Ross, B. Granelli, G. L. Gusella, M. Husain, L. Kaufman, M. Vasievich, V. D. D'Agati, P. D. Wilson, M. E. Klotman and P. E. Klotman (2006). "Role of ubiquitin-like protein FAT10 in epithelial apoptosis in renal disease." J Am Soc Nephrol 17(4): 996-1004.

Rubinsztein, D. C., T. Shpilka and Z. Elazar (2012). "Mechanisms of autophagosome biogenesis." Curr Biol 22(1): R29-34.

Sanz, L., M. T. Diaz-Meco, H. Nakano and J. Moscat (2000). "The atypical PKC-interacting protein p62 channels NF-kappaB activation by the IL-1-TRAF6 pathway." EMBO J 19(7): 1576-1586.

Sanz, L., P. Sanchez, M. J. Lallena, M. T. Diaz-Meco and J. Moscat (1999). "The interaction of p62 with RIP links the atypical PKCs to NF-kappaB activation." EMBO J 18(11): 3044-3053.

Sarikas, A., T. Hartmann and Z. Q. Pan (2011). "The cullin protein family." Genome Biol 12(4): 220.

Schagger, H. and G. von Jagow (1987). "Tricine-sodium dodecyl sulfate-polyacrylamide gel electrophoresis for the separation of proteins in the range from 1 to 100 kDa." Anal Biochem 166(2): 368-379.

Schliehe, C., A. Bitzer, M. van den Broek and M. Groettrup (2012). "Stable antigen is most effective for eliciting CD8+ T-cell responses after DNA vaccination and infection with recombinant vaccinia virus in vivo." J Virol 86(18): 9782-9793.

Schmidtke, G., A. Aichem and M. Groettrup (2013). "FAT10ylation as a signal for proteasomal degradation." Biochim Biophys Acta.

Schmidtke, G., B. Kalveram and M. Groettrup (2009). "Degradation of FAT10 by the 26S proteasome is independent of ubiquitylation but relies on NUB1L." FEBS Lett 583(3): 591-594.

Schmidtke, G., B. Kalveram, E. Weber, P. Bochtler, S. Lukasiak, M. S. Hipp and M. Groettrup (2006). "The UBA domains of NUB1L are required for binding but not for accelerated degradation of the ubiquitin-like modifier FAT10." J Biol Chem 281(29): 20045-20054.

Schrader, E. K., K. G. Harstad and A. Matouschek (2009). "Targeting proteins for degradation." Nat Chem Biol 5(11): 815-822.

Schulman, B. A. (2011). "Twists and turns in ubiquitin-like protein conjugation cascades." Protein Sci 20(12): 1941-1954.

Schulman, B. A. and J. W. Harper (2009). "Ubiquitin-like protein activation by E1 enzymes: the apex for downstream signalling pathways." Nat Rev Mol Cell Biol 10(5): 319-331.

Seibenhener, M. L., J. R. Babu, T. Geetha, H. C. Wong, N. R. Krishna and M. W. Wooten (2004). "Sequestosome 1/p62 is a polyubiquitin chain binding protein involved in ubiquitin proteasome degradation." Mol Cell Biol 24(18): 8055-8068.

Seifert, U., L. P. Bialy, F. Ebstein, D. Bech-Otschir, A. Voigt, F. Schroter, T. Prozorovski, N. Lange, J. Steffen, M. Rieger, U. Kuckelkorn, O. Aktas, P. M. Kloetzel and E. Kruger (2010). "Immunoproteasomes preserve protein homeostasis upon interferon-induced oxidative stress." Cell 142(4): 613-624.

Shabek, N. and A. Ciechanover (2010). "Degradation of ubiquitin: the fate of the cellular reaper." Cell Cycle 9(3): 523-530.

Shaid, S., C. H. Brandts, H. Serve and I. Dikic (2013). "Ubiquitination and selective autophagy." Cell Death Differ 20(1): 21-30.

Shambharkar, P. B., M. Blonska, B. P. Pappu, H. Li, Y. You, H. Sakurai, B. G. Darnay, H. Hara, J. Penninger and X. Lin (2007). "Phosphorylation and ubiquitination of the IkappaB kinase complex by two distinct signaling pathways." EMBO J 26(7): 1794-1805.

Sijts, E. J. and P. M. Kloetzel (2011). "The role of the proteasome in the generation of MHC class I ligands and immune responses." Cell Mol Life Sci 68(9): 1491-1502.

Simonsen, A., H. C. Birkeland, D. J. Gillooly, N. Mizushima, A. Kuma, T. Yoshimori, T. Slagsvold, A. Brech and H. Stenmark (2004). "Alfy, a novel FYVE-domain-containing protein associated with protein granules and autophagic membranes." J Cell Sci 117(Pt 18): 4239-4251.

Smalle, J. and R. D. Vierstra (2004). "The ubiquitin 26S proteasome proteolytic pathway." Annu Rev Plant Biol 55: 555-590.

Snyder, A., Z. Alsauskas, P. Gong, P. E. Rosenstiel, M. E. Klotman, P. E. Klotman and M. J. Ross (2009). "FAT10: a novel mediator of Vpr-induced apoptosis in human immunodeficiency virus-associated nephropathy." J Virol 83(22): 11983-11988.

Spasser, L. and A. Brik (2012). "Chemistry and biology of the ubiquitin signal." Angew Chem Int Ed Engl 51(28): 6840-6862.

Sriram, S. M., R. Banerjee, R. S. Kane and Y. T. Kwon (2009). "Multivalency-assisted control of intracellular signaling pathways: application for ubiquitin- dependent N-end rule pathway." Chem Biol 16(2): 121-131.

Steffan, J. S., N. Agrawal, J. Pallos, E. Rockabrand, L. C. Trotman, N. Slepko, K. Illes, T. Lukacsovich, Y. Z. Zhu, E. Cattaneo, P. P. Pandolfi, L. M. Thompson and J. L. Marsh (2004). "SUMO modification of Huntingtin and Huntington's disease pathology." Science 304(5667): 100-104.

Stumptner, C., H. Heid, A. Fuchsbichler, H. Hauser, H. J. Mischinger, K. Zatloukal and H. Denk (1999). "Analysis of intracytoplasmic hyaline bodies in a hepatocellular carcinoma. Demonstration of p62 as major constituent." Am J Pathol 154(6): 1701-1710.

Szeto, J., N. A. Kaniuk, V. Canadien, R. Nisman, N. Mizushima, T. Yoshimori, D. P. Bazett-Jones and J. H. Brumell (2006). "ALIS are stress-induced protein storage compartments for substrates of the proteasome and autophagy." Autophagy 2(3): 189-199.

Takeda, K. and S. Akira (2005). "Toll-like receptors in innate immunity." Int Immunol 17(1): 1-14.

Tanaka, K. (2013). "The proteasome: from basic mechanisms to emerging roles." Keio J Med 62(1): 1-12.

Tanaka, T., H. Kawashima, E. T. Yeh and T. Kamitani (2003). "Regulation of the NEDD8 conjugation system by a splicing variant, NUB1L." J Biol Chem 278(35): 32905-32913.

Tanida, I. (2011). "Autophagy basics." Microbiol Immunol 55(1): 1-11.

Tasaki, T., S. M. Sriram, K. S. Park and Y. T. Kwon (2012). "The N-end rule pathway." Annu Rev Biochem 81: 261-289.

Thurston, T. L., G. Ryzhakov, S. Bloor, N. von Muhlinen and F. Randow (2009). "The TBK1 adaptor and autophagy receptor NDP52 restricts the proliferation of ubiquitin-coated bacteria." Nat Immunol 10(11): 1215-1221.

Thurston, T. L., M. P. Wandel, N. von Muhlinen, A. Foeglein and F. Randow (2012). "Galectin 8 targets damaged vesicles for autophagy to defend cells against bacterial invasion." Nature 482(7385): 414-418.

Tomaru, U., A. Ishizu, S. Murata, Y. Miyatake, S. Suzuki, S. Takahashi, T. Kazamaki, J. Ohara, T. Baba, S. Iwasaki, K. Fugo, N. Otsuka, K. Tanaka and M. Kasahara (2009). "Exclusive expression of proteasome subunit {beta}5t in the human thymic cortex." Blood 113(21): 5186-5191.

Trempe, J. F. (2011). "Reading the ubiquitin postal code." Curr Opin Struct Biol 21(6): 792-801.

Vadlamudi, R. K., I. Joung, J. L. Strominger and J. Shin (1996). "p62, a phosphotyrosine-independent ligand of the SH2 domain of p56lck, belongs to a new class of ubiquitin-binding proteins." J Biol Chem 271(34): 20235-20237.

Varshavsky, A. (1997). "The N-end rule pathway of protein degradation." Genes Cells 2(1): 13-28.

Varshavsky, A. (2012). "The ubiquitin system, an immense realm." Annu Rev Biochem 81: 167-176.

Voges, D., P. Zwickl and W. Baumeister (1999). "The 26S proteasome: a molecular machine designed for controlled proteolysis." Annu Rev Biochem 68: 1015-1068.

Volz, T., S. Kaesler and T. Biedermann (2012). "Innate immune sensing 2.0 - from linear activation pathways to fine tuned and regulated innate immune networks." Exp Dermatol 21(1): 61-69.

von Muhlinen, N., M. Akutsu, B. J. Ravenhill, A. Foeglein, S. Bloor, T. J. Rutherford, S. M. Freund, D. Komander and F. Randow (2012). "LC3C, bound selectively by a noncanonical LIR motif in NDP52, is required for antibacterial autophagy." Mol Cell 48(3): 329-342.

Wild, P., H. Farhan, D. G. McEwan, S. Wagner, V. V. Rogov, N. R. Brady, B. Richter, J. Korac, O. Waidmann, C. Choudhary, V. Dotsch, D. Bumann and I. Dikic (2011). "Phosphorylation of the autophagy receptor optineurin restricts Salmonella growth." Science 333(6039): 228-233.

Wilkinson, K. D. (2009). "DUBs at a glance." J Cell Sci 122(Pt 14): 2325-2329.

Willis, M. S., W. H. Townley-Tilson, E. Y. Kang, J. W. Homeister and C. Patterson (2010). "Sent to destroy: the ubiquitin proteasome system regulates cell signaling and protein quality control in cardiovascular development and disease." Circ Res 106(3): 463-478.

Wooten, M. W., T. Geetha, M. L. Seibenhener, J. R. Babu, M. T. Diaz-Meco and J. Moscat (2005). "The p62 scaffold regulates nerve growth factor-induced NF-kappaB activation by influencing TRAF6 polyubiquitination." J Biol Chem 280(42): 35625-35629.

Wyatt, A. R., J. J. Yerbury, R. A. Dabbs and M. R. Wilson (2012). "Roles of extracellular chaperones in amyloidosis." J Mol Biol 421(4-5): 499-516.

Xie, Y. (2010). "Structure, assembly and homeostatic regulation of the 26S proteasome." J Mol Cell Biol 2(6): 308-317.

Xu, P., D. M. Duong, N. T. Seyfried, D. Cheng, Y. Xie, J. Robert, J. Rush, M. Hochstrasser, D. Finley and J. Peng (2009). "Quantitative proteomics reveals the function of unconventional ubiquitin chains in proteasomal degradation." Cell 137(1): 133-145.

Yamamoto, A. and A. Simonsen (2011). "Alfy-dependent elimination of aggregated proteins by macroautophagy: can there be too much of a good thing?" Autophagy 7(3): 346-350.

Yang, J. Q., H. Liu, M. T. Diaz-Meco and J. Moscat (2010). "NBR1 is a new PB1 signalling adapter in Th2 differentiation and allergic airway inflammation in vivo." EMBO J 29(19): 3421-3433.

Yang, Y. P., Z. Q. Liang, Z. L. Gu and Z. H. Qin (2005). "Molecular mechanism and regulation of autophagy." Acta Pharmacol Sin 26(12): 1421-1434.

Ye, Y. and M. Rape (2009). "Building ubiquitin chains: E2 enzymes at work." Nat Rev Mol Cell Biol 10(11): 755-764.

Yin, Q., S. C. Lin, B. Lamothe, M. Lu, Y. C. Lo, G. Hura, L. Zheng, R. L. Rich, A. D. Campos, D. G. Myszka, M. J. Lenardo, B. G. Darnay and H. Wu (2009). "E2 interaction and dimerization in the crystal structure of TRAF6." Nat Struct Mol Biol 16(6): 658-666.

Ying, H. and B. Y. Yue (2012). "Cellular and molecular biology of optineurin." Int Rev Cell Mol Biol 294: 223-258.

Yu, X., X. Liu, T. Liu, K. Hong, J. Lei, R. Yuan and J. Shao (2012). "Identification of a novel binding protein of FAT10: eukaryotic translation elongation factor 1A1." Dig Dis Sci 57(9): 2347-2354.

Yuan, J., Y. Tu, X. Mao, S. He, L. Wang, G. Fu, J. Zong and Y. Zhang (2012). "Increased expression of FAT10 is correlated with progression and prognosis of human glioma." Pathol Oncol Res 18(4): 833-839.

Zatloukal, K., C. Stumptner, A. Fuchsbichler, H. Heid, M. Schnoelzer, L. Kenner, R. Kleinert, M. Prinz, A. Aguzzi and H. Denk (2002). "p62 Is a common component of cytoplasmic inclusions in protein aggregation diseases." Am J Pathol 160(1): 255-263.

Zeng, X. and T. J. Kinsella (2011). "Impact of Autophagy on Chemotherapy and Radiotherapy Mediated Tumor Cytotoxicity: "To Live or not to Live"." Front Oncol 1: 30.

8 Abbreviations

aa	amino acid
ABIN	A20-Binding Inhibitors of NF-κB
AID	acidic interaction domain
AIPL1	aryl hydrocarbon receptor-interacting protein-like 1
ALFY	autophagy-linked FYVE
ALIS	aggresome-like induced structures
aPKCs	atypical protein kinase C
ARE	antioxidant response element
ATG	autophagy related genes
ATP	adenosine triphosphate
BAG	bcl-2 associated athanogene
BSA	bovine serum albumin
BUZ	ubiquitin-binding zinc-finger
CALCOCO2	calcium-binding and coiled-coil domain-containing protein 2
CAP	chaperone-assisted proteasomal degradation
CASA	chaperone-assisted selective autophagy
cDNA	complementary DNA
CD8	cluster of differentiation 8
CK2	casein kinase II
CLIR	LIR consensus motif
CMA	chaperone mediated autophagy
COOH	carboxyl
CPI	C-terminal p38 interaction
CRL	cullin-RING E3 ubiquitin ligase
cTECs	cortical thymic epithelial cells
C-terminal	carboxy-terminal
CUL3	cullin3

DALISs	dendritic cell aggresome-like induced structures
DCs	dendritic cells
DFCP1	double FYVE-containing protein 1
CHIP	carboxyl terminus of constitutive HSC70-interacting protein
DHFR	dihydrofolate reductase
DISC	death-inducing signalling complex
DMEM	Dulbecco's Minimal Essential Medium
DMSO	dimethyl sulfoxide
DNA	desoxyribonucleic acid
DRiPs	Defective Ribosomal Products
DUB	deubiquitinating enzyme
EBV	Epstein Barr Virus
E. *coli*	Eschericha. *coli*
eEF1A1	elongation factor 1A1
e.g	for example
EGFP	enhanced green fluorescent protein
E1	ubiquitin-activating enzyme
E2	ubiquitin-conjugating enzyme
E3	ubiquitin protein ligase
E4	ubiquitin-chain elongation factors
ER	endoplasmic reticulum
ERAD	endoplasmic reticulum associated degradation
FADD	f as-associated death domain
FAT10	HLA-F associated transcript 10
fig	figure
GABARAP	γ-aminobutyric acid type A receptor-associated protein
GATE-16	golgi-associated ATPase enhancer of 16 kDa
GFP	green fluorescent protein
GSH	glutathione
GST	glutathione S-transferase

HA	hemagglutinin
HCC	hepatocellular carcinoma
HDAC	histone deacetylase
HECT	homologous to E6-AP carboxyl terminus
HEK	human embryonic kidney cells
HIP	HSP70-interacting protein
HIV	human immunodeficiency virus
HIVAN	HIV-associated nephropathy
HOP	HSP70/HSP90 organizing protein
HRP	horseradish peroxidase
HSP	heat shock proteins
HTT	huntingtin
IFN	interferon
IκB	inhibitor of NF-κB
IKK	IκB kinase
IL	interleukin
IP	immunoprecipitation
ISG15	interferon stimulated gene 15
JunB	jun B proto-oncogene
K	lysine
kDa	kilo Dalton
KEAP1	kelch-like ECH-associated protein 1
KIR	Keap1-interacting region
LCA	leber congenital amaurosis
LC3	light chain 3
LIR	LC3-interacting region
LMP2	low-molecular-weight protein 2
LPS	lipopolysaccharide
LRRFIP2	leucine-rich repeat fli-I-interacting protein 2
LULL1	lumenal domain like LAP1

NAP1	nucleosome assembly protein 1
MAD2	mitotic arrest deficient 2
mAb	monoclonal antibody
MALT1	mucosa-associated lymphoid tissue lymphoma translocation protein 1
MBP	maltose-binding protein
MECL1	multicatalytic endopeptidase-like-complex-1
MeOH	methanol
mM	millimolar
mRNA	messenger RNA
MTOC	microtubule organizing centre.
mTOR	mammalian target of rapamycin
mTORC1	target of rapamycin complex 1
MyD88	myeloid differentiation factor 88
NBR1	neighbour of Brca1 gene1
NDP52	nuclear dot protein 52 kDa
NEDD8	neural precursor cell-expressed developmentally down regulated 8
NEMO	NF-κB essential modulator
NES	nuclear export signal
NF-κB	nuclear factor 'kappa-light-chain-enhancer' of activated B-cells
NLS	nuclear localization signals
NPI	N-terminal p38 interaction
NRCM	neonatal rat cardiac myocytes
NRF2	nuclear factor erythroid-derived 2-related factor 2
N-terminal	amino-terminal
NUB1	NEDD8 ultimate buster 1
NUB1L	NEDD8 ultimate buster 1-Long
OPTN	Optineurin
pAb	polyclonal antibody
PAGE	polyacrylamide gel electrophoresis
PAS	pre autophagosomal structure

PB1	Phox and Bem1
PCR	polymerase chain reaction
PDB	pget's disease of bone
PE	phosphatidylethanolamine
PEST	rich in proline (P), glutamate (E), serine (S), and threonine (T) motif
PHD14	prolyl hydroxylase domain
PI3K	Phosphoinositide 3-kinase
PML	promyelocytic leukemia tumor suppressor
RING	really interesting new gene
RIP	receptor interacting protein
RNA	ribonucleic acid
ROS	reactive oxygen species
RPN	regulatory particle non-ATPase
RPT	regulatory particle triple-A protein
RTEC	renal tubular epithelial cell
SDS	sodium dodecyl sulfate
SH2	Src-homology 2
SQSTM1	Sequestosome-1
SUMO	small ubiquitin-like modifier
siRNA	small interfering RNA
STAT	signal transducer and activator of transcription
TANK	TRAF family member-associated NF-kappa-B activator
TBK1	TANK-binding kinase 1
TCR	T-cell receptor
TEMED	N,N,N’,N’- Tetramethylethylenediamine
Th cells	T helper cells
TLR	toll-like receptor
TNF	tumor necrosis factor
TNFR	tumor necrosis factor receptor
TRADD	Tumor necrosis factor receptor type 1-associated DEATH domain

	protein
TRAF6	TNF receptor-associate factor 6
TRAIL	TNF-related apoptosis inducing ligand
UBA	ubiquitin-associated
UBAN	ubiquitin binding in ABIN and NEMO domain
UBC domain	ubiquitin-conjugating domain
UBD	ubiquitin binding domain
UBE1	ubiquitin-like modifier activating enzyme 1
UBL	ubiquitin-like protein
UBP	ubiquitin-specific proteases
UBZ	ubiquitin-binding zinc-finger
UDP	ubiquitin-domain protein
UFM1	ubiquitin-fold modifier 1
UIM	ubiquitin-interacting motif
ULK	unc-51-like kinase
ULM	ubiquitin-like modifier
UPS	ubiquitin-proteasome system
USE1	UBA6-specific E2 enzyme 1
UVRAG	UV irradiation resistance-associated tumor suppressor gene
VCP	valosin-containing protein
WDFY3	WD repeat and FYVE domain-containing protein 3
WIPI	WD-repeat domain phosphoinositide-interacting)
µg	microgram
µl	microliter
µM	micromolar

9 Appendix

9.1 Supplemental western blots to figure 22

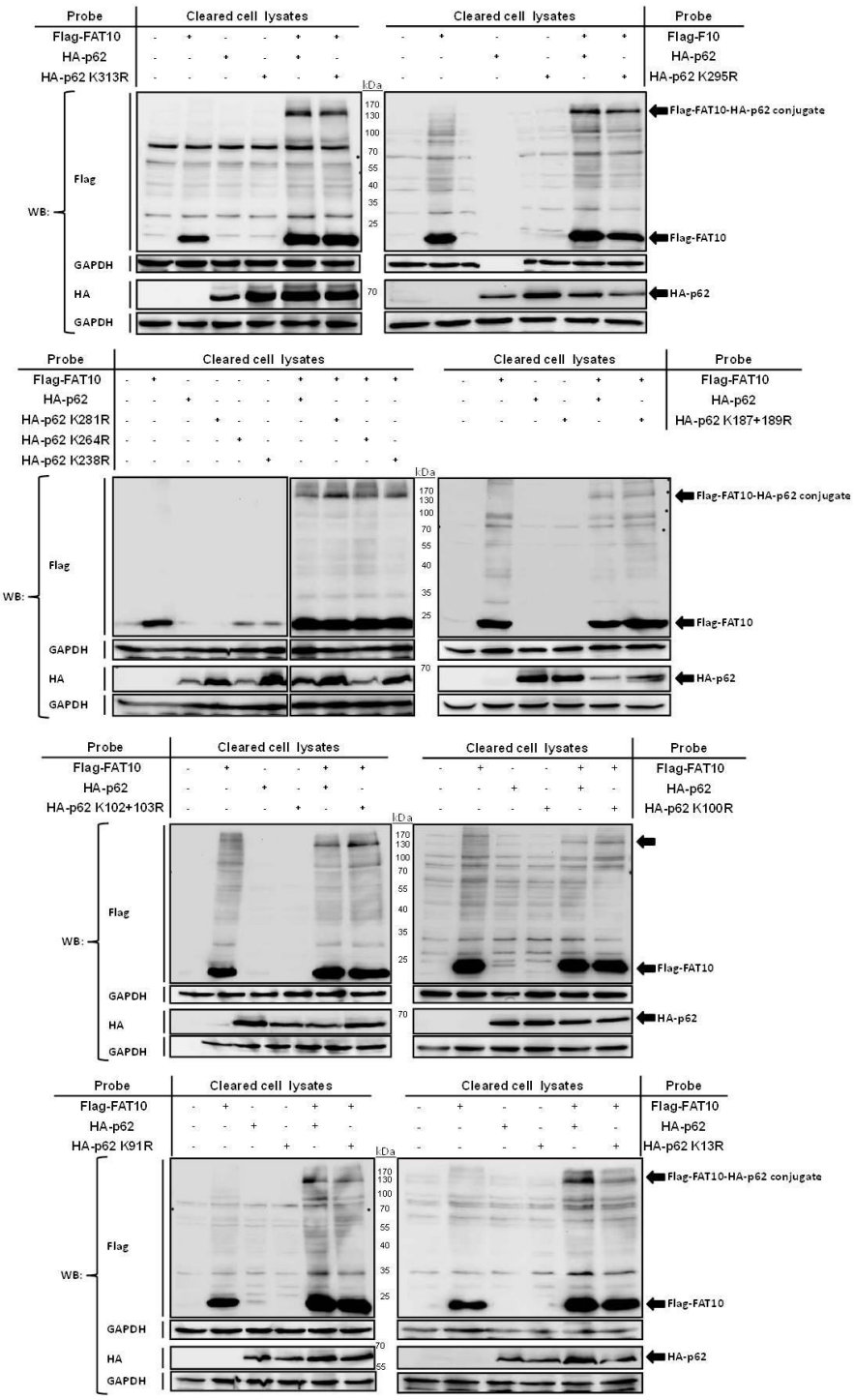

Figure 40: No lysine of p62 which is indispensable for the FAT10ylation could be identified. HEK293T cells were transiently transfected with expression plasmids for Flag-FAT10, HA-p62, and the respective lysine mutants of HA-p62, as indicated. The cleared cell lysates were boiled with a 10 % β-mercaptoethanol containing SDS-sample buffer and separated by SDS PAGE on 10 % or 12 % gels. After wet-blotting, blots were probed with either anti-Flag, or anti-HA reactive antibodies. The experiment was only performed once.

9.2 General facts about the interaction of FAT10 and p62

FAT10 interacts covalently and non-covalently with p62 in HEK293T cells which were transiently co-transfected with FAT10 and p62 constructs. In western blot experiments, the FAT10-p62 conjugate runs at approximately 130 kDa and therefore seems to consist out of one p62 molecule, decorated with up to three FAT10 molecules and/or additional unknown components. However, in contrast to the endogenous data, in the transient transfection experiments there is never a conjugate ladder detectable.

Compared to the amounts of monomeric p62 and FAT10 molecules, the conjugate band is quite faint; indicating that only a low portion of the p62 molecules seems to be FAT10ylated contemporaneously.

In the western blots of transfection experiments, despite using the same amounts of p62 DNA in the samples which were transfected with p62 only as in the samples which were co-transfected with FAT10 and p62, the resulting p62 protein amount often is markedly increased in the FAT10 co-transfected cells. In contrast, the amount of the monomeric FAT10 protein does not differ between the FAT10 only transfected cells and the FAT10 and p62 co-transfected cells.

In western blot analysis and in particular in immunoprecipitation experiments, the FAT10-p62 conjugate derived from overexpressed p62 and FAT10 is detectable under certain conditions only. For all tested tag combinations (Flag-FAT10 + HA-p62 or HA-FAT10 + p62-His), the FAT10-p62 conjugate was detectable only by using the antibody against FAT10 itself, or the FAT10 coupled tag. In the corresponding western blots which were stained with antibodies against either p62 itself, or against the p62 coupled tag, only the monomeric p62 was visible. Also immunoprecipitation

of the conjugate could be achieved only by using the antibodies against FAT10 itself, or against the FAT10 coupled tag.

The co-immunoprecipitation efficiency of the FAT10-p62 conjugate was improved when the incubation time of the immunoprecipitation reaction was reduced from overnight or 4 hours at 4 °C to 1 hour at 4 °C only. Since there are many FAT10ylation targets of different molecular weights, FAT10ylation like ubiquitylation leads to a smear in western blot detection. Due to the small portion of the p62-FAT10 conjugate, it can be easily hidden by this conjugate smear. To reduce at least the additional antibody derived background, directly “horse radish peroxidise” (HRP) labelled primary antibodies were preferentially used for the detection.